The Receptor Tyrosine Phosphatase Ptp69D and the Receptor Tyrosine Kinase Pvr in *Drosophila* Nervous System Development

by

Heather C. Robertson Sears

B.A., Molecular Biology

Pomona College

Submitted to the Department of Biology
in Partial Fulfillment of the Requirements for the Degree of
Doctor of Philosophy in Biology

at the

Massachusetts Institute of Technology

June 2004

Signature of Author.....
Department of Biology
May 21, 2004

Certified by.....
Paul A. Garrity
Assistant Professor of Biology
Thesis Supervisor

Accepted by.....
Stephen P. Bell
Professor of Biology
Co-Chair, Biology Graduate Committee

TABLE OF CONTENTS

The Receptor Tyrosine Phosphatase Ptp69D and the Receptor Tyrosine Kinase Pvr in *Drosophila* Nervous System Development

by

Heather C. Robertson Sears

Submitted to the Department of Biology on May 21, 2004 in partial fulfillment of the requirements for the Degree of Doctor of Philosophy in Biology

ABSTRACT

Cell migration and axon guidance are highly similar processes important for the development of the nervous system. Both processes involve the transduction of signals across the membrane, resulting in changes in the cytoskeleton. I have examined the roles of two receptors that are involved in axon guidance and cell migration in *Drosophila*. Ptp69D is a receptor tyrosine phosphatase required for axon guidance in the developing embryo and for layer-specific axon targeting in the developing visual system. Using a dominant-negative form of Ptp69D, I have identified several genes with which Ptp69D genetically interacts in photoreceptor axon targeting. Removing a single dose of the cytoplasmic tyrosine kinases Src64 or Abl or the repulsive axon guidance receptor robo enhanced the Ptp69D dominant-negative phenotype. In mammalian systems, Src plays a key role in the regulation of cell adhesion, and Abl is a known regulator of actin cytoskeletal dynamics. Removing a single dose of the EGF receptor or Ras85D suppressed the Ptp69D dominant negative phenotype. Interestingly, the cytoplasmic tyrosine kinase PR2 binds Ptp69D, and the *C. elegans* homolog of PR2 has been found to suppress the Egfr/Ras pathway. Other evidence suggests that the Egfr/Ras pathway may be required for axon outgrowth. In addition to PR2, I also identified the receptor tyrosine kinase Pvr in a biochemical screen for proteins that bind Ptp69D. I generated mutants in *Pvr* by gene disruption and EMS mutagenesis. These mutants have disruptions in the embryonic central nervous system, including mispositioning of axon tracts and the glia that wrap them. However, these defects are not inherent to the CNS. Rather, they result from a failure of hemocytes to migrate out of the head and engulf dead cells in the CNS. To identify proteins that signal downstream of Pvr in cell migration, I used a yeast two-hybrid screen to identify 15 proteins that bind the intracellular domain of kinase-active Pvr. One of these proteins, drk, is required for Pvr-dependent Erk MAP kinase activation. None has defects in hemocyte migration when disrupted by RNA interference. Whether these proteins have redundant functions or function downstream of Pvr in other systems remains to be determined.

Thesis Supervisor: Paul Garrity

Title: Assistant Professor of Biology

INTRODUCTION

Directed cell migration is important for the proper formation of most tissues during embryonic development (Armstrong, 1985), as well as proper functioning of the adult immune system. For example, neutrophils migrate through the vasculature and across the blood vessel epithelium to find and kill invading pathogens (Jones, 2000), and fibroblasts and other immune cells migrate into damaged tissue to promote wound healing (Gillitzer and Goebeler, 2001). Failure in cell migration or ectopic cell migration is the cause of a number of disease states, as in atherosclerosis, where smooth muscle cells, macrophages, and lyphocytes accumulate in a plaque in the arterial wall (Worthley et al., 2001), and metastasis, where tumor cells migrate away from their point of origination to invade and destroy other healthy tissues, often in a tissue-specific fashion (Moore, 2001). In most cases, the entire cell body translocates in response to an external cue, beginning with cytoskeletal changes at the leading edge and resulting in the translocation of the nucleus and other organelles. In the nervous system, a number of cell types migrate as whole cell bodies, but most neurons also send out axons and dendrites. At the tips of growing axons and dendrites is the growth cone. While the growth cone has some key differences from a migrating cell, the two are in many ways analogous in the way they sense and respond to cues in the environment.

Mechanisms of guided cell migration and axon guidance

The process of cell migration or axon guidance begins with an extracellular protein ligand binding to receptors on the surface of the migrating cell or navigating growth cone. Activation of the receptor leads to the induction of signaling cascades inside the cell, which may involve formation or disassociation of protein complexes, phosphorylation or dephosphorylation of proteins or lipids, and/or relocalization of cytoplasmic proteins to the membrane or the cytoskeleton. Ultimately these signaling cascades lead to the strengthening or weakening of cell-cell or cell-substrate adhesions and to changes in the actin and microtubule cytoskeletons. When there is a gradient of receptor occupancy from one side of the cell to the other, changes in the cytoskeleton are made locally and, depending on the cell type, lead to the extension of lamellipodia or filopodia in a given direction. In directed cell migration, the cell must extend a pseudopod at the leading edge, stabilize the underlying microtubules and actin meshwork, form

new focal adhesions to stabilize the pseudopod, pull the nucleus and other organelles forward using the stabilized microtubule network, release the focal adhesions at the trailing edge, and destabilize the cytoskeletal networks and focal adhesions at the trailing edge. The process of migration in axon guidance is ostensibly simpler, as the nucleus and cell body stay behind as the growth cone navigates forward. The growth cone extends many actin-rich filopodia, which are rapidly stabilized or destabilized depending on receptor occupancy. As actin-rich protrusions are stabilized in a certain direction, the microtubule cytoskeleton follows to build and stabilize the growing axon.

In recent years much attention has been focused on the mechanisms of chemotaxis in the single-celled amoeba *Dictyostelium discoideum* and leukocytes, professional migratory cells that scour the body for pathogenic invaders. A number of similarities have been found in the chemotaxis of these two cell types (Iijima et al., 2002b). Leukocytes respond to gradients of chemokines, small proteins secreted by other cells of the immune system. Dictyostelium cells respond to gradients of cAMP. These respective chemoattractants bind to G protein-coupled receptors (GPCRs), 7-transmembrane spanning receptors that are constitutively bound to heterotrimeric G proteins. Activation of the GPCR leads to release of the G proteins and their disassociation into Gκ and Gκκ, which mediates chemotaxis (Neptune and Bourne, 1997). Uneven distribution of GPCR occupancy leads to accumulation of PI3 kinase at the leading edge and PTEN at the trailing edge. PI3K and PTEN have antagonistic effects on inositol phospholipids: PI3 kinase phosphorylates phosphatidylinositol (3,4)-bisphosphate [PIP_2] to create phosphatidylinositol (3,4,5)-triphosphate [PIP_3], while PTEN is a phosphatase that reverses this reaction. Thus, accumulation of PI3 kinase at the leading edge results in an accumulation of PIP_3. Inhibition of PI3K or overexpression of PTEN can block chemotaxis (Sasaki et al., 2000; Tamura et al., 1998), while disruption of PTEN or exogenous addition of PIP_3 can enhance motility (Derman et al., 1997; Liliental et al., 2000). Proteins such as PKB/Akt can bind PIP_3 through their PH domains. This binding is thought to be important for mediating chemotaxis (Meili et al., 1999).

Activation of the Rho family of small GTPases is an important step in many chemotactic pathways (Fukata et al., 2003). This family of proteins is primarily composed of three members: Rac, Cdc42, and Rho. The small GTPases are active when bound to GTP and inactive when the GTP is hydrolyzed to GDP. They are activated by guanyl nucleotide exchange factors (GEFs),

which promote the release of GDP, and inactivated by GTPase activating proteins (GAPs). Based on overexpression of activated forms of the GTPases in mammalian fibroblasts, Rac is thought to mediate formation of lamellipodia, Cdc42 formation of filopodia, and Rho formation of focal adhesions, although their involvement in chemotaxis is likely to be far more complex than this simplistic model. PI3K is activated through binding to activated Rac1 or Cdc42 (Zheng et al., 1994), but inhibition of PI3K also prevents Rac and Cdc42 activation (Hawkins et al., 1995). Thus, Rac and Cdc42 can be both upstream and downstream of PI3K. All three small GTPases can lead to stabilization of microtubules, and Rac and Cdc42 lie upstream of a number of effectors of actin cytoskeletal dynamics (Fukata et al., 2003).

Studies of axon guidance have primarily focused on four families of axon guidance molecules and their receptors. Netrins and their receptors, homologs of DCC (deleted in colorectal cancer), primarily mediate long-range attraction; slits and their receptors, the Robo family of proteins, mediate short- and long-range repulsion; semaphorins and their receptors, the neuropilins and plexins, can mediate short- and long-range repulsion; ephrins and their receptors, Eph receptor tyrosine kinase, mediate short-range repulsion. Unlike the GPCR's, these receptors all have a single transmembrane domain and have multiple signaling modules in their intracellular domain capable of binding downstream signaling effectors. The signaling pathways activated downstream of these receptors are discussed in detail in a number of recent reviews (Guan and Rao, 2003; Huber et al., 2003). Of particular note is the fact that all of them lead to activation or inhibition of one or more of the Rho GTPases, and most modulate activity of Ena/VASP proteins, which are important for the elongation of actin filaments.

The signaling pathways and receptors used by migrating cells and navigating growth cones are by no means exclusive from one another. Slits have been found to act as a chemorepellant for leukocytes and migratory neurons as well as in axon guidance (Piper and Little, 2003; Rao et al., 2002; Wong et al., 2002). Conversely, chemokines, which classically are used for leukocyte migration, also are important for neuronal migration through binding to GPCRs (Bagri et al., 2002; Zhu et al., 2002). Sema4D, a non-neuronal semaphorin homolog, is important for leukoctye chemotaxis (Delaire et al., 2001). Clearly, the Rho family of small GTPases is used universally in migration, as are proteins that directly regulate actin filament dynamics.

Cell migration and axon guidance can be regulated by phosphorylation

Protein phosphorylation is a key mechanism for regulating signal transduction pathways in cell migration and axon guidance. Enzyme activity can be turned on or off through phosphorylation, or phosphorylation can create binding sites for other proteins, leading to formation of active signaling complexes. Protein phosphorylation state is regulated by two classes of enzymes: kinases, which add phosphate groups, and phosphatases, which remove phosphate groups. Proteins can be phosphorylated on serine, threonine, and/or tyrosine, although tyrosine phosphorylation is a particularly common mechanism for regulating the proteins involved in transducing migration and guidance signals. Tyrosine phosphatase inhibitors block axon outgrowth and guidance (Mandell and Banker, 1998). Here I will present what is known about how two classes of receptors that transduce signals across the membrane to affect cell migration and axon guidance through changes in tyrosine phosphorylation. The platelet-derived growth factor receptor (PDGFR) is a receptor tyrosine kinase whose ligand, PDGF, is a potent chemoattractant for many cell types. Knock-out mice lacking either PDGFRκ or PDGF-B die in utero of massive hemorrhaging, a result of the failure of pericytes and vascular smooth muscle cells (VSMCs) to migrate into and strengthen the vasculature (Hellstrom et al., 1999; Lindahl et al., 1997). The receptor protein tyrosine phosphatases (RPTPs) are a diverse set of molecules with cell-adhesive properties, many of which have been shown to play important although poorly understood roles in axon outgrowth and guidance. I will first focus on the signaling pathways activated downstream of PDGFR to effect cell migration and then discuss what is known about the downstream mechanisms by which RPTPs effect axon growth and guidance.

PDGF RECEPTOR SIGNALING IN CHEMOTAXIS

Structure and Mechanism of Activation

In mammals, there are two homologues of the PDGFR, PDGFRκ and PDGFRκ. The receptors consist of five immunoglobulin repeats in the extracellular domain and a split tyrosine kinase in the intracellular domain. Four proteins comprise the ligands for PDGFR. PDGF-A and PDGF-B can homo- or heterodimerize, while PDGF-C and PDGF-D only form homodimers. PDGF-A, PDGF-B, and PDGF-C homodimers and the PDGF-AB heterodimer act as ligands for

PDGFRκ, while PDGF-B and PDGF-D homodimers and the PDGF-AB heterodimer act as ligands for PDGFRκ. Binding of ligand results in dimerization of the receptors. The kinase domains of the receptors, when brought in proximity to one another through dimerization, cross-phosphorylate on certain tyrosine residues. Phosphorylation of some tyrosines, such as Y987, results in increased kinase activity, thus acting as a positive feedback loop. Phosphorylation of other key tyrosines creates docking sites for proteins with SH2 (Src homology 2) domains or PTB (phosphotyrosine binding) domains. Some SH2-domain proteins are phosphorylated by PDGFR when bound, which could result in enzymatic activation or the creation of a binding site for another protein. Other proteins are "activated" simply through relocalization to the membrane, or may be constitutively bound to a protein that needs to be translocated to the membrane for activation.

Signaling pathways activated downstream of PDGFR

A myriad of pathways are activated downstream of the activated PDGFR. Some of these are used for mitogenesis, others for chemokinesis or haptotaxis, random cell migration, and others for chemotaxis, directed cell migration. Which pathways are utilized downstream of the PDGFR for which process depends greatly on the cell type examined, and there is a considerable amount of crosstalk between the pathways. The large number of these factors have made clear elucidation of a signal transduction pathway from PDGF to cell movement difficult, if not impossible. Here I will describe recent advances in our understanding of the molecules involved in PDGF-mediated chemotaxis and how they relate to one another.

A key method for investigating the signaling molecules downstream of the mammalian PDGFR has been the mutation of the tyrosines that are phosphorylated and required for activation of various substrates (Figure 1). Phosphotyrosines 579 and 581 (pY579 and pY581) bind the cytoplasmic tyrosine kinase Src, pY740 and pY751 bind PI3K, pY771 binds RasGAP, pY1009 binds the tyrosine phosphatase SHP2, and pY1021 binds phospholipase C (PLCκ). Porcine aortic endothelial (PAE) cells expressing wildtype PDGFRκ migrate toward a gradient of PDGF and form membrane ruffles at the leading edge. When the binding sites for PI3K were mutated to phenylalanine, the cells could no longer migrate towards PDGF and were defective in the formation of membrane ruffles (Wennstrom et al., 1994b), suggesting that PI3K binding is required to mediate cytoskeletal changes and chemotaxis downstream of the PDGFR. Mutation

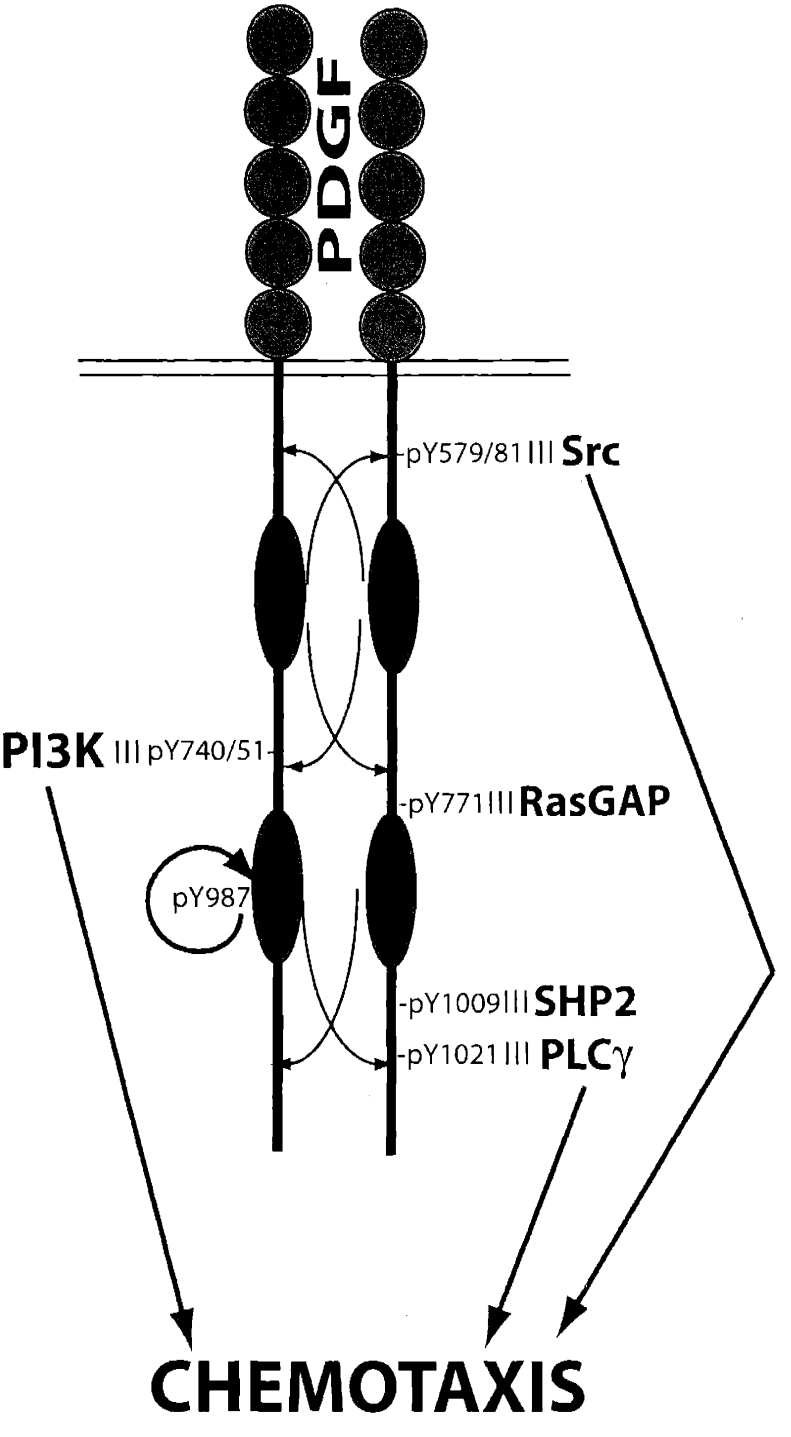

Figure 1. Proteins that bind activated PDGFR. See text for details

of the RasGAP, SHP-2 and PLCκ binding sites had no effect on PDGF-mediated migration in PAE cells. In Ph cells, a derivative of the NIH3T3 cell line that does not endogenously express PDGFRκ, the binding sites for Src, PI3K, and PLCκ in ectopically-expressed PDGFRκ were all required for PDGF-mediated chemotaxis, although none of them were sufficient for migration. Coexpression of PDGFRκ molecules that had only the Src binding sites and either the PI3K or the PLCκ binding sites intact significantly restored PDGF-induced chemotaxis. Mutation of the Src binding sites in PDGFRκ has a negative impact on PDGFR kinase activity (Baxter et al., 1998; Mori et al., 1993), and therefore the requirement for Src activity downstream of PDGFRκ has been difficult to assess using this method. Gelderloos, et al. created a chimeric receptor in which the extracellular domain, transmembrane domain, and the juxtamembrane portion of the intracellular domain containing the Src binding sites were taken from PDGFRκ and the rest of the intracellular domain was taken from PDGFRκ. This chimeric receptor was able to mediate chemotaxis in response to PDGF-AA, and mutation of the Src binding sites did not compromise the receptor kinase activity (Gelderloos et al., 1998). However, changes in Y572 and Y574 (equivalent to Y579 and Y581 in PDGFRκ) resulted in a receptor that could not mediate migration toward PDGF, activation of Src, or phosphorylation of RasGAP, PLCκ, SHP-2, or Shc in response to PDGF stimulation in Ph cells (DeMali and Kazlauskas, 1998). This mutant receptor was capable of mediating chemotaxis towards PDGF in PAE cells (Hooshmand-Rad et al., 1998), suggesting that Src activity is not required in that cell type.

PI3 kinase

PI3K consists of two constitutively bound subunits: p85 is an adaptor protein whose SH2 domain binds the activated PDGFR, and p110 is an enzyme with lipid kinase activity (see above). The lipid kinase activity of PI3K is activitated upon binding of the adaptor to PDGFR. As described above, PDGFR mutants that cannot bind PI3K are defective in PDGF-mediated chemotaxis in both Ph cells and PAE cells. Wortmannin and LY294002, specific inhibitors of PI3K, have been shown to block PDGF-induced chemotaxis in a variety of cell types, including PAE cells, rat and human VSMCs, and smooth muscle cells (SMCs) (Carlin et al., 2003; Hansen et al., 1996; Iijima et al., 2002a; Peppel et al., 2002). Numerous pathways have been shown to be activated downstream of PI3K, but only one, involving the small GTPase Rac, has been shown to have a role in PDGF-dependent chemotaxis (Figure 2). Stimulation with PDGF causes

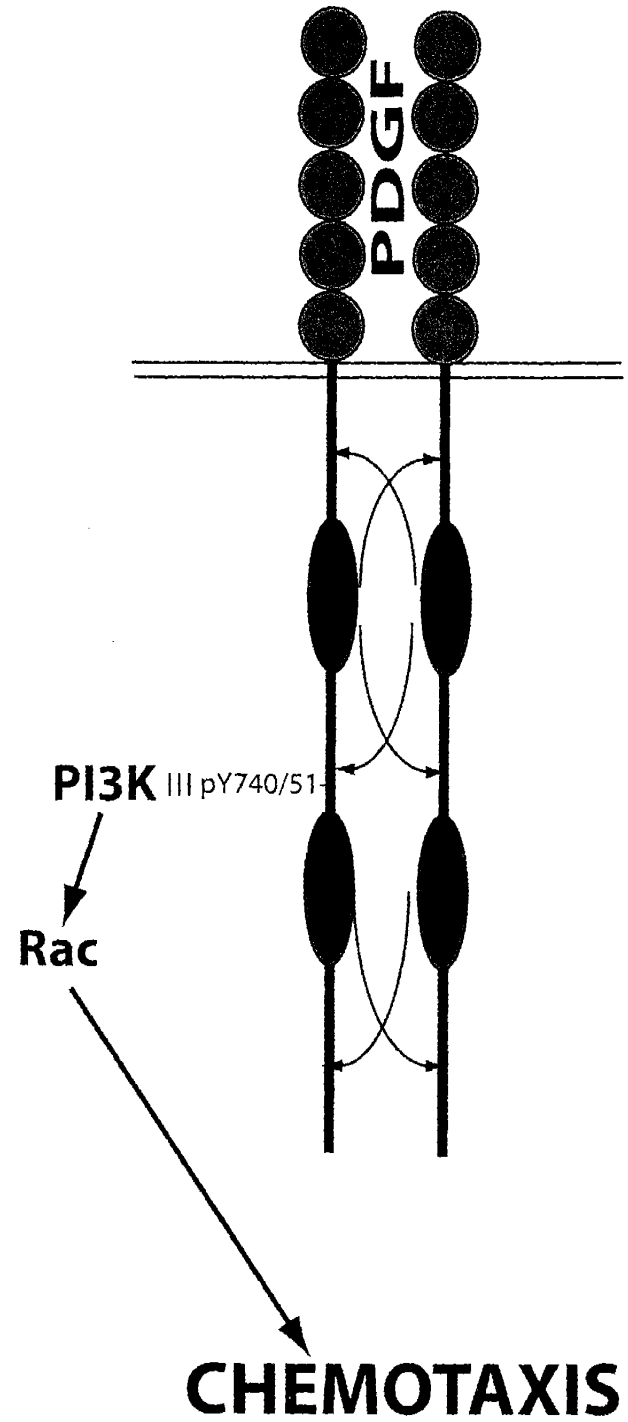

Figure 2. PI3K and Rac are required for PDGF-mediated chemotaxis and membrane ruffling in a variety of cell types.

membrane ruffling in PAE cells, VSMCs, NIH3T3 cells, and fibroblasts. Expression of dominant negative Rac or pharmacological inhibition of PI3K with wortmannin or LY294002 can block this response (Ridley et al., 1992; Ryu et al., 2002; Wennstrom et al., 1994a). Mutation of the PI3K binding sites in PDGFR also prevents formation of PDGF-induced membrane ruffles in PAE cells (Wennstrom et al., 1994a). Furthermore, a mutant form of PDGFRκ in which Y740/51, the PI3K binding sites, were intact, but all other binding sites were mutant, was capable of membrane ruffling and Rac activation upon stimulation with PDGF. Mutation of these sites prevented both membrane ruffling and Rac activation (Kanazawa et al., 2002). Rac is also required for migration toward PDGF gradients. Overexpression of Rac in PAE cells increased PDGF-induced chemotaxis (Hooshmand-Rad et al., 1997), and expression of dominant-negative RacN17 blocked PDGF-induced chemotaxis in fibroblasts (Anand-Apte et al., 1997) and VSMCs (Ryu et al., 2002). Thus, PI3K is a key regulator of PDGF-induced chemotaxis and functions through downstream activation of Rac, which promotes extension of lamellopodia, the first step in the translocation of the cell.

Src family kinases

The Src tyrosine kinase becomes activated upon stimulation with PDGF. The juxtamembrane tyrosines 579 and 581 in PDGFRκ are required for this activation. An inhibitory phosphotyrosine in the C-terminal tail of Src binds to the Src SH2 domain, thus sterically hindering the kinase domain. It is thought that the juxtamembrane phosphotyrosines in PDGFRκ bind the Src SH2 domain and compete away the inhibitory phosphotyrosine. Thus, when Y579/81 are mutated, Src cannot be activated (DeMali et al., 1999). As mentioned above, a receptor in which the Src binding sites are mutated to phenylalanine is incapable of mediating PDGF-induced chemotaxis in Ph cells, although the mutation has no effect on migration in PAE cells. Injection of antibodies against Src into human VSMCs also blocks PDGF-induced chemotaxis (Klinghoffer et al., 1999; Mureebe et al., 1997). However, cells taken from mice lacking three Src family members, Src, Yes, and Fyn, displayed no defects in PDGF-induced chemotaxis. This suggests that despite in vitro evidence to the contrary, these three Src family members do not actually play a role in chemotaxis downstream of PDGFR. It is possible that Src activity is only indirectly involved in PDGF-induced chemotaxis or that there is an additional Src

family member that binds the juxtamembrane phosphotyrosines in PDGFR and is required for migration towards PDGF.

Phospholipase C

Src is capable of phosphorylating Y934 in PDGFRκ. Interestingly, when mutant PDGFRκ in which Y934 was changed to phenylalanine was expressed in PAE cells, it caused an increase in migration towards PDGF (Hansen et al., 1996). In these cells, PLCκ1 activity was increased, as was the level of phosphorylation on PLCκ1 (Ronnstrand et al., 1999). The increase in chemotaxis was blocked by bisindolylmaleimide, a pharmacological inhibitor of PKC, which is activated downstream of PLCκ1. The increase in chemotaxis toward PDGF could not be blocked by LY294002, suggesting that the Y934F mutation released the activation of a PI3K-independent and PLCκ1-dependent chemotactic pathway in PAE cells. In addition, overexpression of PLCκ in PAE cells caused an increase in PDGF-mediated chemotaxis and overrode the requirement for PI3K signaling.

PLCκ is an enzyme that cleaves PIP_2 to produce inositol-1,4,5-triphosphate (IP3) and diacylglycerol (DAG). IP_3 releases intracellular stores of calcium and DAG functions to activate PKC. Binding of PLCκ to Y1021 on PDGFRκ results in phosphorylation and activation of PLCκ (Figure 3). Plattner, et al. found that both the Src binding sites and the PLCκ binding sites on chimeric PDGFRκ/κ were required for PDGF-induced activation of the Abelson tyrosine kinase (Abl) (Plattner et al., 2003). They also found that Abl could not be activated by PDGF stimulation in fibroblasts lacking PLCκ1 or expressing dominant negative PLCκ. Interestingly, neither of the PLCκ enzymatic products was involved in Abl activation. Rather, it was found that the PLCκ substrate, PIP_2, had an inhibitory effect on Abl activity. A kinase-dead form of Abl blocked PDGF-induced chemotaxis in PAE cells overexpressing PLCκ, and expression of constitutively active v-Abl was capable of further increasing PDGF-stimulated chemotaxis in PAE cells overexpressing PLCκ. In mouse embryonic fibroblasts (MEFs) overexpressing PLCκ, migration toward a gradient of PDGF also required Abl (Plattner et al., 2004). The SH2 domain of Abl was found to bind directly to PDGFR. This binding partially required the Src binding sites, Y579/81, suggesting that Abl may bind directly to those sites on PDGFR or that Abl binds to an as yet unidentified site generated by Src phosphorylation. Mutation of the Src, PI3K, RasGAP, SHP2, and PLCκ binding sites together completely

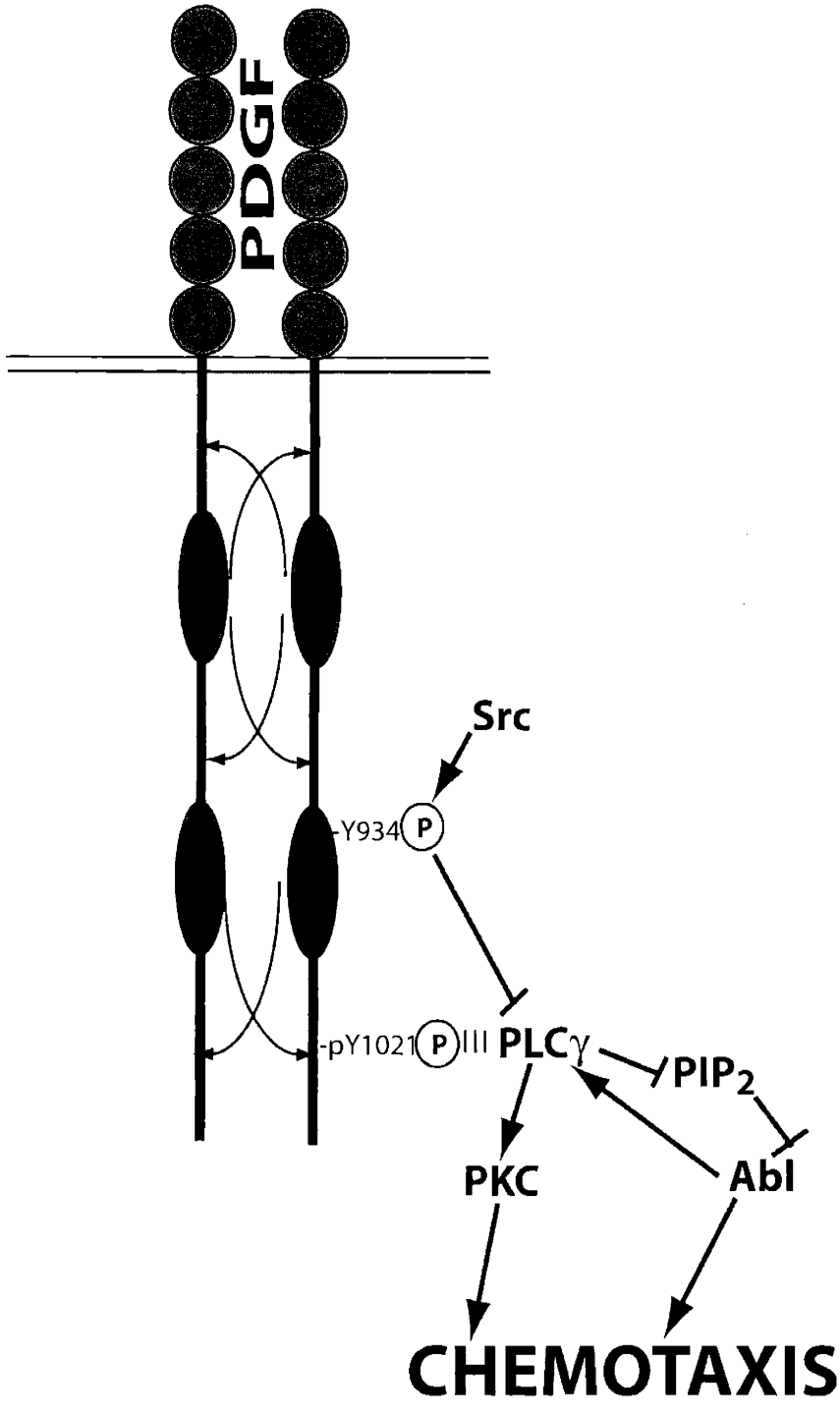

Figure 5. Potential roles of Phospholipase C and Abl in PDGF-mediated chemotaxis.

abolished Abl binding. Abl and PDGFR were capable of phosphorylating one another (Plattner et al., 2004), and Abl was capable of phosphorylating wildtype PLCκ (Plattner et al., 2003), although it was not determined whether any of these steps are required for PDGF-induced chemotaxis. These results suggest the possibility that it is Abl, rather than Src, binding to Y579/81 on PDGFRκ that is important for PDGF-directed motility, and support a novel potential role for Abl both upstream and downstream of PLCκ in PDGF-induced chemotaxis.

Focal adhesion kinase

Focal adhesion kinase (FAK) is a cytoplasmic tyrosine kinase that is a part of the focal adhesion complex and appears to be required for the turnover of focal contacts. The C-terminus of FAK binds to paxillin and talin, which themselves bind to integrins (Chen et al., 1995; Liu et al., 1999; Tachibana et al., 1995). Integrins are transmembrane proteins that link the extracellular matrix to the actin cytoskeleton. Cells lacking FAK are defective in haptotaxis, or random migration, as a result of having increased focal contacts with the substrate (Ilic et al., 1995). Re-expression of FAK in $FAK^{-/-}$ cells can rescue this motility defect. Through transfection of mutant forms of FAK into $FAK^{-/-}$ cells, it was found that three sites are required for FAK-mediated haptotaxis: an SH2-binding site at Y397, the kinase domain, and the SH3 binding site for $p130^{Cas}$ (Sieg et al., 1999). In addition to its role in haptotaxis, FAK is also required for PDGF-directed chemotaxis. Surprisingly, only the SH2-binding site at Y397 was required for migration of cells towards PDGF. The kinase domain and the SH3 binding site were not required (Sieg et al., 2000). The SH2 domain of Src binds to FAK Y397 when cells are stimulated with PDGF. This binding results in activation of Src and subsequent phosphorylation of other tyrosines in FAK. Overexpression of C-terminal Src kinase (Csk), which inhibits Src activity and would thereby prevent phosphorylation of FAK by Src, also inhibited PDGF-directed cell migration. FAK also forms a complex with PDGFR when cells are stimulated with PDGF. Overexpression of the inhibitory domain of FAK, FRNK (FAK-related non-kinase), in VSMCs prevented FAK binding to PDGFR upon stimulation with PDGF, and also inhibited PDGF-directed chemotaxis (Hauck et al., 2000). Thus, while FAK kinase activity is required for focal contact turnover in random cell migration, FAK may have an additional role as an adaptor linking the PDGFR to Src or other SH2 domain-containing proteins in PDGF-mediated chemotaxis (Figure 4).

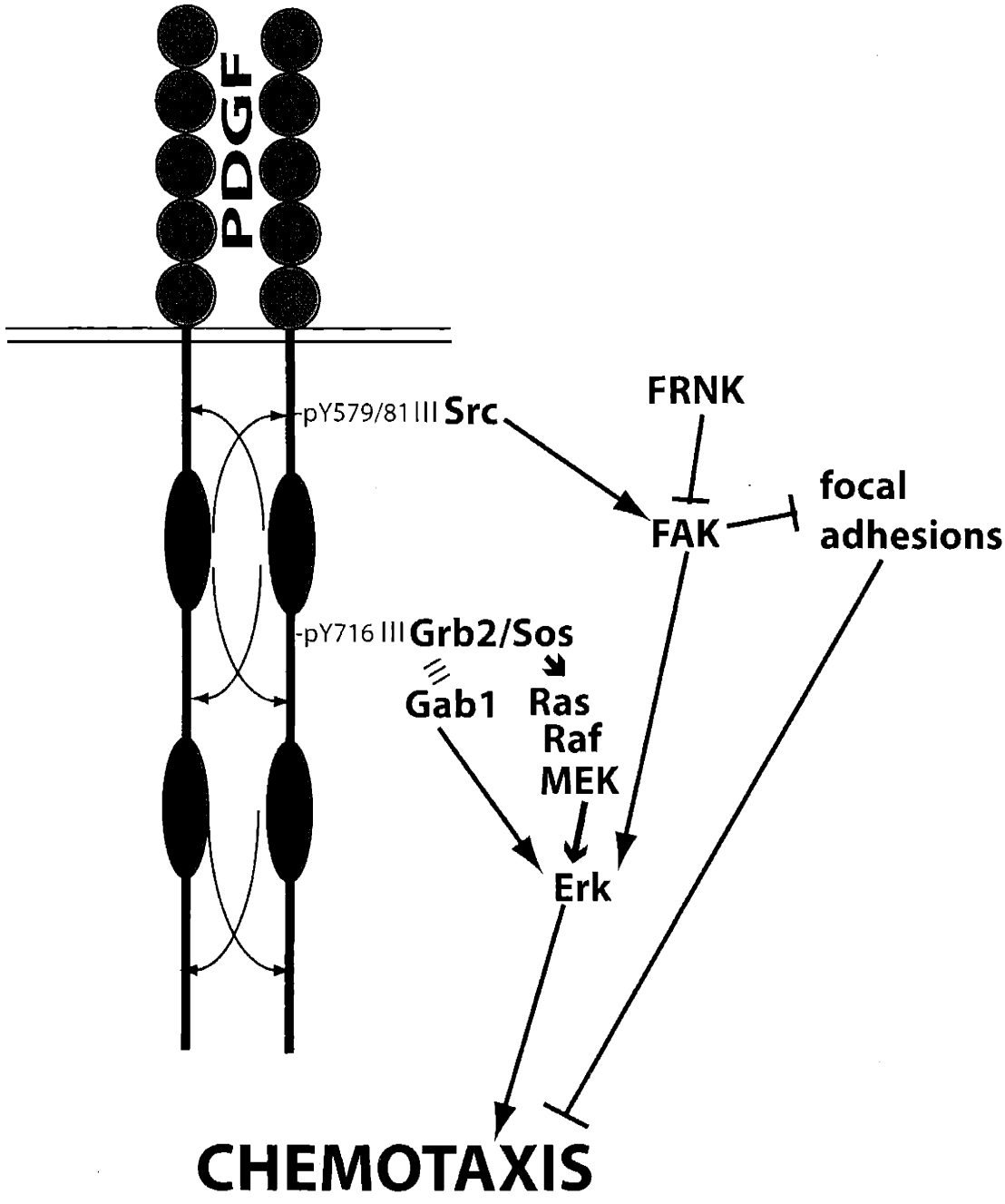

Figure 4. Potential roles of Src, FAK, and Erk pathways in PDGF-mediated chemotaxis. Se text for details.

FAK is a part of a signaling complex that leads to activation of the mitogen-activated protein kinases (MAPKs) Erk1/2 and JNK (Schlaepfer et al., 1999). Expression of FRNK reduced both the extent and duration of phosphorylation of Erk in PDGF-stimulated cells, and activation of Erk in response to PDGF is decreased in $FAK^{-/-}$ cells (Hauck et al., 2000). Erk is also activated downstream of the PDGFR via a pathway including the adaptor proteins Grb-2 and Shc (Figure 4). Grb-2 recruits the GEF Sos to the membrane, where Sos activates the small G protein Ras. Ras activation leads to a cascade of phosphorylation events: Raf kinase phosphorylates MEK, which phosphorylates and activates Erk MAPK. Pharmacological inhibition of MEK by PD98059 inhibited chemotaxis toward 20 ng/ml PDGF in rat aortic SMCs, whereas inhibition of the MAPK p38 had no effect (Hauck et al., 2000). However, Iijima et al. found that PD98059 had no effect on chemotaxis of the same cells toward 10 ng/ml PDGF (Iijima et al., 2002a). Yet another group found that PD98059 blocks PDGF-mediated haptotaxis in VSMCs, and suggested that addition of PDGF and subsequent Erk activation simply functioned to reduce cell adhesion to extracellular matrix proteins (Kingsley et al., 2002). Overexpression of Gab1, an adaptor protein that is recruited to PDGFR by Grb-2 and also binds SHP2 and PI3K, led to increased PDGF-dependent Erk activation, p38 activation, and actin cytoskeleton reorganization. MEFs lacking Gab1 are deficient in chemotaxis towards PDGF (Kallin et al., 2004). Interestingly, expression of PDGFRκ is increased when cells are incubated in high levels of glucose, an effect that was dependent on Erk MAPK activity (Campbell et al., 2003). Thus, Erk MAPK activity is clearly important for PDGF-induced migration. However, which pathways are used to relay activation from PDGFR to Erk in cell migration is unclear, and it is unclear whether Erk is required for cytoskeletal reorganization, focal contact remodeling, or simply for amplifying the PDGF signal through increased expression of PDGFR.

G Protein Coupled Receptors

Many of the molecules required for PDGF-mediated chemotaxis are also required for chemotaxis downstream of GPCRs. An interesting link between PDGFR and GPCRs has emerged in recent years, although not without controversy. Activation of PDGFR leads to activation of sphingosine kinase, which phosphorylates the lipid sphingosine to create sphingosine-1-phosphate (SPP). SPP is a ligand for the EDG-1 family of GPCRs, encoded by the endothelial differentiation genes, and can promote or inhibit migration of cells expressing

EDG-1 or other family members (Figure 5). PDGFR was found to associate with EDG-1 and other members of the GPCR signaling complex, GRK2 and beta-arrestin, when these proteins were co-expressed (Alderton et al., 2001). Additionally, EDG-1 becomes phosphorylated when cells are stimulated with PDGF (Hobson et al., 2001). Hobson et al. observed that *edg*-1 knock-out mice displayed a remarkably similar set of phenotypes to the PDGFRκ and PDGF-B knock-out mice, namely that mural cells, including VSMCs and pericytes, fail to migrate into the arteries and capillaries, leading to vascular hemorrhaging and embryonic death. They found that chemotaxis of MEFs or human aortic SMCs toward PDGF required EDG-1, and that expression of EDG-1 in human embryonic kidney (HEK293) cells, which normally do not migrate toward SPP or PDGF, made them capable of migrating toward both SPP and PDGF (Hobson et al., 2001). Furthermore, inhibition of sphingosine kinase with N,N-dimethylsphingosine or inhibition of G_i with pertussis toxin inhibited migration of MEFs toward PDGF. EDG-1 was also required for PDGF-induced Rac activation. Phosphorylation of GPCRs by G protein receptor kinase 2 (GRK2) desensitizes the receptor to further activation. Overexpression of GRK2 in SMCs blocked PDGF-induced chemotaxis (Peppel et al., 2002). It also blocked PDGF-induced phosphorylation of Akt, which is activated downstream of PI3K. Together these results imply that activation of PDGFR results in activation of EDG-1, which induces migration through activation of the PI3K and Rac signaling pathway. In rat VSMCs, the opposite effect was seen: treatment of cells with SPP actually blocked PDGF-induced migration (Ryu et al., 2002). However, VSMCs predominantly express EDG-5 rather than EDG-1. Engagement of EDG-5 by SPP leads to activation of Rho and inhibition of Rac (Okamoto et al., 2000). Rho activation leads to formation of stress fibers, which tether the cell to its substrate via focal contacts. Thus, activation of Rho has the opposite effect on chemotaxis of Rac, whose activation promotes formation of protrusive lamellipodia. Therefore, EDG-5 and Rho appear to inhibit PDGF-induced chemotaxis, whereas EDG-1 and Rac promote and are required for PDGF-induced chemotaxis. When EDG-1 was overexpressed in rat VSMCs, SPP no longer inhibited PDGF-directed migration (Ryu et al., 2002). In contention with these results, Kluk et al. were unable to reproducibly show a requirement for EDG-1 in rat adult medial VSMCs or MEFs (Kluk et al., 2003). This may have been due to a difference in the cell types used or the methods employed in the chemotaxis assays. This irreproducibility may suggest that PDGFR and EDG-1

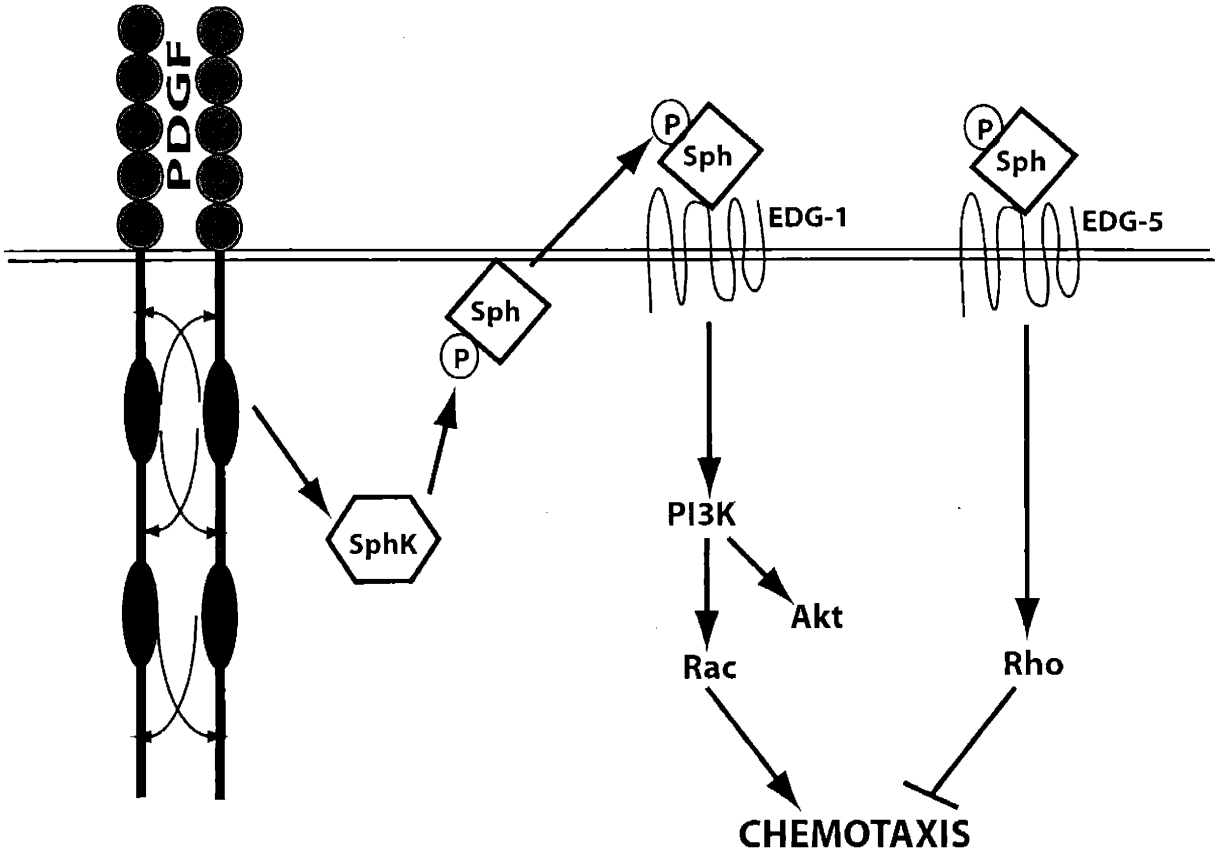

Figure 5. Activated PDGFR activated sphingosine kinase (SphK), which phosphorylates sphingosine (Sph) to create sphingosine-1-phosphate (SPP). SPP is a ligand for the EDG family of GPCRs. EDG-1 mediates PDGF-dependent chemotaxis via PI3K and Rac, while EDG-5 inhibits PDGF-dependent chemotaxis via Rho.

must work together to engage various signaling pathways in some cells, while PDGFR may work alone to engage the same pathways in other cells.

EDG-1 may also be required for PDGF-induced regulation of focal adhesion complexes. Stimulation with PDGF normally causes phosphorylation of FAK and translocation of $p130^{Cas}$ and paxillin to focal adhesions. EDG-1 is required for the appropriate execution of both of these processes (Rosenfeldt et al., 2001). PDGFR activation also results in activation of Src, as described above. Src activation is deregulated in cells lacking *edg*-1. Inhibition of G_i function with pertussis toxin also prevented PDGF-stimulated Src activation. These results collectively suggest that the GPCR EDG-1 may be required to mediate activation of both the PI3K/Rac cytoskeletal remodeling pathway and focal adhesion remodeling downstream of PDGF.

PDGFR Signaling in *Drosophila*

The fruit fly *Drosophila melanogaster* has a single homolog of the PDGF and VEGF receptors, abbreviated Pvr (Duchek et al., 2001). The extracellular domain of Pvr has seven immunoglobulin domains, as does the VEGFR. The intracellular split kinase domain of Pvr, on the other hand, is more closely homologous to the PDGFR, so signaling downstream of Pvr is likely to be more like that of the PDGFR. There are three ligands for Pvr, named Pvf1, Pvf2, and Pvf3. The three ligands are expressed in different subsets of cells, so it is unlikely that they act as heterodimers, but it is unknown whether they act as monomers or homodimers (Cho et al., 2002).

Like PDGFR, Pvr is required for both mitogenesis and chemotaxis of various cells during Drosophila development. During oogenesis, Pvr collaborates with the EGF receptor to control both anterior-posterior and ventral-dorsal migration of the border cells, which form part of the micropyle, the sperm entry point (Duchek et al., 2001). The border cells follow a precise migration route guided primarily by Pvf1. During embryogenesis, Pvr is required for the survival and migration of hemocytes, macrophage-like blood cells that circulate in the hemolymph and scavenge dead cell debris. In *Pvr* mutant embryos, the hemocytes clump together in the anterior part of the embryo, near their point of origination, and fail to spread out throughout the embryo as they do in wildtype animals (Cho et al., 2002; Sears et al., 2003). This clumping is primarily a result of live hemocytes trying to phagocytose the dying hemocytes. When cell death is suppressed in Pvr mutant embryos, the hemocyte clumping is no longer

evident, but rather the hemocytes fail to migrate into the ventral posterior part of the embryo (Katja Brückner and Norbert Perrimon, unpublished data). In their migration, the hemocytes follow stereotyped routes laid out by all three Pvfs. Ectopic expression of a single Pvf, however, is sufficient to misdirect the hemocytes to the ectopic location (Cho et al., 2002). Pvr activation also induces proliferation of larval hemocytes (Munier et al., 2002), but a role for Pvr in larval hemocyte migration has not been demonstrated.

While Pvr's intracellular homology to PDGFR would suggest that the signaling pathways downstream of Pvr might be similar to those downstream of PDGFR, none of the known SH2-binding sites in PDGFR are conserved in Pvr. Thus, the signaling pathways from Pvr to the cytoskeletal and focal contact rearrangements needed for chemotaxis may or may not be conserved. To date, little is known about the signaling pathways activated downstream of Pvr. Rac and the Rac activator myoblast city (mbc), a homolog of DOCK180, appear to be involved in border cell migration downstream of Pvr (Duchek et al., 2001). Expression of dominant active Pvr or Rac in border cells caused the formation of long actin fibers and prevented the border cells from migrating. Co-expression of dominant negative RacN17 with dominant active Pvr quenched this phenotype. Expression of RacN17 alone in border cells blocked their migration. Mutation of *mbc* was also able to quench the dominant active Pvr F-actin-based phenotype and had a border cell migration defect on its own. Activation of Rac by DOCK180 is required for migration of mammalian 293T cells (Grimsley et al., 2004) and C. elegans distal tip cells (Reddien and Horvitz, 2000). More recently, the accumulation of Cortactin, a Src substrate that can stimulate actin polymerization, has been shown to be regulated by Pvr, although Cortactin mutants do not have a defect in border cell migration (Somogyi and Rorth, 2004). Additionally, the ubiquitinating protein Hrs has been shown to be involved in downregulation of Pvr (Jekely and Rorth, 2003). Mutants in the Grb2 homolog drk, Shc, the Nck homolog dock, Pak, or trio did not have any detectable border cell migration defects (Duchek et al., 2001). Zygotic loss of function in drk, Shc, or Sos did not have any defects in hemocyte migration either (Cho et al., 2002), although these genes are heavily maternally contributed. The Ras/MAPK pathway has been loosely implicated in embryonic hemocyte migration. Erk MAPK is phosphorylated in a Pvr-dependent manner in migrating hemocytes (Cho et al., 2002) and in Schneider S2 cells (Duchek et al., 2001), which are derived from embryonic hemocytes. Additionally, expression

of dominant negative RasN17 in hemocytes prevents them from migrating into the tail region of the embryo during the germband-extended stage of development (Cho et al., 2002).

Concluding Remarks

While much progress has been made in elucidating the signaling pathways downstream of PDGFRs in chemotaxis, the picture is far from complete. PDGFR-dependent Rac activation is clearly important for chemotaxis in both mammalian cells in culture and *Drosophila* cells in vivo. In cultured cells, PI3K links PDGFR to Rac activation, but it has not been confirmed that this is the case in vivo. Similarly, PLCκ and the Src-related tyrosine kinases, including Abl, are involved in chemotaxis downstream of PDGFR under non-physiological conditions, but whether these pathways are used by cells in the animal remains to be determined. PDGFR signaling also probably leads to changes in focal adhesion strength and number, which could have an impact on the ability of cells to migrate. Examining these pathways in vivo in mammalian systems is difficult, requiring the creation of knock-out and knock-in mice in each of the pathway components, and compounded by the vast number of cell types in mammals, each of which is likely to respond to gradients of PDGF in a different way. While many of the tyrosines in PDGFR are not conserved in Drosophila Pvr, the signaling pathways downstream of Pvr may be conserved. Due to the increased simplicity of *Drosophila* embryonic development and the *Drosophila* genome, it may be more feasible to examine PDGFR chemotactic signaling in vivo in Drosophila oogenesis and embryogenesis. Further examination of Pvr signaling in border cell migration and hemocyte migration through identification of downstream components and identification of the requisite tyrosines in Pvr could shed light on the pathways used in vivo downstream of PDGFRs.

RECEPTOR TYROSINE PHOSPHATASES IN AXON GUIDANCE

Structures and Mechanisms of Activation

The receptor tyrosine phosphatases are a highly diverse set of molecules that have now been classified into eight types based on the composition of their extracellular domains. However, since even closely homologous receptors in the same class can function quite

differently both in ligand-binding and downstream effects, these classifications are not entirely useful. Most RPTPs have motifs in the extracellular domain that are characteristic of cell adhesion molecules, such as immunoglobulin repeats, Fibronectin type III (FNIII) repeats, or a MAM (meprin-A5-μ) domain. The intracellular domain of RPTPs consists of one or two tandem phosphatase domains. In RPTPs with two phosphatase domains, the first (membrane-proximal) domain is thought to hold the majority of the catalytic activity, although the second (C-terminal) domain in some RPTPs may have catalytic activity or be required as an adaptor module to bind other proteins. How RPTPs are activated is largely unknown, and the mechanism may differ from one RPTP to another. PTPκ, an RPTP with a small highly-glycosylated extracellular domain, crystallizes as a dimer, with a "wedge" motif from one monomer blocking the active site of the other monomer, suggesting that dimerization is inhibitory for PTPκ (Bilwes et al., 1996). However, PTPμ and LAR (leukoctye common antigen-related) crystallize as monomers and do not display such a "wedge" motif (Hoffmann et al., 1997; Nam et al., 1999). PTPκ and PTPκ crystallize as heterodimers, with the second phosphatase domain of PTPκ binding and inhibiting the first phosphatase active site of PTPκ (Wallace et al., 1998). PTPκ/RPTPκ, the only RPTP for which a ligand has been identified, is inactivated upon binding to its ligand (Meng et al., 2000). However, ligand-induced inactivation is unlikely to be a common mechanism among all RPTPs, as each RPTP examined to date appears to be activated or inactivated by a different mechanism.

Mammalian RPTPs: Homophilic attraction and repulsion

A large number of RPTPs are expressed in the nervous system during periods of axon outgrowth and synapse formation and localize to the growing axons and their growth cones (Johnson and Van Vactor, 2003). In Drosophila these include Dlar, Ptp69D, Ptp99A, Ptp10D, and Ptp52F; in vertebrates, LAR and its homologs PTPκ and PTPκ, PTPμ and PTPκ, which are characterized by the presence of an extracellular MAM domain, and CRYP-2; and the LAR homologs HmLAR1 and HmLAR2 in leech. PTPκ, PTPμ, and PTPκ are homophilic cell adhesion molecules that promote neurite outgrowth in vivo and in vitro (Brady-Kalnay and Tonks, 1994; Brady-Kalnay and Tonks, 1995; Drosopoulos et al., 1999; Gebbink et al., 1993; Wang and Bixby, 1999; Zondag et al., 1995). The extracellular domains of PTPμ and PTPκ are strictly homophilic, despite their structural similarity. A fusion protein containing the MAM

domain from PTPκ and the Ig domain from PTPμ was also strictly homophilic and did not bind either PTPμ or PTPκ (Zondag et al., 1995). The soluble extracellular domain of PTPκ was capable of mediating attractive growth cone turning in forebrain neurons in vitro (Wang and Bixby, 1999), and expression of a catalytically inactive PTPκ C-S mutant in Xenopus retinal ganglion cells (RGCs) decreased the rate of axon elongation both in vivo and in vitro on retinal basement membrane (Johnson et al., 2001). The requirement for the catalytic domain of PTPκ and its ability to turn growing axons would suggest it acts as more than just an adhesive to enable growth cones to move along a substrate, but rather that the intracellular phosphatase initiates signals that lead to changes in the cytoskeleton.

The extracellular domains of HmLAR and the chicken RPTP CRYP-2 are also probably capable of homophilic binding, but they mediate repulsion rather than adhesion. In leech, two comb cells extend approximately 70 parallel processes each. HmLAR1 and HmLAR2 are expressed on both the axons and growth cones of these processes (Gershon et al., 1998). A tagged form of the HmLAR extracellular domain bound to the processes, presumably binding to the extracellular domains of endogenously expressed HmLAR molecules (Baker et al., 2000). Interestingly, addition of the tagged extracellular domain also caused the normally parallel processes to cross over one another. Addition of an antibody against the HmLAR extracellular domain or RNA interference (RNAi) against HmLAR caused a similar crossing phenotype (Gershon et al., 1998). The authors of these studies concluded from these data that when filopodia from one process touch another process, the association of HmLAR molecules on the two processes causes them to repel one another. In the chicken visual system, CRYP-2 is expressed on both RGCs and in the optic tectum, the synaptic target of the RGCs (Bodden and Bixby, 1996; Ledig et al., 1999b). Experiments with a tagged form of the CRYP-2 extracellular domain demonstrated that the CRYP-2 ligand (or receptor) is also expressed on RGC axons (Stepanek et al., 2001). In vitro, the extracellular domain of CRYP-2 inhibited RGC neurite outgrowth and mediated growth cone collapse and repulsive turning (Stepanek et al., 2001). Thus, CRYP-2 may act as both a receptor and ligand, although it is unknown whether the receptor for CRYP-2 is CRYP-2 itself or another protein.

Vertebrate LAR and PTPκ are both involved in axon outgrowth, although they may not be involved in axon guidance. The dentate gyrus of $LAR^{-/-}$ knock-out mice is hypoinnervated by cholinergic neurons (Yeo et al., 1997). $PTP\kappa^{-/-}$ mice display more severe defects in motor

coordination, pituitary development, and myelination (Elchebly et al., 1999; Wallace et al., 1999). The expression of both LAR and PTPκ is increased after sciatic nerve crush (Haworth et al., 1998; Xie et al., 2001), and $LAR^{-/-}$ mice are deficient in nerve regeneration after sciatic nerve crush (Haworth et al., 1998). When PTPκ is prevented from binding to its ligand either by addition of an antibody against the extracellular domain or through addition of soluble extracellular domain, RGC axon outgrowth is inhibited (Ledig et al., 1999a). However, expression of a catalytically inactive PTPκ C-S mutant in Xenopus RGCs caused an increase in the rate of axon elongation (Johnson et al., 2001). This discrepancy could be due to the different contexts in which these assays were performed, or alternative functioning of the C-S mutant, as this type of mutant has been shown to act as a partial substrate trap. Expression of C-S mutant forms of LAR, PTPκ, PTPκ, or all three together had no effect on axon guidance.

RPTPs in *Drosophila*

The ease of genetic manipulation in *Drosophila* has made it more feasible to tease apart the signaling pathways downstream of RPTPs in that organism than in the vertebrates. *Drosophila* has six RPTPs, but one, Ptp4E is not expressed in the nervous system. Mutants in *Ptp69D* or *Dlar* cause partially penetrant defects in the targeting of the embryonic motor neurons (Desai et al., 1996; Krueger et al., 1996). The most well-characterized of these nerves is ISNb. INSb exits from the CNS with another nerve, ISN, but then splits off from ISN as they enter the muscle field. Axons in ISNb then defasciculate from the main nerve at various points to innervate the ventrolateral muscles. In some segments of both *Ptp69D* and *Dlar* mutants ISNb exhibits a bypass phenotype, where the axons in ISNb stay fasciculated and fail to innervate their target muscles. However, *Dlar* mutants more often exhibit a parallel bypass phenotype, where ISNb defasciculates from ISN and continue to grow parallel to it, while *Ptp69D* mutants more often display a fusion bypass phenotype, where ISNb fails to defasciculate from ISN. In the development of the Drosophila compound eye, Ptp69D is also required for the axons of photoreceptors R1-R6 to defasciculate from the R8 axon, which precedes R1-R6 axons into the brain (Garrity et al., 1999). These data suggest that Ptp69D acts as a defasciculation receptor, rather than an attractive or repulsive guidance receptor. *Ptp69D* and *Dlar* double mutants have more highly penetrant ISNb phenotypes, and overexpression of Dlar can rescue the *Ptp69D* mutant defects, suggesting that these two RPTPs may be redundant (Desai et al., 1997).

Mutations in *Ptp99A* also enhance the *Ptp69D* ISNb fusion bypass phenotype (Desai et al., 1996), although they suppress the *Dlar* ISNb defects (Desai et al., 1997). In the embryonic CNS, *Ptp69D* and *Ptp52F* single mutants cause breaks in the outermost fascicle and cause some longitudinal axons to cross the midline, as detected by staining with an antibody against Fasciclin II, which stains only the longitudinal axons and the motor axons (Schindelholz et al., 2001; Sun et al., 2000). *Ptp10D*, *Ptp99A*, and *Dlar* mutants enhance the Ptp69D mutant phenotype, and in triple or quadruple mutants most longitudinal axons can be seen crossing the midline (Sun et al., 2000). *Ptp10D* and *Ptp69D* mutations enhance the *Ptp52F* CNS defects, but *Dlar* suppresses them (Schindelholz et al., 2001). These interactions suggest that the interplay between the RPTPs in Drosophila is likely to be complex, and they may act synergistically or antagonistically depending on the context.

Some progress has been made in teasing apart the pathways downstream of Dlar in embryonic axon guidance (Figure 6). Wills, et al. found that *Dlar* and *Abl* have an antagonistic genetic relationship in axon guidance (Wills et al., 1999a). Overexpression of wildtype Abl, but not kinase-dead Abl, in neurons caused an ISNb bypass phenotype similar to that found in Dlar mutant embryos. Reduction of *Abl* dosage by half suppressed the Dlar mutant ISNb bypass phenotype, and increasing the dosage of Dlar suppressed the ISNb bypass phenotype caused by Abl overexpression. Furthermore, in the CNS of *Abl* mutants some longitudinal axons cross the midline, a phenotype that is suppressed by removing *Dlar* (Wills et al., 2002). *Enabled* (*ena*) was originally identified as a suppressor of *Abl* mutant lethality and a subtrate of Abl kinase activity (Gertler et al., 1995; Gertler et al., 1990). Studies of the mouse homolog of ena, Mena, in mouse fibroblasts demonstrated that ena promotes F-actin extension by blocking binding of capping protein, which inhibits F-actin extension (Bear et al., 2002; Gertler et al., 1996). As would be expected from *Abl's* genetic relationships with *Dlar* and *ena*, *ena* mutants phenocopy *Dlar* loss of function and Abl overexpression in having an ISNb bypass phenotype (Wills et al., 1999a). The second phosphatase domain of Dlar, but not the first phosphatase domain, specifically binds both Abl and ena in vitro, and Abl specifically phosphorylates the second phosphatase domain (Wills et al., 1999a). Dlar was also capable of dephosphorylating Abl and ena in vitro, but the specificity of this dephosphorylation was not demonstrated, and tyrosine phosphatases have been shown to be rather promiscuous in vitro. Collectively these data suggest a model where Abl and Dlar have antagonistic effects on the phosphorylation state of ena, which

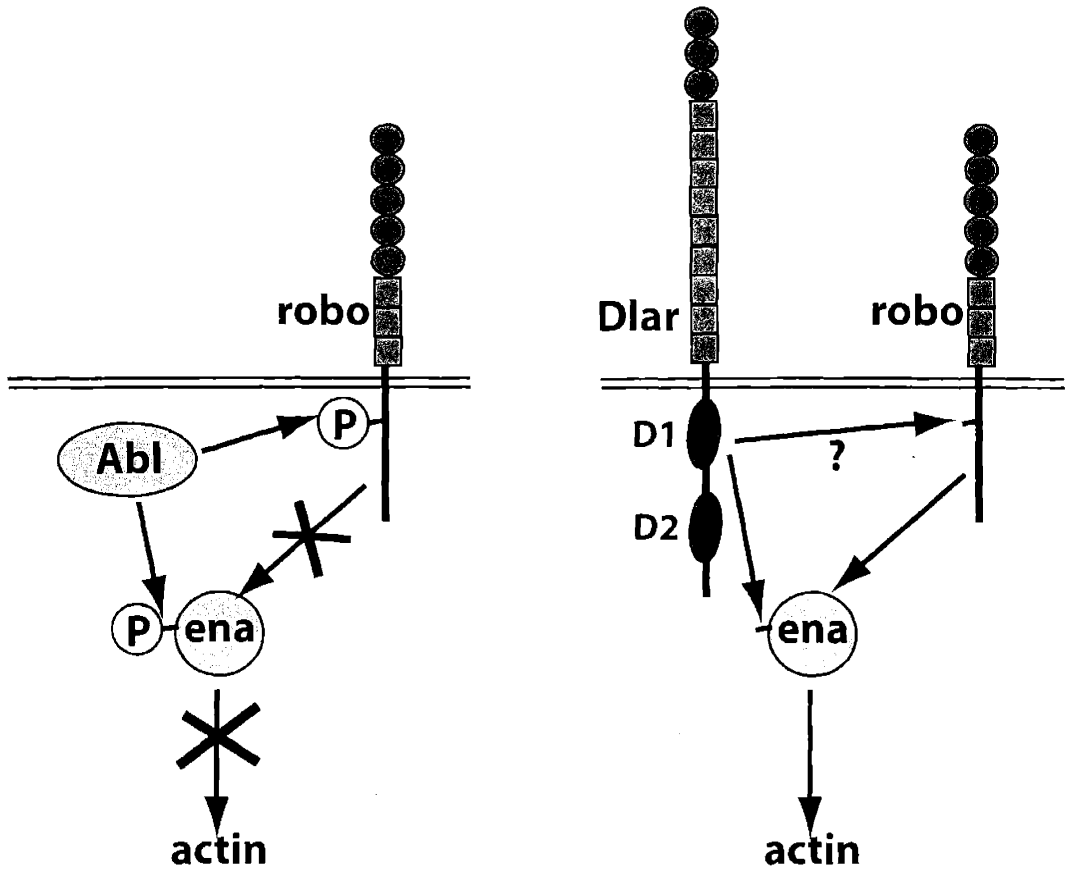

Figure 6. Dlar and Abl have antagonistic effects on ena and possibly robo. Ena and robo are activated by dephosphorylation. Details may be found in the text.

in its dephosphorylated state promotes axon extension and may allow axons within ISNb to defasciculate from the main nerve.

Ena also functions downstream of the repulsive axon guidance receptor robo, which functions to repel axons from the embryonic CNS midline (Figure 6). Mutation of *ena* or overexpression of Abl enhances robo and slit midline crossing phenotypes in a dose dependent fashion, and *Abl* loss of function suppresses the *robo* and *slit* midline crossing phenotypes (Bashaw et al., 2000). In addition to downregulating ena, Abl also appears to be capable of downregulating robo through phosphorylation. Interestingly, *Ptp10D* and *Ptp69D* loss of function enhances the *robo* and *slit* loss of function midline crossing phenotype (Sun et al., 2000). The commissureless (comm) protein functions to downregulate robo in axons crossing the midline, and *comm* loss of function ablates normal midline crossing. *Ptp10D* and *Ptp69D* loss of function partially suppress the *comm* mutant phenotype. Together these data suggest that RPTPs positively regulate robo activity, and that they may positively regulate ena activity both directly and indirectly through robo. Alternatively, robo may act as a scaffolding protein to bring RPTPs and ena together. The biochemical relationship between robo and RPTPs needs to be further investigated.

The intracellular domain of mammalian LAR was found to bind Trio in a yeast two-hybrid interaction trap (Debant et al., 1996). Trio is a GEF for the small GTPases Rac and Rho, and also has a kinase domain that is most similar to the calcium/calmodulin-dependent kinases. In *Drosophila* embryos, mutation of *trio* causes ISNb axons to stall before reaching their targets (Bateman et al., 2000), a phenotype that is also found in *Abl* mutants (Wills et al., 1999b), However, reducing the genetic dosage of *trio* by half enhanced the *Dlar* mutant ISNb bypass phenotype (Bateman et al., 2000). It is possible that trio plays a Dlar-independent role early in axon outgrowth, and later is required downstream of Dlar for axons to grow out away from the ISNb fascicle. Alteration of Rac activity, which putatively is activated by trio, also affects ISNb guidance (Kaufmann et al., 1998). Expression of dominant active RacV12 causes ISNb to stall before reaching its targets, and expression of dominant negative RacN17 causes an ISNb bypass phenotype. Reducing *Dlar* genetic dosage by half moderately enhances the RacN17 ISNb bypass phenotype, and RacN17 expression strongly enhances the *Dlar* mutant phenotype. Thus, in addition to its regulation of ena, Dlar may also promote axon outgrowth and turning by

activating trio, which in turn activates Rac, which leads to actin cytoskeletal rearrangement and extension.

Drosophila Ptp10D binds and dephosphorylates a cell adhesion molecule-like protein, gp150, in cultured cells. gp150 is phosphorylated by Src and forms a complex with Src and another as-yet unidentified 40 kD protein (Fashena and Zinn, 1997). Gp150 has been shown to be required for downregulation of Notch during eye development and refinement of photoreceptor specification (Fetchko et al., 2002; Li et al., 2003), but a role in axon guidance or an in vivo relationship with Ptp10D has not been demonstrated.

RPTPs Regulate Adherens Junctions

Several mammalian RPTPs have been implicated in the regulation of adherens junctions through modulation of cadherin/catenin complexes (Figure 7). Cadherins are homophilic receptors that tether cells to one another when their intracellular domains are bound to catenins (Nelson and Nusse, 2004). The intracellular domains of cadherins bind κ-catenin, which binds κ-catenin, which tethers the complex to the actin cytoskeleton. Tyrosine phosphorylation of κ-catenin disrupts its binding to both cadherin and κ-catenin, thereby disrupting the adherens junction. Release of κ-catenin into the cytoplasm has been correlated with increased cell migration (Hollande et al., 2001; Liu et al., 1997; Muller et al., 1999), although increased adherens junction formation may also be positively correlated with axon outgrowth. PTPμ binds both cadherins and catenins (Brady-Kalnay et al., 1995), and axon outgrowth on a substrate of N-cadherin requires PTPμ (Burden-Gulley and Brady-Kalnay, 1999). PTPκ has also been shown to bind and dephosphorylate κ-catenin (Fuchs et al., 1996), suggesting a role for PTPκ in increasing adherens junction stability. PTPκ/RPTPκ also binds and dephosphorylates κ-catenin, but interaction of PTPκ/RPTPκ with its ligand pleiotrophin inhibits its activity and leads to increased κ-catenin phosphorylation (Meng et al., 2000). Drosophila N-cadherin (Ncad) mutants phenocopy Dlar mutants in photoreceptor axon guidance. In both mutants, photoreceptor R7 axons fail to target to the appropriate layer of the medulla in the optic lobe of the brain, and late events in R1-R6 axon targeting fail to occur (Lee et al., 2001; Maurel-Zaffran et al., 2001). Mammalian LAR associates with and dephosphorylates κ-catenin, and overexpression of LAR inhibits epithelial cell migration (Muller et al., 1999), suggesting that LAR may regulate adherens junction stability, the balance of which is important for migration. It will be interesting

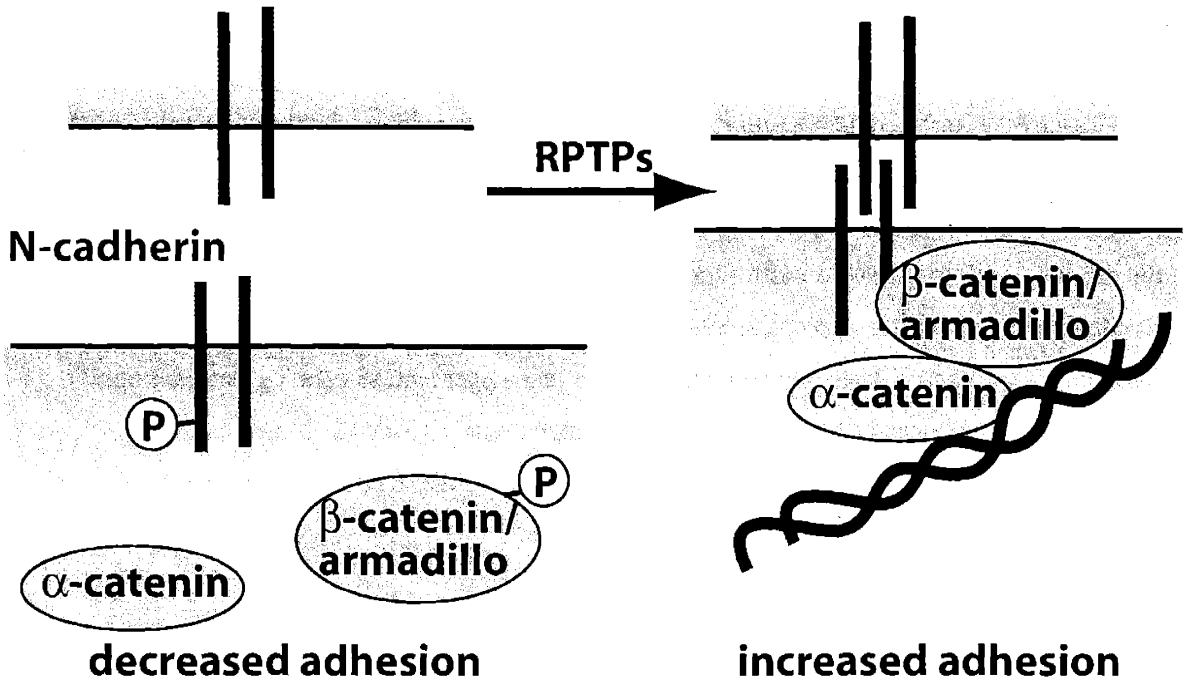

Figure 7. Dephosphorylation of N-cadherin or β-catenin by RPTPs can lead to increased adherens junction formation.

to see whether Ncad, the Drosophila κ-catenin homolog armadillo, and Dlar interact during axon guidance in the Drosophila embryo or in the developing visual system.

PTPμ was found to bind RACK1 (Receptor for activated Protein C Kinase) in a two-hybrid interaction trap (Mourton et al., 2001). RACK1 is thought to be a scaffolding protein that activates PKC signaling pathways. In fact, PTPμ, RACK1, and PKCκ all bind to one another in retinal cells (Rosdahl et al., 2002), and RACK1 is recruited to points of cell-cell contact by PTPμ (Mourton et al., 2001). Furthermore, pharmacological inhibition of PKC inhibited RGC neurite outgrowth on PTPμ. These data suggest a pathway in which PTPμ leads to axon outgrowth by recruiting RACK1 and PKCκ to points of cell-cell contact. RACK1 also binds and is phosphorylated by Src tyrosine kinase (Chang et al., 2002). RACK1 binding to PTPμ or Src appears to be mutually exclusive, as expression of constitutively active v-Src prevented RACK-PTPμ binding (Mourton et al., 2001). When PTPμ is added to neurites exogenously, it causes the growth cones to take on a more filopodial morphology, with a very small lamellipodium. Rosdahl, et al. found that expression of dominant negative Cdc42N17, but not dominant-negative Rac, prevented this PTPμ-dependent growth cone rearrangement, suggesting that homophilic binding of PTPμ causes actin cytoskelectal rearrangements via Cdc42. It has not been determined whether Cdc42 acts in the same pathway or a different pathway from RACK1 and PKCκ.

PTP-alpha in cell migration and neurite outgrowth

PTPκ is abundantly expressed in neural tissue and has recently been shown to be involved in both neuronal migration in vivo and neurite outgrowth in vitro. In PTPκ$^{-/-}$ knock-out mice, the radial migration of pyramidal neurons in the hippocampus is defective (Petrone et al., 2003). However, the authors of this study postulate that this defect is likely to be cell non-autonomous, resulting from a primary defect in radial glia. In cultured cells, PTPκ dephosphorylates the inhibitory phosphotyrosine in the C-terminal tail of Src family kinases. This has an activating effect on Src family kinases, and in fact overexpression of PTPκ does activate Src and Fyn (Bhandari et al., 1998; Harder et al., 1998; Zheng et al., 2000), and loss of PTPκ results in decreased Src and Fyn activity (Ponniah et al., 1999). Activated Src is capable of phosphorylating a number of proteins, including FAK, p130^{Cas}, and Sin (Honda et al., 1998; O'Neill et al., 2000). Phosphorylation of Sin creates binding sites for the adaptor proteins Crk

and Nck (Yang et al., 2002). Expression of wild type PTPκ in PC12 cells resulted in neurite outgrowth in response to the epidermal growth factor (EGF) (Yang et al., 2002). This response was dependent on Src activity, and was also dependent on physical association between Sin and Crk. Crk has been shown to participate in the DOCK180-dependent activation of Rac (Reddien and Horvitz, 2000), although it is unknown whether Rac is required for neurite outgrowth in the pathway described here. Thus, PTPκ serves to activate Src family kinases, enabling them to participate in growth factor-initiated pathways leading to neurite outgrowth. PTPκ-dependent activation of Src also leads to changes in focal adhesions. PTPκ localizes to focal adhesions (Lammers et al., 2000), and cells overexpressing PTPκ display increased adhesiveness to a fibronectin substrate (Harder et al., 1998). MEFs lacking PTPκ fail to generate lamellipodial or filopodial protrusions, and are defective in both a wound healing migration assay and in haptotactic migration on fibronectin (Zeng et al., 2003). In these cells, FAK phosphorylation on Src SH2 binding site Y397 is severely diminished, as is Src-FAK binding. Fyn completely fails to bind FAK in PTPκ$^{-/-}$ MEFs. Interestingly, wild type MEFs treated with the Src inhibitor PP2 are phenotypically identical to MEFs lacking PTPκ, suggesting that the primary and possibly only role of PTPκ in cell migration and neurite outgrowth is to dephosphorylate and activate Src.

CD45

CD45, a receptor tyrosine phosphatase abundantly expressed in T cells, also activates Src family kinases through dephosphorylation of the inhibitory C-terminal phosphotyrosine. CD45 has clearly been shown to participate in T cell receptor (TCR) signaling through dephosphorylation of Y505 of the Src family kinase Lck, thus maintaining Lck in an activated state capable of phosphorylating the TCR (Alexander, 2000). However, CD45 is also capable of dephosphorylating a positive regulatory tyrosine in the active site loop of Src family kinases. In macrophages, CD45 colocalizes with integrins and Src family kinases to sites of focal contact (Roach et al., 1997). Both macrophages and T lymphocytes adhere more strongly to their substrates in CD45$^{-/-}$ cell lines than in their wild type counterparts, an effect which is dependent on integrins (Roach et al., 1997; Shenoi et al., 1999). This would suggest a role for CD45 in regulating the formation and/or turnover of focal adhesions, a process that is regulated in large part by Src kinases, as described above. In fact, in CD45$^{-/-}$ macrophages the activity of Src family kinases Hck and Lyn is increased as a result of increased phosphorylation on the active

site tyrosine (Roach et al., 1997). This would suggest that while activation of Src family kinases by CD45-mediated dephosphorylation of the C-terminal inhibitory residue is important for TCR signaling, CD45 is more important for dephosphorylation of the active site residue and therefore inhibition of Src family kinases in cell adhesion and possibly migration. Further support for this hypothesis came from studies of $CD45^{-/-}$ T lymphocytes. Li, et al. found that cells lacking CD45, but not wild type cells, spread out when plated on dishes coated with antibody against CD44, a cell adhesion molecule that binds hyaluronan, a component of the extracellular matrix (Li et al., 2001). The total phosphorylation levels of Lck and Fyn were higher in $CD45^{-/-}$ cells than in non-mutant cells. Although the authors of this study did not test the activity of Lck and Fyn in $CD45^{-/-}$ cells, they did find that treatment with PP2 prevented the $CD45^{-/-}$ cells from spreading out on CD44 antibody. This strongly suggests that the increased spreading in cells lacking CD45 is a result of increased Src family kinase activity, which in turn is a result of hyperphosphorylation of the Src active site tyrosine. Furthermore, Pyk2 and FAK, which regulate focal adhesions and are Src kinase substrates, were hyperphosphorylated in $CD45^{-/-}$ T cells. The downregulation of focal adhesions through CD45-mediated Src inhibition is likely to be important for cell migration. In fact, T cell-derived Jurkat cells lacking CD45 were unable to migrate toward the chemokine CXCL12 (Fernandis et al., 2003), and antibody-mediated inhibition of CD45 blocked chemotaxis in neutrophils (Harvath et al., 1991).

Concluding Remarks

In summary, RPTPs play a variety of roles in chemotaxis. They are involved in axon outgrowth and guidance and cell migration, through modulation of the actin cytoskeleton and remodeling of cell-cell and cell-substrate contacts. Genetic studies in the Drosophila embryo have yielded great insight into how RPTPs contribute to the control of axon guidance through interactions with Abl, its kinase substrate ena, and the axon guidance receptor robo, molecules that are primarily involved in altering the actin cytoskeleton. It will be interesting to see the extent to which RPTPs, ena, and robo interact with one another and whether robo's interaction with ena is dependent on RPTPs. Mammalian RPTPs have also been shown to be involved in axon outgrowth, although whether or not they are involved in axon guidance is unclear. However, unlike the Drosophila RPTPs, what is known to date about mammalian RPTPs points toward roles in modulating focal adhesions and adherens junctions. The proper balance of

adhesion is important for both cell migration and axon guidance: too much adhesion and the cell or growth cone cannot move forward; too little adhesion and the cell or growth cone does not have enough traction to maintain forward progress. Unlike Dlar, Ptp69D seems to be primarily involved in defasciculation and deadhesion. It will be interesting to see whether, like the mammalian RPTPs, Ptp69D regulates focal adhesions or adherens junctions.

COMPARISON OF PDGFR AND RPTP SIGNALING

While PDGFRs and RPTPs are opposite in their catalytic function, they do not necessarily have opposite functions in cellular signaling pathways. Both are important in chemotaxis, although PDGFRs are primarily used for cell migration and RPTPs are primarily used in axon outgrowth and guidance. Both types of receptors can effect changes in the actin cytoskeleton as well as changes in adhesion, both of which are important in cell or growth cone navigation. Specifically activation of Rac is likely to be used to effect changes in the actin cytoskeleton downstream of both LAR phosphatases and the PDGFR. However, the pathways used to activate Rac are different between the two. Rac activation downstream of PDGFR is mediated primarily by PI3K, while trio is likely to mediate Rac activation downstream of LAR phosphatases. Interestingly, Src tyrosine kinases can be activated by both PDGFRs and RPTPs. The autoinhibition mediated by the C-terminal phosphotyrosine on Src can be relieved either through the binding of the Src SH2 domian to PDGFR or through dephosphorylation of the C-terminal phosphotyrosine. Activation of Src by either method is likely to result in the same outputs, namely activation of FAK and modulation of focal adhesion complexes. It is possible that RPTPs cooperate with PDGFR to activate Src. It would be interesting to examine whether PTPκ or CD45 have an effect on chemotaxis of cells toward PDGF. There may be further similarities and interplay between these two classes of receptors that have not yet been discovered, as the downstream signaling pathways for both are far from complete.

DISSECTION OF PDGFR AND RPTP SIGNALING

In my work I have sought to understand the signaling pathways regulated by Pvr and Ptp69D in cell migration and axon guidance. I took two general approaches to identify other molecules involved in these signaling pathways. The first was a genetic approach, in which I sought to identify genes that were required for a given process in conjunction with Ptp69D or Pvr. With Ptp69D, I used a dominant negative form of Ptp69D that disrupted photoreceptor axon targeting in a similar fashion to the *Ptp69D* loss of function. I used the dominant negative as a sensitized genetic background to then identify genes that could enhance or suppress the axon mistargeting phenotype when mutated. Taking this approach I was able to identify several candidate modifiers of the *Ptp69D* phenotype from a collection of genes that seemed like reasonable candidates based on their functions in actin regulation or cell adhesion. The strength of this approach came from the fact that any modifiers were likely to be involved in photoreceptor axon targeting. In addition, looking for mutant effects in the sensitized background caused by Ptp69D dominant negative allowed us to identify genes that may be involved in axon targeting but may not have been identified in a straightforward screen for photoreceptor axon targeting mutants. For example, *Src64* enhanced the *Ptp69D* shoot-through phenotype, but photoreceptor axons mutant for *Src64* target normally. Conversely, mutants in *Egfr* or *Ras* suppress the Ptp69D dominant negative phenotype, but these genes are required for eye development and so an axon guidance phenotype would have been impossible to detect in mutant clones of these genes. This approach, however, has limitations. Since many pathways converge and intersect to give an output such as proper axon targeting, genes that appeared to interact with *Ptp69D* could be upstream or downstream of Ptp69D or in a parallel pathway with a common factor downstream. Genes that control expression of the Ptp69D dominant negative transgene would artifactually appear to genetically interact with *Ptp69D* as well. Additionally, since I was dealing with only partial loss-of-function in each gene, it was impossible to establish epistatic relationships. Using the genetic approach alone, I could not determine the nature of the relationship between *Ptp69D* and its interactors. Similarly, I used RNA interference to test whether potential Pvr interactors had loss-of-function phenotypes similar to *Pvr* mutants in hemocyte migration or MAPK activation. Having a similar phenotype would suggest that the

potential interactor was involved in that process, but it could be in the same pathway as Pvr or in a parallel pathway.

The second approach I took to identify proteins involved in signaling with Ptp69D and Pvr was to identify proteins that physically bind to either of these molecules. This approach has the opposite advantages and disadvantages of the genetic approach. Whereas with the genetic approach alone, the nature of the interaction is difficult or impossible to ascertain, with a biochemical approach, the only proteins identified are ones that physically bind, and therefore are potentially directly connected to the protein of interest. With Ptp69D, I sought to identify proteins from *Drosophila* cultured cell lysates that bound to a substrate-trapping form of the phosphatase. Any protein identified was likely to be a substrate of Ptp69D phosphatase activity. With Pvr, I used a yeast two-hybrid approach to identify proteins that bind the intracellular domain of Pvr. Both of these were unbiased screens, having an advantage over the biased genetic screens because unexpected binding proteins could be identified and weak interactions would not necessarily be identified. However, both screens were also done in artificial systems. Whether the proteins that were found to bind Ptp69D *in vitro* or Pvr in yeast actually bind those proteins in photoreceptor axons or hemocytes respectively is unknown. Whether those proteins are also required for axon targeting or hemocyte migration was also unknown.

In the case of Ptp69D, the genetic approach and the biochemical approach yielded non-overlapping sets of genes and proteins. It is possible that in an unbiased genetic screen for *Ptp69D* interactors, I might have identified some of the genes encoding the proteins that physically bind Ptp69D. However, in the case of Pvr, only one of 15 proteins found to physically bind Pvr displayed a genetic requirement similar to Pvr. What is the cause of this discrepancy? The signaling pathways involved in cell movement are rather complex, and perhaps should be called "signal transduction webs" rather than "signal transduction cascades." While in some cases the pathways used to relay signals for cell fate decisions can be fairly simple and linear, the pathways used for cell movement can be fairly complex. For example, the sevenless pathway, used to determine the fate of photoreceptor R7, consists primarily of a single pathway starting with activation of the sevenless receptor by its ligand, boss. Without sevenless activity the process of specification completely fails. This may be because the failure to turn on the appropriate set of genes causes R7 precursors to take another developmental path. There appears to be a single key target of sevenless in this process, the MAP kinase cascade, whose

activation largely suffices to trigger the specification of R7 neuron. This single pathway can be used to determine the fate of the R7 because it maintains a fixed positional relationship with its neighboring cells, and its environment does not change with time. Migrating cells and navigating axons face much more complex choices. Because migrating cells and navigating axons are constantly changing their position within the organism, they must have the capability to dynamically respond to cues in their environment in order to accurately navigate their path. Unlike cell fate determination, this is not just a matter of turning on a pathway that is off, but rather one of providing spatial regulation of cytoskeletal pathways that are already working to promote navigation of the axon. A plethora of extracellular signaling cues are integrated by webs of interacting and overlapping signal transduction cascades that in turn regulate the activity of a diverse array of cytoskeletal regulatory proteins. Thus, there may be less reliance on a single switch to make a decision. This complex process is shared by many cell types; cells with vastly different fates and morphologies and positions within the organism must undergo the same process of migration or guidance, although each must respond to the cues in its environment in a unique way. Organisms have adapted to the complexity of this problem by using just a few molecules, which through different levels of expression or different subcellular localization can interact with one another in a combinatorial fashion, depending on the cell type and the changing position of the cell or growth cone within the organism. It is for this reason that the signaling pathways involved in cell movement have been relatively difficult to tease apart. Because the signaling systems have been designed to be adaptable to a changing environment, the cell is capable of compensating for the removal of a single signaling component by upregulating or downregulating another component. Additionally, the exact pathways used within a given cell are likely to change given its position within the organism. During photoreceptor axon targeting, for example, many pathways are likely to intersect and converge to give the output of certain axons stopping at certain layers (Araujo and Tear, 2003). Ptp69D and the other receptor tyrosine phosphatases, given their redundancy and their ability to functionally replace one another, are likely to be modulators of these various pathways, rather than predominantly exerting their effects through a single pathway in growth cone navigation. Members of these various pathways could be found to genetically interact with *Ptp69D* without actually having a direct physical interaction. Conversely, it is possible that even the genes encoding proteins that directly associate with Ptp69D *in vivo* would fail to act as genetic modifiers of the Ptp69D phenotype

either because their loss is moot in the absence of Ptp69D function or because other proteins in the complex web of signal transduction are able to take their place.

REFERENCES

Alderton, F., Rakhit, S., Kong, K. C., Palmer, T., Sambi, B., Pyne, S., and Pyne, N. J. (2001). Tethering of the platelet-derived growth factor beta receptor to G-protein-coupled receptors. A novel platform for integrative signaling by these receptor classes in mammalian cells. J Biol Chem *276*, 28578-28585.

Alexander, D. R. (2000). The CD45 tyrosine phosphatase: a positive and negative regulator of immune cell function. Semin Immunol *12*, 349-359.

Anand-Apte, B., Zetter, B. R., Viswanathan, A., Qiu, R. G., Chen, J., Ruggieri, R., and Symons, M. (1997). Platelet-derived growth factor and fibronectin-stimulated migration are differentially regulated by the Rac and extracellular signal-regulated kinase pathways. J Biol Chem *272*, 30688-30692.

Araujo, S. J., and Tear, G. (2003). Axon guidance mechanisms and molecules: lessons from invertebrates. Nat Rev Neurosci *4*, 910-922.

Armstrong, P. B. (1985). The control of cell motility during embryogenesis. Cancer Metastasis Rev *4*, 59-79.

Bagri, A., Gurney, T., He, X., Zou, Y. R., Littman, D. R., Tessier-Lavigne, M., and Pleasure, S. J. (2002). The chemokine SDF1 regulates migration of dentate granule cells. Development *129*, 4249-4260.

Baker, M. W., Rauth, S. J., and Macagno, E. R. (2000). Possible role of the receptor protein tyrosine phosphatase HmLAR2 in interbranch repulsion in a leech embryonic cell. J Neurobiol *45*, 47-60.

Bashaw, G. J., Kidd, T., Murray, D., Pawson, T., and Goodman, C. S. (2000). Repulsive axon guidance: Abelson and Enabled play opposing roles downstream of the roundabout receptor. Cell *101*, 703-715.

Bateman, J., Shu, H., and Van Vactor, D. (2000). The guanine nucleotide exchange factor trio mediates axonal development in the Drosophila embryo. Neuron *26*, 93-106.

Baxter, R. M., Secrist, J. P., Vaillancourt, R. R., and Kazlauskas, A. (1998). Full activation of the platelet-derived growth factor beta-receptor kinase involves multiple events. J Biol Chem *273*, 17050-17055.

Bear, J. E., Svitkina, T. M., Krause, M., Schafer, D. A., Loureiro, J. J., Strasser, G. A., Maly, I. V., Chaga, O. Y., Cooper, J. A., Borisy, G. G., and Gertler, F. B. (2002). Antagonism between Ena/VASP proteins and actin filament capping regulates fibroblast motility. Cell *109*, 509-521.

Bhandari, V., Lim, K. L., and Pallen, C. J. (1998). Physical and functional interactions between receptor-like protein-tyrosine phosphatase alpha and p59fyn. J Biol Chem *273*, 8691-8698.

Bilwes, A. M., den Hertog, J., Hunter, T., and Noel, J. P. (1996). Structural basis for inhibition of receptor protein-tyrosine phosphatase-alpha by dimerization. Nature *382*, 555-559.

Bodden, K., and Bixby, J. L. (1996). CRYP-2: a receptor-type tyrosine phosphatase selectively expressed by developing vertebrate neurons. J Neurobiol *31*, 309-324.

Brady-Kalnay, S. M., Rimm, D. L., and Tonks, N. K. (1995). Receptor protein tyrosine phosphatase PTPmu associates with cadherins and catenins in vivo. J Cell Biol *130*, 977-986.

Brady-Kalnay, S. M., and Tonks, N. K. (1994). Identification of the homophilic binding site of the receptor protein tyrosine phosphatase PTP mu. J Biol Chem *269*, 28472-28477.

Brady-Kalnay, S. M., and Tonks, N. K. (1995). Protein tyrosine phosphatases as adhesion receptors. Curr Opin Cell Biol *7*, 650-657.

Burden-Gulley, S. M., and Brady-Kalnay, S. M. (1999). PTPmu regulates N-cadherin-dependent neurite outgrowth. J Cell Biol *144*, 1323-1336.

Campbell, M., Allen, W. E., Silversides, J. A., and Trimble, E. R. (2003). Glucose-induced phosphatidylinositol 3-kinase and mitogen-activated protein kinase-dependent upregulation of the platelet-derived growth factor-beta receptor potentiates vascular smooth muscle cell chemotaxis. Diabetes *52*, 519-526.

Carlin, S. M., Roth, M., and Black, J. L. (2003). Urokinase potentiates PDGF-induced chemotaxis of human airway smooth muscle cells. Am J Physiol Lung Cell Mol Physiol *284*, L1020-1026.

Chang, B. Y., Harte, R. A., and Cartwright, C. A. (2002). RACK1: a novel substrate for the Src protein-tyrosine kinase. Oncogene *21*, 7619-7629.

Chen, H. C., Appeddu, P. A., Parsons, J. T., Hildebrand, J. D., Schaller, M. D., and Guan, J. L. (1995). Interaction of focal adhesion kinase with cytoskeletal protein talin. J Biol Chem *270*, 16995-16999.

Cho, N. K., Keyes, L., Johnson, E., Heller, J., Ryner, L., Karim, F., and Krasnow, M. A. (2002). Developmental control of blood cell migration by the Drosophila VEGF pathway. Cell *108*, 865-876.

Debant, A., Serra-Pages, C., Seipel, K., O'Brien, S., Tang, M., Park, S. H., and Streuli, M. (1996). The multidomain protein Trio binds the LAR transmembrane tyrosine phosphatase, contains a protein kinase domain, and has separate rac-specific and rho-specific guanine nucleotide exchange factor domains. Proc Natl Acad Sci U S A *93*, 5466-5471.

Delaire, S., Billard, C., Tordjman, R., Chedotal, A., Elhabazi, A., Bensussan, A., and Boumsell, L. (2001). Biological activity of soluble CD100. II. Soluble CD100, similarly to H-SemaIII, inhibits immune cell migration. J Immunol *166*, 4348-4354.

DeMali, K. A., Godwin, S. L., Soltoff, S. P., and Kazlauskas, A. (1999). Multiple roles for Src in a PDGF-stimulated cell. Exp Cell Res *253*, 271-279.

DeMali, K. A., and Kazlauskas, A. (1998). Activation of Src family members is not required for the platelet-derived growth factor beta receptor to initiate mitogenesis. Mol Cell Biol *18*, 2014-2022.

Derman, M. P., Toker, A., Hartwig, J. H., Spokes, K., Falck, J. R., Chen, C. S., Cantley, L. C., and Cantley, L. G. (1997). The lipid products of phosphoinositide 3-kinase increase cell motility through protein kinase C. J Biol Chem *272*, 6465-6470.

Desai, C. J., Gindhart, J. G., Jr., Goldstein, L. S., and Zinn, K. (1996). Receptor tyrosine phosphatases are required for motor axon guidance in the Drosophila embryo. Cell *84*, 599-609.

Desai, C. J., Krueger, N. X., Saito, H., and Zinn, K. (1997). Competition and cooperation among receptor tyrosine phosphatases control motoneuron growth cone guidance in Drosophila. Development *124*, 1941-1952.

Drosopoulos, N. E., Walsh, F. S., and Doherty, P. (1999). A soluble version of the receptor-like protein tyrosine phosphatase kappa stimulates neurite outgrowth via a Grb2/MEK1-dependent signaling cascade. Mol Cell Neurosci *13*, 441-449.

Duchek, P., Somogyi, K., Jekely, G., Beccari, S., and Rorth, P. (2001). Guidance of cell migration by the Drosophila PDGF/VEGF receptor. Cell *107*, 17-26.

Elchebly, M., Wagner, J., Kennedy, T. E., Lanctot, C., Michaliszyn, E., Itie, A., Drouin, J., and Tremblay, M. L. (1999). Neuroendocrine dysplasia in mice lacking protein tyrosine phosphatase sigma. Nat Genet *21*, 330-333.

Fashena, S. J., and Zinn, K. (1997). Transmembrane glycoprotein gp150 is a substrate for receptor tyrosine phosphatase DPTP10D in Drosophila cells. Mol Cell Biol *17*, 6859-6867.

Fernandis, A. Z., Cherla, R. P., and Ganju, R. K. (2003). Differential regulation of CXCR4-mediated T-cell chemotaxis and mitogen-activated protein kinase activation by the membrane tyrosine phosphatase, CD45. J Biol Chem *278*, 9536-9543.

Fetchko, M., Huang, W., Li, Y., and Lai, Z. C. (2002). Drosophila Gp150 is required for early ommatidial development through modulation of Notch signaling. Embo J *21*, 1074-1083.

Fuchs, M., Muller, T., Lerch, M. M., and Ullrich, A. (1996). Association of human protein-tyrosine phosphatase kappa with members of the armadillo family. J Biol Chem *271*, 16712-16719.

Fukata, M., Nakagawa, M., and Kaibuchi, K. (2003). Roles of Rho-family GTPases in cell polarisation and directional migration. Curr Opin Cell Biol *15*, 590-597.

Garrity, P. A., Lee, C. H., Salecker, I., Robertson, H. C., Desai, C. J., Zinn, K., and Zipursky, S. L. (1999). Retinal axon target selection in Drosophila is regulated by a receptor protein tyrosine phosphatase. Neuron *22*, 707-717.

Gebbink, M. F., Zondag, G. C., Wubbolts, R. W., Beijersbergen, R. L., van Etten, I., and Moolenaar, W. H. (1993). Cell-cell adhesion mediated by a receptor-like protein tyrosine phosphatase. J Biol Chem *268*, 16101-16104.

Gelderloos, J. A., Rosenkranz, S., Bazenet, C., and Kazlauskas, A. (1998). A role for Src in signal relay by the platelet-derived growth factor alpha receptor. J Biol Chem *273*, 5908-5915.

Gershon, T. R., Baker, M. W., Nitabach, M., and Macagno, E. R. (1998). The leech receptor protein tyrosine phosphatase HmLAR2 is concentrated in growth cones and is involved in process outgrowth. Development *125*, 1183-1190.

Gertler, F. B., Comer, A. R., Juang, J. L., Ahern, S. M., Clark, M. J., Liebl, E. C., and Hoffmann, F. M. (1995). enabled, a dosage-sensitive suppressor of mutations in the Drosophila Abl tyrosine kinase, encodes an Abl substrate with SH3 domain-binding properties. Genes Dev *9*, 521-533.

Gertler, F. B., Doctor, J. S., and Hoffmann, F. M. (1990). Genetic suppression of mutations in the Drosophila abl proto-oncogene homolog. Science *248*, 857-860.

Gertler, F. B., Niebuhr, K., Reinhard, M., Wehland, J., and Soriano, P. (1996). Mena, a relative of VASP and Drosophila Enabled, is implicated in the control of microfilament dynamics. Cell *87*, 227-239.

Gillitzer, R., and Goebeler, M. (2001). Chemokines in cutaneous wound healing. J Leukoc Biol *69*, 513-521.

Grimsley, C. M., Kinchen, J. M., Tosello-Trampont, A. C., Brugnera, E., Haney, L. B., Lu, M., Chen, Q., Klingele, D., Hengartner, M. O., and Ravichandran, K. S. (2004). Dock180 and ELMO1 proteins cooperate to promote evolutionarily conserved Rac-dependent cell migration. J Biol Chem *279*, 6087-6097.

Guan, K. L., and Rao, Y. (2003). Signalling mechanisms mediating neuronal responses to guidance cues. Nat Rev Neurosci *4*, 941-956.

Hansen, K., Johnell, M., Siegbahn, A., Rorsman, C., Engstrom, U., Wernstedt, C., Heldin, C. H., and Ronnstrand, L. (1996). Mutation of a Src phosphorylation site in the PDGF beta-receptor leads to increased PDGF-stimulated chemotaxis but decreased mitogenesis. Embo J *15*, 5299-5313.

Harder, K. W., Moller, N. P., Peacock, J. W., and Jirik, F. R. (1998). Protein-tyrosine phosphatase alpha regulates Src family kinases and alters cell-substratum adhesion. J Biol Chem *273*, 31890-31900.

Harvath, L., Balke, J. A., Christiansen, N. P., Russell, A. A., and Skubitz, K. M. (1991). Selected antibodies to leukocyte common antigen (CD45) inhibit human neutrophil chemotaxis. J Immunol *146*, 949-957.

Hauck, C. R., Hsia, D. A., and Schlaepfer, D. D. (2000). Focal adhesion kinase facilitates platelet-derived growth factor-BB-stimulated ERK2 activation required for chemotaxis migration of vascular smooth muscle cells. J Biol Chem *275*, 41092-41099.

Hawkins, P. T., Eguinoa, A., Qiu, R. G., Stokoe, D., Cooke, F. T., Walters, R., Wennstrom, S., Claesson-Welsh, L., Evans, T., Symons, M., and et al. (1995). PDGF stimulates an increase in GTP-Rac via activation of phosphoinositide 3-kinase. Curr Biol *5*, 393-403.

Haworth, K., Shu, K. K., Stokes, A., Morris, R., and Stoker, A. (1998). The expression of receptor tyrosine phosphatases is responsive to sciatic nerve crush. Mol Cell Neurosci *12*, 93-104.

Hellstrom, M., Kalen, M., Lindahl, P., Abramsson, A., and Betsholtz, C. (1999). Role of PDGF-B and PDGFR-beta in recruitment of vascular smooth muscle cells and pericytes during embryonic blood vessel formation in the mouse. Development *126*, 3047-3055.

Hobson, J. P., Rosenfeldt, H. M., Barak, L. S., Olivera, A., Poulton, S., Caron, M. G., Milstien, S., and Spiegel, S. (2001). Role of the sphingosine-1-phosphate receptor EDG-1 in PDGF-induced cell motility. Science *291*, 1800-1803.

Hoffmann, K. M., Tonks, N. K., and Barford, D. (1997). The crystal structure of domain 1 of receptor protein-tyrosine phosphatase mu. J Biol Chem *272*, 27505-27508.

Hollande, F., Choquet, A., Blanc, E. M., Lee, D. J., Bali, J. P., and Baldwin, G. S. (2001). Involvement of phosphatidylinositol 3-kinase and mitogen-activated protein kinases in glycine-extended gastrin-induced dissociation and migration of gastric epithelial cells. J Biol Chem *276*, 40402-40410.

Honda, H., Oda, H., Nakamoto, T., Honda, Z., Sakai, R., Suzuki, T., Saito, T., Nakamura, K., Nakao, K., Ishikawa, T., *et al.* (1998). Cardiovascular anomaly, impaired actin bundling and resistance to Src-induced transformation in mice lacking p130Cas. Nat Genet *19*, 361-365.

Hooshmand-Rad, R., Claesson-Welsh, L., Wennstrom, S., Yokote, K., Siegbahn, A., and Heldin, C. H. (1997). Involvement of phosphatidylinositide 3'-kinase and Rac in platelet-derived growth factor-induced actin reorganization and chemotaxis. Exp Cell Res *234*, 434-441.

Hooshmand-Rad, R., Yokote, K., Heldin, C. H., and Claesson-Welsh, L. (1998). PDGF alpha-receptor mediated cellular responses are not dependent on Src family kinases in endothelial cells. J Cell Sci *111 (Pt 5)*, 607-614.

Huber, A. B., Kolodkin, A. L., Ginty, D. D., and Cloutier, J. F. (2003). Signaling at the growth cone: ligand-receptor complexes and the control of axon growth and guidance. Annu Rev Neurosci *26*, 509-563.

Iijima, K., Yoshizumi, M., Hashimoto, M., Akishita, M., Kozaki, K., Ako, J., Watanabe, T., Ohike, Y., Son, B., Yu, J., *et al.* (2002a). Red wine polyphenols inhibit vascular smooth muscle cell migration through two distinct signaling pathways. Circulation *105*, 2404-2410.

Iijima, M., Huang, Y. E., and Devreotes, P. (2002b). Temporal and spatial regulation of chemotaxis. Dev Cell *3*, 469-478.

Ilic, D., Furuta, Y., Kanazawa, S., Takeda, N., Sobue, K., Nakatsuji, N., Nomura, S., Fujimoto, J., Okada, M., and Yamamoto, T. (1995). Reduced cell motility and enhanced focal adhesion contact formation in cells from FAK-deficient mice. Nature *377*, 539-544.

Jekely, G., and Rorth, P. (2003). Hrs mediates downregulation of multiple signalling receptors in Drosophila. EMBO Rep *4*, 1163-1168.

Johnson, K. G., McKinnell, I. W., Stoker, A. W., and Holt, C. E. (2001). Receptor protein tyrosine phosphatases regulate retinal ganglion cell axon outgrowth in the developing Xenopus visual system. J Neurobiol *49*, 99-117.

Johnson, K. G., and Van Vactor, D. (2003). Receptor protein tyrosine phosphatases in nervous system development. Physiol Rev *83*, 1-24.

Jones, G. E. (2000). Cellular signaling in macrophage migration and chemotaxis. J Leukoc Biol *68*, 593-602.

Kallin, A., Demoulin, J. B., Nishida, K., Hirano, T., Ronnstrand, L., and Heldin, C. H. (2004). Gab1 contributes to cytoskeletal reorganization and chemotaxis in response to platelet-derived growth factor. J Biol Chem.

Kanazawa, H., Ohsawa, K., Sasaki, Y., Kohsaka, S., and Imai, Y. (2002). Macrophage/microglia-specific protein Iba1 enhances membrane ruffling and Rac activation via phospholipase C-gamma -dependent pathway. J Biol Chem *277*, 20026-20032.

Kaufmann, N., Wills, Z. P., and Van Vactor, D. (1998). Drosophila Rac1 controls motor axon guidance. Development *125*, 453-461.

Kingsley, K., Huff, J. L., Rust, W. L., Carroll, K., Martinez, A. M., Fitchmun, M., and Plopper, G. E. (2002). ERK1/2 mediates PDGF-BB stimulated vascular smooth muscle cell proliferation and migration on laminin-5. Biochem Biophys Res Commun *293*, 1000-1006.

Klinghoffer, R. A., Sachsenmaier, C., Cooper, J. A., and Soriano, P. (1999). Src family kinases are required for integrin but not PDGFR signal transduction. Embo J *18*, 2459-2471.

Kluk, M. J., Colmont, C., Wu, M. T., and Hla, T. (2003). Platelet-derived growth factor (PDGF)-induced chemotaxis does not require the G protein-coupled receptor S1P1 in murine embryonic fibroblasts and vascular smooth muscle cells. FEBS Lett *533*, 25-28.

Krueger, N. X., Van Vactor, D., Wan, H. I., Gelbart, W. M., Goodman, C. S., and Saito, H. (1996). The transmembrane tyrosine phosphatase DLAR controls motor axon guidance in Drosophila. Cell *84*, 611-622.

Lammers, R., Lerch, M. M., and Ullrich, A. (2000). The carboxyl-terminal tyrosine residue of protein-tyrosine phosphatase alpha mediates association with focal adhesion plaques. J Biol Chem *275*, 3391-3396.

Ledig, M. M., Haj, F., Bixby, J. L., Stoker, A. W., and Mueller, B. K. (1999a). The receptor tyrosine phosphatase CRYPalpha promotes intraretinal axon growth. J Cell Biol *147*, 375-388.

Ledig, M. M., McKinnell, I. W., Mrsic-Flogel, T., Wang, J., Alvares, C., Mason, I., Bixby, J. L., Mueller, B. K., and Stoker, A. W. (1999b). Expression of receptor tyrosine phosphatases during development of the retinotectal projection of the chick. J Neurobiol *39*, 81-96.

Lee, C. H., Herman, T., Clandinin, T. R., Lee, R., and Zipursky, S. L. (2001). N-cadherin regulates target specificity in the Drosophila visual system. Neuron *30*, 437-450.

Li, R., Wong, N., Jabali, M. D., and Johnson, P. (2001). CD44-initiated cell spreading induces Pyk2 phosphorylation, is mediated by Src family kinases, and is negatively regulated by CD45. J Biol Chem *276*, 28767-28773.

Li, Y., Fetchko, M., Lai, Z. C., and Baker, N. E. (2003). Scabrous and Gp150 are endosomal proteins that regulate Notch activity. Development *130*, 2819-2827.

Liliental, J., Moon, S. Y., Lesche, R., Mamillapalli, R., Li, D., Zheng, Y., Sun, H., and Wu, H. (2000). Genetic deletion of the Pten tumor suppressor gene promotes cell motility by activation of Rac1 and Cdc42 GTPases. Curr Biol *10*, 401-404.

Lindahl, P., Johansson, B. R., Leveen, P., and Betsholtz, C. (1997). Pericyte loss and microaneurysm formation in PDGF-B-deficient mice. Science *277*, 242-245.

Liu, D., el-Hariry, I., Karayiannakis, A. J., Wilding, J., Chinery, R., Kmiot, W., McCrea, P. D., Gullick, W. J., and Pignatelli, M. (1997). Phosphorylation of beta-catenin and epidermal growth factor receptor by intestinal trefoil factor. Lab Invest *77*, 557-563.

Liu, S., Thomas, S. M., Woodside, D. G., Rose, D. M., Kiosses, W. B., Pfaff, M., and Ginsberg, M. H. (1999). Binding of paxillin to alpha4 integrins modifies integrin-dependent biological responses. Nature *402*, 676-681.

Mandell, J. W., and Banker, G. A. (1998). Selective blockade of axonogenesis in cultured hippocampal neurons by the tyrosine phosphatase inhibitor orthovanadate. J Neurobiol *35*, 17-28.

Maurel-Zaffran, C., Suzuki, T., Gahmon, G., Treisman, J. E., and Dickson, B. J. (2001). Cell-autonomous and -nonautonomous functions of LAR in R7 photoreceptor axon targeting. Neuron *32*, 225-235.

Meili, R., Ellsworth, C., Lee, S., Reddy, T. B., Ma, H., and Firtel, R. A. (1999). Chemoattractant-mediated transient activation and membrane localization of Akt/PKB is required for efficient chemotaxis to cAMP in Dictyostelium. Embo J *18*, 2092-2105.

Meng, K., Rodriguez-Pena, A., Dimitrov, T., Chen, W., Yamin, M., Noda, M., and Deuel, T. F. (2000). Pleiotrophin signals increased tyrosine phosphorylation of beta beta-catenin through inactivation of the intrinsic catalytic activity of the receptor-type protein tyrosine phosphatase beta/zeta. Proc Natl Acad Sci U S A *97*, 2603-2608.

Moore, M. A. (2001). The role of chemoattraction in cancer metastases. Bioessays *23*, 674-676.

Mori, S., Ronnstrand, L., Yokote, K., Engstrom, A., Courtneidge, S. A., Claesson-Welsh, L., and Heldin, C. H. (1993). Identification of two juxtamembrane autophosphorylation sites in the PDGF beta-receptor; involvement in the interaction with Src family tyrosine kinases. Embo J *12*, 2257-2264.

Mourton, T., Hellberg, C. B., Burden-Gulley, S. M., Hinman, J., Rhee, A., and Brady-Kalnay, S. M. (2001). The PTPmu protein-tyrosine phosphatase binds and recruits the scaffolding protein RACK1 to cell-cell contacts. J Biol Chem *276*, 14896-14901.

Muller, T., Choidas, A., Reichmann, E., and Ullrich, A. (1999). Phosphorylation and free pool of beta-catenin are regulated by tyrosine kinases and tyrosine phosphatases during epithelial cell migration. J Biol Chem *274*, 10173-10183.

Munier, A. I., Doucet, D., Perrodou, E., Zachary, D., Meister, M., Hoffmann, J. A., Janeway, C. A., Jr., and Lagueux, M. (2002). PVF2, a PDGF/VEGF-like growth factor, induces hemocyte proliferation in Drosophila larvae. EMBO Rep *3*, 1195-1200.

Mureebe, L., Nelson, P. R., Yamamura, S., Lawitts, J., and Kent, K. C. (1997). Activation of pp60c-src is necessary for human vascular smooth muscle cell migration. Surgery *122*, 138-144; discussion 144-135.

Nam, H. J., Poy, F., Krueger, N. X., Saito, H., and Frederick, C. A. (1999). Crystal structure of the tandem phosphatase domains of RPTP LAR. Cell *97*, 449-457.

Nelson, W. J., and Nusse, R. (2004). Convergence of Wnt, beta-catenin, and cadherin pathways. Science *303*, 1483-1487.

Neptune, E. R., and Bourne, H. R. (1997). Receptors induce chemotaxis by releasing the betagamma subunit of Gi, not by activating Gq or Gs. Proc Natl Acad Sci U S A *94*, 14489-14494.

O'Neill, G. M., Fashena, S. J., and Golemis, E. A. (2000). Integrin signalling: a new Cas(t) of characters enters the stage. Trends Cell Biol *10*, 111-119.

Okamoto, H., Takuwa, N., Yokomizo, T., Sugimoto, N., Sakurada, S., Shigematsu, H., and Takuwa, Y. (2000). Inhibitory regulation of Rac activation, membrane ruffling, and cell migration by the G protein-coupled sphingosine-1-phosphate receptor EDG5 but not EDG1 or EDG3. Mol Cell Biol *20*, 9247-9261.

Peppel, K., Zhang, L., Huynh, T. T., Huang, X., Jacobson, A., Brian, L., Exum, S. T., Hagen, P. O., and Freedman, N. J. (2002). Overexpression of G protein-coupled receptor kinase-2 in smooth muscle cells reduces neointimal hyperplasia. J Mol Cell Cardiol *34*, 1399-1409.

Petrone, A., Battaglia, F., Wang, C., Dusa, A., Su, J., Zagzag, D., Bianchi, R., Casaccia-Bonnefil, P., Arancio, O., and Sap, J. (2003). Receptor protein tyrosine phosphatase alpha is essential for hippocampal neuronal migration and long-term potentiation. Embo J *22*, 4121-4131.

Piper, M., and Little, M. (2003). Movement through Slits: cellular migration via the Slit family. Bioessays *25*, 32-38.

Plattner, R., Irvin, B. J., Guo, S., Blackburn, K., Kazlauskas, A., Abraham, R. T., York, J. D., and Pendergast, A. M. (2003). A new link between the c-Abl tyrosine kinase and phosphoinositide signalling through PLC-gamma1. Nat Cell Biol *5*, 309-319.

Plattner, R., Koleske, A. J., Kazlauskas, A., and Pendergast, A. M. (2004). Bidirectional signaling links the abelson kinases to the platelet-derived growth factor receptor. Mol Cell Biol *24*, 2573-2583.

Ponniah, S., Wang, D. Z., Lim, K. L., and Pallen, C. J. (1999). Targeted disruption of the tyrosine phosphatase PTPalpha leads to constitutive downregulation of the kinases Src and Fyn. Curr Biol *9*, 535-538.

Rao, Y., Wong, K., Ward, M., Jurgensen, C., and Wu, J. Y. (2002). Neuronal migration and molecular conservation with leukocyte chemotaxis. Genes Dev *16*, 2973-2984.

Reddien, P. W., and Horvitz, H. R. (2000). CED-2/CrkII and CED-10/Rac control phagocytosis and cell migration in Caenorhabditis elegans. Nat Cell Biol *2*, 131-136.

Ridley, A. J., Paterson, H. F., Johnston, C. L., Diekmann, D., and Hall, A. (1992). The small GTP-binding protein rac regulates growth factor-induced membrane ruffling. Cell *70*, 401-410.

Roach, T., Slater, S., Koval, M., White, L., Cahir McFarland, E. D., Okumura, M., Thomas, M., and Brown, E. (1997). CD45 regulates Src family member kinase activity associated with macrophage integrin-mediated adhesion. Curr Biol *7*, 408-417.

Ronnstrand, L., Siegbahn, A., Rorsman, C., Johnell, M., Hansen, K., and Heldin, C. H. (1999). Overactivation of phospholipase C-gamma1 renders platelet-derived growth factor beta-receptor-expressing cells independent of the phosphatidylinositol 3-kinase pathway for chemotaxis. J Biol Chem *274*, 22089-22094.

Rosdahl, J. A., Mourton, T. L., and Brady-Kalnay, S. M. (2002). Protein kinase C delta (PKCdelta) is required for protein tyrosine phosphatase mu (PTPmu)-dependent neurite outgrowth. Mol Cell Neurosci *19*, 292-306.

Rosenfeldt, H. M., Hobson, J. P., Maceyka, M., Olivera, A., Nava, V. E., Milstien, S., and Spiegel, S. (2001). EDG-1 links the PDGF receptor to Src and focal adhesion kinase activation leading to lamellipodia formation and cell migration. Faseb J *15*, 2649-2659.

Ryu, Y., Takuwa, N., Sugimoto, N., Sakurada, S., Usui, S., Okamoto, H., Matsui, O., and Takuwa, Y. (2002). Sphingosine-1-phosphate, a platelet-derived lysophospholipid mediator, negatively regulates cellular Rac activity and cell migration in vascular smooth muscle cells. Circ Res *90*, 325-332.

Sasaki, T., Irie-Sasaki, J., Jones, R. G., Oliveira-dos-Santos, A. J., Stanford, W. L., Bolon, B., Wakeham, A., Itie, A., Bouchard, D., Kozieradzki, I., *et al.* (2000). Function of PI3Kgamma in thymocyte development, T cell activation, and neutrophil migration. Science *287*, 1040-1046.

Schindelholz, B., Knirr, M., Warrior, R., and Zinn, K. (2001). Regulation of CNS and motor axon guidance in Drosophila by the receptor tyrosine phosphatase DPTP52F. Development *128*, 4371-4382.

Schlaepfer, D. D., Hauck, C. R., and Sieg, D. J. (1999). Signaling through focal adhesion kinase. Prog Biophys Mol Biol *71*, 435-478.

Sears, H. C., Kennedy, C. J., and Garrity, P. A. (2003). Macrophage-mediated corpse engulfment is required for normal Drosophila CNS morphogenesis. Development *130*, 3557-3565.

Shenoi, H., Seavitt, J., Zheleznyak, A., Thomas, M. L., and Brown, E. J. (1999). Regulation of integrin-mediated T cell adhesion by the transmembrane protein tyrosine phosphatase CD45. J Immunol *162*, 7120-7127.

Sieg, D. J., Hauck, C. R., Ilic, D., Klingbeil, C. K., Schaefer, E., Damsky, C. H., and Schlaepfer, D. D. (2000). FAK integrates growth-factor and integrin signals to promote cell migration. Nat Cell Biol *2*, 249-256.

Sieg, D. J., Hauck, C. R., and Schlaepfer, D. D. (1999). Required role of focal adhesion kinase (FAK) for integrin-stimulated cell migration. J Cell Sci *112 (Pt 16)*, 2677-2691.

Somogyi, K., and Rorth, P. (2004). Cortactin modulates cell migration and ring canal morphogenesis during Drosophila oogenesis. Mech Dev *121*, 57-64.

Stepanek, L., Sun, Q. L., Wang, J., Wang, C., and Bixby, J. L. (2001). CRYP-2/cPTPRO is a neurite inhibitory repulsive guidance cue for retinal neurons in vitro. J Cell Biol *154*, 867-878.

Sun, Q., Bahri, S., Schmid, A., Chia, W., and Zinn, K. (2000). Receptor tyrosine phosphatases regulate axon guidance across the midline of the Drosophila embryo. Development *127*, 801-812.

Tachibana, K., Sato, T., D'Avirro, N., and Morimoto, C. (1995). Direct association of pp125FAK with paxillin, the focal adhesion-targeting mechanism of pp125FAK. J Exp Med *182*, 1089-1099.

Tamura, M., Gu, J., Matsumoto, K., Aota, S., Parsons, R., and Yamada, K. M. (1998). Inhibition of cell migration, spreading, and focal adhesions by tumor suppressor PTEN. Science *280*, 1614-1617.

Wallace, M. J., Batt, J., Fladd, C. A., Henderson, J. T., Skarnes, W., and Rotin, D. (1999). Neuronal defects and posterior pituitary hypoplasia in mice lacking the receptor tyrosine phosphatase PTPsigma. Nat Genet *21*, 334-338.

Wallace, M. J., Fladd, C., Batt, J., and Rotin, D. (1998). The second catalytic domain of protein tyrosine phosphatase delta (PTP delta) binds to and inhibits the first catalytic domain of PTP sigma. Mol Cell Biol *18*, 2608-2616.

Wang, J., and Bixby, J. L. (1999). Receptor tyrosine phosphatase-delta is a homophilic, neurite-promoting cell adhesion molecular for CNS neurons. Mol Cell Neurosci *14*, 370-384.

Wennstrom, S., Hawkins, P., Cooke, F., Hara, K., Yonezawa, K., Kasuga, M., Jackson, T., Claesson-Welsh, L., and Stephens, L. (1994a). Activation of phosphoinositide 3-kinase is required for PDGF-stimulated membrane ruffling. Curr Biol *4*, 385-393.

Wennstrom, S., Siegbahn, A., Yokote, K., Arvidsson, A. K., Heldin, C. H., Mori, S., and Claesson-Welsh, L. (1994b). Membrane ruffling and chemotaxis transduced by the PDGF beta-receptor require the binding site for phosphatidylinositol 3' kinase. Oncogene *9*, 651-660.

Wills, Z., Bateman, J., Korey, C. A., Comer, A., and Van Vactor, D. (1999a). The tyrosine kinase Abl and its substrate enabled collaborate with the receptor phosphatase Dlar to control motor axon guidance. Neuron *22*, 301-312.

Wills, Z., Emerson, M., Rusch, J., Bikoff, J., Baum, B., Perrimon, N., and Van Vactor, D. (2002). A Drosophila homolog of cyclase-associated proteins collaborates with the Abl tyrosine kinase to control midline axon pathfinding. Neuron *36*, 611-622.

Wills, Z., Marr, L., Zinn, K., Goodman, C. S., and Van Vactor, D. (1999b). Profilin and the Abl tyrosine kinase are required for motor axon outgrowth in the Drosophila embryo. Neuron *22*, 291-299.

Wong, K., Park, H. T., Wu, J. Y., and Rao, Y. (2002). Slit proteins: molecular guidance cues for cells ranging from neurons to leukocytes. Curr Opin Genet Dev *12*, 583-591.

Worthley, S. G., Osende, J. I., Helft, G., Badimon, J. J., and Fuster, V. (2001). Coronary artery disease: pathogenesis and acute coronary syndromes. Mt Sinai J Med *68*, 167-181.

Xie, Y., Yeo, T. T., Zhang, C., Yang, T., Tisi, M. A., Massa, S. M., and Longo, F. M. (2001). The leukocyte common antigen-related protein tyrosine phosphatase receptor regulates regenerative neurite outgrowth in vivo. J Neurosci *21*, 5130-5138.

Yang, L. T., Alexandropoulos, K., and Sap, J. (2002). c-SRC mediates neurite outgrowth through recruitment of Crk to the scaffolding protein Sin/Efs without altering the kinetics of ERK activation. J Biol Chem *277*, 17406-17414.

Yeo, T. T., Yang, T., Massa, S. M., Zhang, J. S., Honkaniemi, J., Butcher, L. L., and Longo, F. M. (1997). Deficient LAR expression decreases basal forebrain cholinergic neuronal size and hippocampal cholinergic innervation. J Neurosci Res *47*, 348-360.

Zeng, L., Si, X., Yu, W. P., Le, H. T., Ng, K. P., Teng, R. M., Ryan, K., Wang, D. Z., Ponniah, S., and Pallen, C. J. (2003). PTP alpha regulates integrin-stimulated FAK autophosphorylation and cytoskeletal rearrangement in cell spreading and migration. J Cell Biol *160*, 137-146.

Zheng, X. M., Resnick, R. J., and Shalloway, D. (2000). A phosphotyrosine displacement mechanism for activation of Src by PTPalpha. Embo J *19*, 964-978.

Zheng, Y., Bagrodia, S., and Cerione, R. A. (1994). Activation of phosphoinositide 3-kinase activity by Cdc42Hs binding to p85. J Biol Chem *269*, 18727-18730.

Zhu, Y., Yu, T., Zhang, X. C., Nagasawa, T., Wu, J. Y., and Rao, Y. (2002). Role of the chemokine SDF-1 as the meningeal attractant for embryonic cerebellar neurons. Nat Neurosci *5*, 719-720.

Zondag, G. C., Koningstein, G. M., Jiang, Y. P., Sap, J., Moolenaar, W. H., and Gebbink, M. F. (1995). Homophilic interactions mediated by receptor tyrosine phosphatases mu and kappa. A critical role for the novel extracellular MAM domain. J Biol Chem *270*, 14247-14250.

Chapter 2.

Identification of proteins involved in Ptp69D signaling in *Drosophila* photoreceptor axon guidance

Experiments in Figure 12d-e were done by Rita Khodosh.

SUMMARY

Photoreceptors in the developing *Drosophila* eye extend axons that target to different layers of the optic lobe. One set of photoreceptors, R1-R6, has axons that target to the lamina, while R7 and R8 axons target to different layers of the medulla. The receptor tyrosine phosphatase Ptp69D is required for both R1-R6 and R7 targeting. In *Ptp69D* mutants, many R1-R6 and R7 axons stay fasciculated to R8 and terminate in the R8 layer of the medulla. Expression of Ptp69D lacking the intracellular domain (Ptp69DλC) causes R1-R6 axon mistargeting similar to that in *Ptp69D* loss of function, and genetic interaction between Ptp69DλC overexpression and *Ptp69D* loss of function suggests that Ptp69DλC acts as a dominant negative. I have identified several genes that display a dosage-sensitive genetic interaction with Ptp69DλC. Removal of a single genetic dose of the cytoplasmic tyrosine kinases *Src* or *Abl* enhances the Ptp69DλC phenotype. The genetic interaction between *Ptp69D* and *Src* was confirmed with loss-of-function Ptp69D. Mutations in the receptor tyrosine kinase Egfr and its downstream effector, the small GTPase Ras, were found to suppress the Ptp69DλC R1-R6 mistargeting phenotype. Expression of dominant-negative Egfr or Ras in postmitotic neurons caused axons to stop before reaching their targets, and expression of dominant-active Egfr caused R1-R6 axons to overshoot their targets. In a biochemical screen for proteins that physically bind a substrate-trapping form of Ptp69D, the tyrosine kinase PR2 was found to interact with Ptp69D. The *C. elegans* homolog of PR2 negatively regulates the Egfr/Ras pathway. Together these data suggest that Ptp69D may act to stop R1-R6 axons at the lamina by activating PR2, which then blocks axon outgrowth by inhibiting the Egfr pathway.

INTRODUCTION

The establishment of neuronal circuitry in the developing brain requires that neurons make specific connections with other neurons through the extension and correct navigation of axons. The array of connections in the brain is complex yet precise, with axons often having to travel long distances, traversing a diversity of cell types, but reproducibly terminating and

choosing targets in a certain region. Much of the vertebrate brain is organized in layers, and axons often must make layer-specific targeting decisions. For example, the mammalian cortex is composed of five distinct layers (Bolz et al., 1996), and the avian optic tectum has fifteen layers. Retinal ganglion cell axons arborize on only a few layers of the optic tectum (Acheson et al., 1980), and each subtype of retinal ganglion cell appears to form synapses in only one layer (Cowan, 1971; Reperant and Angaut, 1977). The molecular cues guiding these layer-specific decisions are poorly understood (Inoue and Sanes, 1997).

Axons navigate to their targets by sensing signals in the extracellular environment and responding to that environment by moving in a certain direction (Tessier-Lavigne and Goodman, 1996). Navigation decisions are carried out largely by the leading edge of the axon, the growth cone, which extends and retracts thin actin-rich protrusions called filopodia that sense cues in the environment. Axon growth and motility depends on actin polymerization and microtubule extension, and contact with the substrate on which it is growing. Navigation is directed by cues from other cells that bind receptors on the surface of the growth cone, which in turn transduce the information to the cytoskeleton or cell adhesion machinery, resulting in changes in movement or attachment. These cues can be attractive or repulsive and diffusible or cell-surface bound. The signal sent by some receptors can be interpreted by the cell as either attractive or repulsive, depending on the internal state of the cell (Song et al., 1997). It has been shown that interpretation of cues also depends on the combination of cues that a growth cone is receiving at a given moment(Hopker et al., 1999). The signaling pathways involved in transducing information from guidance receptors remain elusive.

The visual system of *Drosophila* provides a simple model for studying layer-specific axon targeting. Each of the 750 facets (ommatidia) in the eye contains eight uniquely identifiable photoreceptor neurons (R cells), which send axons into the brain and choose targets in one of two ganglia of the optic lobe. R8, the first cell to differentiate in each ommatidium, sends the first axon into the brain, going through the developing lamina, the most superficial optic ganglion, and choosing targets in one layer of the next optic ganglion, the medulla. R1-R6 develop next, and send axons along the path laid by R8 into the brain. However, rather than following R8 all the way to the medulla, R1-R6 axons defasciculate from R8 and choose targets in one layer of the lamina. Finally, R7 differentiates and sends an axon along the same fascicle, eventually choosing a target in a layer just below R8 in the medulla.

The repetitive nature of the eye and the apparent binary nature of the R1-R6 targeting decision makes the eye a relatively simple system in which to study how genes interact in the signal transduction pathways that lead to proper axon targeting. However, very little is known about the signaling pathways involved in the decision of R1-R6 to stop at the lamina, although several isolated genes have been identified as playing a role in R1-R6 targeting. Mutations in dreadlocks (dock), an SH2-SH3 adaptor protein; p21-activated kinase (Pak), which binds to dock; and trio, a Rac-GEF that signals upstream of Pak, cause massive defects in R cell targeting (Newsome et al., 2000). Mutations in the receptor tyrosine phosphatase Ptp69D cause more subtle defects(Garrity et al., 1999), with about 25% of R1-R6 axons bypassing the lamina and shooting through into the medulla.

Four receptor tyrosine phosphatases (RPTPs) in *Drosophila*, Ptp69D, Ptp99A, Dlar, and Ptp52F, have been shown to play a role in axon guidance. Dlar has been shown to be involved in targeting the R7 axon to the proper layer of the medulla (Frydman and Spradling, 2001) and later stages of R1-R6 target selection within the lamina (Clandinin et al., 2001). It has also been shown to be involved in motor neuron synapse formation (Kaufmann et al., 2002). Single mutations in any of the RPTPs cause partially penetrant defects in targeting of axons in the embryonic motor nerve ISNb. However, double, triple, and quadruple mutants in any combination have much more penetrant ISNb phenotypes, and overexpression of Ptp69D in the CNS can partially rescue the *dlar* mutant phenotype, suggesting that the phosphatases play overlapping roles in targeting (Desai et al., 1996; Desai et al., 1997; Schindelholz et al., 2001).

Little is known about how RPTPs help axons choose the correct target. One possibility is that activation of the phosphatase leads to a change in the actin cytoskeleton, thus causing axons to stop or change direction. Another possibility is that phosphatase activity is required for changes in fasciculation, which enables the growing axon to respond to other cues at the target that lead to cytoskeletal changes. To date, only one RPTP ligand has been found, and little is known about downstream targets. The involvement of Ptp69D in R1-R6 targeting in the eye poses a good entry point for studying the signaling mechanism used by RPTPs in axon choicepoint navigation. The intracellular domain of Ptp69D has two tandem phosphatase domains, as do many RPTPs. Deletion of the second phosphatase domain has no effect on R1-R6 targeting, suggesting that this domain is not required for activity (Garrity et al., 1999). On the other hand, the intracellular domain is required, as expression of a C-terminal truncation that

removes all of the intracellular domain causes an early lethality phenotype in the absence of endogenous Ptp69D (Garrity et al., 1999). Here I demonstrate that this intracellular deletion acts as a dominant negative phosphatase.

I have used Ptp69DλC as a genetic tool to identify genes that partner with Ptp69D in R1-R6 target selection. I have found three genes that are putative enhancers of the *Ptp69D* R1-R6 mistargeting phenotype. These include two cytoplasmic tyrosine kinases, Abl and Src64, and the axon guidance receptor robo. The EGF receptor and the small GTPase Ras, which have long been known to play a crucial role in the development of the eye, appear to be suppressors of the *Ptp69D* phenotype. This implicates a novel role for the Egfr/Ras signaling pathway in axon guidance. I have also examined the effects of substrate-trapping mutant forms of Ptp69D on embryonic motor nerve axon guidance and have used these substrate-trapping forms to identify potential targets of dephosphorylation by Ptp69D.

RESULTS

R1-R6 photoreceptor axons are mistargeted in *Ptp69D* mutants

In third instar larvae mutant for *Ptp69D*, photoreceptor axon bundles projecting into the medulla appear thicker than normal (Garrity et al., 1999). I sought to determine whether this was due to aberrant projection of R1-R6 axons into the medulla. I labeled a subset of R1-R6 axons using ro-tauLacZ, a fusion of the tau microtubule binding protein and λ-galactosidase driven under the control of the rough promoter. The rough promoter drives gene expression specifically in R2-R5 photoreceptors (Kimmel et al., 1990). In wild type animals, most axons labeled by ro-taulacZ stop at the lamina, with only 5 ± 3 axons projecting into the medulla (Garrity et al., 1999). In *Ptp69D* mutants, however, 29 ±12 labeled axons fail to stop at the lamina and project into the medulla, representing 20-25% of the total number of labeled axons (Garrity et al., 1999).

An intracellular deletion of Ptp69D acts as a dominant negative

The molecular mechanism of Ptp69D activity is unknown. Other receptor tyrosine phosphatases have been shown to be inactive when homo- or hetero-dimerized (Jiang et al.,

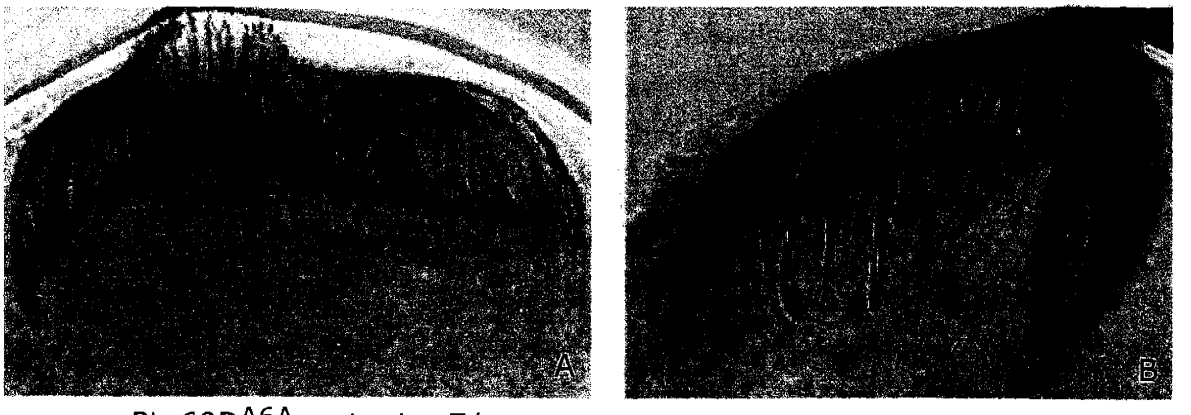

Ptp69D^{A6A},ro-tauLacZ/+ Ptp69D^{A6A},ro-tauLacZ/Ptp69D^{8ex34}

Figure 1. R2-R5 photoreceptor axons mistarget to the medulla in Ptp69D mutants. R2-R5 axons were labeled using the ro-tauLacZ reporter construct and stained using anti-b-galactosidase antibody. (A) In wildtype, R2-R5 axons stop at the lamina. (B) In Ptp69D mutants, many R2-R5 axons shoot through the lamina at stop in the medulla.

1999; Majeti et al., 1998; Wallace et al., 1998). Receptor tyrosine kinases, conversely, are activated when dimerized (Hubbard and Till, 2000). Ptp69D could be activated through homo-dimerization, dedimerization, or hetero-dimerization with other receptor tyrosine phosphatases or other receptors. In identifying which regions of Ptp69D are required for its function, Garrity et al. found that ectopic expression of a Ptp69D transgene lacking the intracellular domain (Ptp69DλC) enhanced the lethality of Ptp69D mutants (Paul Garrity, personal communication). The fact that overexpression of Ptp69DλC enhances lethality in a *Ptp69D* null background would suggest that Ptp69D is not activated by homodimerization, as there would be nothing with which a truncated protein could dimerize in a null background. If Ptp69D were activated by dedimerization, Ptp69DλC would be predicted to act as a dominant active form. Alternatively, if Ptp69D acts by binding to other receptors, Ptp69DλC could act as a general dominant negative phosphatase. I first examined whether Ptp69DλC had a dominant lethality phenotype when expressed in all neurons using the elav promoter. The number of animals expressing Ptp69DλC was as expected according to Mendelian genetics (data not shown). Therefore, overexpressing Ptp69DλC in neurons has no effect on viability. To determine whether Ptp69DλC had a dominant phenotype in R1-R6 axon targeting, I expressed Ptp69DλC in the developing eye in a wild type background using the GMR promoter. I found that overexpression of Ptp69DλC resulted in a phenotype similar to *Ptp69D* loss of function, with 23 ± 7 R2-R5 axons aberrantly projecting into the medulla (Figure 2a). This phenotype was enhanced to 43 ± 17 ($p<0.01$) mistargeted R2-R5 axons by the removal of a single copy of endogenous *Ptp69D* (Figure 2b) and was suppressed to 7 ± 8 ($p<0.01$) mistargeted axons by concomitant expression of a wild type Ptp69D transgene (Figure 2c). The quantification of these results is presented in Figure 2d. I concluded from these results that Ptp69DλC acts as a dominant negative phosphatase, and thus is likely to be activated through heterodimerization.

Genetic screen for modifiers of Ptp69D

The results of overexpressing Ptp69DλC in the developing eye suggested that Ptp69D may act by binding to another receptor. This complex could then induce a signal transduction cascade that would lead to changes in the cytoskeleton or cell-cell adhesion. I sought to identify other genes in this pathway by conducting a pilot screen for dominant enhancers or suppressors of the Ptp69DλC overexpression phenotype. Genes that dominantly enhanced the number of

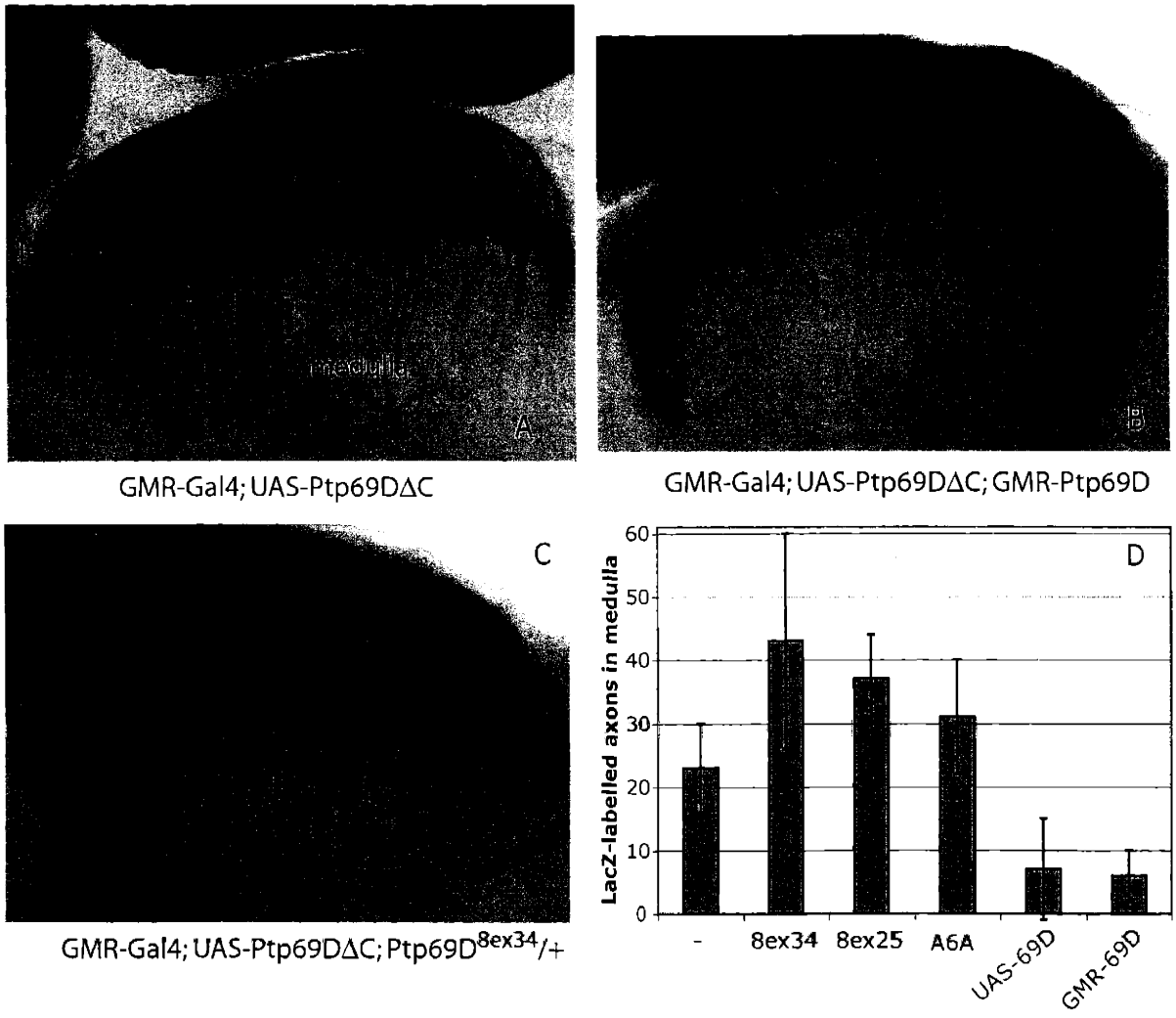

Figure 2. Ptp69DΔC acts as a dominant negative. All animals carry the ro-tauLacZ reporter construct. Eye-brain complexes were dissected from third instar larvae, and R2-R5 axons were visualized with anti-β-galactosidase antibody. (A) Ptp69DΔC was expressed in photoreceptor neurons under the control of the GMR promoter, causing R2-R5 to mistarget to the medulla. (B) Co-expressing wildtype Ptp69D suppresses the number of axons mistargeting to the medulla. (C) Removing a single copy of endogenous Ptp69D enhances the Ptp69DΔC phenotype. (D) Quantitation of results presented in (A-C). Genotypes are GMR-Gal4;UAS- Ptp69DΔC and heterozygous for the chromosome indicated. 8ex34 and 8ex25 are C-terminal deletions of Ptp69D. A6A is an N-terminal deletion of Ptp69D.

Table 1. Genes tested for dominant genetic interaction with Ptp69DλC.

Mutant gene	# Mistargeted axons	n=	p value
-	23 ± 7	20	n/a
$Ptp99A^{HA64}$	22 ± 11	8	0.77
$dlar^{5.5}$	21 ± 4	6	0.51
Abl^{2}	9 ± 4	10	<0.01
Abl^{1}	41 ± 13	16	<0.01
Abl^{4}	39 ± 12	20	<0.01
Df(3L)st-j7	44 ± 14	19	<0.01
UAS-Abl #6	8 ± 8	12	<0.01
UAS-Abl #11	10 ± 6	10	<0.01
$UAS\text{-}Abl^{KN}$	26 ± 7	15	0.22
ena^{210}	24 ± 6	15	0.66
ena^{GC1}	27 ± 5	15	0.07
abl^{1} dab^{m54}	16 ± 9	16	0.01
abl^{1} fax^{m12} p[Abl2.8]	12 ± 7	12	<0.01
$robo^{1}$	39 ± 9	23	<0.01
FasIII $robo^{Z420}$	41 ± 17	12	<0.01
comm	23 ± 12	12	1.0
slit	22 ± 7	17	0.67
$Src64^{PI}$	36 ± 3	16	<0.01
$Src64^{\lambda 17}$	17 ± 9	16	0.03
Src42A	19 ± 9	13	0.16
$Btk29^{e482}$	14 ± 8	12	<0.01
$Btk29^{KO5610}$	10 ± 8	13	<0.01
scb^{1}	20 ± 8	16	0.24
mys^{10}	24 ± 12	14	0.76
arm^{4}	27 ± 14	18	0.27
$LamA^{6\text{-}36}$	22 ± 10	15	0.73
$Ncad^{M19}$	23 ± 8	17	1.0
$FasI^{R401}$	23 ± 7	15	1.0
btl^{LG19}	16 ± 7	14	<0.01
htl^{AB42}	29 ± 8	13	0.03
$Egfr^{F2}$	10 ± 5	18	<0.01
$Egfr^{f10}$	14 ± 6	19	<0.01
$Egfr^{f8}$	16 ± 6	16	0.03
$argos^{\lambda 7}$	17 ± 9	15	0.03
Ras85D	13 ± 8	17	<0.01

R1-R6 axons mistargeting to the medulla could be positive regulators of Ptp69D signaling, whereas genes that suppressed the number of mistargeted axons could be negative regulators of Ptp69D signaling. The genes I tested and their effects on R2-R5 axon targeting are listed in Table 1. This approach had a number of advantages over a more standard genetic modification screen, although it also had some disadvantages. The animals examined were fully viable, as expression of Ptp69DλC does not cause lethality, and so a large number of animals of each genotype could be examined. In addition, a single cross generated the relevant genotypes, which would not have been feasible in a screen using loss-of-function *Ptp69D*. The genes examined for an interaction with Ptp69DλC were already known to be regulators of axon guidance, actin polymerization, and/or adhesion, so it was likely that among them would be genes that interact with Ptp69D, and by examining known genes we spared ourselves the difficulty of cloning newly generated mutations. However, it is always possible that overexpression of a dominantly acting construct does not perfectly mimic the corresponding loss of function in every way. Ptp69DλC could interfere with the function of other receptors not related to Ptp69D, or possibly induce the activation of ectopic pathways. Additionally, mutations interfering with the expression of Ptp69DλC would appear to suppress the dominant negative phenotype. Due to these caveats, any genes found to interact with Ptp69DλC must also be confirmed to interact with loss-of-function *Ptp69D*. By limiting ourselves to a select set of genes, we very likely missed a number of genes that do interact with Ptp69D. Conversely, due to the higher level of stringency that is required in an unbiased complete genomic screen, several of the genes that were found to be enhancers or suppressors in this pilot screen may not have been identified.

Abl is an enhancer of Ptp69D

The cytoplasmic tyrosine kinase Abl has been shown to be involved in axon guidance in the *Drosophila* embryonic CNS and motor nerves (Gertler et al., 1989; Gertler et al., 1993). Work from the Van Vactor lab has suggested that Dlar interacts with Abl and its substrate ena in embryonic motor neurons (Wills et al., 1999). They propose a model in which Dlar phosphatase and Abl kinase have antagonistic effects on ena, which has recently been shown to promote actin filament extension through its anti-capping activity (Bear et al., 2002). Wills et al. show that *ena* mutants, like *Dlar* mutants, cause ISNb axons to bypass their targets. Conversely, in *Abl* mutants targeting is largely normal, but one axon in ISNb fails to reach its target. *Abl* mutations

dominantly suppress the bypass caused by *Dlar*. It has also been postulated that Abl and RPTPs may have opposite effects on the axon guidance receptor robo (Bashaw et al., 2000). If Abl and Ptp69D act to respectively phosphorylate and dephosphorylate a common target involved in photoreceptor axon guidance, mutations in *Abl* should suppress the Ptp69DλC dominant phenotype. However, two loss-of-function alleles of *Abl*, Abl^{1} and Abl^{4}, and a deficiency that removes *Abl* act as strong dominant enhancers of the Ptp69DλC phenotype (Figure 3b,e), and overexpression of two different wild type Abl transgenes suppresses the Ptp69DλC phenotype (Figure 3c,e). Mutations in *ena* have no effect (Figure 3e). The kinase activity of Abl has been shown to be required for its involvement in axon guidance, but not for proper eye development (Henkemeyer et al., 1990). Expression of a kinase-dead form of Abl (UAS-Abl^{KN}) had no effect on the Ptp69DλC phenotype (Figure 3d,e), suggesting that the kinase activity is required for its interaction with Ptp69D in R1-R6 axon guidance. Thus, *Abl* does not interact with *Ptp69D* as it has been proposed to interact with other RPTPs in embryonic axon guidance. Rather, Abl and Ptp69D appear to cooperate in targeting R1-R6 photoreceptor axons to the lamina.

To determine whether *Abl* alone has a phenotype similar to Ptp69D, I examined animals that were mutant for *Abl*, but expressed a kinase-dead Abl transgene (p[Abl^{KN}]). This transgene rescues the eye development defects caused by Abl loss-of-function(Henkemeyer et al., 1990), but should not rescue its function in photoreceptor axon guidance. Contrary to expectation, photoreceptor axons in these animals either stop before reaching the lamina or fail to enter the brain altogether (Figure 4a-b).

Figure 3. Abl is a positive regulator in the Ptp69D signaling pathway. Dissections and staining were as in figure 3. (A) Ptp69DλC was expressed in photoreceptor neurons under the control of the GMR promoter in a wildtype background. (B) Abl4 dominantly enhances the Ptp69DλC phenotype. (C) Overexpression of wildtype Abl suppresses the number of mistargeted R2-R5 axons. (D) Overexpression of kinase-dead Abl has no effect. (E) Quantitation of results presented in (A-D). Genotypes are GMR-Gal4;UAS- Ptp69DλC and heterozygous for the allele or insertion indicated. Df(Abl) is Df(3L)st-j7, a deficiency that removes Abl and argos, but not fax, Dab, or Nrt. UAS-Abl#6 and UAS-Abl#11 are two independent insertions of the UAS-Abl transgene.

GMR-Gal4; UAS-Ptp69DΔC

GMR-Gal4; UAS-Ptp69DΔC; *Abl*^{4}/+

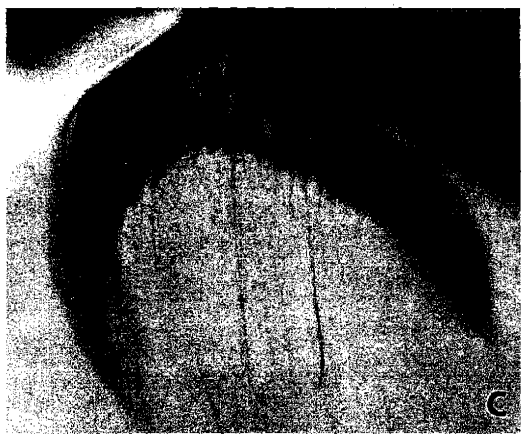

GMR-Gal4; UAS-Ptp69DΔC; UAS-Abl

GMR-Gal4; UAS-Ptp69DΔC; UAS-Abl^{KN}

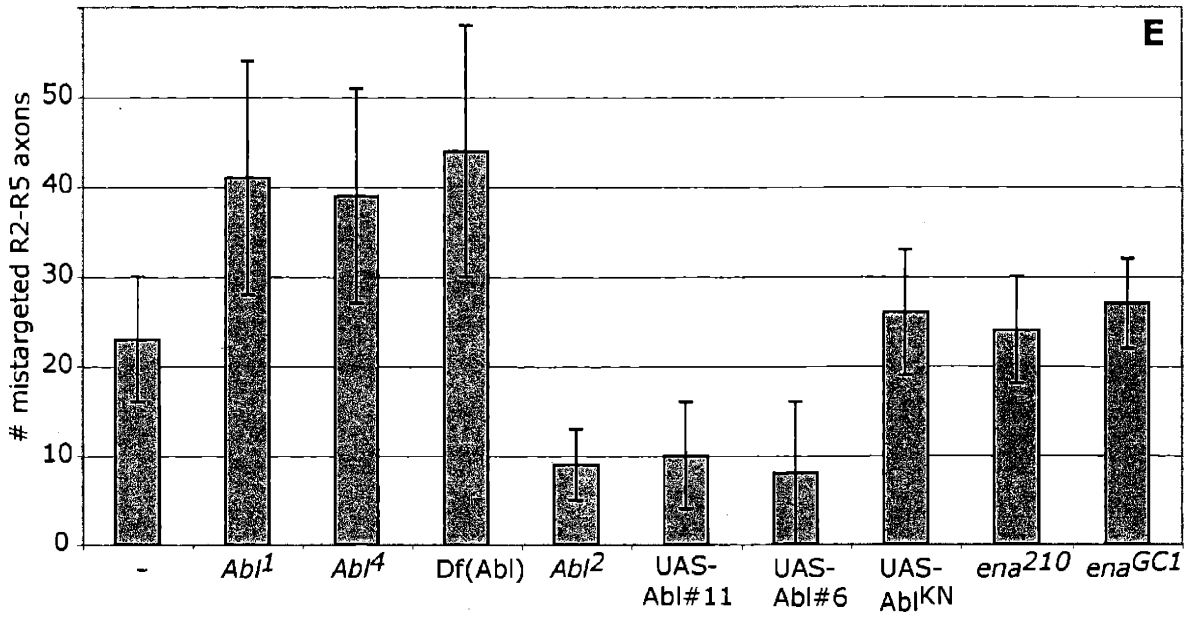

Figure 4. Photoreceptor axons stall before reaching their targets in *Abl* homozygous mutant animals. Eye-brain complexes were dissected from third instar larvae and stained with mAb 24B10, which labels all photoreceptor axons. (A) Homozygous Abl^{1} mutants expressing kinase-dead Abl under the control of the Abl promotor. p[Abl^{KN}] rescues Abl function in eye development, but not axon guidance. Arrows indicate axons stopping above the lamina. (B) Abl^{1} hemizygous over *Abl* deficiency Df(3L)st-j7 with p[Abl^{KN}].

One allele of *Abl*, Abl^2, acts as a strong dominant suppressor of the Ptp69DλC phenotype (Figure 3e). This is inconsistent with the direction of interaction of Abl^1, Abl^4, the *Abl* deficiency, and the Abl overexpression constructs. Abl^1 encodes a 65 kD truncated protein that localizes to the cell body, failing to translocate to the growth cone (Henkemeyer et al., 1990). It thus could act as a dominant negative or straight loss-of-function allele. Abl^4 is thought to be the Abl mutation closest to being a protein null, as it encodes a 25-35 kD truncated protein, the majority of which appears to be degraded (Bennett and Hoffmann, 1992). Abl^2 encodes a 51-53 kD truncated protein. Its subcellular localization is unknown, but in lethality and external phenotype tests, it displayed a less severe phenotype than Abl^1 (Henkemeyer et al., 1987). It is conceivable that Abl^2 could behave as a hypermorph or neomorph in its interaction with Ptp69D in photoreceptor axon guidance. Alternatively, an additional lesion on the Abl^2 mutant chromosome could cause the aberrant interaction with Ptp69DΔC.

Src64 is an enhancer of Ptp69D

There are three Src homologs in *Drosophila*, Src64B, Src42A, and Btk29A. A *Src42A* allele had little effect on the Ptp69DλC phenotype (Figure 5e). Two P-element alleles in *Btk29A* mildly suppressed the Ptp69DλC phenotype (Figure 5e), but this interaction was not pursued further. $Src64^{Pl}$, containing a P-element in the second intron of *Src64* (Dodson et al., 1998), dominantly enhanced the Ptp69DλC phenotype (Figure 5c,e). $Src64^{\lambda 17}$ had no effect on the PTP69DλC phenotype (Figure 5e), but also displays reduced phenotype penetrance in other assays (Dodson et al., 1998). To confirm the interaction between *Ptp69D* and *Src64*, I created *Ptp69D*, *Src64* double mutants. I found that $Src64^{Pl}$ strongly dominantly enhanced the *Ptp69D* loss-of-function phenotype (Figure 5d). In *Ptp69D* mutants, as described above, approximately 20-25% of R2-R5 axons fail to stop at the lamina and instead protrude into the medulla. In *Ptp69D* mutants with one copy of *Src64* removed, almost all of the labeled R2-R5 axons can be seen protruding into the medulla. The penetrance of this phenotype was 100%. To further confirm the interaction between *Src64* and *Ptp69D*, additional null alleles of *Src64* should be tested for interaction. *Src64* homozygous mutants alone are viable and have no photoreceptor axon guidance defects (Myles Robichaux, unpublished data).

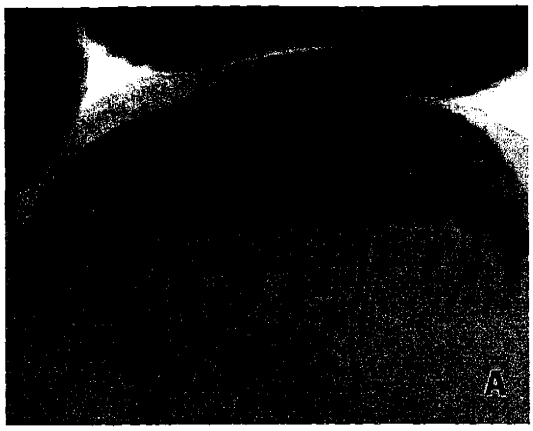

GMR-Gal4; UAS-Ptp69DΔC

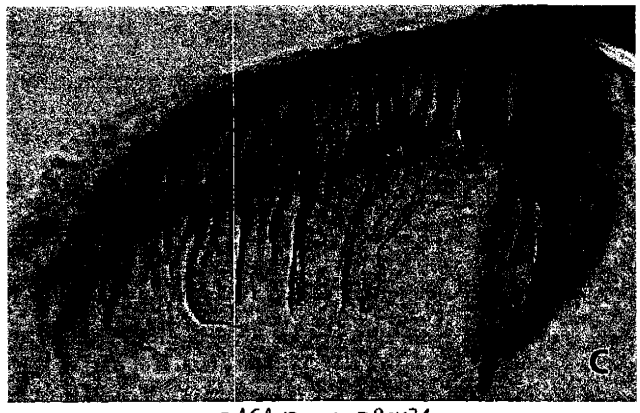

Ptp69D^{A6A}/*Ptp69D*^{8ex34}

GMR-Gal4; UAS-Ptp69DΔC; *Src64*^{PI}/+

Ptp69D^{A6A},*Src64*^{PI}/*Ptp69D*^{8ex34},+

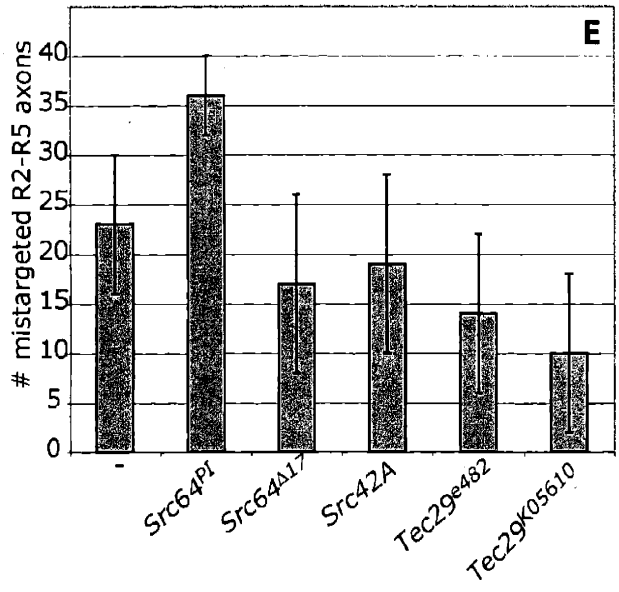

Figure 5. Src64 is a positive regulator in the Ptp69D signaling pathway. Dissections and staining were as in Figure 3.

(A) GMR-Gal4; UAS-Ptp69DΔC.

(B) GMR-Gal4; UAS-Ptp69DΔC; *Src64*^{PI}/+. *Src64* dominantly enhances the Ptp69DΔC phenotype. (C) *Ptp69D*^{A6A}/*Ptp69D*^{8ex34}. About 20-25% of R2-R5 axons mistarget in *Ptp69D* loss-of-function mutants.

(D) *Ptp69D*^{A6A},*Src64*^{PI}/*Ptp69D*^{8ex34},+. *Src64*^{PI} dominantly enhances *Ptp69D* loss of function, so that no R2-R5 axons can be seen stopping at the lamina. (E) Quantitation of results presented in (A-B) and other Src-related alleles not shown. Genotypes are GMR-Gal4; UAS-Ptp69DΔC and heterozygous for the indicated alleles.

Robo is an enhancer of Ptp69D

The axon guidance receptor robo has been shown to be important for axon repulsion at the *Drosophila* CNS midline(Kidd et al., 1998). Tissue-specific mutations in its ligand, slit, cause R1-R6 photoreceptor axons to overshoot their targets, although this is likely due to defects in other parts of the visual system (Tim Tayler, unpublished data). Robo has also been shown to be important for proper axon guidance in other areas of the larval and adult brain. Two loss-of-function mutations in *robo* strongly enhanced the Ptp69DλC phenotype (Figure 6b,c). This result was perplexing, as overexpression of wild type robo in a wild type background also causes a large number of R2-R5 axons to mistarget to the medulla (Rita Khodosh, unpublished data). Reduction of robo mRNA in the developing eye does not itself cause an R1-R6 targeting defect (Tim Tayler, unpublished data). However, the possibility remains that the expression of Ptp69DλC creates a sensitized background that reveals a novel function for robo in photoreceptor axon guidance that cannot be observed in robo mutants.

Egfr and Ras are suppressors of Ptp69D

I tested a number of growth factor receptor tyrosine kinases for modulation of the Ptp69DλC phenotype. The FGF receptors heartless and breathless had little effect. However, three alleles of the EGF receptor suppressed the Ptp69DλC phenotype (Figure 7a,c). The small GTPase Ras acts downstream of Egfr. An allele of *Ras85D* also suppressed the Ptp69DλC phenotype (Figure 7b-c), suggesting that Ptp69D could negatively interact with the Egfr/Ras pathway. This pathway is also involved in every step of eye development (Dominguez et al., 1998), so I was unable to examine the effect of loss-of-function mutants on photoreceptor axon guidance. However, the elav promotor drives expression in postmitotic neurons, after photoreceptor differentiation has taken place. I therefore used the elav promoter to drive expression of dominant-negative and dominant-active Egfr and Ras and examined the animals for defects in photoreceptor targeting. Overexpression of Ras^{V12}, a dominant active form of Ras, caused a severe phenotype that is suggestive of structural defects in the brain (Figure 8b). Expression of a constitutively dimerized activated form of Egfr (lambda-Egfr) caused R1-R6 axons to bypass the lamina and shoot into the medulla, reminiscent of the *Ptp69D* loss of function phenotype (Figure 8a). Expression of either RasN17, a dominant-negative form of Ras, or a dominant-negative intracellular deletion of Egfr caused axons to stop above the lamina

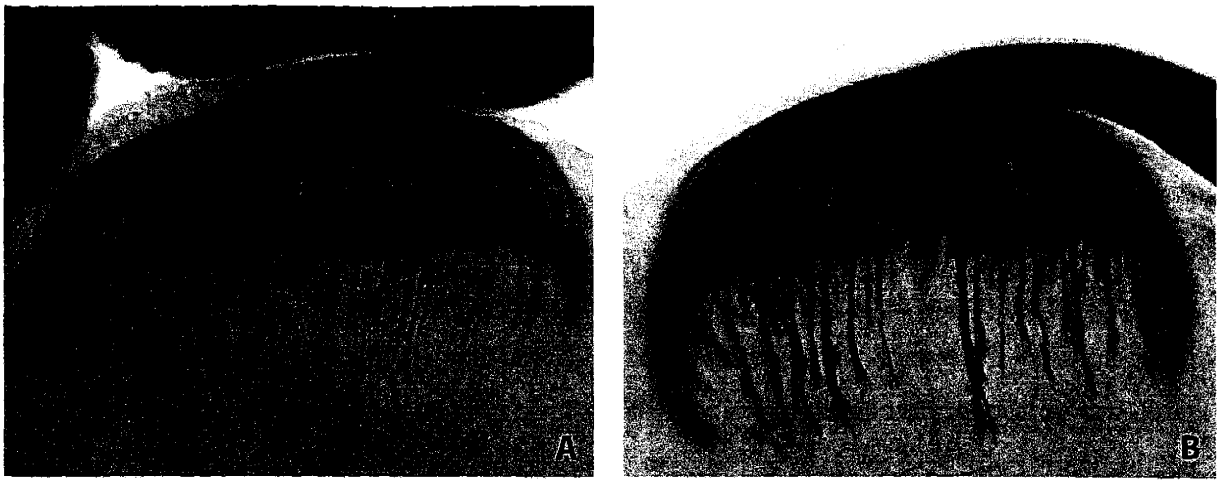

GMR-Gal4; UAS-Ptp69DΔC

GMR-Gal4; UAS-Ptp69DΔC; *FasIII, robo*^{Z570}/+,+

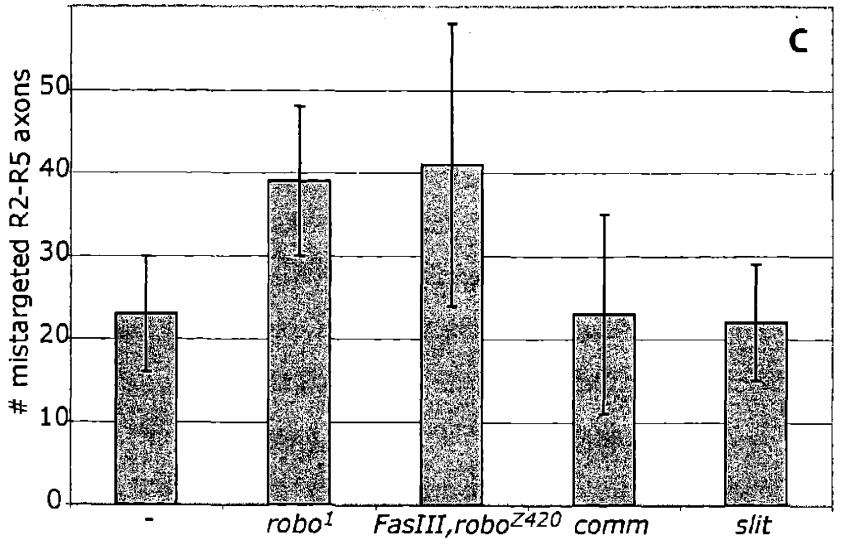

Figure 6. robo dominantly enhances the Ptp69DΔC phenotype. Dissections and staining were as in Figure 3. (A) GMR-Gal4; UAS-Ptp69DΔC. (B) GMR-Gal4; UAS-Ptp69DΔC; *FasIII,robo*^{Z570}/+,+. Removing a single copy of *FasIII* and *robo* enhances the Ptp69DΔC phenotype. (C) Quantitation of R2-R5 mistargeting in GMR-Gal4; UAS-Ptp69DΔC animals heterozygous for the indicated alleles. Two alleles of *robo* strongly enhance the Ptp69DΔC phenotype, but neither comm nor slit has any effect.

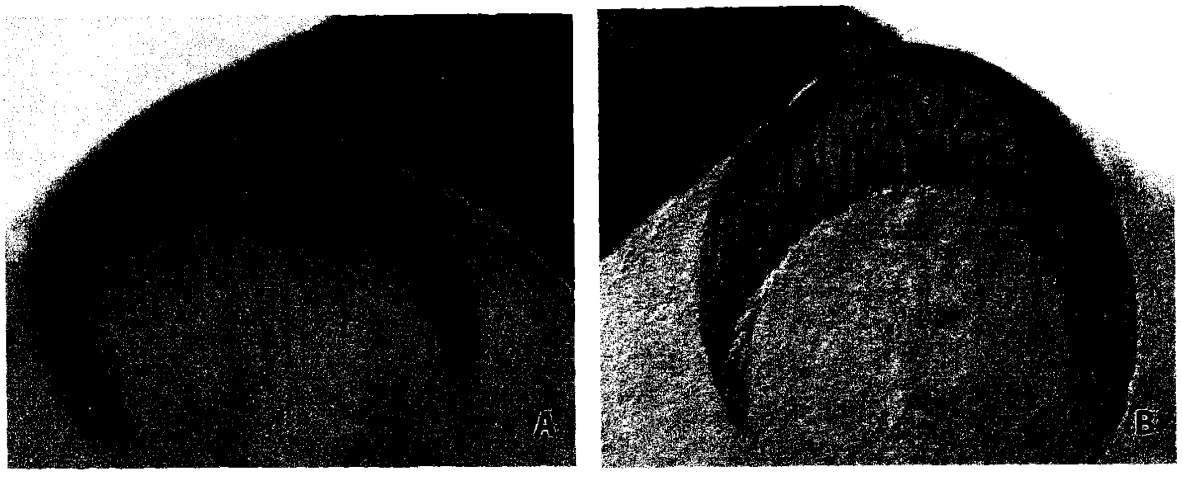

GMR-Gal4; UAS-Ptp69DΔC; *Egfr*^{f8}/+ GMR-Gal4; UAS-Ptp69DΔC; *Ras85D*/+

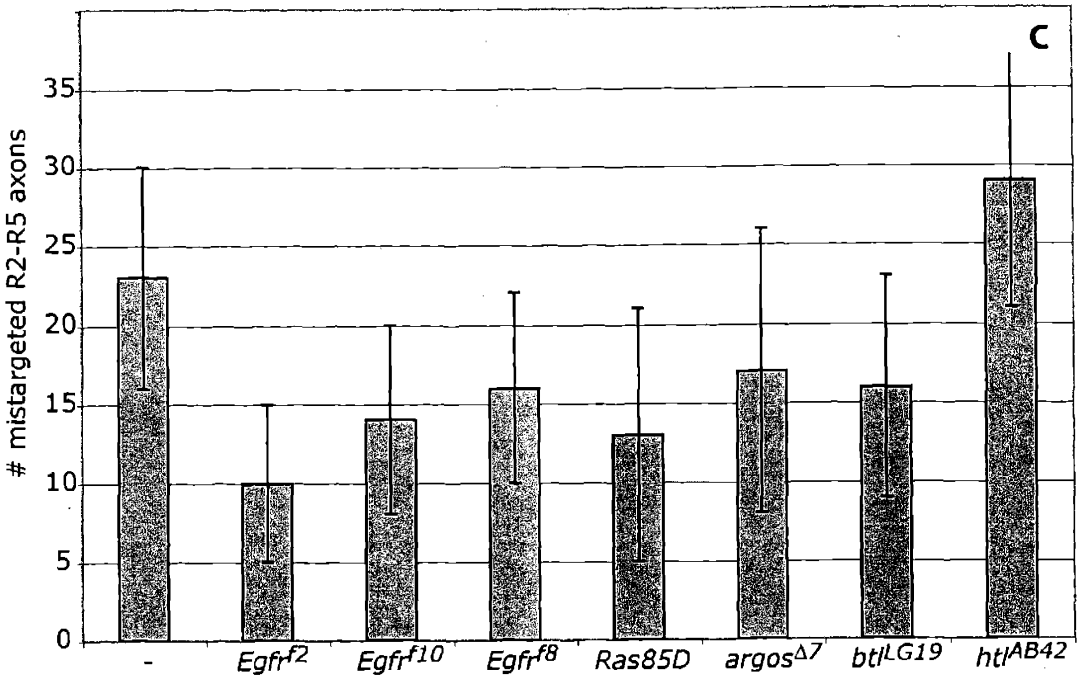

Figure 7. Mutations in *Egfr* or *Ras* dominantly suppress the mistargeting caused by Ptp69DΔC. Dissections and staining were as in Figure 3. (A) GMR-Gal4; UAS-Ptp69DΔC; *Egfr*^{f8}/+. *Egfr*^{f8} dominantly suppresses the Ptp69DΔC phenotype. (B) GMR-Gal4; UAS-Ptp69DΔC; *Ras85D*/+. *Ras85D* dominantly suppresses the Ptp69DΔC phenotype. (C) Quantitation of results depicted in (A-B) and other receptor tyrosine kinases not shown. Three alleles of *Egfr* dominantly suppress Ptp69DΔC to varying degrees. The Egfr ligand argos and the FGF receptor btl had a minimal effect. The FGF receptor htl had no effect.

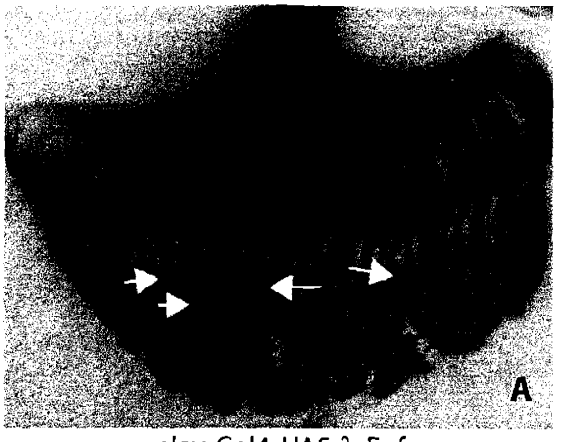

elav-Gal4; UAS-λ-Egfr

elav-Gal4; UAS-Ras^{V12}

elav-Gal4; UAS-λ-Egfr

elav-Gal4; UAS-EgfrΔC

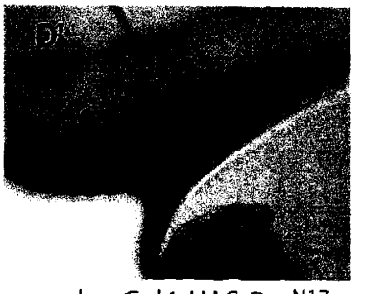

elav-Gal4; UAS-Ras^{N17}

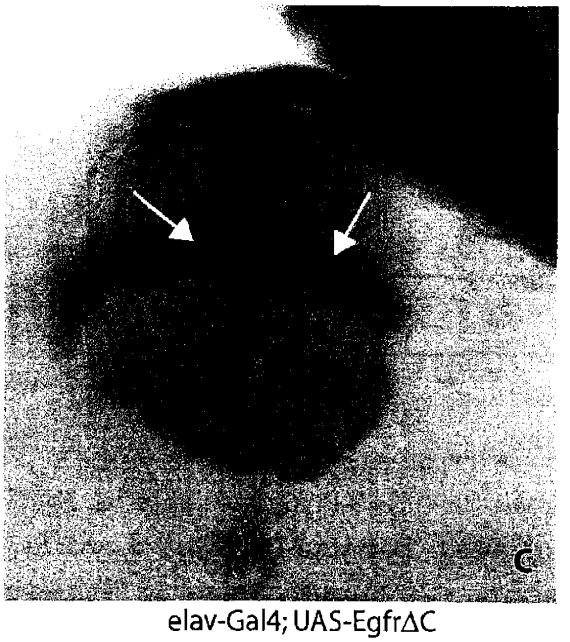

elav-Gal4; UAS-EgfrΔC

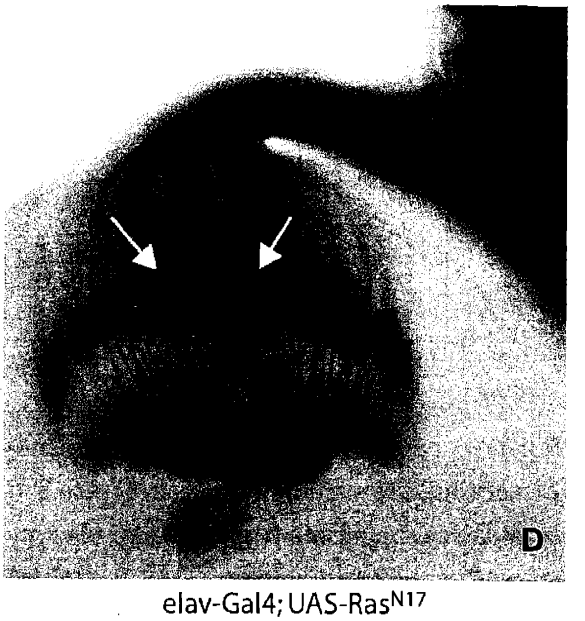

elav-Gal4; UAS-Ras^{N17}

(Figure 8c-d). The eye discs in all of these animals develop normally (Figure 8a'-d'), indicating that photoreceptor development is not perturbed by expression of these constructs.

A substrate trapping form of Ptp69D displays dominant CNS phenotypes

In the catalytic cleft of tyrosine phosphatases, an aspartate residue serves as a proton acceptor for the catalytic cysteine (Zhang et al., 1994). When this aspartate is mutated to alanine, the phosphatase is still able to bind its phosphorylated substrate, but the catalytic reaction cannot proceed and the substrate remains bound to the phosphatase. These mutants have been dubbed "substrate traps" (Flint et al., 1997). Ptp69D has two tandem phosphatase domains in its intracellular domain. Only the membrane-proximal of these is thought to be catalytically active, although the terminal domain may still be able to bind substrates. A mutant protein in which only the membrane-proximal phosphatase domain is converted to a substrate trap ($Ptp69D^{DA1}$) is able to partially rescue the *Ptp69D* loss of function phenotype. However, a mutant protein in which both phosphatase domains are mutated ($Ptp69D^{DA3}$) does not rescue the *Ptp69D* phenotype (Garrity et al., 1999). To determine whether the substrate-trapping versions of Ptp69D have a dominant phenotype, I expressed them in all postmitotic neurons using the elav promoter. I tested six insertions of the UAS-$Ptp69D^{DA1}$ transgene and two insertions of the $Ptp69D^{DA3}$ transgene (Figure 9). Three of the UAS-$Ptp69D^{DA1}$ lines were partially lethal when

Figure 8. Egfr or Ras activity is necessary and sufficient to drive photoreceptor axons forward. Eye-brain complexes were dissected from third instar larvae and stained with mAb 24B10, which labels all photoreceptor axons. Dominant negative or dominant active Egfr or Ras was expressed in all postmitotic neurons using elav-Gal4. (A) elav-Gal4; UAS-λEgfr. Dominant active Egfr causes R1-R6 to mistarget to the medulla. Thicker-than-normal bundles can be seen projecting into the medulla (arrows). (B) elav-Gal4; UAS-RasV12. Dominant active Ras disrupts the structure of the lamina, suggestive of defects in the lamina target region. (C) elav-Gal4; UAS-EgfrDC. (D) elav-Gal4; UAS-RasN17. Both dominant negative Egfr and dominant negative Ras cause photoreceptor axons to stop before reaching their targets (arrows). (A',C',D') Eye discs corresponding to the brains depicted in (A, C, and D). Eye development proceeds normally in these animals.

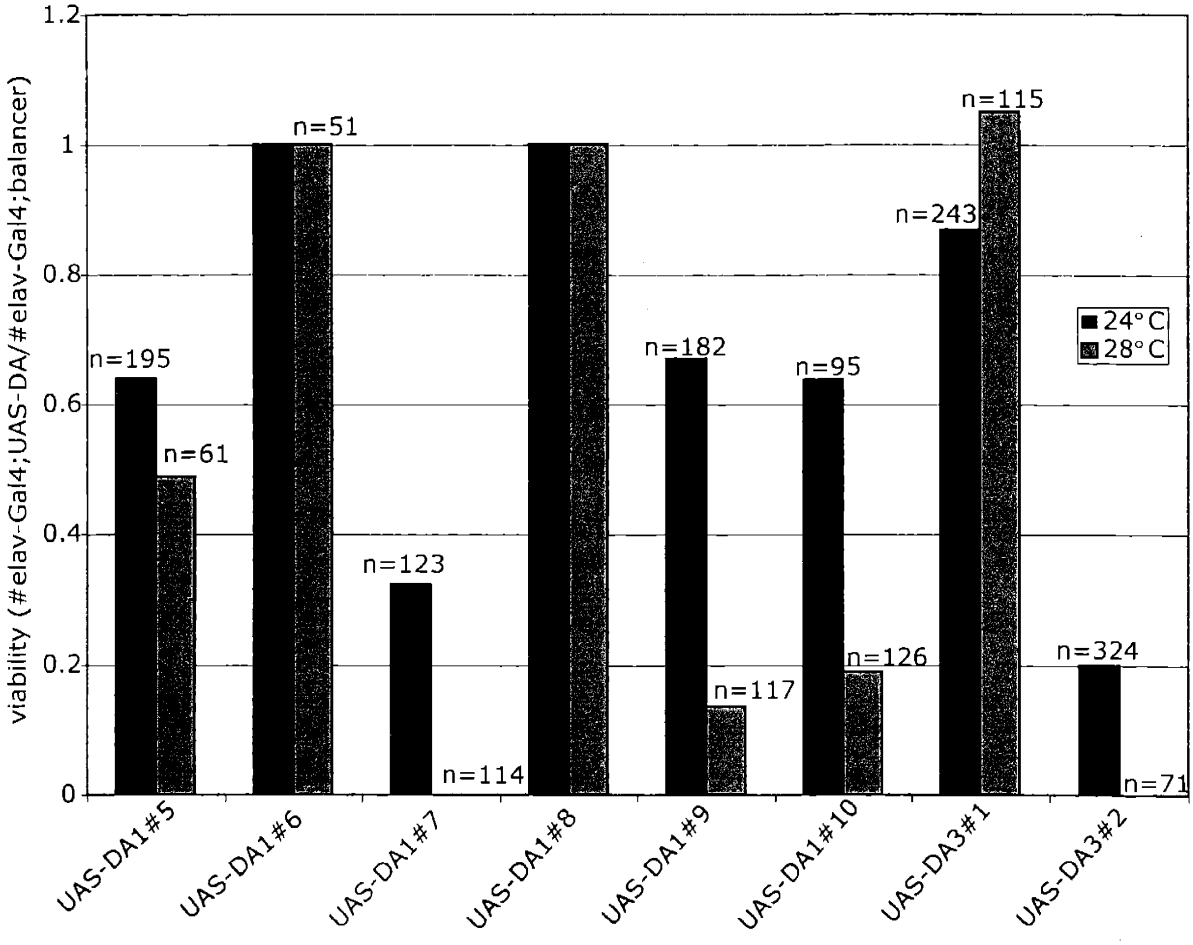

Figure 9. Expression of Ptp69D substrate traps in neurons is lethal. elav-Gal4 homozygotes were crossed to various balanced substrate trap insertions. Progeny were grown at 24°C or 28°C. Gal4 has higher activity at higher temperatures, resulting in elevated transgene expression. Values are expressed as a ratio of the actual number to the expected number of elav-Gal4;UAS-DA flies. The expected number was determined by the number of balancer-carrying progeny.

crossed to elav-Gal4. UAS-Ptp69D^{DA1}#7, which has two insertions of the transgene on one chromosome, is partially lethal when the flies are grown at 25°C and fully lethal at 28°C, which induces a higher level of Gal4 expression. Of the two UAS-Ptp69D^{DA3} lines, one causes partial lethality at 25°C and complete lethality at 28°C.

Ptp69D displays a requirement for choicepoint navigation in all three major embryonic motor nerves, ISN, ISNb, and SNa, when mutated in combination with other phosphatases such as Ptp99A or Dlar (Desai et al., 1996; Desai et al., 1997). I examined whether the motor nerve projections were also disturbed in embryos expressing the double substrate trap in neurons. I found that expression of Ptp69D^{DA3} caused all three motor nerves to stall before reaching their respective targets. ISN stalled before reaching its final targets in 14.7% of segments (n=109; Figure 10a). ISNb stalled before reaching the ventrolateral muscles in 24.8% of segments (Figure 10c); an additional 5.5% of segments had other defects in ISNb, including bypass and mistargeting. SNa was lacking its dorsal-extending branch in 34.7% of segments (Figure 10e) and the lateral-extending branch in 8.3% of segments.

Figure 10. Expression of Ptp69D substrate traps in neurons causes embryonic motor axons to stall before reaching their targets. Stage 16-17 embryos were stained with antibody against Fasciclin II, which labels all motor neurons and their axons. Stained embryos were filleted and mounted with the inside surface of the body wall facing up. (B,D) Wildtype. (A,C,E) elav-Gal4; UAS-Ptp69DDA3. (A) ISN normally reaches past the trachea by stage 16 (left and right segments), but stalls before reaching the trachea in some segments. (B) Axons of ISNb normally defasciculate from the primary nerve at defined branchpoints to innervate the ventrolateral muscles. However, in animals expressing the substrate trap (C), ISNb often forms a clump and stalls before entering the muscle region. In ISNb of the segments depicted, a single axon escapes from the clump to contact muscle 13. This pattern is not typical. (D) SNa normally forms a dorsal branch (D) and a lateral branch (L). However, in substrate trap-expressing embryos (E), the dorsal branch is frequently missing and the lateral branch is occasionally missing (not shown).

elav-Gal4; UAS-Ptp69D^{DA3}

wildtype

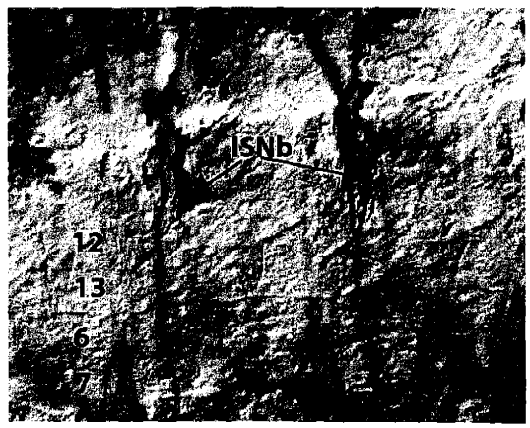

elav-Gal4; UAS-Ptp69D^{DA3}

wildtype

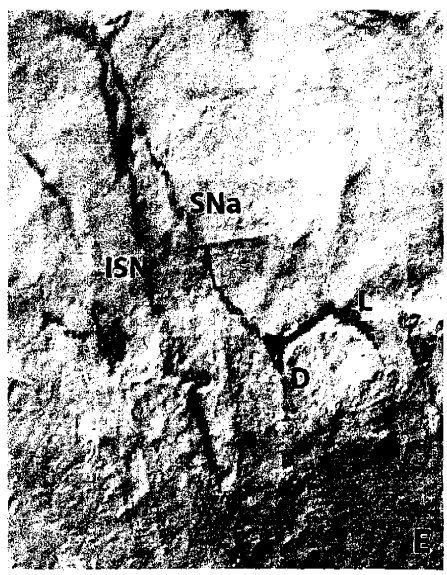

elav-Gal4; UAS-Ptp69D^{DA3}

I also tested whether expressing the substrate traps using other Gal4 drivers could generate any dominant phenotypes. A number of drivers caused lethality, especially when the flies were grown at 28°C. The full data set is presented in Figure 11. Of particular note, when $Ptp69D^{DA1}$ was expressed using c701b-Gal4 at 28°C, 43.5% of adult animals had deformities in the third legs (n=24). Deformed legs had the correct number of segments, but were curled under rather than extending straight as in wild type. c701b-Gal4 has been reported to be expressed throughout the eye disc, in the brain, and in the anterior region of the wing, haltere, and leg discs (Manseau et al., 1997).

Biochemical screen for Ptp69D substrates

As an additional approach to identifying downstream components of the Ptp69D signaling pathway, I used the membrane-proximal phosphatase domain substrate trap fused to a GST moiety (GST-DA1) to biochemically purify potential substrates from Schneider cell extracts. The use of Schneider cells has several advantages: Schneider cells grow relatively quickly, one can obtain large numbers of cells fairly easily, and the cells express *Ptp69D* and other genes that are involved in axon guidance.

I was able to selectively pull down five tyrosine-phosphorylated bands from Schneider cell extract, representing a different set of bands than are in bulk cell extract (Figure 12a). These proteins are not pulled down with GST alone or with substrate trap that has been treated with vanadate, an inhibitor that binds the phosphatase active site, suggesting that these proteins bind to the Ptp69D active site. They also do not bind wild type Ptp69D, which suggests that Ptp69D dephosphorylates these proteins. I was able to obtain enough protein for identification by mass spectrometry by using extract from $2x10^9$ cells and staining the gels with Sypro Ruby Red, a fluorescent dye which allows detection of ~100 ng protein (Figure 12b). Five bands approximately corresponding to the five bands seen by phosphotyrosine Western blot were sequenced. Three proteins were identified from each of three gel slices containing the two bands at 45 kD, the band at 105 kD, and the two bands at 200 kD. In the 45 kD doublet were Nmda1, CG7635 (a stomatin homolog), and CG11009 (a WBP-2 homolog). In the 105 kD band were Lasp, Scar, and Belle. In the 200 kD doublet were PR2, lingerer, and Pvr.

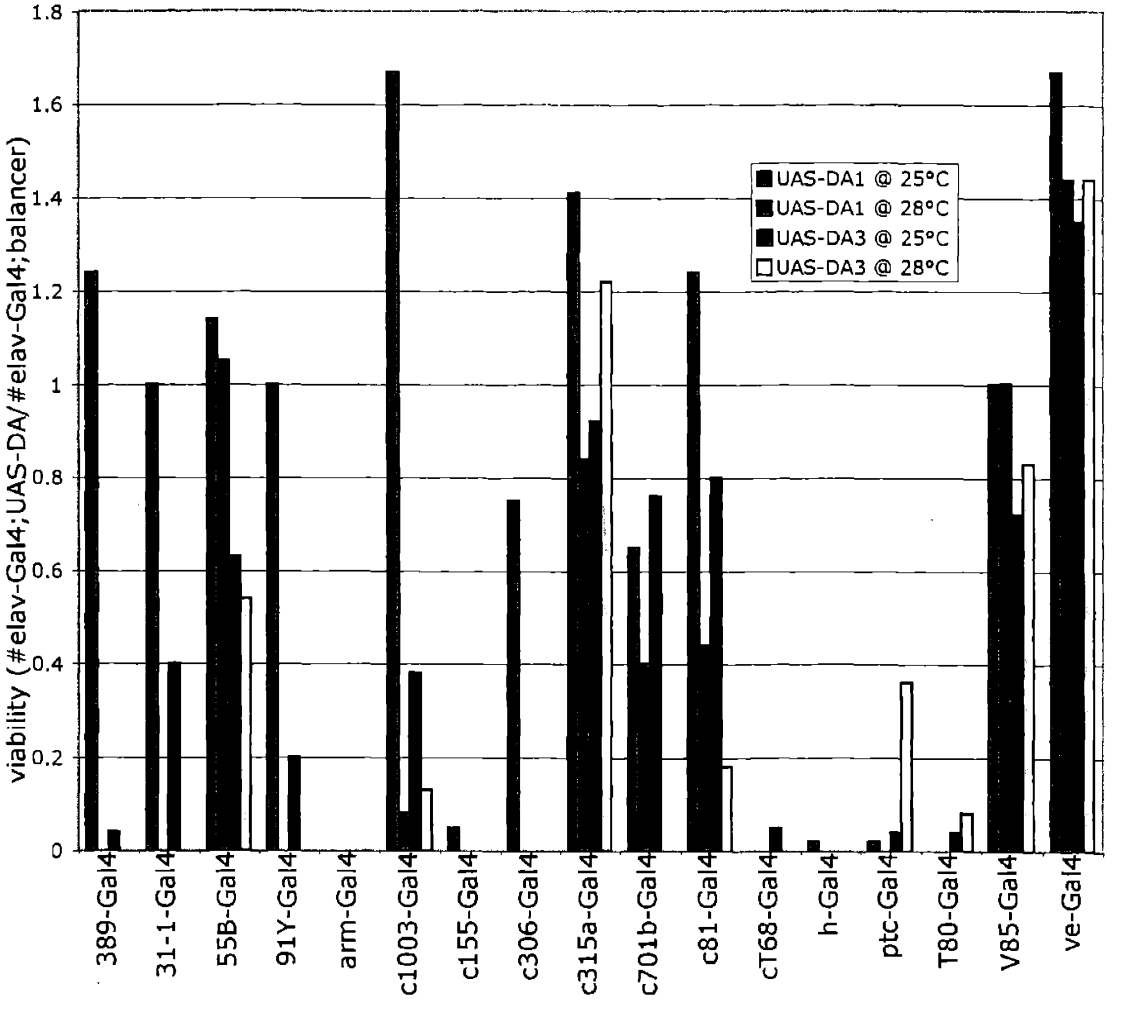

Figure 11. Expression of Ptp69D substrate traps in a variety of neuronal subsets is lethal. UAS-DA1#7 and UAS-DA3#2, which were the most lethal substrate trap insertions when driven with elav-Gal4, were expressed with a number of other Gal4 drivers and tested for their effects on lethality at 25°C and 28°C.

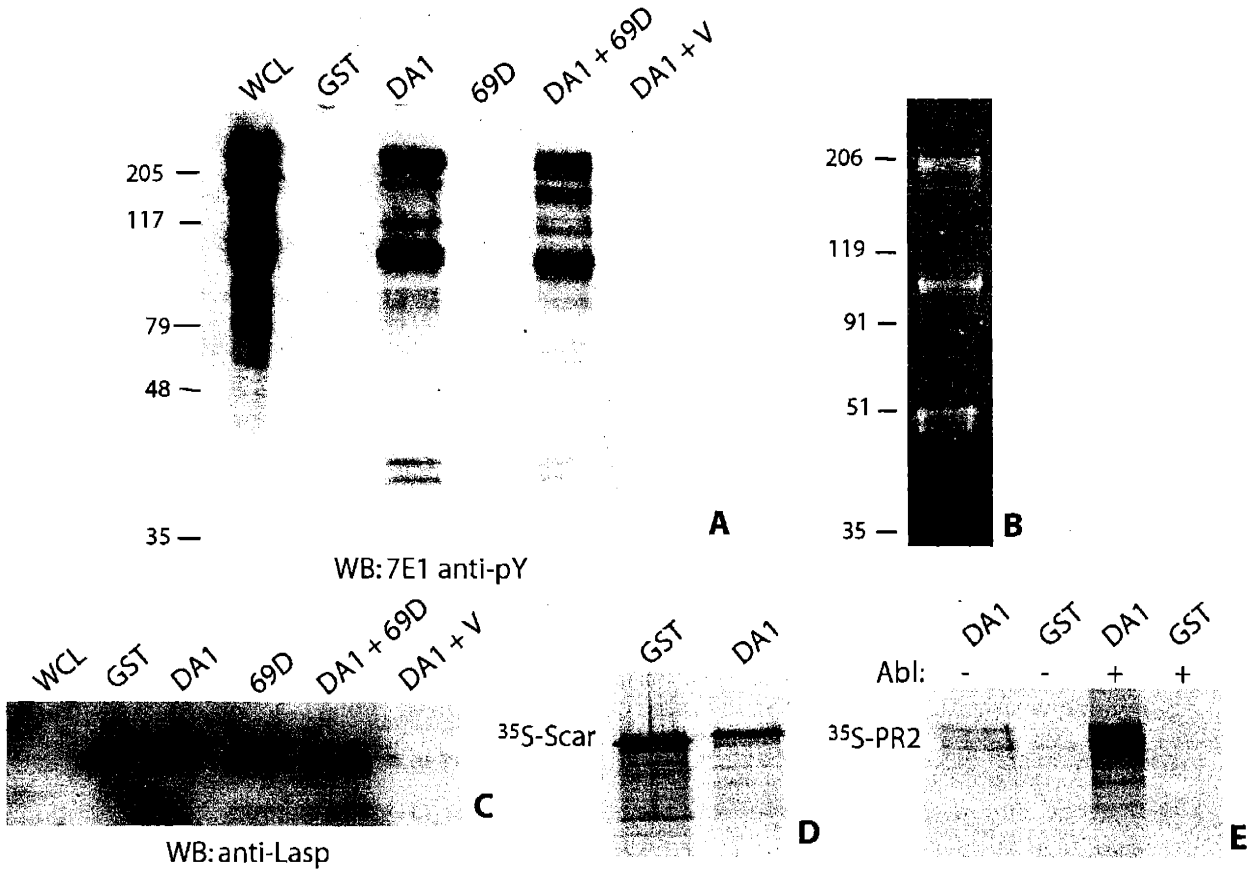

Figure 12. Ptp69D substrate trap selectively binds a few proteins from S2 cells that had been pre-treated with 0.1 mM vanadate. (A) GST fusion proteins were used to bind and pull Ptp69D substrates out of 0.5 ml S2 cell lysate at 1.2 mg/ml protein. WCL: 0.4% of whole cell lysate. GST: glutathione beads bound to GST used in pulldown. DA1: First Ptp69D phosphatase domain substrate trap fused to GST used in pulldown 69D: Wildtype Ptp69D first phosphatase domain fused to GST used in pulldown. DA1 + V: GST-DA1 fusion protein was treated with 0.1 mM vanadate prior to pulldown. Proteins were Western blotted and the Western blot was probed with anti-phosphotyrosine antibody. (B) Ptp69D substrates were trapped as in (A), but using 300 mg of protein from 2.5x109 cells. The gel was stained using Sypro Ruby Red from BioRad. Protein bands were excised and sequenced. (C) Same blot as in (A) reprobed with anti-Lasp antibody. (D) Scar was transcribed and translated in vitro in the presence of ^{35}S. Labeled protein was pulled down with GST or GST-DA1. (E) PR2 protein was synthesized as in (D), but protein was tyrosine phosphorylated with Abl tyrosine kinase prior to pulldowns (lanes 3-4).

Reprobing the blot from Figure 12a with Lasp antibody demonstrated that Lasp binds to GST alone, but binds more strongly to GST-DA1 and GST-69D (Figure 12c). It did not appear to bind to GST-DA1 that had been treated with vanadate. However, these results could not be repeated. The anti-Lasp antibody recognizes a band that runs slightly below the predominant 105 kD tyrosine-phosphorylated band. Radioactively labeled Scar was made *in vitro* and assayed for its ability to bind GST and GST-DA1 (Rita Khodosh; Figure 12d). It was found to bind both GST and GST-DA1 equally well. PR2 was also synthesized and labeled in vitro. It did not bind GST, and was found to bind GST-DA1 more strongly when tyrosine-phosphorylated by Abl (Rita Khodosh; Figure 12e).

Pvr is not co-expressed with Ptp69D, but is required for CNS development

No antibody was available for Pvr, and I anticipated that such a large transmembrane protein would be difficult to translate *in vitro*. I therefore used RNA *in situ* hybridization to determine whether it is expressed in the same cells as Ptp69D. In young embryos, after gastrulation and during germband extension (stages 8-10), Pvr is expressed in a group of cells in the anteroventral part of the embryo, between the stomodeum (an invagination that joins the midgut) and the cephalic furrow. In germband retraction (stages 11-12) the expression becomes more diffuse. During dorsal closure (stages 13-15), Pvr begins to be expressed in the midline glia, and continues to be expressed there through the end of embryogenesis. In stages 16 and 17, expression also comes on in the hemocytes, circulating blood cells that differentiate into macrophages when in contact with dead cell debris (Cho et al., 2002; Heino et al., 2001). Pvr is not expressed in an overlapping pattern with Ptp69D, which would suggest that Pvr is not a physiological substrate of Ptp69D.

Injection of gene-specific dsRNA into the posterior end of pre-cellularization embryos disrupts expression of the corresponding gene. I used RNA interference to determine whether Pvr may have a glial development or axon guidance phenotype. Embryos were injected with 1 mg/ml of a 600 bp dsRNA from a region of the Pvr cDNA encoding the transmembrane domain. Staining injected embryos with slit antibody showed that the midline glia are present and in roughly the right positions (Figure 14a-b). Repo antibody staining indicated that longitudinal glia are present in roughly normal numbers, although their arrangement was disrupted (Figure 14c-d). I observed that the nervous system in these embryos develops normally for the most

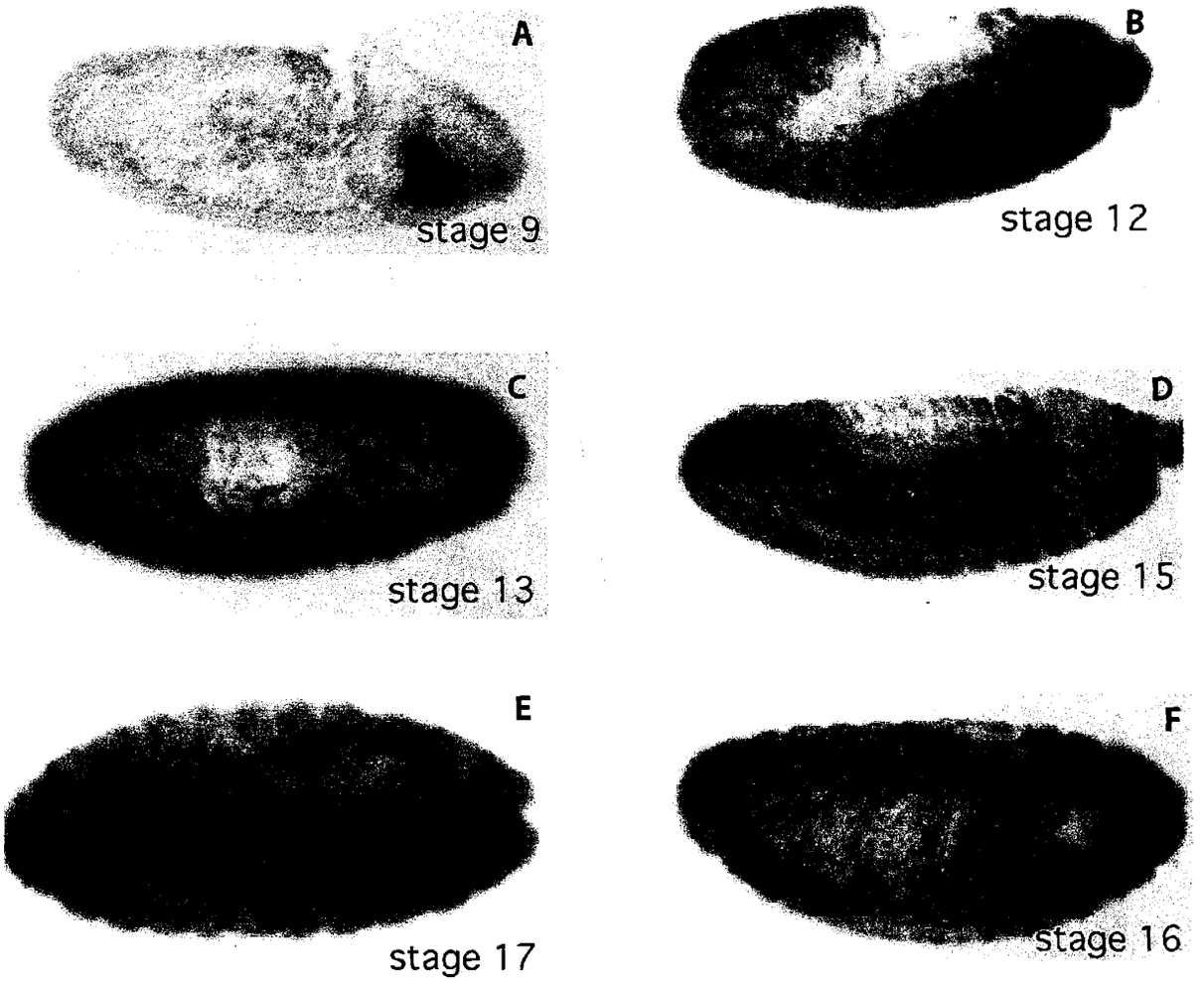

Figure 13. Pvr mRNA expression pattern throughout embryonic development. Anterior is to the right in all images and dorsal is up in A, B, D, and F. (A) Stage 9. (B) Stage 12. (C) Stage 13. (D) Stage 15. (E) Stage 17. (F) Stage 16.

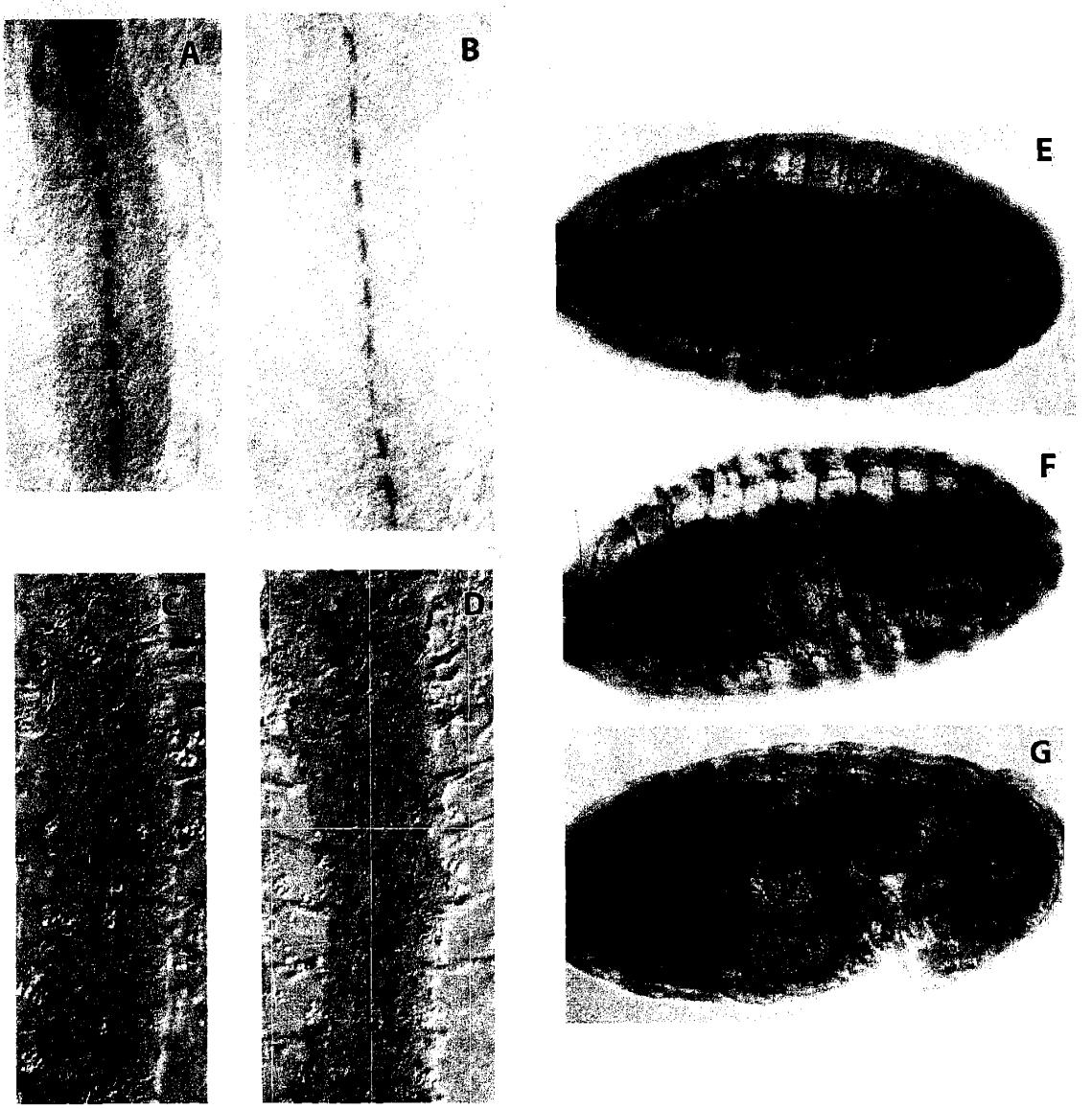

Figure 14. Pvr RNAi embryonic phenotypes. (A-B) Embryos were stained with anti-slit antibody to detect midline glia. (A) Control injected. (B) Pvr RNAi. (C-D) Embryos were stained with anti-repo antibody to detect longitudinal glia. (C) Wildtype. (D) Pvr RNAi. (E-G) Embryos were stained with anti-FasII to detect CNS and motor axons. 13% of injected embryos are like wildypte (E), 80% of inject embryos fail to contract the nerve cord (F), and 7% of injected embryos fail germband retraction (G).

part, although in 80% of embryos the nerve cord fails to contract (Figure 14f) and an additional 7% of injected embryos fail to complete germband retraction (Figure 14g). Increasing the dsRNA concentration to 4 mg/ml increased the percentage of embryos that fail germband retraction to 26% and caused slight defasciculation of the longitudinal axons (data not shown).

DISCUSSION

Ptp69D is a receptor tyrosine phosphatase involved in axon guidance in the embryonic central nervous system and motor nerves and in photoreceptor R1-R6 axon targeting. I have sought to understand the mechanism by which Ptp69D acts to stop R1-R6 axons at the lamina. There is considerable evidence that other mammalian receptor tyrosine phosphatases exist as inactive homodimers. A wedge motif in the membrane-proximal phosphatase domain binds and inhibits the active site in trans when homodimerized (Jiang et al., 1999; Majeti et al., 1998). It is thought that these phosphatases are activated through monomerization or an otherwise open conformation of the intracellular domain (Blanchetot et al., 2002). It is unlikely that Ptp69D is activated in this manner. First, a Ptp69D construct in which the wedge motif is mutated completely rescues the Ptp69D loss-of-function phenotype (Garrity et al., 1999). Second, I have found that a construct in which the intracellular domain of Ptp69D is deleted acts as a dominant negative phosphatase. If homodimers were inactive, overexpression of an intracellular deletion should act as a dominant active. Finally, expression of the Ptp69D intracellular deletion enhances lethality in a *Ptp69D* mutant background. These data combine to suggest a model in which Ptp69D monomers are inactive, but when Ptp69D heterodimerizes with another receptor, either Ptp69D itself is activated or Ptp69D activates its coreceptor. This coreceptor has not been identified. It could be another receptor tyrosine phosphatase such as Lar or Ptp99A, or it could be a non-phosphatase axon guidance receptor such as robo or Egfr.

In order to further understand how Ptp69D acts to stop R1-R6 axons at the lamina, I sought to identify other components of the Ptp69D signaling pathway using both a genetic and a biochemical approach. Overexpression of Ptp69DλC causes a dominant R1-R6 mistargeting

phenotype that can be enhanced by removal of one copy of endogenous Ptp69D and suppressed by concomitant overexpression of wild type Ptp69D. I was able to identify a number of other genes that were capable of enhancing or suppressing the Ptp69DλC phenotype.

I found that a mutation in the cytoplasmic tyrosine kinase Src64 dominantly enhances both the Ptp69DλC overexpression phenotype and the *Ptp69D* loss-of-function phenotype. In mammalian systems, Src has been found to be catalytically active and bound to the cytoskeleton when dephosphorylated at Y527 (Cooper and King, 1986; Helmke and Pfenninger, 1995). It has been suggested that Ptp-alpha, a mammalian receptor tyrosine phosphatase, is recruited to focal adhesion complexes in response to integrin binding laminin, and that once there it dephosphorylates and activates Src (Helmke et al., 1998). Activated Src could then serve to attach the focal adhesion complex to the cytoskeleton, thus anchoring the cell at the attachment site. A similar model could be operating in R1-R6 targeting. When R1-R6 growth cones reach the lamina, Ptp69D could be recruited to focal adhesion sites to dephosphorylate Src, which would in turn allow the growth cone to attach to its targets in the lamina. Loss of function in *Ptp69D* would lead to diminished Src activity, which would prevent R1-R6 growth cones from attaching at the lamina. To test this hypothesis, it would be interesting to see whether Ptp69D is capable of dephosphorylating Src64 and whether Src64 is hyperphosphorylated in the absence of Ptp69D. There is one homolog of C-Src kinase in *Drosophila*, Csk. Mutations in Csk would be expected to dominantly suppress the Ptp69DλC overexpression or *Ptp69D* loss of function phenotypes, although they may not display an R1-R6 targeting phenotype as single mutants. Experiments with Ptp-alpha and Src were done with growth cone particles (GCPs) from homogenized rat brain (Helmke et al., 1998). Similar experiments could be done with larval or pupal brains to determine whether Ptp69D is recruited to adhesion complexes in the presence of laminin. Single mutations in *Drosophila* integrins did not have a dominant effect on the Ptp69DλC phenotype, but this could be due to redundancy between the integrins. It would be difficult to examine the effect of integrin loss of function on photoreceptor axon guidance, as the integrins are required for ommatidial assembly (Zusman et al., 1993; Zusman et al., 1990). However, expression of laminin at the lamina and/or expression of integrins in photoreceptor growth cones would lend support to this hypothesis.

Mutations in both the axon guidance receptor *robo* and the cytoplasmic tyrosine kinase *Abl* were found to dominantly enhance the Ptp69DΔC phenotype. In addition, overexpression of wild type Abl suppressed the Ptp69DΔC phenotype, although overexpression of a kinase-dead form of Abl had no effect. These data suggest that Abl kinase activity is required with Ptp69D to stop axons at the lamina. However, in *Abl* mutant animals, photoreceptor axons stall before reaching their targets, suggesting that Abl is also required for axon outgrowth, although Abl may also be required for development of the target region. *Abl* and *robo* have been found to genetically interact in axon guidance in the embryonic central nervous system (Bashaw et al., 2000). *Abl* mutations were found to dominantly suppress the midline crossing defects of *robo,slit* heterozygotes, and overexpression of Abl enhanced the *robo,slit* heterozygous phenotype. The authors of this study also found that Abl phosphorylates robo, which they propose to be inactivating. However, more recently it has been shown that *Abl* loss of function or gain of function can cause axons to aberrantly cross the midline (Hsouna et al., 2003). Thus, Abl's function in axon guidance is clearly complex, and it may feed into multiple signal transduction pathways to fine-tune whether a growth cone extends forward or stops. In photoreceptor axon guidance, a model in which robo is activated through dephosphorylation is consistent with the interaction that I see between Ptp69D and robo; it is possible that Ptp69D dephosphorylates and activates robo, which causes axons to stop. However, no *robo* loss-of-function phenotype has been observed in photoreceptor axons, although this may be due to redundant robo activity (Tim Tayler, unpublished data). Ptp69D activity may also be somehow redundant with robo activity. Abl may also interact with robo in photoreceptors, but it is clear from Abl's interactions with Ptp69DΔC that Abl and Ptp69D do not act antagonistically, for example by respectively phosphorylating and dephosphorylating robo. Abl may perform some previously undescribed function in its interaction with Ptp69D. It may phosphorylate and activate Ptp69D to dephosphorylate robo (or Src), or conversely Ptp69D could dephosphorylate Abl and activate it to promote stopping through another pathway. It would be worthwhile to see whether Ptp69D is capable of dephosphorylating robo or Abl and whether tyrosine-phosphorylated Abl or robo could be pulled out of a lysate using the Ptp69D substrate trap. It would also be interesting to see whether Ptp69D is phosphorylated in the presence of Abl. If it is, one could mutate the phosphorylated tyrosine to phenylalanine to assess whether that phosphorylation was required for Ptp69D function.

The Ras signaling pathway has been well studied for its roles in differentiation, cell type specification, and cell survival. Several members of this pathway, including the adaptor protein drk, the Ras activator Sos, and Ras itself were identified as members of a single pathway activated by both sevenless and Egfr receptor tyrosine kinases during the development of the Drosophila retina. (Olivier et al., 1993; Rozakis-Adcock et al., 1993; Simon et al., 1991; Simon et al., 1993). The Egfr/Ras pathway is used over and over again throughout development, and even in the retina is used to specify almost every cell type (Dominguez et al., 1998). Due to the central role of the Egfr signaling pathway in cell type determination and survival, it has not been feasible to ascertain whether this pathway also plays a role in later steps in cell differentiation, such as axon outgrowth or other cell shape changes. The EGF receptor has been shown to be involved in cell migration in mammalian tissue culture systems (Chen et al., 1994a), with phospholipase C and gelsolin required downstream, but not involving MAP kinase (Chen et al., 1996; Chen et al., 1994b; Xie et al., 1998). The Egfr has also been shown to modify *neuroglian* mutant defects in ocellar axon guidance in *Drosophila*, but the *Egfr* loss-of-function defects are difficult to interpret in this system (Garcia-Alonso et al., 2000). I have found that mutations in *Egfr* or *Ras85D* dominantly suppress the Ptp69DλC photoreceptor mistargeting phenotype. Consistent with this finding, I have also found that overexpression of dominant-active Egfr in postmitotic neurons causes R1-R6 axons to mistarget to the medulla, phenocopying *Ptp69D* loss of function. Conversely, expression of dominant-negative Egfr or Ras causes photoreceptor axons to stop before reaching their targets. These data suggest a role for Egfr and Ras in axon extension and suggest that Ptp69D may act to inhibit that pathway once R1-R6 axons reach the lamina. These interactions could be confirmed and extended with a number of genetic experiments. First, I would like to see that *Egfr* and *Ras* loss of function could also suppress the *Ptp69D* loss-of-function phenotype. *Elp* is a dominant active *Egfr* allele that is viable when heterozygous. *Elp* should dominantly enhance both the Ptp69DλC and *Ptp69D* loss-of-function phenotypes. The experiments I have done with dominant forms of Egfr and Ras were done by expressing these constructs in all neurons. To ensure that the phenotypes I see are not due to defects generated in the target region, I would express the dominant negative and active forms using glass-Gal4, which drives expression specifically in postmitotic photoreceptors. To determine whether Ptp69D acts upstream or downstream of

Egfr, I would co-express the dominant negative forms of each protein. A *Ptp69D*-like phenotype, with R1-R6 axons mistargeting to the medulla, would suggest that Ptp69D acts downstream of Egfr, perhaps by dephosphorylating a downstream component. An early stopping phenotype, reminiscent of dominant negative Egfr or Ras, would suggest that Ptp69D acts upstream of Egfr, perhaps deactivating one of the proteins through dephosphorylation or preventing activation by binding and preventing Egfr homodimerization. I would also want to test other components of the Egfr/Ras pathway both for phenotypes by themselves and for interactions with Ptp69D. These would include the adaptor proteins drk and Shc, the guanine nucleotide exchange factor Sos, and MAP kinase. I would also want to test the molecules that have been shown to act downstream of Egfr in fibroblast motility, such as PLC-gamma (Wells et al., 1999), PKC-delta (Iwabu et al., 2004), and Gelsolin (Chen et al., 1996).

I have also taken a biochemical approach to identify the downstream substrates of Ptp69D. I used a substrate-trapping version of the Ptp69D membrane-proximal phosphatase domain fused to GST (GST-DA1) to pull substrates out of *Drosophila* Schneider S2 cell lysate. I purified nine proteins that bind to the GST-DA1 fusion protein. One of these, Scar, was found to also bind GST alone. Lasp and PR2 appear to preferentially bind GST-DA1, but these interactions were not pursued further. Lasp is an actin-binding protein with LIM and SH3 domains. Human Lasp localizes to F-actin-rich cell extensions and is phosphorylated by constitutively-active Src (Schreiber et al., 1998). No studies have been done on *Drosophila* Lasp. PR2 is a cytoplasmic tyrosine kinase with an SH3 domain and a CRIB (Cdc42/Rac Interactive Binding) domain. There is one functional homolog of PR2 in *C. elegans*, called ARK-1 (Ack-Related tyrosine Kinase). ARK-1 has been shown to genetically interact with the Egfr/Ras pathway in worm vulval development, such that *ark-1* is thought to negatively regulate either *let-23* (*Egfr*) or *sem-5* (*drk*/*Grb*-2). SEM-5 was found to bind ARK-1 in a yeast two-hybrid assay (Hopper et al., 2000). This is consistent with the interactions that I have observed between Ptp69D and the Egfr/Ras pathway. PR2 could be an effector of Ptp69D-induced inhibtion of the Egfr/Ras pathway. In such a model, the Egfr/Ras pathway would serve to drive R1-R6 axons forward into the brain. Ptp69D would stop R1-R6 axons at the lamina by activation or relocalization of PR2, which in turn would inactivate Egfr or drk, potentially through phosphorylation, thus removing the driving force of extension. By this model, mutants

in *PR2* should phenocopy *Ptp69D* loss of function and dominantly enhance the Ptp69DλC phenotype. Mutants in *Ptp69D* or *PR2* would also be expected to dominantly enhance the mistargeting phenotype induced by dominant active Egfr, although the early stopping phenotypes caused by dominant negative Egfr or Ras would be epistatic to *Ptp69D* or *PR2* loss of function phenotypes.

Pvr is not co-expressed with Ptp69D in the embryo, but RNAi on Pvr demonstrated a role for Pvr in CNS morphogenesis. This phenotype was pursued further and is described in the next chapter. CG8715 has since been renamed lingerer, because mutants have a phenotype in male copulatory behavior (Kuniyoshi et al., 2002). As mutants are viable, this gene is unlikely to be required for Ptp69D function, but its involvement in behavior may be due to a defect in axon guidance. Nmda1, CG7635, CG11009, and Belle were not analyzed further for specificity of binding to GST-DA1, and no mutants are available in any of these genes, which prevented us from analyzing them for a genetic interaction with *Ptp69D*.

Tsuboi et al. identified p85, the regulatory subunit of PI3K, as a substrate of CD148, a mammalian receptor tyrosine phosphatase, using the CD148 substrate trap as bait in a yeast three-hybrid assay, co-expressing v-Src to tyrosine-phosphorylate the prey proteins (Nobuo Tsuboi, personal communication; MBC 2002 abstract book). This could be a second approach to identify Ptp69D substrates. Proteins found to bind the Ptp69D substrate trap in yeast could be assayed for their ability to bind to GST-DA3 in vitro. Mutants in the corresponding genes, where available, could be assayed for their ability to genetically interact with Ptp69DλC and *Ptp69D* loss of function in photoreceptor axon guidance.

Based on results from genetic interactions with *Ptp69D*, I have hypothesized three different mechanisms by which Ptp69D could act to stop R1-R6 photoreceptor axons at the lamina. First, Ptp69D could dephosphorylate and activate components of the focal adhesion complex in response to a signal at the lamina. This could act to tether the extending growth cone at the lamina. Second, Ptp69D could feed positively into known axon guidance pathways that induce changes in the cytoskeleton, repelling R1-R6 growth cones from the medulla or attracting them to the lamina. Third, Ptp69D could inhibit the driving force of axon extension when activated by a signal from the lamina. These models are not mutually exclusive; it is likely that Ptp69D, with the other RPTPs, performs multiple functions in R1-R6 guidance. It will require

further experimentation to determine whether any of these models have merit. Further, experiments with Ptp69DλC suggest that Ptp69D acts by heterodimerizing with another receptor. Ptp69D could have multiple co-receptors, activating or deactivating other guidance receptors such as robo or Egfr through dephosphorylation.

MATERIALS AND METHODS

Quantification of R1-R6 mistargeting

Eye-brain complexes were dissected from crawling third instar larvae or white prepupae having the ro-tauLacZ reporter and stained with anti-λ-galactosidase antibody as described. After mounting, the number of stained axons projecting into the medulla region was counted while visualized with a 40X objective on a Zeiss Axioplan upright microscope. If there were bundles of axons projecting into the medulla, as many individual axons as could be discerned within the bundle were counted. Thus, brains with a large number of mistargeted R1-R6 axons may have been undercounted. Only eye-brain complexes that had more than 15 rows of development in the eye were analyzed. P values were determined using the unpaired student t test (http://www.graphpad.com/quickcalcs/ttest1.cfm).

Substrate trap fusion protein construction

The intracellular domains of the Ptp69D substrate trap were cloned into the pGEX-2TK vector. The multiple cloning site of the vector was first modified by inserting an oligonucleotide containing three new restriction sites between the BamHI and EcoRI sites. The sequence of this oligonucleotide, excluding overhangs, is 5'-CATGGCCGGCTCGAG-3', and includes an NcoI site, a NaeI site, and an XhoI site. The modified plasmid was renamed pGEX-2TK+. The substrate-trapping phosphatase domains were amplified by PCR from the GMR-DA3 plasmid (Garrity 1999). The membrane proximal domain (DA1) was amplified using primers 5'-CTGACCCATGGAACTGCAGGGCGAAGAC-3' and 5'-GTCTGACTCGAGGCCAGTAGTTTCTCGAATTC-3'. The terminal domain (DA2) was amplified using primers 5'-GTCTGACCATGGAATTCGAGAAACTACTGGC-3' and 5'-

GTCTGACTCGAGCTCGGCTATGTGATGTAGTC-3'. Both domains were amplified together using the first and last primers. The PCR products were digested with NcoI and XhoI (underlined sequences) and cloned into pGEX-2TK+ that had been digested with the same enzymes. This produced pGST-DA1, pGST-DA2, and pGST-DA3. These plasmids were transformed into BL21(DE3) cells. Cultures were grown in 2XYT with 100 μg/ml ampicillin and 2% glucose to OD600=1.0. Protein expression was induced with 0.05 mM IPTG overnight. Cells were lysed in PBS using a French press and 30 minute incubation with 1% Triton-X 100. Lysates were incubated with 0.5 ml glutathione beads for 30 minutes. The beads were washed 3 times with 10 ml PBS and stored as a 50% slurry in PBS. The highest expression levels were obtained with GST-DA1.

Substrate trap pulldowns

S2 cells were grown to confluence in Schneider's medium supplemented with 10% FBS. Cells were treated with 0.1 mM vanadate prior to lysis to accumulate the phosphorylated forms of substrates, washed in phosphate-buffered saline, and lysed for 30 minutes on ice in lysis buffer (20 mM Tris pH 7.5, 100 mM NaCl, 1% Triton, 1 mM EDTA, 10% glycerol, 5 mM iodoacetic acid, 1 μg/ml aprotinin, 1μg/ml leupeptin, 1 mM benzamidine). Insoluble material was removed by centrifugation, and the lysate was incubated with glutathione-sepharose beads for 1 hour at 4°C to clear away non-specifically binding proteins. 150 μg of cleared lysate was incubated 2 hours at 4°C with 10 μl GST-DA1 beads containing ~2 μg GST-DA1 fusion protein. Beads were washed three times in lysis buffer lacking iodoacetic acid and protease inhibitors. Bound proteins were resolved on a 9% SDS-PAGE gel and transferred to Hybond-P membrane (Amersham). Membranes were probed with 1:1000 7E1 mouse anti-phosphotyrosine antibody (Zymed) and 1:5000 HRP-conjugated goat anti-mouse secondary antibody. Bands were visualized using ECL (Amersham).

Purification of trapped proteins

To scale up the substrate-trapping purification for protein sequencing, 2.5×10^9 log-phase S2 cells were washed and lysed in 30 ml lysis buffer. Lysate containing 300 mg total protein was cleared with 1.5 ml glutathione-Sepharose beads and subsequently diluted to a total volume of 200 ml. Substrates were pulled out using 1 ml glutathione-Sepharose beads containing 1 mg GST-DA1

protein. Beads were washed four times in 40 ml lysis buffer and then boiled for 10 minutes in lysis buffer with 1% SDS. Tyrosine-phosphorylated proteins were pulled out of the cooled, boiled lysate with 700 μl PY20 beads (Zymed) for 1 hour at 4°C. PY20 beads were washed three times with 10 ml lysis buffer and proteins were eluted with 2 ml of 50 mM pNPP for 30 minutes. Eluted proteins were concentrated with Microcon YM-30 filtration units (Millipore) and separated on a 9% SDS-PAGE gel. The gel was stained with Sypro Ruby Red (BioRad) according to manufacturer's protocol. Protein bands were excised and sequenced at the Harvard Microchemistry Facility by microcapillary reverse-phase HPLC nano-electrospray tandem mass spectrometry on a Finnigan LCQ DECA quadrupole ion trap mass spectrometer.

REFERENCES

Acheson, D. W., Kemplay, S. K., and Webster, K. E. (1980). Quantitative analysis of optic terminal profile distribution within the pigeon optic tectum. Neuroscience *5*, 1067-1084.

Bashaw, G. J., Kidd, T., Murray, D., Pawson, T., and Goodman, C. S. (2000). Repulsive axon guidance: Abelson and Enabled play opposing roles downstream of the roundabout receptor. Cell *101*, 703-715.

Bear, J. E., Svitkina, T. M., Krause, M., Schafer, D. A., Loureiro, J. J., Strasser, G. A., Maly, I. V., Chaga, O. Y., Cooper, J. A., Borisy, G. G., and Gertler, F. B. (2002). Antagonism between Ena/VASP proteins and actin filament capping regulates fibroblast motility. Cell *109*, 509-521.

Bennett, R. L., and Hoffmann, F. M. (1992). Increased levels of the Drosophila Abelson tyrosine kinase in nerves and muscles: subcellular localization and mutant phenotypes imply a role in cell-cell interactions. Development *116*, 953-966.

Blanchetot, C., Tertoolen, L. G., Overvoorde, J., and den Hertog, J. (2002). Intra- and intermolecular interactions between intracellular domains of receptor protein-tyrosine phosphatases. J Biol Chem *277*, 47263-47269.

Bolz, J., Castellani, V., Mann, F., and Henke-Fahle, S. (1996). Specification of layer-specific connections in the developing cortex. Prog Brain Res *108*, 41-54.

Chen, P., Gupta, K., and Wells, A. (1994a). Cell movement elicited by epidermal growth factor receptor requires kinase and autophosphorylation but is separable from mitogenesis. J Cell Biol *124*, 547-555.

Chen, P., Murphy-Ullrich, J. E., and Wells, A. (1996). A role for gelsolin in actuating epidermal growth factor receptor-mediated cell motility. J Cell Biol *134*, 689-698.

Chen, P., Xie, H., Sekar, M. C., Gupta, K., and Wells, A. (1994b). Epidermal growth factor receptor-mediated cell motility: phospholipase C activity is required, but mitogen-activated protein kinase activity is not sufficient for induced cell movement. J Cell Biol *127*, 847-857.

Cho, N. K., Keyes, L., Johnson, E., Heller, J., Ryner, L., Karim, F., and Krasnow, M. A. (2002). Developmental control of blood cell migration by the Drosophila VEGF pathway. Cell *108*, 865-876.

Clandinin, T. R., Lee, C. H., Herman, T., Lee, R. C., Yang, A. Y., Ovasapyan, S., and Zipursky, S. L. (2001). Drosophila LAR regulates R1-R6 and R7 target specificity in the visual system. Neuron *32*, 237-248.

Cooper, J. A., and King, C. S. (1986). Dephosphorylation or antibody binding to the carboxy terminus stimulates pp60c-src. Mol Cell Biol *6*, 4467-4477.

Cowan, W. M. (1971). Studies on the development of the avian visual system. UCLA Forum Med Sci *14*, 177-222.

Desai, C. J., Gindhart, J. G., Jr., Goldstein, L. S., and Zinn, K. (1996). Receptor tyrosine phosphatases are required for motor axon guidance in the Drosophila embryo. Cell *84*, 599-609.

Desai, C. J., Krueger, N. X., Saito, H., and Zinn, K. (1997). Competition and cooperation among receptor tyrosine phosphatases control motoneuron growth cone guidance in Drosophila. Development *124*, 1941-1952.

Dodson, G. S., Guarnieri, D. J., and Simon, M. A. (1998). Src64 is required for ovarian ring canal morphogenesis during Drosophila oogenesis. Development *125*, 2883-2892.

Dominguez, M., Wasserman, J. D., and Freeman, M. (1998). Multiple functions of the EGF receptor in Drosophila eye development. Curr Biol *8*, 1039-1048.

Flint, A. J., Tiganis, T., Barford, D., and Tonks, N. K. (1997). Development of "substrate-trapping" mutants to identify physiological substrates of protein tyrosine phosphatases. Proc Natl Acad Sci U S A *94*, 1680-1685.

Frydman, H. M., and Spradling, A. C. (2001). The receptor-like tyrosine phosphatase lar is required for epithelial planar polarity and for axis determination within drosophila ovarian follicles. Development *128*, 3209-3220.

Garcia-Alonso, L., Romani, S., and Jimenez, F. (2000). The EGF and FGF receptors mediate neuroglian function to control growth cone decisions during sensory axon guidance in Drosophila. Neuron *28*, 741-752.

Garrity, P. A., Lee, C. H., Salecker, I., Robertson, H. C., Desai, C. J., Zinn, K., and Zipursky, S. L. (1999). Retinal axon target selection in Drosophila is regulated by a receptor protein tyrosine phosphatase. Neuron *22*, 707-717.

Gertler, F. B., Bennett, R. L., Clark, M. J., and Hoffmann, F. M. (1989). Drosophila abl tyrosine kinase in embryonic CNS axons: a role in axonogenesis is revealed through dosage-sensitive interactions with disabled. Cell *58*, 103-113.

Gertler, F. B., Hill, K. K., Clark, M. J., and Hoffmann, F. M. (1993). Dosage-sensitive modifiers of Drosophila abl tyrosine kinase function: prospero, a regulator of axonal outgrowth, and

disabled, a novel tyrosine kinase substrate [published erratum appears in Genes Dev 1996 Sep 1;10(17):2234]. Genes Dev *7*, 441-453.

Heino, T. I., Karpanen, T., Wahlstrom, G., Pulkkinen, M., Eriksson, U., Alitalo, K., and Roos, C. (2001). The Drosophila VEGF receptor homolog is expressed in hemocytes. Mech Dev *109*, 69-77.

Helmke, S., Lohse, K., Mikule, K., Wood, M. R., and Pfenninger, K. H. (1998). SRC binding to the cytoskeleton, triggered by growth cone attachment to laminin, is protein tyrosine phosphatase-dependent. J Cell Sci *111 (Pt 16)*, 2465-2475.

Helmke, S., and Pfenninger, K. H. (1995). Growth cone enrichment and cytoskeletal association of non-receptor tyrosine kinases. Cell Motil Cytoskeleton *30*, 194-207.

Henkemeyer, M., West, S. R., Gertler, F. B., and Hoffmann, F. M. (1990). A novel tyrosine kinase-independent function of Drosophila abl correlates with proper subcellular localization. Cell *63*, 949-960.

Henkemeyer, M. J., Gertler, F. B., Goodman, W., and Hoffmann, F. M. (1987). The Drosophila Abelson proto-oncogene homolog: identification of mutant alleles that have pleiotropic effects late in development. Cell *51*, 821-828.

Hopker, V. H., Shewan, D., Tessier-Lavigne, M., Poo, M., and Holt, C. (1999). Growth-cone attraction to netrin-1 is converted to repulsion by laminin- 1. Nature *401*, 69-73.

Hopper, N. A., Lee, J., and Sternberg, P. W. (2000). ARK-1 inhibits EGFR signaling in C. elegans. Mol Cell *6*, 65-75.

Hsouna, A., Kim, Y. S., and VanBerkum, M. F. (2003). Abelson tyrosine kinase is required to transduce midline repulsive cues. J Neurobiol *57*, 15-30.

Hubbard, S. R., and Till, J. H. (2000). Protein tyrosine kinase structure and function. Annu Rev Biochem *69*, 373-398.

Inoue, A., and Sanes, J. R. (1997). Lamina-specific connectivity in the brain: regulation by N-cadherin, neurotrophins, and glycoconjugates. Science *276*, 1428-1431.

Iwabu, A., Smith, K., Allen, F. D., Lauffenburger, D. A., and Wells, A. (2004). EGF induces fibroblast contractility and motility via a PKCdelta -dependent pathway. J Biol Chem.

Jiang, G., den Hertog, J., Su, J., Noel, J., Sap, J., and Hunter, T. (1999). Dimerization inhibits the activity of receptor-like protein-tyrosine phosphatase-alpha. Nature *401*, 606-610.

Kaufmann, N., DeProto, J., Ranjan, R., Wan, H., and Van Vactor, D. (2002). Drosophila liprin-alpha and the receptor phosphatase Dlar control synapse morphogenesis. Neuron *34*, 27-38.

Kidd, T., Brose, K., Mitchell, K. J., Fetter, R. D., Tessier-Lavigne, M., Goodman, C. S., and Tear, G. (1998). Roundabout controls axon crossing of the CNS midline and defines a novel subfamily of evolutionarily conserved guidance receptors. Cell *92*, 205-215.

Kimmel, B. E., Heberlein, U., and Rubin, G. M. (1990). The homeo domain protein rough is expressed in a subset of cells in the developing Drosophila eye where it can specify photoreceptor cell subtype. Genes Dev *4*, 712-727.

Kuniyoshi, H., Baba, K., Ueda, R., Kondo, S., Awano, W., Juni, N., and Yamamoto, D. (2002). lingerer, a Drosophila gene involved in initiation and termination of copulation, encodes a set of novel cytoplasmic proteins. Genetics *162*, 1775-1789.

Majeti, R., Bilwes, A. M., Noel, J. P., Hunter, T., and Weiss, A. (1998). Dimerization-induced inhibition of receptor protein tyrosine phosphatase function through an inhibitory wedge. Science *279*, 88-91.

Manseau, L., Baradaran, A., Brower, D., Budhu, A., Elefant, F., Phan, H., Philp, A. V., Yang, M., Glover, D., Kaiser, K., *et al.* (1997). GAL4 enhancer traps expressed in the embryo, larval brain, imaginal discs, and ovary of Drosophila. Dev Dyn *209*, 310-322.

Newsome, T. P., Schmidt, S., Dietzl, G., Keleman, K., Asling, B., Debant, A., and Dickson, B. J. (2000). Trio combines with dock to regulate Pak activity during photoreceptor axon pathfinding in Drosophila. Cell *101*, 283-294.

Olivier, J. P., Raabe, T., Henkemeyer, M., Dickson, B., Mbamalu, G., Margolis, B., Schlessinger, J., Hafen, E., and Pawson, T. (1993). A Drosophila SH2-SH3 adaptor protein implicated in coupling the sevenless tyrosine kinase to an activator of Ras guanine nucleotide exchange, Sos. Cell *73*, 179-191.

Reperant, J., and Angaut, P. (1977). The retinotectal projections in the pigeon. an experimental optical and electron microscope study. Neuroscience *2*, 119-140.

Rozakis-Adcock, M., Fernley, R., Wade, J., Pawson, T., and Bowtell, D. (1993). The SH2 and SH3 domains of mammalian Grb2 couple the EGF receptor to the Ras activator mSos1. Nature *363*, 83-85.

Schindelholz, B., Knirr, M., Warrior, R., and Zinn, K. (2001). Regulation of CNS and motor axon guidance in Drosophila by the receptor tyrosine phosphatase DPTP52F. Development *128*, 4371-4382.

Schreiber, V., Moog-Lutz, C., Regnier, C. H., Chenard, M. P., Boeuf, H., Vonesch, J. L., Tomasetto, C., and Rio, M. C. (1998). Lasp-1, a novel type of actin-binding protein accumulating in cell membrane extensions. Mol Med *4*, 675-687.

Simon, M. A., Bowtell, D. D., Dodson, G. S., Laverty, T. R., and Rubin, G. M. (1991). Ras1 and a putative guanine nucleotide exchange factor perform crucial steps in signaling by the sevenless protein tyrosine kinase. Cell *67*, 701-716.

Simon, M. A., Dodson, G. S., and Rubin, G. M. (1993). An SH3-SH2-SH3 protein is required for p21Ras1 activation and binds to sevenless and Sos proteins in vitro. Cell *73*, 169-177.

Song, H. J., Ming, G. L., and Poo, M. M. (1997). cAMP-induced switching in turning direction of nerve growth cones [published erratum appears in Nature 1997 Sep 25;389(6649):412]. Nature *388*, 275-279.

Tessier-Lavigne, M., and Goodman, C. S. (1996). The molecular biology of axon guidance. Science *274*, 1123-1133.

Wallace, M. J., Fladd, C., Batt, J., and Rotin, D. (1998). The second catalytic domain of protein tyrosine phosphatase delta (PTP delta) binds to and inhibits the first catalytic domain of PTP sigma. Mol Cell Biol *18*, 2608-2616.

Wells, A., Ware, M. F., Allen, F. D., and Lauffenburger, D. A. (1999). Shaping up for shipping out: PLCgamma signaling of morphology changes in EGF-stimulated fibroblast migration. Cell Motil Cytoskeleton *44*, 227-233.

Wills, Z., Bateman, J., Korey, C. A., Comer, A., and Van Vactor, D. (1999). The tyrosine kinase Abl and its substrate enabled collaborate with the receptor phosphatase Dlar to control motor axon guidance. Neuron *22*, 301-312.

Xie, H., Pallero, M. A., Gupta, K., Chang, P., Ware, M. F., Witke, W., Kwiatkowski, D. J., Lauffenburger, D. A., Murphy-Ullrich, J. E., and Wells, A. (1998). EGF receptor regulation of cell motility: EGF induces disassembly of focal adhesions independently of the motility-associated PLCgamma signaling pathway. J Cell Sci *111 (Pt 5)*, 615-624.

Zhang, Z. Y., Wang, Y., and Dixon, J. E. (1994). Dissecting the catalytic mechanism of protein-tyrosine phosphatases. Proc Natl Acad Sci U S A *91*, 1624-1627.

Zusman, S., Grinblat, Y., Yee, G., Kafatos, F. C., and Hynes, R. O. (1993). Analyses of PS integrin functions during Drosophila development. Development *118*, 737-750.

Zusman, S., Patel-King, R. S., Ffrench-Constant, C., and Hynes, R. O. (1990). Requirements for integrins during Drosophila development. Development *108*, 391-402.

Chapter 3.

Macrophage-mediated corpse engulfment is required for normal *Drosophila* CNS morphogenesis

As published in Development 2003 Aug; 130(15):3557-65.

Experiments in Figures 3e-f, 5a-b,i, and 6d,h were done by Caleb Kennedy.

SUMMARY

Cell death plays an essential role in development, and the removal of cell corpses presents an important challenge for the developing organism. Macrophages are largely responsible for the clearance of cell corpses in *Drosophila melanogaster* and mammalian systems. Here we examine the developmental requirement for macrophages in *Drosophila* and find that macrophage function is essential for central nervous system (CNS) morphogenesis. We generate and analyze mutations in the *Pvr* locus, which encodes a receptor tyrosine kinase of the PDGF/VEGF family that is required for hemocyte migration. We find that loss of *Pvr* function causes the mispositioning of glia within the CNS and the disruption of the CNS axon scaffold. We further find that inhibition of hemocyte development or of Croquemort, a receptor required for macrophage-mediated corpse engulfment, cause similar CNS defects. These data indicate that macrophage-mediated clearance of cell corpses is required for proper morphogenesis of the *Drosophila* CNS.

INTRODUCTION

Programmed cell death plays an important role in sculpting tissues and neuronal circuitry during development (Jacobson et al., 1997). In *Drosophila melanogaster*, large numbers of cells die during development, and these deaths serve to shape tissue, to delete unnecessary structures, to control cell numbers and to eliminate damaged or developmentally defective cells (Abrams, 2002; Baehrecke, 2002; Bangs and White, 2000). For example, activation of cell death is essential for sculpting the embryonic head (Lohmann et al., 2002), eliminating cells at metamorphosis (Jiang et al., 1997), limiting the divisions of post-embryonic neuroblasts (Bello et al., 2003), and specifying the precise number of neurons in each cartridge within the lamina ganglion of the visual system (Huang et al., 1998). Such widespread occurrence of cell death creates many cell corpses, and the engulfment and removal of cell corpses is a prominent feature of animal development (Fadok and Chimini, 2001).

Macrophages are responsible for the majority of cell corpse removal during mammalian development (Hopkinson-Woolley et al., 1994; Hume et al., 1983; Morris et al., 1991). In *Drosophila,* cell corpse removal also relies on specialized phagocytic cells that resemble mammalian macrophages in a number of cellular and molecular properties (Franc, 2002). *Drosophila* macrophages are derived from hematopoietic precursor cells termed hemocytes

which differentiate into macrophages displaying phagocytic and scavenger properties in response to cell corpse exposure (Tepass et al., 1994). Work on mammalian macrophages and other phagocytic cells has identified several classes of receptors implicated in corpse recognition, including lectins, integrins, the MER tyrosine kinase, the phosphatidylserine receptor (PSR), and scavenger receptors such as CD36 (Fadok and Chimini, 2001). *Drosophila* macrophages express a CD36-related receptor, Croquemort (Franc et al., 1996), and *croquemort* (*crq*) function is required for macrophages to take up dead cells efficiently in the developing embryo (Franc et al., 1999).

As macrophages are responsible for much of the dead cell engulfment in developing animals, an important role for macrophages in tissue morphogenesis during development has been suggested (Morris et al., 1991). However, direct evidence of a required role for macrophage-mediated cell corpse engulfment in development is limited. In the feet of PU.1 mutant mice that lack macrophages, for example, other cell types take over the engulfing role and permit morphogenesis to proceed, albeit at a slower pace (Wood et al., 2000). In contrast, in the developing mouse retina macrophages are essential for cell death-mediated morphogenesis (Lang et al., 1994; Lang and Bishop, 1993). In this case, the primary defect is not caused by a failure of engulfment. Rather, macrophages are required to initiate the cell deaths that normally eliminate the hyaloid vessels and the pupillary membrane during the development of the mouse eye.

In the CNS of *Drosophila melanogaster* embryos, programmed cell death eliminates many neurons and glia (Jacobs, 2000; Sonnenfeld and Jacobs, 1995b). In the case of the midline glia, approximately ten midline glial cells are generated in each segment by stage 13 of embryonic development. As development proceeds, most of these glia are eliminated by programmed cell death, leaving two to three midline glia per segment by stage 17 (Klambt et al., 1991; Sonnenfeld and Jacobs, 1995a; Zhou et al., 1995). Recent work indicates that midline glial cell survival is mediated through activation of MAP kinase signaling in the midline glia via the reception of the EGFR ligand Spitz, which is provided by the developing neurons (Bergmann et al., 2002). In addition to midline glia, a subset of developing neurons and longitudinal glia (which flank the midline) are also removed through cell death (Hidalgo et al., 2001; Sonnenfeld and Jacobs, 1995b). Electron microscopic studies by Sonnenfeld and Jacobs demonstrated that the majority of cell corpses are expelled from the CNS and engulfed by macrophages

(Sonnenfeld and Jacobs, 1995b). Cell corpses can also be detected in glial cells both within and at the surface of the CNS, indicating that glial cells also contribute to removal of dead cells. These authors also examined macrophage-less embryos derived from *Bic-D* mothers and found an increase in the number of unengulfed cells within the CNS as well as increased numbers in subperineurial glial cells at the periphery of the CNS. However, embryos derived from *Bic-D* mutant mothers have widespread patterning defects (duplication of posterior structures at the expense of anterior structures), complicating analysis of the consequences of macrophage loss on development.

Pvr encodes the *Drosophila* member of the vertebrate PDGF/VEGF receptor tyrosine kinase family (Duchek et al., 2001; Heino et al., 2001). *Pvr* was initially shown by Duchek et al. to regulate border cell migration during oogenesis (Duchek and Rorth, 2001) and subsequently shown by Cho et al. to control hemocyte migration (Cho et al., 2002). Cho et al. found that hemocytes fail to disperse normally in *Pvr* mutant animals and that expression of the Pvr ligand Pvf2 in an ectopic location can attract hemocytes to the site of Pvf2 expression (Cho et al., 2002). We independently isolated mutations in *Pvr* and have used our analysis of *Pvr* as a starting point to investigate the previously unexplored function of hemocytes in CNS development.

In this work, we use a combination of gene targeting by homologous recombination and chemical mutagenesis to create mutations in *Pvr*. We find that *Pvr* mutations, which disrupt hemocyte migration, cause defects in the patterning of the CNS axon scaffold and the positioning of CNS glia without affecting the pattern of midline glial cell death. We further find that *serpent (srp)* mutant animals (which lack hemocytes) and animals in which the function of the macrophage scavenger receptor Croquemort has been inhibited both show defects in CNS patterning similar to those of *Pvr* mutants. Taken together, these data suggest that macrophage-mediated engulfment is necessary for proper *Drosophila* CNS development.

RESULTS

Targeted disruption of the *Pvr* locus

To initiate our studies of *Pvr* function, the *Pvr* locus was disrupted using a recently described procedure for gene disruption by homologous recombination (Fig.1A) (Rong and Golic, 2000; Rong and Golic, 2001). Ten independent homologous recombination events were recovered from the progeny of 3000 females, and the products of the targeting events were examined by a combination of long-range PCR and Southern blotting. Nine of ten targeted insertions, including Pvr^{KO2}, yield the products expected for a successful targeting event in both PCR and Southern blot analysis (Figure 1B and Figure 1C). These alleles all failed to complement the lethality of *Df(2L)TE128x11*, a chromosomal deficiency that removes *Pvr*, completing embryogenesis but failing to hatch. One targeted insertion allele, Pvr^{KO8}, appeared to have undergone a complex combination of DNA insertion and duplication and was not analyzed further.

In addition to creating targeted insertions at the *Pvr* locus, we identified multiple *Pvr* alleles though a genetic non-complementation screen. 9810 lines of EMS-mutagenized flies were screened for failure to complement the lethality of *Df(2L)TE128x11*, a chromosomal deficiency that removes *Pvr*. 185 lethal or semi-lethal lines were recovered, of which twenty failed to complement Pvr^{KO} lethality. Among these putative *Pvr* alleles, we have identified four that carry missense mutations in the extracellular domain, four that create stop codons in the extracellular domain, and three that carry missense mutations in the kinase domain (Figure 2A). The mutations in the kinase domain disrupt residues highly conserved among protein kinases (Hanks et al., 1988; Johnson et al., 1996). In Pvr^{729} an alanine residue in the catalytic loop, highly conserved among tyrosine kinases, is changed to a threonine. In Pvr^{4187} a glutamate residue in the activation loop, highly conserved among all protein kinases, is changed to a lysine. Finally, in Pvr^{7508} an aspartate residue in the DFG motif at the base of the activation loop is changed to a valine. Crystallographic data indicates this residue is involved in the divalent cation binding that contributes to nucleotide triphosphate recognition (Johnson et al., 1996). The recovery of these changes in the kinase region are consistent with the importance of catalytic activity for *Pvr* function. All eleven of these EMS-induced *Pvr* alleles behave as embryonic lethal mutations.

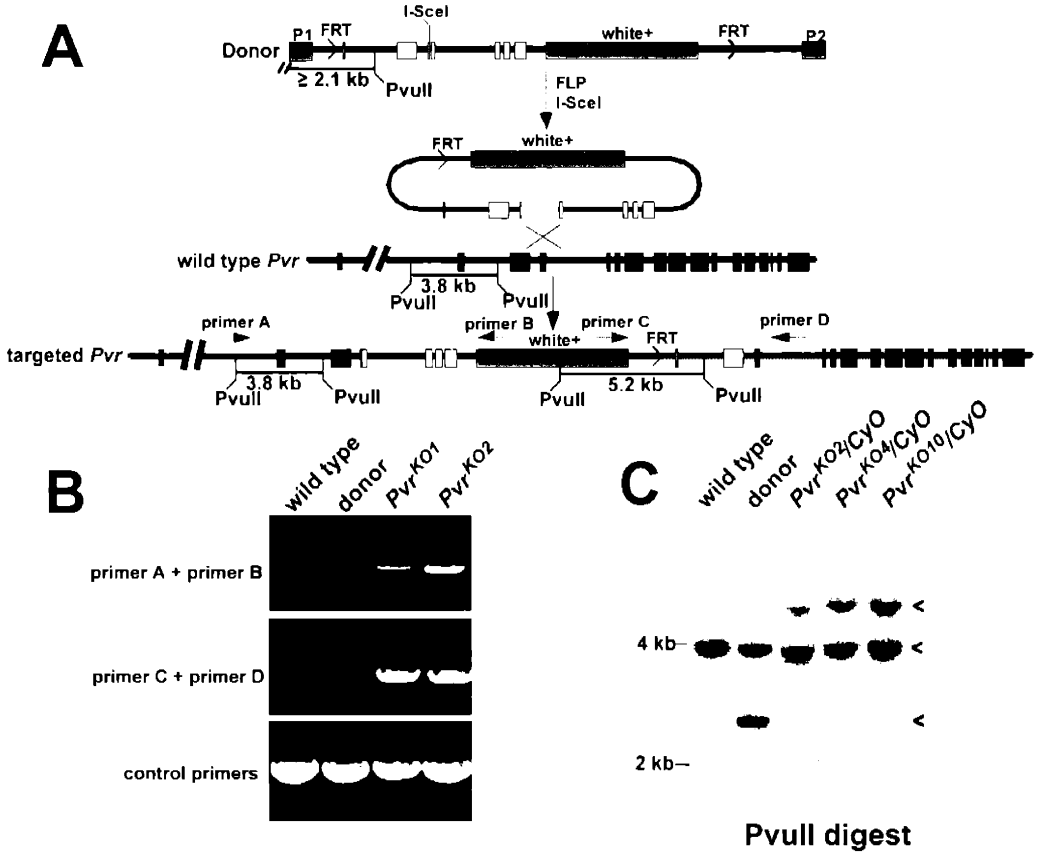

Fig. 1. Disruption of the *Pvr* locus through homologous recombination-mediated gene targeting. (A) A P-element containing 4.5kb of Pvr genomic sequence, a mini-white gene and FRT sequences was randomly inserted by transposition onto the third chromosome. This DNA was circularized through expression of FLP recombinase and linearized through expression of the yeast restriction endonuclease I-Sce-I. This linear fragment recombined with the endogenous *Pvr* locus to produce two tandem partial copies of the *Pvr* gene. White boxes indicate exons that originate from the donor fragment. Black boxes indicate exons that originate from the endogenous locus. (B) PCR analysis of homologous recombinants using the primer pairs indicated in (A). One primer of each pair anneals to DNA in the mini-white gene in the targeting construct, while the other primer of each pair anneals to genomic DNA from the endogenous locus. In the top panel, primers A and B were used to amplify DNA to the left of the mini-white gene. In the center panel, primers C and D were used to amplify DNA to the right of the mini-white gene. As expected, DNA from wild-type flies or flies with the donor P-element yield no PCR product in either case. DNA from homozygous *Pvr* knock-out embryos gives the expected size PCR products. In the bottom panel, control primers were used to amplify a fragment from the same genomic DNA used in the top and center panels. (C) Southern blot analysis of homologous recombinants. The locations and sizes of the fragments recognized by the probe are indicated in (A). Red arrowhead,

homologous recombinant-specific band. Green arrowhead, endogenous Pvr locus band. Blue arrowhead, pre-recombination donor-specific band. As Pvr^{KO2}, Pvr^{KO4}, and Pvr^{KO10} are homozygous lethal early in development, DNA was obtained from adults heterozygous for each Pvr^{KO} allele and a wild-type copy of *Pvr* on a CyO chromosome. As expected, the endogenous *Pvr* locus band (green) is approximately twice as intense as the homologous recombinant-specific band (red), as the endogenous *Pvr* locus band is generated from both alleles.

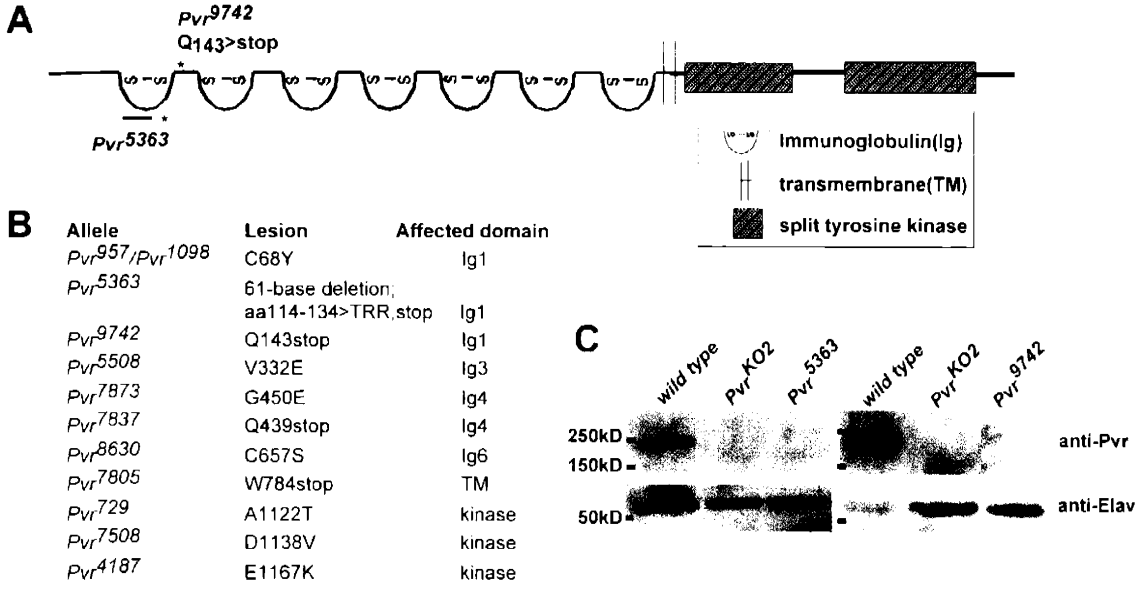

Figure 2. *Pvr* alleles generated by EMS mutagenesis. (A) Schematic of the Pvr proteins noting the location of lesions predicted to severely truncate the Pvr protein. In Pvr^{9742} Q143 is converted to a stop codon. In Pvr^{5363}, a 61-base deletion results in the deletion of amino acids 114-134 and a subsequent frameshift that results in three new amino acids and a stop codon. (B) Molecular lesions in *Pvr* alleles. Four alleles truncate the protein, four alleles contain missense mutations in the extracellular domain and three contain missense mutations in the kinase domain. (C) Western blots containing protein from the genotypes indicated probed with anti-Pvr antiserum. A single major protein species is detected in wild-type flies. This species cannot be detected in the Pvr mutants. Blots were reprobed with anti-Elav antiserum to confirm that similar or greater levels of protein were present in mutant lanes compared to wild-type controls.

We have focused our analysis on three alleles predicted to yield severely truncated *Pvr* proteins. Pvr^{KO2} contains two truncated copies of *Pvr*: one copy encodes a Pvr protein truncated after the fourth Ig domain, while the other copy lacks promoter sequences and predicted start codons. Pvr^{9742} contains a stop codon immediately after the first Ig domain, while Pvr^{5363} has a 61-base deletion that removes amino acids 114-134 from the first Ig domain and replaces them with three new residues and a stop codon. Stage 16/17 Pvr^{KO2}, Pvr^{9742}, and Pvr^{5363} embryos were examined for Pvr protein expression by Western blot using antisera raised against the C-terminal 275 amino acids of Pvr. Pvr expression was not detected in any of these mutant animals (Figure 1C). This was the case even when lanes containing protein derived from *Pvr* mutant embryos contained substantially more total protein than lanes containing protein from wild type control embryos, as assessed by reprobing the blots with a monoclonal antibody against the pan-neuronal protein Elav (Figure 1C). Pvr^{KO2}, Pvr^{9742}, and Pvr^{536} give equivalent results in the studies described below.

Pvr is required for proper CNS axon scaffold formation and glial positioning

We next examined CNS patterning in *Pvr* mutants. CNS axons in the *Drosophila* embryo establish a precise pattern reiterated in each segment (Figure 3a). CNS Axons establish two longitudinal tracts that run the length of the embryo on either side of the midline, with a subset of these axons crossing the midline of the embryo, forming two commissural axon bundles per segment. CNS axons are guided in part by signals from glia precisely positioned at the midline and along the longitudinal tracts (Hidalgo and Booth, 2000a; Kidd et al., 1999). Although CNS axon architecture was grossly normal in *Pvr* mutants, the precise ladder-like axon scaffold seen in wild-type embryos was disrupted (Figure 3b). The scaffold in each segment had a rounded appearance, due to changes in the separation between the anterior and posterior commissures and the longitudinal tracts.

As a metric of CNS shape change in *Pvr* mutants, we calculated the ratio of the distance between the longitudinal tracts in each segment of late stage 16 embryos to the distance between anterior and posterior commissures. As shown in Table 1, this ratio was significantly smaller in *Pvr* mutants than in wild type or *Pvr* heterozygote controls (unpaired t-test, $P<.01$). As glial cells within the CNS are required for proper axon tract formation, we examined the positioning of glial cells in *Pvr* mutants. Many CNS glial cells express the homeobox protein Repo and

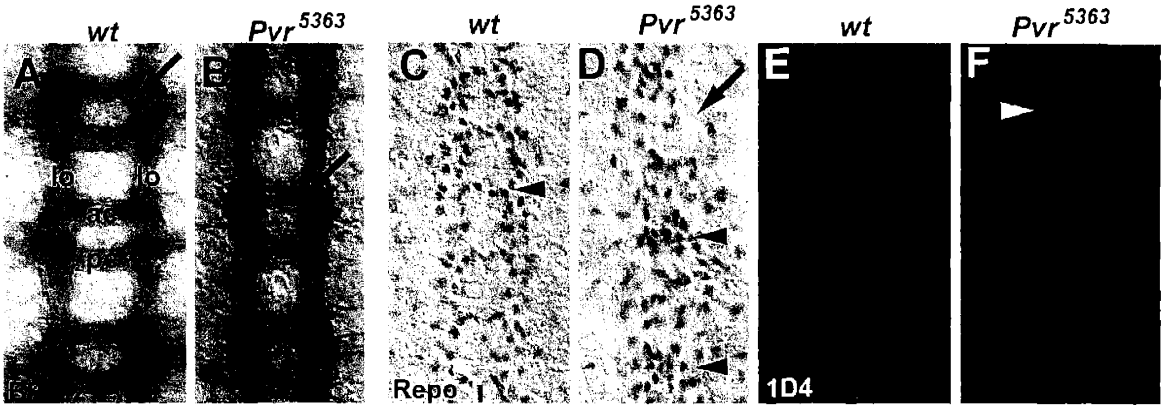

Figure 3. Pvr is required for proper CNS morphogenesis. (A,B) Stage 16 (A) wild type (Canton-S) and (B) *Pvr*^{5363} embryos stained with MAb BP102 to visualize CNS axons. ac, anterior commissure. pc, posterior commissure. lo, longitudinal tracts. Red line, CNS midline. In wild type the commissures and longitudinal tracts form a rectangular axon scaffold in each segment (arrow), while in *Pvr* the longitudinal tracts are closer together than in wild type, giving the axon scaffold a rounded appearance in each segment (arrow). (C,D) Stage 16 (C) wild type (Canton-S) and (D) *Pvr*^{5363} embryos stained with anti-Repo to visualize glia. In wild type, Repo-positive glia are arranged in a patterned array along the two longitudinal tracts, with a single row of Repo-positive glia between the longitudinal tracts in each segment (arrowhead). In *Pvr* mutants, Repo-positive glia accumulate at the midline (arrowheads), and there are fewer Repo-positive glia in the longitudinal tract region (arrow). The longitudinal tracts appear in outline in the photograph, which was taken using differential interference contrast (DIC) optics. (E,F) Longitudinal axon tracts of stage 17 embryos are stained with the anti-Fasciclin II monoclonal antibody 1D4. (E) Wild type. Three tightly bundled axon tracts can be seen on each side of the midline. (F) *Pvr*^{5363} mutants also form three axon tracts on either side of the midline. No ectopic axon crossing of the midline can be detected, although minor defasciculation of axon tracts can be seen in some segments (arrowhead).

require Repo for their proper development (Campbell et al., 1994; Halter et al., 1995). Repo-expressing glia form a patterned array along the longitudinal axon tracts and are largely excluded from the midline, except for a thin line of glia that enter the midline in each embryonic segment (Campbell et al., 1994; Jacobs and Goodman, 1989) (Figure 3C, arrowhead). In *Pvr* mutants, however, large numbers of Repo-positive glia accumulated in the midline (Figure 3D, arrowheads). Thus, *Pvr* mutants have defects in both CNS axon tract morphology and glial positioning.

Table 1. Quantitative representation of CNS commissure morphology of late stage 16/early stage 17 embryos

Genotype	ratio of distance between longitudinals and commissures[a]
+/+	2.5±0.09 (n=40)
Pvr^{KO2}/+	2.6±0.09 (n=40)
Pvr^{KO2}	1.6±0.06* (n=40)
Pvr^{5363}	1.7±0.07* (n=32)
srp^{neo45}	1.6±0.08* (n=40)
crq RNAi	1.8±0.07* (n=32)

[a]In each embryonic segment, the distance between the longitudinal axon bundles and the distance between the commissural axon bundles was measured, and the ratio of the two quantities was calculated. A ratio was used so that variations in overall embryo size between individuals would not contribute to the result. Error is given as standard error of the mean.
*Significantly different from wild type, P-value <0.01 (unpaired t-test).
n=number of segments quantitated

As *Pvr* mutants showed disruptions in CNS axon tract shape and glial cell positioning near the CNS midline, the pathfinding of CNS axons near the midline in *Pvr* mutants was examined in greater detail. The monoclonal antibody 1D4 (MAb 1D4) recognizes the fasciclin II protein (Van Vactor et al., 1993) and labels a subset of longitudinal bundles that grow adjacent to the CNS midline. Mab1D4 is a commonly used tool for assessing axon fasciculation patterns

and detecting inappropriate axon crossing of the CNS midline (Hidalgo and Brand, 1997; Kidd et al., 1998; Lin et al., 1994). Despite the changes in CNS axon scaffold shape and longitudinal glial distribution observed in *Pvr* mutants, no inappropriate axon crossing of the midline was detected (Fig. 3E,F). In addition, in wild-type animals three major tracts of fasciclin II-positive axons are observed near the dorsal surface of the CNS on either side of the midline (Fig. 3E). Three major tracts of fasciclin II-positive axons were also observed in *Pvr* mutants (Fig. 3F). Although these tracts were relatively normal, they did show very mild defasciculation in some segments, with axons in *Pvr* mutants occasionally separating from one another by greater distances than normal (Fig. 3F). As disruptions in longitudinal glial cell development disrupt the formation of these axon bundles (Hidalgo and Booth, 2000b), the minor axon tract defects observed in *Pvr* mutants were not unexpected given the glial cell mispositioning seen in *Pvr* mutants (Figure 3D).

Pvr functions in hemocytes

To investigate the source of the CNS defects in *Pvr* mutants, we identified the cell populations expressing Pvr. Pvr protein was detected on several cell populations during embryonic development. In stage 16 embryos, Pvr was prominently expressed by cells at the surface of the embryo, as well as by cells scattered throughout the embryo and by cells at the CNS midline (Fig. 4A). The large number of Pvr-expressing cells scattered throughout the embryo were hemocytes, as they co-expressed the hemocyte marker Peroxidasin (Fig. 4B-D). The Pvr-expressing cells at the CNS midline were midline glia (a population distinct from the Repo-positive glia mentioned above) and were intimately associated with the CNS commissures (Fig. 4E-F). Pvr expression could not be detected in Pvr^{KO2}, Pvr^{5363}, or Pvr^{9742} embryos, confirming the specificity of the antiserum (Fig. 4G).

Drosophila midline glia play important roles in separating and wrapping CNS axon commissures (Jacobs, 2000). Although midline glia expressed Pvr and *Pvr* mutants exhibited defects in commissure morphology, we could detect no role for Pvr in the midline cells. We first examined the number of midline glia present in *Pvr* mutant embryos using the midline glial marker *sli(1.0)-lacZ* (Nambu et al., 1991). Wild-type stage 17 embryos contained 2.8±0.2 glia per segment (n=18; ± s.e.m.), while Pvr^{KO2} embryos contained 2.7±0.2 glia per segment (n=25). Thus, there was no detectable alteration in the number of midline glia. Midline glial cell

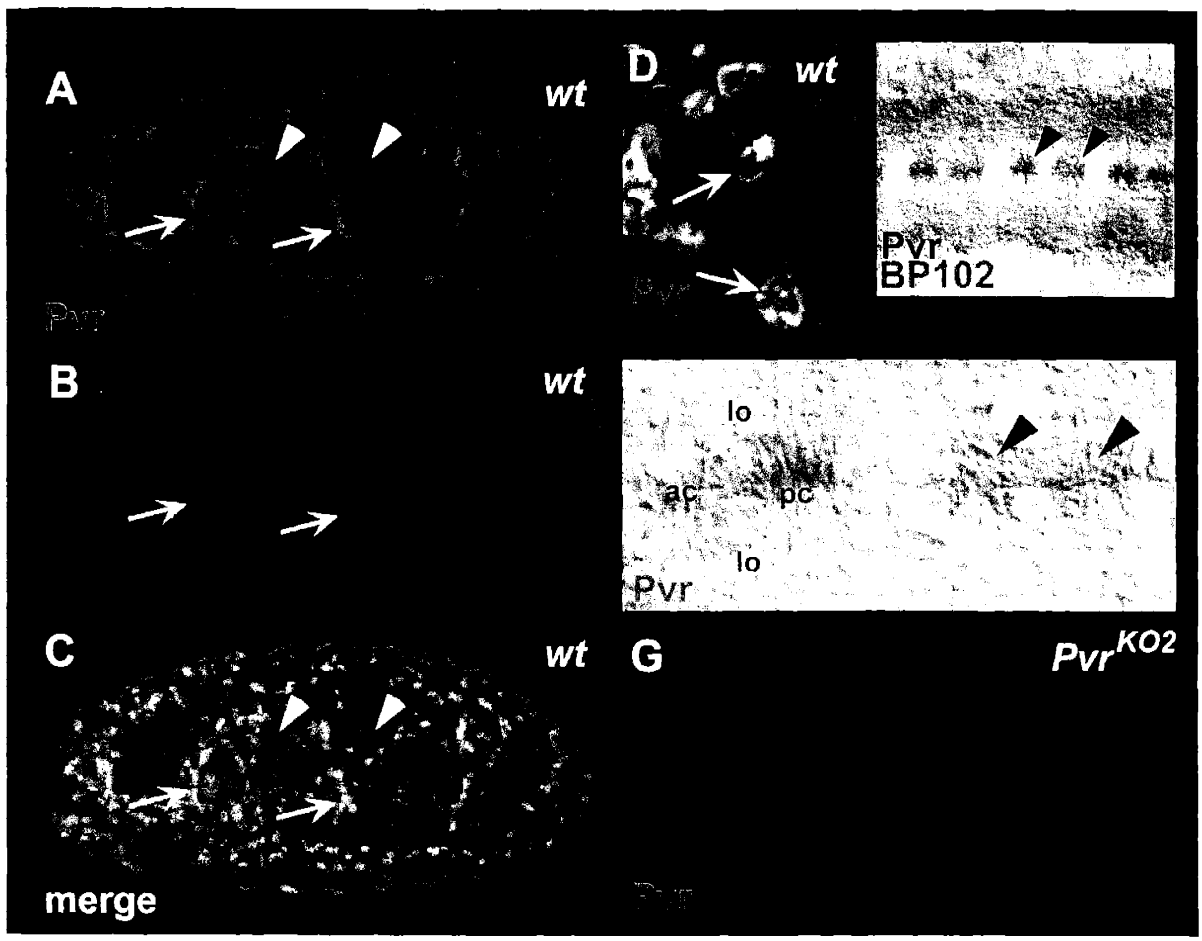

Figure 4. Pvr protein is present on midline glia and hemocytes. (A-D) Wild type stage 16 embryo stained with anti-Pvr (red) and anti-Peroxidasin (Pxn) (green). Yellow indicates overlap in the merged images (C-D). Pvr protein can be detected at the midline (arrowheads), in hemocytes (arrows), and at the surface of the embryo. (D) Higher magnification image of embryo depicted in (A-C). The expression of Pvr in hemocytes is confirmed by co-expression with Peroxidasin in (C) and (D). (E) Stage 17 embryo double-labelled with anti-Pvr (black) and BP102 (brown). Pvr protein is expressed on midline glia that surround the CNS commissures (arrowhead). (F) Higher magnification image of wild type stage 16 embryo stained with anti-Pvr. CNS axon tracts are visualized using DIC optics. Pvr protein is expressed on midline glia (arrowheads) that surround the anterior and posterior CNS commissures. ac, anterior commissure. pc, posterior commissure. lo, longitudinal axons tracts. (G) *Pvr*^{KO2} mutant embryo stained with anti-Pvr. Anti-Pvr staining cannot be detected in mutant animals.

development was further examined by staining for Wrapper, an immunoglobulin superfamily protein specifically expressed in midline glia and required for midline glial survival (Noordermeer et al., 1998). Wrapper was appropriately expressed by midline glia in *Pvr* mutants (Fig. 5 A, B). To directly test whether *Pvr* acted in midline glia, high-level expression of a dominant-negative form of Pvr (Duchek et al., 2001) was driven in all midline cells using the *Sim:Gal4* driver or specifically in midline glia using the *Slit:Gal4* driver. However, in neither case was a detectable CNS axon or Repo-positive glia phenotype generated (Fig. 5C,E and H. C. Sears, C. J. Kennedy, and P. A. Garrity, unpublished).

We next examined whether the CNS phenotype was related to Pvr expression in hemocytes. In the *Pvr* alleles recovered in our studies, hemocytes largely failed to migrate away from their birthplace in the head (Fig. 5G,H), consistent with the recent observations of Cho et al. (Cho et al., 2002). To test whether Pvr function in hemocytes was important for CNS development, we drove expression of dominant-negative Pvr in the developing hemocytes. While no solely hemocyte-specific Gal4 driver is available, *Gcm:Gal4* has been used previously to drive gene expression in embryonic hemocytes (Cho et al., 2002). We find that *Gcm:Gal4* drives gene expression specifically in hemocytes beginning at stage 11 and later, beginning at stage 15, in other cells that do not detectably express Pvr (H. C. Sears, C. J. Kennedy, and P. A. Garrity, unpublished). Embryos expressing dominant-negative Pvr under the control of *Gcm:Gal4* had hemocyte migration defects resembling those of *Pvr* mutants, consistent with *Pvr* acting cell-autonomously to control hemocyte migration (Fig. 5I). Most importantly, embryos expressing dominant-negative Pvr under *Gcm:Gal4* control also exhibited rounding of CNS axon commissures and mispositioning of Repo-positive glial cells similar to *Pvr* mutants (Fig. 5D,F). These data are consistent with Pvr acting in hemocytes to control CNS patterning and suggest that hemocyte function is required during CNS development.

Macrophage function is required for CNS patterning

To further examine the potential contribution of hemocytes to CNS development, we examined animals mutant for *serpent (srp)*, which encodes a GATA-family transcription factor required for hemocyte development (Rehorn et al., 1996). srp^{neo45} is a hemocyte-specific allele of *serpent*, and srp^{neo45} animals lack all hemocytes (Lebestky et al., 2000; Rehorn et al., 1996). Examination of srp^{neo45} embryos demonstrated that not only did srp^{neo45} mutants lack

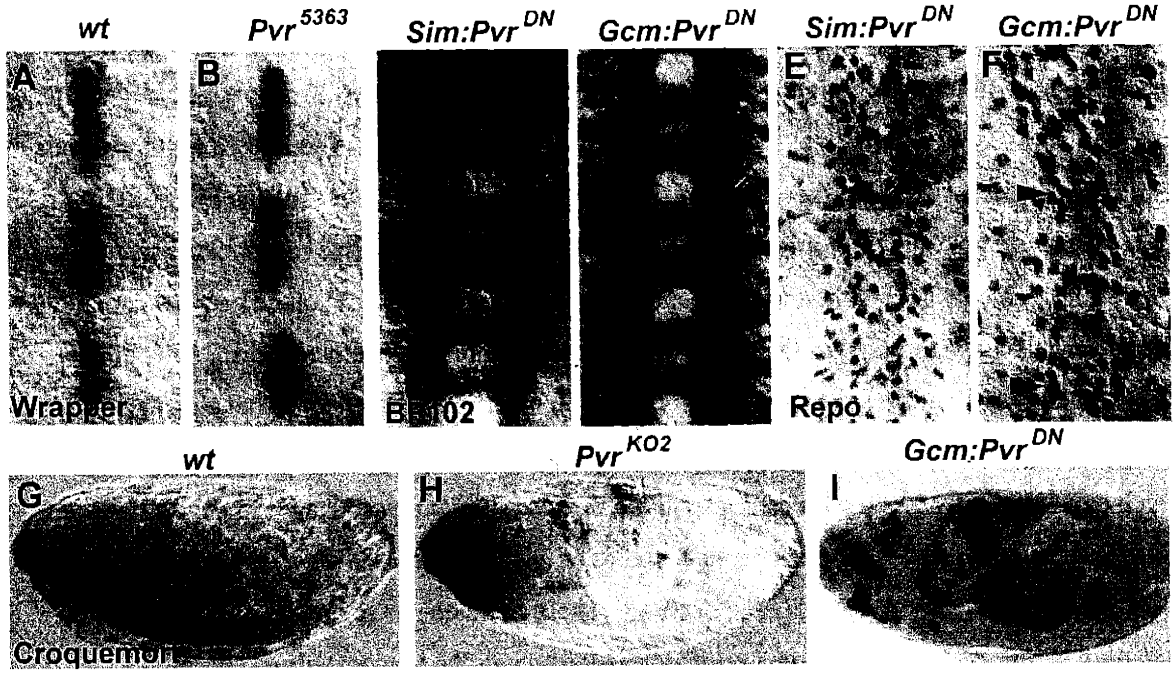

Figure 5. Pvr acts in hemocytes and not midline glia for proper CNS patterning. (A,B) Stage 16 embryos stained with anti-wrapper antibody to visualize midline glia. *Pvr*^{5363} midline glia (B) are indistinguishable from wildtype (A). (C,D) Stage 16 (C) Sim-Gal4;UAS-PvrDN and (D) Gcm-Gal4;UAS-PvrDN embryos stained with mAb BP102 to visualize CNS axons. Sim-Gal4;UAS-PvrDN embryos are indistinguishable from wild type, with commissures and longitudinal tracts forming a rectangular axon scaffold in each segment (arrow), while Gcm-Gal4;UAS-PvrDN embryos resemble *Pvr* embryos, with the axon scaffold having a rounded appearance in each segment (arrow). (E,F) Stage 16 (E) Sim-Gal4;UAS-PvrDN and (F) Gcm-Gal4;UAS-PvrDN embryos stained with anti-Repo antibody to visualize glia. Sim-Gal4;UAS-PvrDN embryos have glia in normal positions, with only few glia located between commissures in each segment (arrowhead), while many segments of Gcm-Gal4;UAS-PvrDN embryos have clusters of glia near the midline (arrowheads). (G-I) Stage 16 (G) wild type (Canton-S), (H) Pvr^{KO2}, and (I) Gcm-Gal4;UAS-PvrDN embryos stained with anti-Croquemort to visualize hemocytes. In wild type hemocytes are dispersed throughout the embryo, while in *Pvr* mutants and Gcm-Gal4;UAS-PvrDN embryos hemocytes are largely clustered near the dorsal and anterior regions of the embryo. Anterior is at left and dorsal is at top.

macrophages, they also exhibited CNS axon scaffold defects similar to those in *Pvr* mutants, with characteristic rounding of commissures (Fig. 6C). Quantitative representation of CNS axon tract morphology in srp^{neo45} mutants confirmed this observation (Table 1). The ratio of the distance between the longitudinal axon tracts and the distance between the commissural axon tracts in srp^{neo45} mutants was significantly different from wild type ($P<.01$), but not significantly different from *Pvr* homozygotes ($P>0.2$) (Table 1). srp^{neo45} animals also showed longitudinal glia positioning defects similar to those seen in *Pvr* mutants (Fig. 6G). Thus mutants that disrupt either hemocyte production or migration cause similar alterations in CNS morphogenesis.

One possible explanation for dependence of CNS morphogenesis on hemocytes is that hemocyte-derived macrophages are needed to engulf cell corpses generated during development. To test this possibility we examined animals in which macrophages appear to develop normally, but fail to engulf cell corpses. This was achieved using animals with reduced function of *crq*, which encodes a CD36-related receptor required for *Drosophila* macrophages to engulf dead cells (Franc et al., 1999). Previous genetic studies of *crq* function used the chromosomal deficiencies *Df(2L)al* and *Df(2L)TE99(Z)XW88*. These deficiencies remove a number of genes, including *u-shaped*, a transcriptional regulator which acts in the hemocyte lineage and is involved in germ-band contraction (Fossett et al., 2001; Franc et al., 1999). Since the elimination of multiple genes affecting potentially related processes complicates the use of *Df(2L)al* and *Df(2L)TE99(Z)XW88* in the analysis of CNS development, *crq* loss-of-function was examined using RNAi. Embryos injected with dsRNA corresponding to either of two non-overlapping regions within the Crq transcript had CNS axon scaffold defects similar to those in *Pvr* and *srp* mutants (Figure 6D). In *crq* RNAi embryos the ratio of distance between longitudinals to distance between commissures was significantly different from wild type ($P<.01$), but not significantly different from *Pvr* or *srp* mutants ($P>0.2$) (Table 1). In addition, *crq* RNAi animals also showed defects in the positioning of Repo-positive glia similar to those seen in *Pvr* and *srp* mutants (Figure 6H). These data further support the importance of hemocytes in CNS morphogenesis and specifically suggest that engulfment of dead cells by hemocyte-derived macrophages is essential for CNS development.

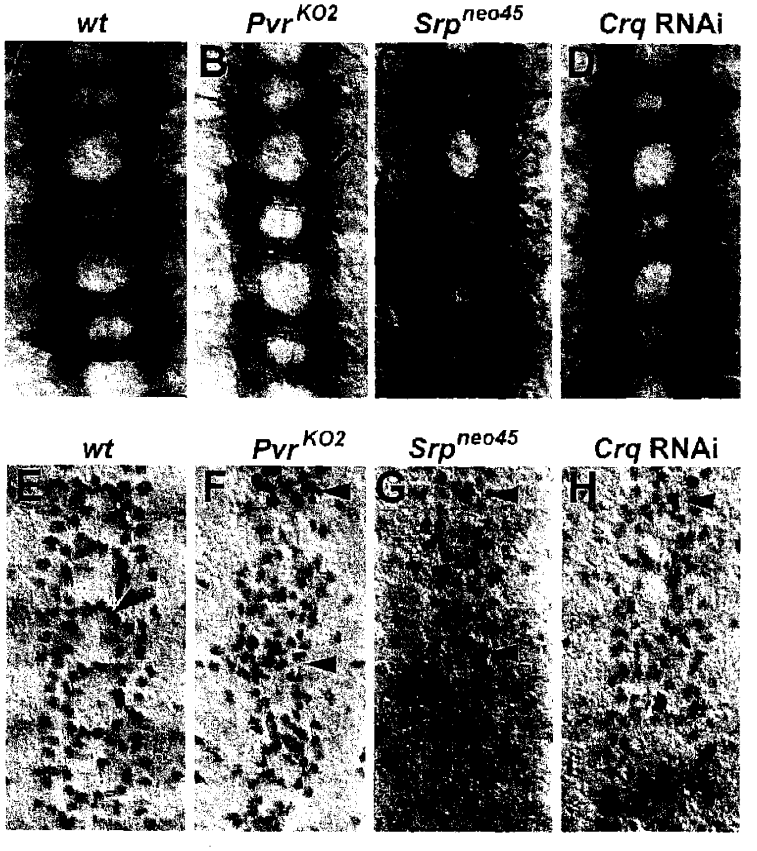

Figure 6. Macrophage function is required for proper CNS patterning. (A-D) Stage 16 (A) wild type, (B) Pvr^{KO2} , (C) Srp^{neo45}, and (D) *Crq* RNAi embryos stained with BP102 to visualize CNS axons. Srp^{neo45} and *Crq* RNAi embryos resemble *Pvr* embryos, with the axon scaffold having a rounded appearance in each segment (arrows). (E-H) Stage 16 (E) wild type, (F) Pvr^{KO2} , (G) Srp^{neo45}, and (H) *Crq* RNAi embryos stained with Repo to visualize glia. Pvr^{KO2} , Srp^{neo45} and *Crq* RNAi embryos all have disruptions in the pattern of Repo-positive glia. Srp^{neo45} mutant embryos have increased numbers of Repo-positive glia at the midline in each segment (arrowheads). In *Crq* RNAi embryos, there are also increased numbers of glia at the midline (arrowheads), while the glia associated with longitudinal tracts appear more dispersed than in wild type (arrow).

DISCUSSION

We have examined the role of macrophage function in *Drosophila* development using several genetic approaches. Through a combination of site-specific gene targeting and chemical mutagenesis we generated and characterized a series of mutations in *Pvr*, which encodes a receptor tyrosine kinase of the PDGF/VEGF receptor family. In addition to disrupting macrophage migration, a function of *Pvr* recently described by Cho et al. (Cho et al., 2002), we find that *Pvr* mutants have defects in glial positioning and axon scaffold formation in the CNS. Tissue-specific expression of dominant-negative Pvr suggests that the CNS defects result from the disruption in macrophage positioning. Consistent with this interpretation, similar defects in CNS patterning are observed in animals which completely lack macrophages (srp^{neo45} mutants) and in animals in which expression of Croquemort (Crq), a receptor required for macrophage engulfment of dead cells, is inhibited. Taken together, these data suggest that macrophages play an important role in CNS development. Furthermore, since the effects on CNS morphogenesis of inhibiting *croquemort* function are essentially indistinguishable from eliminating macrophages altogether, our data suggest that corpse engulfment is a major aspect, and perhaps the most important aspect, of macrophage function in CNS development.

There are several possible explanations for the observed contribution of macrophages to CNS morphogenesis. As engulfment is capable of promoting cell death in some situations (Reddien et al., 2001), the inhibition of macrophage function could potentially change patterns of cell death. However, previous work found that substantial cell death still occurs in *Drosophila* embryos in the absence of macrophages (Tepass et al., 1994). Similarly, we find no alteration in the number of midline glia in *Pvr* mutants, suggesting that the death of midline glia proceeds normally. Acridine orange staining of developing embryos likewise shows no detectable alteration in the pattern of dead cell generation (H. C. Sears, C. J. Kennedy, and P. A. Garrity, unpublished). Thus, while subtle changes in pattern of cell death would escape detection by these methods, there is no large-scale alteration in cell death in *Drosophila* in the absence of macrophages. Interestingly, when cell death is blocked in homozygous *Df(3L)H99* animals, which lack the cell death promoting genes *hid*, *grim*, and *reaper*, the CNS axon scaffolds are wider than normal (Zhou et al., 1995)(H. C. Sears, C. J. Kennedy, and P. A. Garrity, unpublished). The phenotypic contrast between the absence of cell death and the absence of

macrophages suggests that macrophages are not simply required to remove material from the developing midline.

An alternative explanation for the need for macrophage-mediated engulfment is that the accumulation of cell corpses within the CNS disrupts axon and glial positioning. Cell corpses could exert a toxic effect or could disrupt the function of particular cell populations by abnormally accumulating within these cells. Such possibilities are consistent with Sonnenfeld and Jacobs' observation that in embryos from *Bic-D* mutant mothers (which, in addition to severe embryonic patterning defects, lack macrophages) cell corpses accumulate at the CNS periphery and in CNS glial cells (Sonnenfeld and Jacobs, 1995b). In the case of glial cells, it is interesting to note that the CNS defects of *Pvr*, *serpent*^{neo45} and *crq* RNAi animals resemble those of *repo* mutant animals in which glial positioning and survival is disrupted (Campbell et al., 1994; Halter et al., 1995). Thus, a disruption in glial positioning could lead to the disruption of the CNS axon scaffold observed in the absence of macrophage-mediated engulfment.

Another possible requirement for the engulfment of dead cells by macrophages could be that engulfment stimulates the release by macrophages of factors required for proper CNS morphogenesis. *Drosophila* macrophages produce extracellular matrix components such as collagen IV, laminin, papilin, glutactin, and macrophage-derived proteoglycan-1 (MDP-1) (Fessler et al., 1994; Gullberg et al., 1994; Hortsch et al., 1998), and the presence of cell corpses is known to enhance production of at least one of these, MDP-1 (Hortsch et al., 1998). That *Pvr*, *serpent*^{neo45} and *crq* RNAi animals all show a mild elongation of the nerve cord (H. C. Sears, C. J. Kennedy, and P. A. Garrity, unpublished) could reflect defects in extracellular matrix production.

Cell death is a major component of many morphogenetic processes during development in vertebrates and invertebrates. However, an essential role for macrophages in these morphogenetic events has been established only in the mouse retina, where macrophages appear to act by triggering cell death (Lang et al., 1994; Lang and Bishop, 1993). Unlike the mouse retina, cell death in the *Drosophila* CNS does not require macrophages (Tepass et al., 1994). Our data support a different role for macrophages in *Drosophila* CNS morphogenesis: mediating clearance of dead cells. These observations indicate that both cell death and the interaction of macrophages with cell corpses are required for proper *Drosophila* CNS development.

MATERIALS AND METHODS

Genetics and Molecular Biology

Fly stocks and plasmids for creating the Pvr disruption allele were obtained from K. Golic. To create the targeting construct, bases 125741-130091 from AE003620 were excised as a SacII/SgrA1 fragment and cloned into pTV2. An I-SceI recognition site was inserted at the BstEII site at base 128126. Targeting was done as described (Rong and Golic, 2000). EMS alleles were sequenced by the MGH DNA Sequencing Core Facility.

Genomic DNA was prepared for long-range PCR by crushing single flies (Canton-S, *Pvr* knock-out donor, or heterozygous *Pvr* knock-out) in 50 μl squishing buffer (10 mM Tris-HCl pH8.2, 1 mM EDTA, 25 mM NaCl, 200 μg/ml Proteinase K). Crushed flies were incubated at 37°C for 30 min and Proteinase K was inactivated at 95°C for 2 min. Long-range PCR was performed using the Expand Long Template PCR System (Roche). Primers used to confirm homologous recombination were 5'-AATCGTACCGTTGCGAATAAGTGGG-3' (Primer A), 5'-AGAAGCGAGAGGAGTTTTGGCACAGC-3' (Primer B), 5'-TTTGTTCGACGACCTTGGAGCGAC-3' (Primer C), and 5'-TGGATAAAGTTCCATCACCACCACGG-3' (Primer D). Control PCR was performed with primers against Pvr genomic DNA, 5'-CAGTGCAACGCTAAGTGAGCC-3' and 5'-TCTTCACGCAATAGTAGGCTGCC-3'.

The following fly stocks were kindly provided by those indicated: *slit(1.0)-LacZ* (I. Rebay), *Sim-Gal4* (C. Goodman), *Gcm-Gal4* (U. Tepass), *UAS-Pvr*^{DN} (P. Rorth), *srp*^{neo45} (U. Banerjee), and *Df(3L)H99* (Bloomington Stock Center). Homozygous *Pvr* and *srp*^{neo45} mutant embryos were identified through the use of balancers marked with GFP (Bloomington Stock Center).

Southern Blotting

Genomic DNA isolated from 25 Canton-S or Pvr^{KO}/CyO flies was digested with PvuII. Digested DNAs were electrophoresed on an 0.8% agarose gel and transferred by downward capillary transfer to a Zeta-Probe GT membrane (BioRad). Membrane was subsequently treated following manufacturer's protocol. The probe template was amplified by PCR using genomic DNA and primers 5'-ATCGCTCGTATGCCCTACAACG-3' and 5'-

CTTCCTGTCAACAATCGCACATTC-3', which span 776 bases of the Pvr locus. ^{32}P-labelled probe was made from this template using the DECAprime II Kit (Ambion).

Immunohistochemistry and Western Blotting

All embryos were stained as described (Patel, 1994) using: rat polyclonal antiserum against Repo (Campbell et al., 1994) (1:500); mouse monoclonal antibody against LacZ (1:100; Promega); mouse polyclonal antiserum against Peroxidasin (Nelson et al., 1994) (1:500) and rabbit polyclonal antiserum against Croquemort (Franc et al., 1999) (1:500). The mouse monoclonal antibody BP102 developed by C. Goodman was obtained from the Developmental Studies Hybridoma Bank developed under the auspices of the NICHD and maintained by The University of Iowa, Department of Biological Sciences, Iowa City, IA 52242. Secondary antibodies labelled with HRP, FITC, or Cy3 were obtained from Jackson Laboratories. Polyclonal antiserum against Pvr was produced in rats (Covance) against a 30 kD peptide containing the 275 C-terminal amino acids of Pvr fused to a 6XHis tag. Anti-Pvr antiserum was used at 1:300 on embryos. Fluorescent images were obtained using a Nikon PCM2000 confocal microscope.

For each lane of Western blots, 10 embryos of each genotype were homogenized in PBS (130 mM NaCl, 175 mM Na_2HPO_4, 60 mM NaH_2PO_4). Lysates were run on a 9% polyacrylamide gel and transferred to Hybond-P membrane (Amersham Pharmacia). Membranes were blocked in 5% nonfat milk and probed with anti-Pvr antisera diluted 1:2000 and HRP-conjugated goat anti-rat antibody diluted at 1:5000. Blots were stripped and reprobed with rat monoclonal antibody against Elav to confirm that each *Pvr* mutant lane contained similar or greater amounts of total protein than wild type control.

RNAi

Inhibition of Crq by RNAi was performed as described(Kennerdell and Carthew, 1998). Bases 681-1203 and 1209-1737 of Crq cDNA RE02070 (ResGen; Genbank accession AY070904) were PCR-amplified using primer 5'-GAATTAATACGACTCACTATAGGGAGAGGGACTGATGCCTATGAAAGCTG-3' with 5'-GAATTAATACGACTCACTATAGGGAGAAGCCATCGTAAGTCAGCGACTC-3' and 5'-GAATTAATACGACTCACTATAGGGAGAACTATTCACACGGGCACTGACG-3' with

5'-GAATTAATACGACTCACTATAGGGAGATAATCTGGATGCGTCCATGCAC-3'. The 5'-end of each oligonucleotide contains a T7 RNA polymerase promoter sequence. dsRNA's were synthesized with T7 RNA polymerase from the MEGAscript High Yield Transcription Kit (Ambion). dsRNA was injected into Canton-S embryos at 1 $\mu g/\mu l$. Both Crq dsRNA's gave similar results. Control embryos injected with dsRNA from the Gal4 gene or Ptp99A gave no detectable phenotype.

We thank C. Thomas and M. Robichaux for technical assistance; U. Banerjee, P. Duchek, R. Ezekowitz, J. and L. Fessler, K. Golic, C. Goodman, Y. Rong, P. Rorth, J. Simpson, U. Tepass, and the Developmental Studies Hybridoma Bank for antibodies and fly stocks; A. Chess, N. Franc, H.R. Horvitz, L. Huang, E. Nedivi, T. Orr-Weaver, S.L. Zipursky, and Garrity lab members for discussions. This work was supported by grants to P.A.G. from the National Institutes of Health (1RO1EY/MH13874-01), the Raymond and Beverly Sackler Foundation, the Leukemia and Lymphoma Society, and the McKnight Foundation. H.C.S. is supported by a Centocor Fellowship. P.A.G is an investigator and C.J.K. is a research associate of the Raymond and Beverly Sackler Foundation.

REFERENCES

Abrams, J. M. (2002). Competition and compensation: coupled to death in development and cancer. *Cell* **110**, 403-6.

Baehrecke, E. H. (2002). How death shapes life during development. *Nat Rev Mol Cell Biol* **3**, 779-87.

Bangs, P. and White, K. (2000). Regulation and execution of apoptosis during Drosophila development. *Dev Dyn* **218**, 68-79.

Bello, B. C., Hirth, F. and Gould, A. P. (2003). A Pulse of the *Drosophila* Hox Protein Abdominal-A Schedules the Endo of Neural Proliferatin via Neuroblast Apoptosis. *Neuron* **37**, 209-219.

Bergmann, A., Tugentman, M., Shilo, B. Z. and Steller, H. (2002). Regulation of cell number by MAPK-dependent control of apoptosis: a mechanism for trophic survival signaling. *Dev Cell* **2**, 159-70.

Campbell, G., Goring, H., Lin, T., Spana, E., Andersson, S., Doe, C. Q. and Tomlinson, A. (1994). RK2, a glial-specific homeodomain protein required for embryonic nerve cord condensation and viability in Drosophila. *Development* **120**, 2957-66.

Cho, N. K., Keyes, L., Johnson, E., Heller, J., Ryner, L., Karim, F. and Krasnow, M. A. (2002). Developmental control of blood cell migration by the Drosophila VEGF pathway. *Cell* **108**, 865-76.

Duchek, P. and Rorth, P. (2001). Guidance of cell migration by EGF receptor signaling during drosophila oogenesis. *Science* **291**, 131-3.

Duchek, P., Somogyi, K., Jekely, G., Beccari, S. and Rorth, P. (2001). Guidance of cell migration by the Drosophila PDGF/VEGF receptor. *Cell* **107**, 17-26.

Fadok, V. A. and Chimini, G. (2001). The phagocytosis of apoptotic cells. *Semin Immunol* **13**, 365-72.

Fessler, L. I., Nelson, R. E. and Fessler, J. H. (1994). Drosophila extracellular matrix. *Methods Enzymol* **245**, 271-94.

Fossett, N., Tevosian, S. G., Gajewski, K., Zhang, Q., Orkin, S. H. and Schulz, R. A. (2001). The Friend of GATA proteins U-shaped, FOG-1, and FOG-2 function as negative regulators of blood, heart, and eye development in Drosophila. *Proc Natl Acad Sci U S A* **98**, 7342-7.

Franc, N. C. (2002). Phagocytosis of apoptotic cells in mammals, caenorhabditis elegans and Drosophila melanogaster: molecular mechanisms and physiological consequences. *Front Biosci* **7**, d1298-313.

Franc, N. C., Dimarcq, J. L., Lagueux, M., Hoffmann, J. and Ezekowitz, R. A. (1996). Croquemort, a novel Drosophila hemocyte/macrophage receptor that recognizes apoptotic cells. *Immunity* **4**, 431-43.

Franc, N. C., Heitzler, P., Ezekowitz, R. A. and White, K. (1999). Requirement for croquemort in phagocytosis of apoptotic cells in Drosophila. *Science* **284**, 1991-4.

Gullberg, D., Fessler, L. I. and Fessler, J. H. (1994). Differentiation, extracellular matrix synthesis, and integrin assembly by Drosophila embryo cells cultured on vitronectin and laminin substrates. *Dev Dyn* **199**, 116-28.

Halter, D. A., Urban, J., Rickert, C., Ner, S. S., Ito, K., Travers, A. A. and Technau, G. M. (1995). The homeobox gene repo is required for the differentiation and maintenance of glia function in the embryonic nervous system of Drosophila melanogaster. *Development* **121**, 317-32.

Hanks, S. K., Quinn, A. M. and Hunter, T. (1988). The protein kinase family: conserved features and deduced phylogeny of the catalytic domains. *Science* **241**, 42-52.

Heino, T. I., Karpanen, T., Wahlstrom, G., Pulkkinen, M., Eriksson, U., Alitalo, K. and Roos, C. (2001). The Drosophila VEGF receptor homolog is expressed in hemocytes. *Mech Dev* **109**, 69-77.

Hidalgo, A. and Booth, G. E. (2000a). Glia dictate pioneer axon trajectories in the Drosophila embryonic CNS. *Development* **127**, 393-402.

Hidalgo, A. and Booth, G. E. (2000b). Glia dictate pioneer axon trajectories in the Drosophila embryonic CNS. *Development* **127**, 393-402.

Hidalgo, A. and Brand, A. H. (1997). Targeted neuronal ablation: the role of pioneer neurons in guidance and fasciculation in the CNS of Drosophila. *Development* **124**, 3253-62.

Hidalgo, A., Kinrade, E. F. and Georgiou, M. (2001). The Drosophila neuregulin vein maintains glial survival during axon guidance in the CNS. *Dev Cell* **1**, 679-90.

Hopkinson-Woolley, J., Hughes, D., Gordon, S. and Martin, P. (1994). Macrophage recruitment during limb development and wound healing in the embryonic and foetal mouse. *J Cell Sci* **107 (Pt 5)**, 1159-67.

Hortsch, M., Olson, A., Fishman, S., Soneral, S. N., Marikar, Y., Dong, R. and Jacobs, J. R. (1998). The expression of MDP-1, a component of Drosophila embryonic basement membranes, is modulated by apoptotic cell death. *Int J Dev Biol* **42**, 33-42.

Huang, Z., Shilo, B. Z. and Kunes, S. (1998). A retinal axon fascicle uses spitz, an EGF receptor ligand, to construct a synaptic cartridge in the brain of Drosophila. *Cell* **95**, 693-703.

Hume, D. A., Perry, V. H. and Gordon, S. (1983). Immunohistochemical localization of a macrophage-specific antigen in developing mouse retina: phagocytosis of dying neurons and differentiation of microglial cells to form a regular array in the plexiform layers. *J Cell Biol* **97**, 253-7.

Jacobs, J. R. (2000). The midline glia of Drosophila: a molecular genetic model for the developmental functions of glia. *Prog Neurobiol* **62**, 475-508.

Jacobs, J. R. and Goodman, C. S. (1989). Embryonic development of axon pathways in the Drosophila CNS. I. A glial scaffold appears before the first growth cones. *J Neurosci* **9**, 2402-11.

Jacobson, M. D., Weil, M. and Raff, M. C. (1997). Programmed cell death in animal development. *Cell* **88**, 347-54.

Jiang, C., Baehrecke, E. H. and Thummel, C. S. (1997). Steroid regulated programmed cell death during Drosophila metamorphosis. *Development* **124**, 4673-83.

Johnson, L. N., Noble, M. E. and Owen, D. J. (1996). Active and inactive protein kinases: structural basis for regulation. *Cell* **85**, 149-58.

Kennerdell, J. R. and Carthew, R. W. (1998). Use of dsRNA-mediated genetic interference to demonstrate that frizzled and frizzled 2 act in the wingless pathway. *Cell* **95**, 1017-26.

Kidd, T., Bland, K. S. and Goodman, C. S. (1999). Slit is the midline repellent for the robo receptor in Drosophila. *Cell* **96**, 785-94.

Kidd, T., Brose, K., Mitchell, K. J., Fetter, R. D., Tessier-Lavigne, M., Goodman, C. S. and Tear, G. (1998). Roundabout controls axon crossing of the CNS midline and defines a novel subfamily of evolutionarily conserved guidance receptors. *Cell* **92**, 205-15.

Klambt, C., Jacobs, J. R. and Goodman, C. S. (1991). The midline of the Drosophila central nervous system: a model for the genetic analysis of cell fate, cell migration, and growth cone guidance. *Cell* **64**, 801-15.

Lang, R., Lustig, M., Francois, F., Sellinger, M. and Plesken, H. (1994). Apoptosis during macrophage-dependent ocular tissue remodelling. *Development* **120**, 3395-403.

Lang, R. A. and Bishop, J. M. (1993). Macrophages are required for cell death and tissue remodeling in the developing mouse eye. *Cell* **74**, 453-62.

Lebestky, T., Chang, T., Hartenstein, V. and Banerjee, U. (2000). Specification of Drosophila hematopoietic lineage by conserved transcription factors. *Science* **288**, 146-9.

Lin, D. M., Fetter, R. D., Kopczynski, C., Grenningloh, G. and Goodman, C. S. (1994). Genetic analysis of Fasciclin II in Drosophila: defasciculation, refasciculation, and altered fasciculation. *Neuron* **13**, 1055-69.

Lohmann, I., McGinnis, N., Bodmer, M. and McGinnis, W. (2002). The Drosophila Hox gene deformed sculpts head morphology via direct regulation of the apoptosis activator reaper. *Cell* **110**, 457-66.

Morris, L., Graham, C. F. and Gordon, S. (1991). Macrophages in haemopoietic and other tissues of the developing mouse detected by the monoclonal antibody F4/80. *Development* **112**, 517-26.

Nambu, J. R., Lewis, J. O., Wharton, K. A., Jr. and Crews, S. T. (1991). The Drosophila single-minded gene encodes a helix-loop-helix protein that acts as a master regulator of CNS midline development. *Cell* **67**, 1157-67.

Nelson, R. E., Fessler, L. I., Takagi, Y., Blumberg, B., Keene, D. R., Olson, P. F., Parker, C. G. and Fessler, J. H. (1994). Peroxidasin: a novel enzyme-matrix protein of Drosophila development. *Embo J* **13**, 3438-47.

Noordermeer, J.N., Kopczynski, C.C., Fetter, R.D., Bland, K.S., Chen, W.Y., and Goodman, C.S. (1998). Wrapper, a novel member of the Ig superfamily, is expressed by midline glia and is required for them to ensheath commissural axons in Drosphila. *Neuron* **21**, 991-1001.

Patel, N. H. (1994). Imaging Neuronal Subsets and Other Cell Types in Whole-Mount *Drosophila* Embryos and Larvae Using Antibody Probes. In *Methods in Cell Biology*, vol. 44 (ed. E. A. Fyrberg), pp. 445-487. San Diego: Academic Press.

Reddien, P. W., Cameron, S. and Horvitz, H. R. (2001). Phagocytosis promotes programmed cell death in C. elegans. *Nature* **412**, 198-202.

Rehorn, K. P., Thelen, H., Michelson, A. M. and Reuter, R. (1996). A molecular aspect of hematopoiesis and endoderm development common to vertebrates and Drosophila. *Development* **122**, 4023-31.

Rong, Y. S. and Golic, K. G. (2000). Gene targeting by homologous recombination in Drosophila. *Science* **288**, 2013-8.

Rong, Y. S. and Golic, K. G. (2001). A targeted gene knockout in drosophila. *Genetics* **157**, 1307-12.

Sonnenfeld, M. J. and Jacobs, J. R. (1995a). Apoptosis of the midline glia during Drosophila embryogenesis: a correlation with axon contact. *Development* **121**, 569-78.

Sonnenfeld, M. J. and Jacobs, J. R. (1995b). Macrophages and glia participate in the removal of apoptotic neurons from the Drosophila embryonic nervous system. *J Comp Neurol* **359**, 644-52.

Tepass, U., Fessler, L. I., Aziz, A. and Hartenstein, V. (1994). Embryonic origin of hemocytes and their relationship to cell death in Drosophila. *Development* **120**, 1829-37.

Van Vactor, D. V., Sink, H., Fambrough, D., Tsoo, R. and Goodman, C. S. (1993). Genes that control neuromuscular specificity in *Drosophila*. *Cell* **73**, 1137-1153.

Wood, W., Turmaine, M., Weber, R., Camp, V., Maki, R. A., McKercher, S. R. and Martin, P. (2000). Mesenchymal cells engulf and clear apoptotic footplate cells in macrophageless PU.1 null mouse embryos. *Development* **127**, 5245-52.

Zhou, L., Hashimi, H., Schwartz, L. M. and Nambu, J. R. (1995). Programmed cell death in the Drosophila central nervous system midline. *Curr Biol* **5**, 784-90.

Chapter 4.

Identification and characterization of proteins that bind the intracellular domain of Pvr

Experiments in Figure 7 were done with the assistance of Paul Phelps

SUMMARY

The receptor tyrosine kinase Pvr (PDGF/VEGF Receptor) is required for migration of border cells during oogenesis and hemocytes during embryogenesis, as well as proliferation and survival of both embryonic and larval hemocytes. I have sought to identify proteins that bind to the intracellular domain of Pvr through the use of a yeast-two hybrid interaction trap. Proteins that bind the intracellular domain of Pvr may be involved in signaling downstream of Pvr in cell migration or proliferation. I identified 15 proteins that bind Pvr in a phosphorylation-dependent manner. These include homologues of proteins known to bind the mammalian PDGFR and others that have no known connection to PDGFR signaling. Most of the interactors have SH2 domains that are likely to be required for binding to Pvr. Shc, drk, dock, and Lnk are adaptor proteins; vav is a GEF for the small GTPase Rac; kurtz is a homolog of beta-arrestin, which in mammalian cells is important for GPCR signaling and has recently been shown to bind PDGFR; tensin is a part of the focal adhesion complex, which has been shown to be regulated by PDGFR signaling. Twelve of the 15 interactors are expressed in Schneider S2 cells and larval hemocytes, although all but two are expressed to some extent in embryonic hemocytes. Two novel SH2-domain proteins, CG32406 and CG13289, and the potassium channel Ork1 are not expressed in either cell type. mRNA in situ hybridization showed that while many of the genes are expressed ubiquitously, none are expressed in an overlapping pattern with Pvr. I found that drk, but not any of the other interactors, is required for Pvr-dependent Erk MAP kinase activation. A novel FHA-domain protein, CG1135, is required for activation of Erk by dominant-active Pvr, although this is unlikely to be a pathway used by the endogenous receptor. RNAi of any of the Pvr interactors failed to give a hemocyte migration phenotype in embryos, but this could could reflect redundancy in the pathway or maternal contribution of protein.

INTRODUCTION

PDGF receptor signaling has been shown to play a role in directed cell migration in a number of mammalian cell types. Parts of the PDGF receptor signaling pathway have begun to be elucidated, although different pathways appear to be in effect in different cell types (Ronnstrand and Heldin, 2001). In PAE cells, activation of PI3 kinase by the PDGF receptor is required for PDGF-induced chemotaxis (Wennstrom et al., 1994b). Activation of PI3 kinase can lead to activation of the small GTPase Rac (Wennstrom et al., 1994a), which is required for PDGF-induced migration in PAE cells and Rat1 fibroblasts (Anand-Apte et al., 1997; Hooshmand-Rad et al., 1997). Activation of PI3 kinase also can lead to activation of PDK1, which can activate PKC (Vanhaesebroeck and Alessi, 2000). Inhibition of PKC activity blocks PDGF-induced migration (Derman et al., 1997). However, links between every step in this pathway have not been shown, and the PI3 kinase pathway does not appear to be involved in PDGF-induced chemotaxis in vascular smooth muscle cells or Swiss 3T3 cells (Higaki et al., 1996). Conversely, activation of PLCα1 by the PDGF receptor is required for migration in CHO cells and canine kidney epithelial cells, but not PAE cells (Kundra et al., 1994; Wennstrom et al., 1994b). It has been suggested that the PDGF receptor may serve to remodel the actin cytoskeleton via its interaction with the adaptor protein Nck, which binds the WASP-interacting protein WIRE, which relocalizes WASP to actin filaments to regulate actin polymerization (Aspenstrom, 2002). However, Nck has not actually been shown to be required for PDGF-induced migration.

Activation of the small GTPase Ras through binding of the adaptor proteins Grb2/drk or Shc to the activated PDGF receptor (Arvidsson et al., 1994; Rozakis-Adcock et al., 1992) is required for migration towards PDGF in NIH3T3 cells (Kundra et al., 1995). Activation of Erk MAP kinase downstream of Ras is required for PDGF-dependent migration in human mesangial cells and retinal pigment epithelial cells, but not Rat1 fibroblasts (Anand-Apte et al., 1997; Choudhury et al., 1997; Hinton et al., 1998). Other pathways may also be activated downstream of Ras in PDGF-induced chemotaxis.

The intracellular domain of *Drosophila* receptor tyrosine kinase Pvr is most homologous to the PDGF receptor (35% identity/55% similarity), although none of the tyrosine residues that are required for signaling in the mammalian PDGF receptor are conserved in Pvr. Pvr has been

shown to be required for migration of border cells during oogenesis (Duchek et al., 2001) and of hemocytes during embryogenesis (Cho et al., 2002). Rac and the Rac activator mbc were shown to be required for potentiating the actin-polymerizing effects of dominant active Pvr in the oocyte. Rac and mbc are also required for border cell migration, although a link to Pvr in border cell migration has not been demonstrated. Erk MAP kinase is activated downstream of Pvr both in hemocytes and in cultured S2 cells, which are thought to be derived from embryonic hemocytes. Cho, et al. observed that hemocyte migration is blocked by expression of dominant negative Ras, suggesting that the Ras/MAPK pathway may be important for hemocyte migration. They could not detect a requirement for the adaptor proteins drk (Grb2 homolog) or Shc, but both of these mRNAs are heavily maternally contributed.

I have conducted a yeast two-hybrid screen for embryonic proteins that bind to the Pvr intracellular domain. Identification of Pvr substrates and adaptor proteins could lead to insight into which signaling pathways are involved downstream of Pvr in cell migration or potentially identify novel signaling mechanisms used by the PDGF receptor family of receptor tyrosine kinases. The adaptor proteins Shc, drk, and dock bind to Pvr in a phosphorylation-dependent manner. The mammalian homologs of these proteins, Shc, Grb2, and Nck respectively bind to the PDGF receptor and may be important for both cell proliferation and migration. I did not identify *Drosophila* homologues of any other proteins that bind to the PDGF receptor as binding to Pvr, although I did not test them directly. I did identify a number of proteins as Pvr binding partners that had not previously been implicated downstream of the PDGF receptor. Three of these, vav, tensin and kurtz (α-arrestin), have homologues in mammalian systems that have been implicated in cell migration. Expression analysis indicated that all of the Pvr interactors except for two novel SH2-domain proteins and a potassium channel are likely to be expressed in hemocytes.

RESULTS

Several SH2 binding sites are predicted in Pvr

A comparison of the PDGFR and Pvr intracellular domains revealed that none of the nine tyrosine residues important for binding other signaling molecules in PDGFR are conserved in Pvr. Eight other intracellular tyrosines are conserved from fly to mammals. One of these, corresponding to PDGFRα Y857 and Pvr Y1160, is important for enhancing catalytic activity in PDGFRα. Another, corresponding to Y934 in PDGFRα and Y1237 in Pvr, is phosphorylated by Src tyrosine kinase on PDGFRα. Several tyrosines in the C-terminal tail of Pvr were predicted to be SH2 binding sites by Scansite 2.0, a web-based program that scans proteins for motifs such as phosphorylation sites or binding sites for common protein modules (Obenauer et al., 2003). Y1237 was predicted to bind the SH2 domain of PI3K and Y1273 was predicted to bind PLCα. Both of these tyrosines are conserved in mammalian PDGFRα. Y1330 was predicted to bind PI3K, Y1460 was predicted to bind PI3K, PLCα, and Grb2, and Y1495 was predicted to bind the Shc PTB domain. These three tyrosines are conserved between Pvr and the homolog of Pvr in *Anopheles gambiae*, the malaria-carrying mosquito. Y1437 was predicted to bind PLCα, Nck, and Crk, but this tyrosine is not even conserved in the mosquito Pvr homolog.

Two-hybrid screen for Pvr-interacting proteins

I conducted a yeast two-hybrid screen to identify proteins that bind to the intracellular domain of Pvr. The entire intracellular domain of Pvr was fused to the Gal4 DNA-binding domain (DBD) and used as bait in the screen. The DBD-Pvr fusion protein is tyrosine-phosphorylated in yeast, thus mimicking the activated form of Pvr (Figure 1, lane 2). A mutated form of DBD-Pvr in which the catalytic lysine is changed to alanine (DBD-PvrKA) is not phosphorylated (Figure 1, lane 3), suggesting both that DBD-Pvr is catalytically active and cross-phosphorylates in yeast and that DBD-PvrKA is a kinase-dead form of DBD-Pvr. Yeast strain PJ69-4a (James et al., 1996) was co-transformed with DBD-Pvr and a *Drosophila* embryonic cDNA library fused to the Gal4 activation domain (AD). Binding of bait and prey proteins in this strain results in the expression of reporter genes ADE2, HIS3, and MEL1, which encodes the α-galactosidase protein. 10^7 co-transformed colonies were screened for ability to grow on media lacking ura, leu, and his and supplemented with 5 mM 3-AT, a competitive

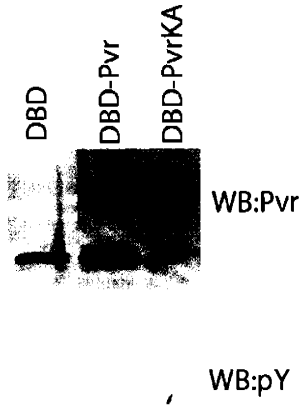

Figure 1. DBD-Pvr is phosphorylated in yeast, while kinase-dead DBD-PvrKA is not. Yeast strain PJ69-4A cells transformed with pDBD, pDBD-Pvr, or pDBD-PvrKA were lysed and whole cell lysate was separated by SDS-PAGE. Western blot was probed with anti-Pvr antiserum, which recognizes the C-terminus of Pvr (top panel) and then reprobed with PY20 anti-phosphotyrosine antibody (bottom panel). The bottom band in the top panel is a non-specific protein recognized by Pvr antiserum.

inhibitor with histidine. Of approximately 2000 colonies that passed this first selection, 784 colonies were able to grow on media lacking ura, leu, his, and ade. These colonies were forced to lose the URA3-expressing bait plasmid through growth on 5-FOA, which creates a toxic byproduct when digested by the URA3 enzyme. Most clones grew pink after losing the bait plasmid due to lack of ADE2 reporter expression. However, 46 clones grew white after losing the bait plasmid, suggesting that they were contaminant yeast wild type for ADE2 or that the prey plasmid alone was capable of inducing expression of ADE2. These clones were discarded. The remaining 738 clones were crossed to PJ69-4α containing DBD-LaminC, a bait protein commonly used to identify "sticky" proteins that bind non-specifically to any prey protein. 571 clones failed to interact with LaminC; the remainder was discarded. Clones that did not interact with LaminC were recrossed to PJ69-4α containing DBD-Pvr. Only 256 clones were found to interact with DBD-Pvr in this second test. The inserts from these 256 clones were amplified by PCR and sequenced. Clones encoding transcription factors or heat-shock proteins, common false positives in yeast two-hybrid screens, were discarded. Clones in which the insert was out of frame with the AD were also discarded. The remaining 219 clones represented 15 genes: CG1135, dreadlocks (dock), Pellino (Pli), Shc, drk, vav, CG32406, kurtz (krz), Lnk, CG13289/CG13290, CG17168, tensin, Ork1, Socs16D, and Socs44A. The total number of clones as well as the number of independent clones representing each of these genes is depicted in Table 1. Diploid yeast expressing DBD-Pvr and the AD fusion with the longest cDNA of each of these genes are shown in Figure 2 growing on plates supplemented with X-α-Gal, which forms a blue byproduct when digested with α-galactosidase. To determine whether Pvr must be phosphorylated or kinase-active in order for the interactors to bind, yeast carrying each AD fusion were also crossed to yeast carrying DBD-PvrKA. DBD-PvrKA did not interact with any of the Pvr-interacting proteins (Figure 2).

Figure 2. Positive two-hybrid Pvr interactors. PJ69-4a carrying the AD plasmid indicated were mated to PJ69-4α carrying DBD-Pvr or DBD-PvrKA. After mating, yeast were plated on selective media to select for diploids carrying both AD and DBD plasmids. Diploids were then struck on SC-leu,ura,his,ade + X-α-Gal plates. Blue color results from digestion of X-α-Gal by α-galactosidase, a marker for AD/DBD interaction. Diploids carrying DBD-Pvr are shown on the plates on the left. Diploids carrying DBD-PvrKA and any AD plasmid were unable to grow on the reporter plates (right).

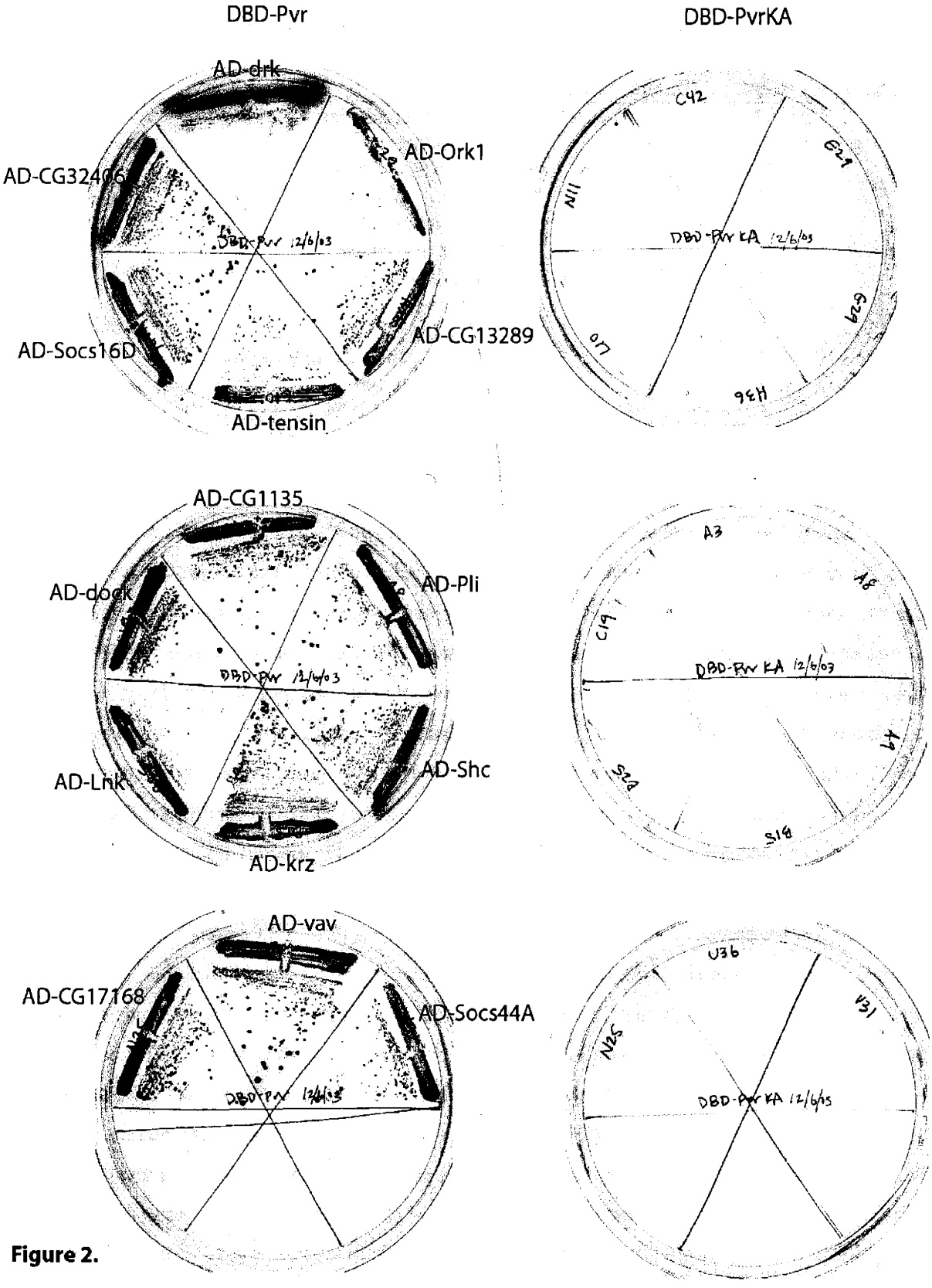
DBD-Pvr
DBD-PvrKA
AD-drk
AD-Ork1
AD-CG32406
AD-Socs16D
AD-CG13289
AD-tensin
AD-CG1135
AD-dock
AD-Pli
AD-Lnk
AD-Shc
AD-krz
AD-vav
AD-CG17168
AD-Socs44A

Figure 2.

Table 1. Yeast two-hybrid interactors

Interactor	# clones (total)	# clones (independent)	Description
drk	92	13	Grb2; SH3/SH2 adapter
Shc	41	5	PTB/SH2 adapter
dock	17	7	Nck; SH3/SH2 adapter
vav	8	4	Rho-GEF
kurtz	11	2	non-visual arrestin
Pellino	7	2	binds Pelle S/T kinase
Lnk	2	2	PH/SH2 adapter
tensin	5	1	focal adhesion
CG1135	9	4	microspherule protein
CG17168	3	3	Smad Nuclear Interacting Protein
CG32406	5	3	SH2; novel N-terminus
CG13289	8	5	SH2; novel N-terminus
Socs44A	1	1	Suppressor of Cytokine Signaling
Socs16D	1	1	Suppressor of Cytokine Signaling

Ninety-two clones encoded drk, an adaptor protein known to act downstream of most receptor tyrosine kinases. These represented 14 independent clones. The drk protein has an SH2 domain flanked by two SH3 domains. The longest clones were full-length, and the shortest clones encoded the C-terminal SH2 and SH3 domains. The SH2 domain is responsible for binding to other receptor tyrosine kinases, so it is likely that the drk SH2 domain also is required for binding Pvr. 41 clones encoded Shc, another adaptor protein that has been shown to be involved in RTK signaling. These represented 5 independent clones. Shc has an N-terminal PTB domain and a C-terminal SH2 domain. The longest clones were full-length, and the shortest clones encoded only the SH2 domain, suggesting that it is the SH2 domain that binds Pvr. 17 clones encoded dock, an adaptor protein involved in CNS and photoreceptor axon guidance. These represented 7 independent clones. Dock has three SH3 domains with an SH2 domain at the C-terminus. The longest clones lacked the first 50 amino acid residues, and the shortest clones encoded only the C-terminal SH2 domain suggesting that dock too binds Pvr with its SH2 domain. CG13289/90 and CG32406 both encode novel proteins with one SH2 domain at the C-terminus. Eight CG13289/90 clones represented 5 independent cDNAs, and 5 CG32406 clones represented 3 independent cDNAs. None of these clones were full-length, and the shortest clones encoded little more than the SH2 domain of both proteins. tensin, a focal adhesion protein with an SH2 domain, was pulled out of the screen five times. However, all of these clones were identical and encoded only the SH2 domain. Lnk is an adaptor protein with a

PH domain and an SH2 domain that has been shown to negatively regulate B cell and T cell proliferation in mammalian systems. Two independent cDNAs encoding Lnk were identified. One is full-length and the other lacks only the first 11 amino acids.

11 clones encoded kurtz, a non-visual arrestin of which mutants develop melanotic tumors in the third instar larvae due to disassociation of the fat bodies. These 11 clones represented two independent cDNAs. One cDNA was full-length and the other encoded a protein lacking the first 42 amino acids.

CG1135 and CG17168 encode proteins with SMAD/FHA domains, which have been found to be important modules for both signal transduction and transcription. CG1135 is homologous to microspherule protein 1, a nucleolar protein. CG17168 is partially homologous to SNIP (Smad Nuclear Interacting Protein), which negatively regulates the TGFα signal transduction pathway. Nine clones representing four independent cDNAs were found to encode CG1135. The longest clones are full-length, and the shortest clone encodes more than half of the protein. Three clones, each independent of the others, encoded CG17168. These cDNAs encode truncated proteins that start at amino acids 64, 68, and 99.

Eight clones representing four independent cDNAs encoded vav, a GEF for Rac involved in cytoskeletal organization. The shortest vav clone encoded only the C-terminal SH2 and SH3 domains. However, even the longest clones lacked the GEF domain, suggesting that the GEF domain may inhibit binding to Pvr. 7 clones corresponded to Pellino, a protein that was originally identified in a two-hybrid screen with Pelle, a serine/threonine kinase putatively involved in hematopoiesis. All but one clone were full-length, and the one truncated clone encoded a protein lacking only the first nine amino acids. Three clones representing two independent cDNAs encoded a potassium channel, Ork1. All three clones encode only the C-terminal cytoplasmic portion of the channel. I pulled out one clone each of Socs16D and Socs44A. Socs proteins are Suppressors of Cytokine Signaling, negatively regulating Jak/Stat signaling. Both clones encode little more than the C-terminal SH2 domain.

Expression patterns of Pvr-binding candidates

In order to determine whether any of these genes are expressed in an overlapping pattern with Pvr, I analyzed the mRNA expression patterns by RNA *in situ*. The expression patterns of vav, CG13289/90, and dock have been determined by the BDGP Expression Pattern Project

(http://www.fruitfly.org/cgi-bin/ex/bquery.pl). None of the genes I analyzed are expressed specifically in hemocytes. CG1135, krz, Lnk, CG17168, and Socs16D are expressed broadly throughout embryonic development (Figure 3a-c,g-o,v-x). CG32406 is expressed specifically in a subset of cells in the CNS late in embryogenesis (Figure 3d-f). Tensin is expressed in a ring of cells just inside the germband from germband extension through germband retraction (Figure 3p-q), coincident with the location of the developing dorsal vessel, the larval heart. It is expressed semi-ubiquitously late in embryogenesis (Figure 3r). The tensin expression patterns have recently been published (Torgler et al., 2004).

I used RT-PCR to determine whether any candidates were expressed in S2 cells, which are reported to have been derived from embryonic hemocytes. CG1135, dock, Pli, Shc, drk, vav, krz, Lnk, CG17168, tensin, Socs16D, and Socs44A are all expressed in S2 cells (Figure 4a). I also used larval hemocyte RNA as template in gene-specific RT-PCR (Guilherme Neves and Andy Chess). This RNA was isolated by FACS sorting cells from larvae expressing GFP under the hml promoter, which drives expression specifically in the larval hemocytes (Goto et al., 2001; data not shown). Larval hemocytes are developmentally distinct from embryonic hemocytes, but perform similar functions and respond to Pvr ligands. RT-PCR with this RNA gave the same results as with S2 cell RNA, but with a range of expression levels. Pli, Shc, drk, CG17168, and Socs16D had the highest expression levels (Figure 4b). Lastly, I isolated GFP-expressing cells from Pxn-Gal4, UAS-GFP stage 16-17 embryos. The pxn promoter drives expression specifically in embryonic hemocytes beginning around stage 15 (see Figure 7b) and later in larval hemocytes (data not shown). RNA from these cells, which should have been primarily embryonic hemocytes, was used in RT-PCR with the same gene-specific primers

---

Figure 3. mRNA expression patterns were determined by RNA in situ hybridization using probes against each Pvr interactor not already described by the BDGP Expression Project. 3-17 hour Canton-S embryos were used. Representative samples of each of three different stages are shown. In most cases, anterior is to the left and ventral is down. In some stage 15-17 embryos, the ventral nerve cord is shown facing the viewer. (A,D,G,J,M,P,S,V) Stage 8-11: germband extension. (B,E,H,K,N,Q,T,W) Stage 13: after germband retraction, before dorsal closure. (C,F,I,L,O,R,U,X) Stage 15-17: after dorsal closure, before hatching. (A-C) CG1135. (D-F) CG32406. (G-I) kurtz. (J-L) Lnk. (M-O) CG17168. (P-R) tensin. (S-U) Ork1. (V-X) Socs16D.

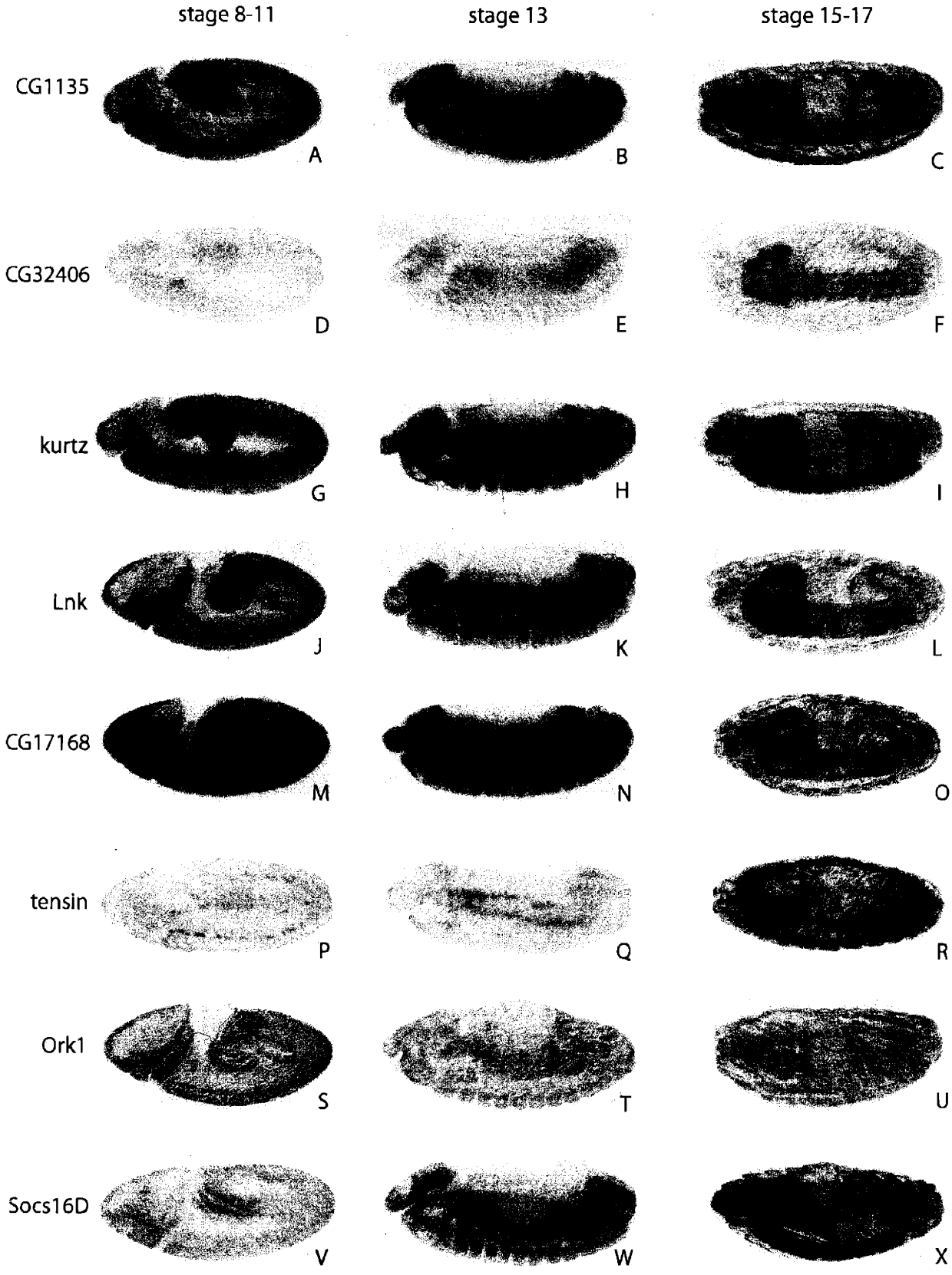
stage 8-11
stage 13
stage 15-17
CG1135
A
B
C
CG32406
D
E
F
kurtz
G
H
I
Lnk
J
K
L
CG17168
M
N
O
tensin
P
Q
R
Ork1
S
T
U
Socs16D
V
W
X

Figure 3.

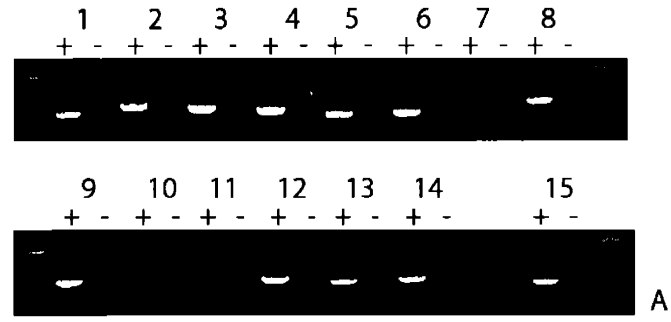

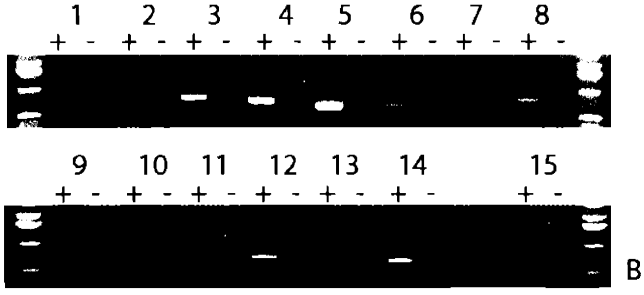

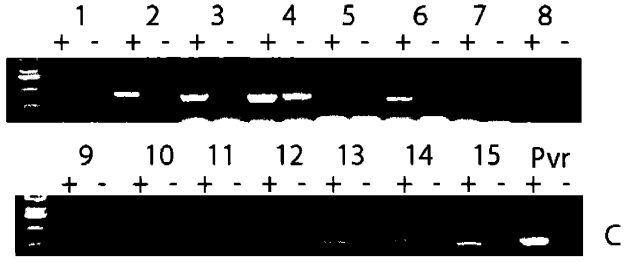

Figure 4. Cell-specific expression of Pvr interactor mRNAs. RT-PCR was performed from RNA isolated from S2 cells (A), larval hemocytes (B), or embryonic hemocytes (C) using gene-specific primers. +: RT-PCR. -: no reverse transcriptase control PCR. Lanes 1, CG1135. Lanes 2, dock. Lanes 3, Pli. Lanes 4, Shc. Lanes 5, drk. Lanes 6, vav. Lanes 7, CG32406. Lanes 8, krz. Lanes 9, Lnk. Lanes 10, CG13289. Lanes 11, Ork1. Lanes 12, CG17168. Lanes 13, tensin. Lanes 14, Socs16D. Lanes 15, Socs44A.

(Figure 4c). Pvr-specific primers were used as a positive control in this experiment, and these do give a PCR product. As in the S2 cell and larval hemocyte RT-PCRs, neither CG13289 nor Ork1 were found to be expressed in embryonic hemocytes. However, drk, CG32406, and kurtz appeared to be very weakly expressed, Only dock, Pli, Shc, and vav gave PCR products with an intensity similar to that of Pvr. However, the Shc primers were also able to amplify a PCR product from the negative control lacking reverse transcriptase. Thus, the results of RT-PCR with Shc is inconclusive. It is interesting to note that with this set of genes the expression profile of S2 cells is closer to that of larval hemocytes, and the expression profile of embryonic hemocytes appears to be somewhat distinct from the larval hemocyte expression profile.

drk is required for Pvr-dependent activation of Erk MAPK

I began a functional analysis of the Pvr interactors by testing them for a role in Erk MAP kinase activation. It has been shown that MAPK is phosphorylated in S2 cells in response to conditioned media. This response is dependent on Pvr (Duchek et al., 2001). Erk is also activated in migrating embryonic hemocytes. This activation is dependent on Pvr and is enhanced when Pvf1 is overexpressed (Cho et al., 2002). In addition, hemocyte migration is blocked when a dominant negative form of Ras is overexpressed, suggesting that the Ras/Erk pathway is involved in hemocyte migration (Cho et al., 2002). The transmembrane and intracellular portions of Pvr were fused to the lambda repressor protein cI, which constitutively dimerizes. The constitutive dimerization of the chimeric protein (lambda-Pvr) results in constitutive phosphorylation and activation of the Pvr intracellular domain. Expression of lambda-Pvr in S2 cells resulted in an increase in the level of Erk phosphorylation over the basal phosphorylation level, as detected with an antibody that specifically recognizes the di-phosphorylated form of Erk (Figure 5a-b, lanes 2). I sought to block this response by conducting RNAi on the candidate Pvr interactors. RNAi of CG1135 blocked the lambda-Pvr-dependent increase in Erk phosphorylation without reducing the basal level of phosphorylation (Figure 5a, lanes 3-4). RNAi of drk or vav reduced the basal level of Erk phosphorylation, but the amount of phosphorylation on Erk increased with lambda-Pvr (Figure 4a, lanes 5-8). However, I found that RNAi of endogenous Pvr also significantly decreased the basal level of Erk phosphorylation (Figure 5b, lanes 3-4). This suggested that overexpression of an activated form of Pvr activates MAPK through a potentially distinct pathway from endogenous Pvr. CG1135 could be a part of

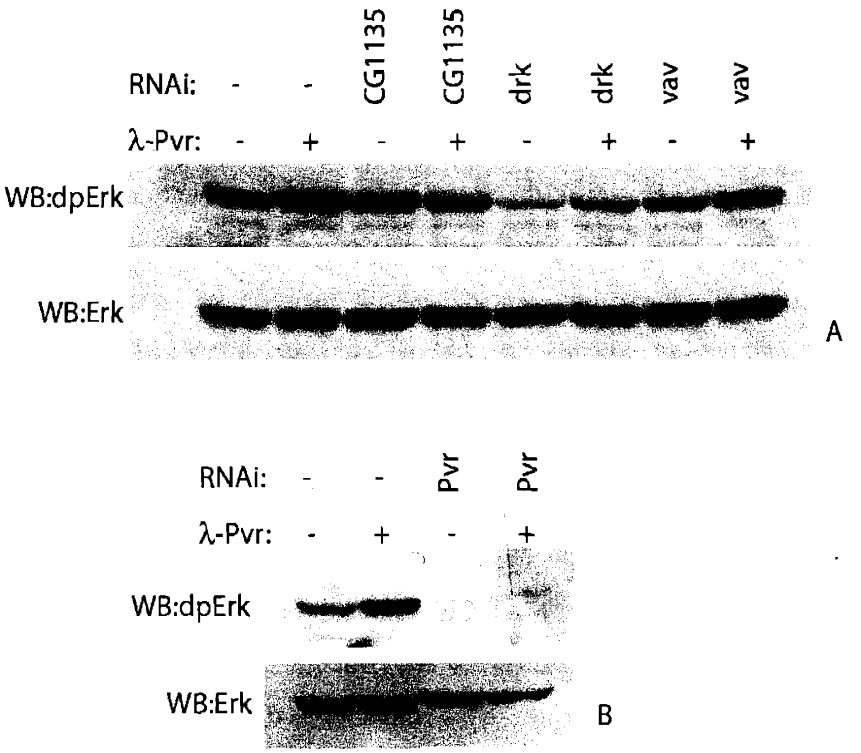

Figure 5. CG1135 RNAi blocks induction of Erk activation by constitutively active lambda-Pvr, but not endogenous Pvr. Schneider cells were transfected with pAc-lambda-Pvr and/or the dsRNA indicated. Cell lysates were analyzed by Western blot for Erk phosphorylation (top panels) and total Erk expression (bottom panels). (A) Expression of lambda-Pvr increased Erk phosphorylation (lane 2). This effect was blocked by CG1135 RNAi (lane 4). RNAi against drk or vav decreased the basal level of Erk phosphorylation (lanes 5 and 7), but did not affect the increase caused by expression of lambda-Pvr (lanes 6 and 8). (B) RNAi of Pvr completely eliminates the basal level of Erk phosphorylation (lane 3).

this ectopically-induced pathway. It has been suggested that dominant active torso also induces ectopic signaling cascades that are not activated by endogenous torso in the *Drosophila* embryo (Li and Li, 2003).

Addition of S2 cell-conditioned media to serum-starved S2 cells specifically activates endogenous Pvr. Therefore, only RNAi of genes in the endogenous Pvr/MAPK pathway would block induction of MAPK activation by conditioned media. In order to limit the level of Pvr activation prior to addition of conditioned media, I performed RNAi on the three Pvr ligands, Pvf1, Pvf2, and Pvf3. Pvf1 and Pvf3 RNAi together caused the greatest reduction in basal MAPK phosphorylation levels (Figure 6a), suggesting that activation of Pvr by Pvf1 or Pvf3 leads to activation of MAPK. S2 cells were transfected with Pvf1/3 dsRNA alone or Pvf1/3 dsRNA and dsRNA against one of the Pvr-interacting genes. Two days after transfection, cells were treated with fresh (control) media or conditioned media and analyzed for Erk phosphorylation. Conditioned media treatment of cells that had only been transfected with Pvf1/3 dsRNA resulted in approximately two-fold increase in Erk phosphorylation over cells that had been treated with control media (Figure 6b). RNAi of drk blocked this activation. This is not surprising, as drk has been found to act downstream of most receptor tyrosine kinases in activation of Erk. RNAi of any other gene had no effect on Erk activation.

None of the Pvr interactors display a requirement in hemocyte migration

I used RNAi to determine whether any of the Pvr interactors have a requirement in embryonic hemocyte migration. dsRNAs were injected into the ventral posterior portion of 1-hour-old Pxn-Gal4,UAS-GFP embryos at 3-4 $\mu g/\mu l$. These embryos express GFP in hemocytes beginning at embryonic stage 16, which allowed us to look for hemocyte migration phenotypes in live embryos approximately 17 hours after injection. Control injection of injection buffer with no dsRNA caused about 57% of the embryos to die or have severely defective morphologies (Figure 7a). Any embryos with normal morphology had hemocytes distributed throughout the embryo (Figure 7b). Injection of dsRNA against Pvr caused 48% of the embryos to have hemocyte migration defects, although 38% of the injected embryos had severely disrupted morphologies, indicative of injection-related damage (Figure 7a,c). RNAi of drk, Shc, dock, kurtz, vav, Lnk, Pli CG1135, CG17168, CG13289/90, or Socs16D and Socs44A together caused a distribution of phenotypes virtually indistinguishable from the control injection (Figure 7a),

Figure 6. Of the Pvr interactors, only drk is required for activation of Erk through endogenous Pvr. (A) Schneider cells were transfected with dsRNA against Pvr ligands Pvf1, Pvf2, Pvf3, or some combination of the three. Cells were starved overnight and treated with control medium for 10 minutes. Cell lysates were analyzed by Western blot for dpErk content. RNAi of Pvf1 and Pvf3 together causes the greatest reduction in the basal level of Erk phosphorylation. The bar graph indicates the relative levels of Erk phosphorylation (see Materials and Methods). (B) Schneider cells were transfected with dsRNA against Pvf1, Pvf3, and the gene indicated. Cells were starved overnight and treated for 10 minutes with control medium or conditioned medium. Lysates were analyzed by Western blot for dpErk (top panel) or total Erk (bottom panel) content. Values in the graph are as in (A), and represent the average of two independent experiments.

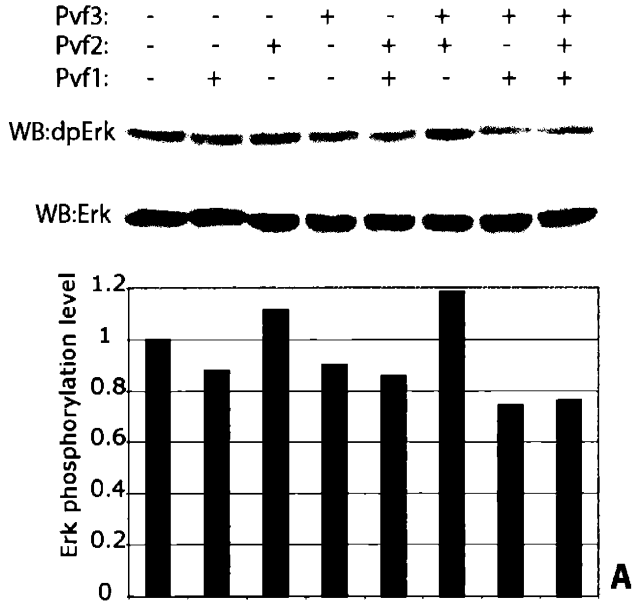

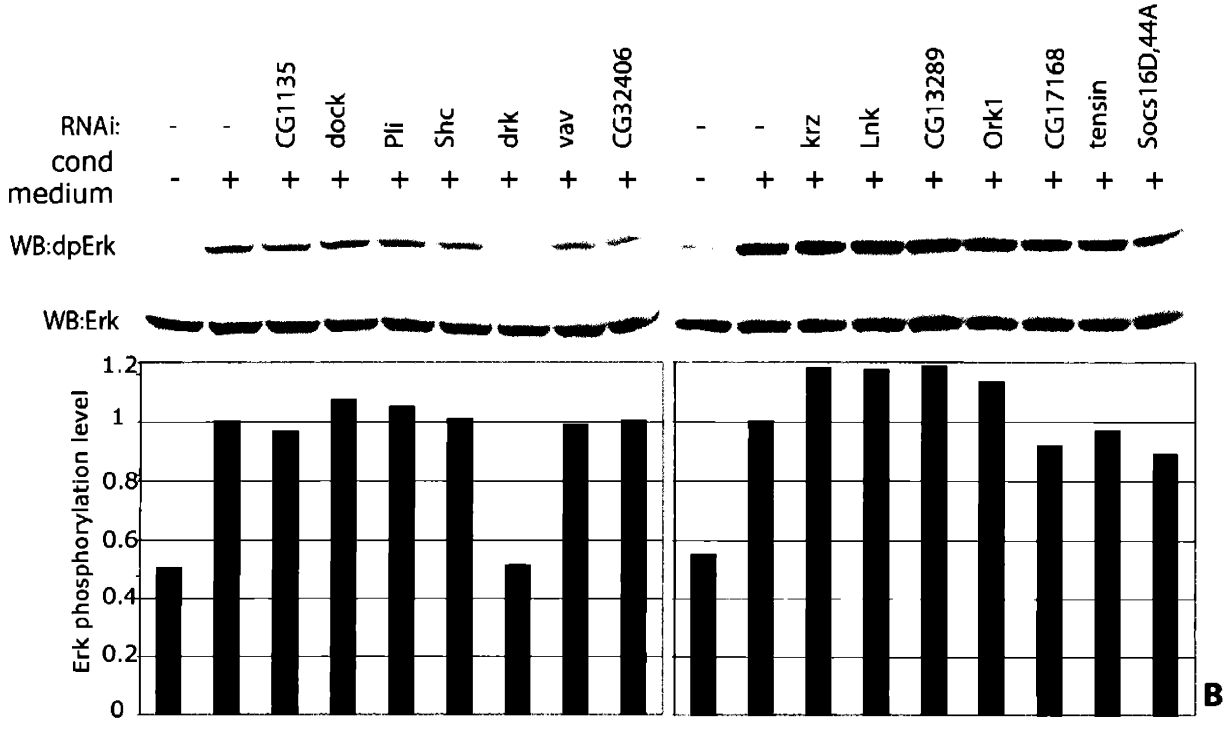

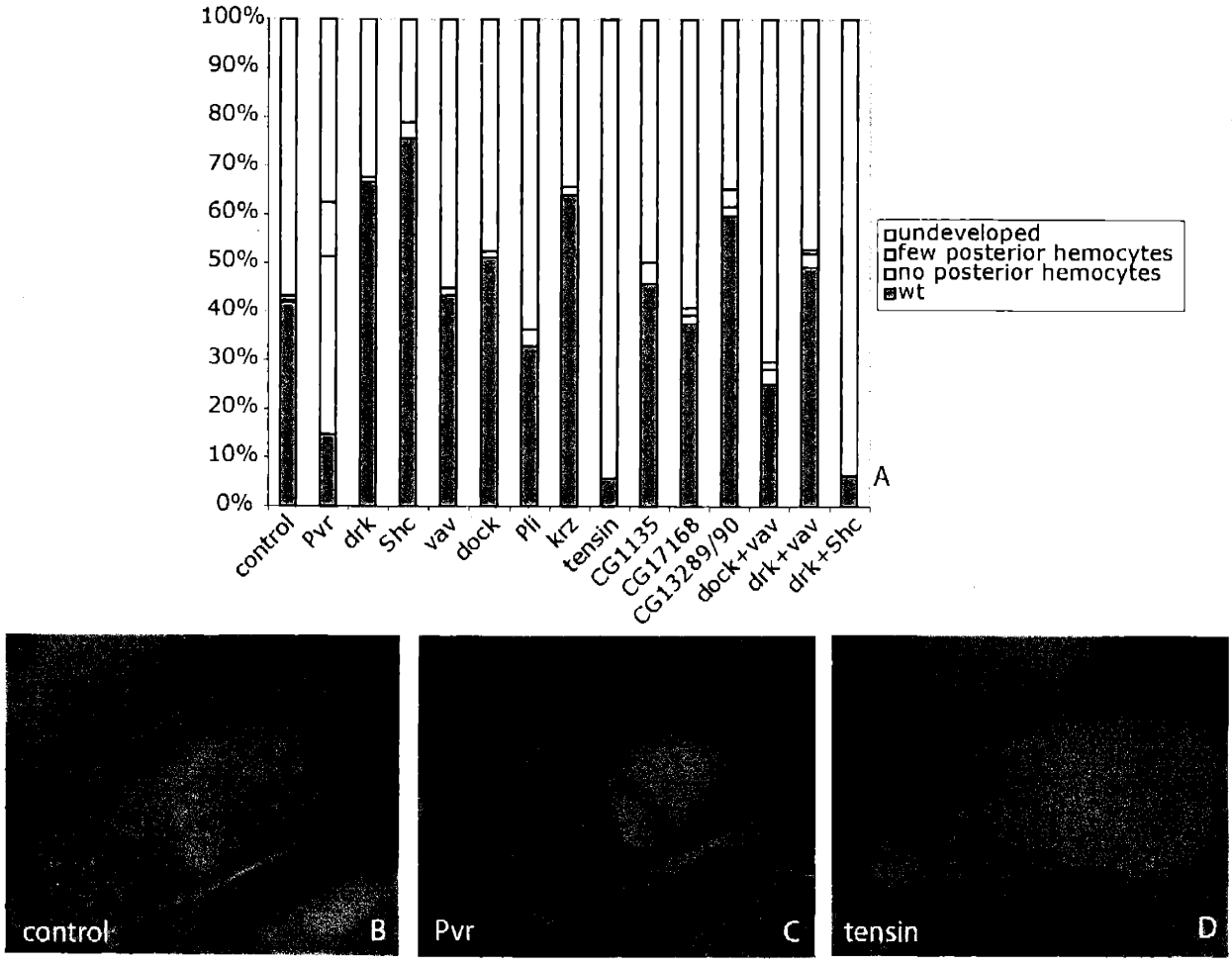

Figure 7. Pvr interactors do not have hemocyte migration phenotypes when inhibited by RNAi. dsRNA against each Pvr interactor was injected into Psn-Gal4;UAS-GFP embryos. (A) The graph shows the percentage of embryos from each injection that had a normal distribution of hemocytes, apparent defects in hemocyte migration (no hemocytes in posterior or few hemocytes in posterior), or were completely destroyed morphologically (undeveloped). (B-D) Embryos pictured are at stage 16-17 or the equivalent in hours of development. Anterior is down and to the left, ventral is up and to the left. (B) Control embryos injected with injection buffer. (C) Embryos injected with Pvr dsRNA. (D) Embryos injected with tensin dsRNA.

although gut development appeared to be perturbed when Socs16D and Socs44A were eliminated (data not shown). RNAi of tensin caused severe defects in embryogenesis such that it was impossible to assess whether tensin has a role in hemocyte migration (Figure 7d). In most of the tensin dsRNA-injected embryos, development in the posterior half was completely disrupted, but hemocytes could be seen clustering together in the anterior half of the embryo, which may have been a result of extensive cell death. Three pairwise combinitations of dsRNAs were also injected. Embryos injected with dock and vav or drk and vav dsRNAs were indistinguishable from control-injected embryos. Injection of drk and Shc dsRNAs together caused a severe disruption of development, such that in 94% of the embryos no embryonic structures whatsoever could be seen.

DISCUSSION

From a two-hybrid screen of an embryonic cDNA library I have identified 15 proteins that bind to the intracellular domain of Pvr in a phosphotyrosine-dependent manner. Twelve of the corresponding genes are expressed in larval hemocytes and S2 cells, and one more is expressed at low levels in embryonic hemocytes. Drk was found to be required for Pvr-dependent activation of MAPK, but neither drk nor any of the other interactors were found to have a hemocyte migration phenotype when gene expression was inhibited in embryos by RNAi. However, it is possible that these genes are redundant in their function or that they participate in Pvr signaling in other tissues. The proteins that were found to bind Pvr suggest potential roles for Pvr in MAPK signaling, Rac activation, GPCR signaling, integrin-mediated regulation of focal adhesions, and hematopoiesis.

drk is an adaptor protein homologous to Grb2 in mammals. It is composed of an SH2 domain flanked by two SH3 domains. The SH2 domain is likely to be required for binding to Pvr. drk/Grb2 acts as an adaptor protein for most receptor tyrosine kinases, including EGF receptors, FGF receptors, PDGF and VEGF receptors, and *Drosophila* sevenless. It serves to translocate the GEF Sos to the membrane, where Sos can activate Ras. A number of factors lie downstream of Ras, such as MAP kinase, Rac, and PI3 kinase. All three of these downstream effectors have been implicated in cell migration and regulation of the cytoskeleton. I have

demonstrated that drk is required for Pvr-dependent Erk MAP kinase activation. Erk is activated in response to Pvr ligand in embryonic hemocytes, and Ras activity is thought to be required for hemocyte migration (Cho et al., 2002; Heino et al., 2001). However, elimination of drk RNA by RNAi had no effect on hemocyte migration, although RNAi of drk would not eliminate maternal contribution of drk protein. The mouse protein Gab1, which binds Grb2, is required for PDGF-induced activation of MAP kinase and PDGF-induced changes in the cytoskeleton in mouse embryonic fibroblasts (Kallin et al., 2004). Interestingly, MAP kinase activity was not required for the cytoskeletal changes, but rather this effect was mediated by Rac. It would be interesting to compare the effects of dominant negative Ras, Rac, Rho, and Cdc42 on hemocyte migration to determine whether one of the small GTPases is preferentially required for this process.

The adaptor protein Shc is required in some cells for drk/Grb2 to bind to activated RTKs. Shc has an N-terminal PTB domain, which binds to drk/Grb2, and a C-terminal SH2 domain, which binds to the activated RTK. In fact, only the SH2 domain of Shc is required for binding to Pvr. Shc has not directly been shown to mediate PDGF-induced chemotaxis, but its requirement for mediating activation of Ras would suggest a possible role in cell migration. However, RNAi of Shc does not result in an embryonic hemocyte migration defect and Shc is not required for Pvr-dependent activation of Erk. Neither Shc nor drk were shown to be required for border cell migration in the oocyte (Duchek et al., 2001).

dreadlocks (dock) is an adaptor protein homologous to mammalian Nck with three N-terminal SH3 domains and a C-terminal SH2 domain. Only the SH2 domain is required for binding to Pvr. dock is required for guidance of axons in both the embryonic CNS and the retina. Nck binds to and is phosphorylated by the PDGF receptor (Li et al., 1992), but a requirement for Nck in PDGF-induced proliferation or chemotaxis has not been convincingly demonstrated. dock is not required for Pvr-dependent activation of Erk, and RNAi of dock in embryos does not cause a hemocyte migration defect.

vav is a guanyl nucleotide exchange factor (GEF) for the small GTPase Rac. It is composed of a calponin-homology (CH) domain at the N-terminus, a GEF domain, a pleckstrin homology (PH) domain, an SH2 domain, and an SH3 domain at the C-terminus. CH domains bind F-actin, and PH domains bind inositol phosphates, which are important for signaling and are enzymatic targets of PLCαand PI3 kinase. The SH2 domain of vav is probably required for binding to Pvr, and the GEF domain may be inhibitory for binding to Pvr, as even the longest

cDNAs identified in the two-hybrid screen lacked sequences encoding the GEF domain. Expression of dominant active vav in S2 cells causes extension of an actin-based lamellipodial network, which is blocked by co-expression of dominant negative Rac (Hornstein et al., 2003). It has also been shown that vav is phosphorylated upon Egfr stimulation and that vav is required for Egfr-dependent Erk activation (Hornstein et al., 2003). Vav was not required for Pvr-dependent Erk activation. *Drosophila* vav has not been implicated in cell migration. The mammalian Vav proteins are required for migration of neutrophils and macrophages during wound healing (Hall et al., 2003), and the migration of primitive hematopoietic cells in response to cytokines is dependent on Vav1 (Whetton et al., 2003).

kurtz is a non-visual arrestin with a high level of homology to the mammalian beta-arrestins. Even the shortest cDNAs isolated from the Pvr two-hybrid screen encode all conserved protein domains, so it is impossible to say without further analysis which part of the protein is required for Pvr binding. The beta-arrestins are clathrin adaptor proteins that are recruited to activated G protein coupled receptors (GPCRs) and are thought to mediate signaling of the ligand-bound receptor through endocytosis. The PDGF receptor has been shown to constitutively bind to beta-arrestin, the GPCR EDG-1, and the GPCR activator GRK2 when the corresponding genes are exogenously co-expressed (Alderton et al., 2001). It has similarly been shown that stimulation of the PDGF receptor leads to EDG-1 phosphorylation and recruitment of beta-arrestin to EDG-1 (Hobson et al., 2001). Furthermore, EDG-1 is required for PDGF-induced chemotaxis and enhances PDGF-induced stimulation of Erk MAP kinase activation. beta-Arrestin also binds to the protease-activated receptor (PAR-2). PAR-2 sequesters ERK in the cytoplasm when bound to beta-arrestin, and activation of PAR-2 leads to reorganization of the cytoskeleton and cell motility dependent on Erk and beta-arrestin. *Drosophila* kurtz is expressed in the embryonic CNS, and its expression there is required for viability. Third instar larvae mutant for kurtz develop melanotic tumors resulting from encapsulation of disassociated fat bodies by hemocytes (Roman et al., 2000). Because kurtz appears to be required only in the CNS for viability, it seems unlikely that it is required for migration of the embryonic hemocytes. In fact, disruption of kurtz expression by RNAi had no effect on hemocyte migration. However, kurtz may play a role downstream of Pvr later in development, such as in development of the fat bodies or in the proper functioning of larval hemocytes. kurtz is not required for Pvr-dependent Erk activation in S2 cells.

Tensin is a part of the focal adhesion complex. Sequences at the N-terminus bind to actin filaments and a PTB domain at the C-terminus binds to integrins. Tensin thus serves as a link between the membrane and the actin cytoskeleton in focal adhesions. An SH2 domain N-terminal of the PTB domain binds tyrosine-phosphorylated proteins, and may be the route by which tensin itself becomes tyrosine phosphorylated. The SH2 domain of *Drosophila* tensin is likely to be required for binding to Pvr, as all isolated clones were N-terminally truncated just 10 amino acids upstream of the SH2 domain. A direct link between the PDGF receptor and tensin has not been demonstrated, but stimulation of mammalian cells with PDGF does lead to phosphorylation of tensin (Jiang et al., 1996) and association of tensin with PI3 kinase (Auger et al., 1996). As would be expected for a focal adhesion protein, tensin is required for migration of a number of mammalian cell types both *in vivo* and *ex vivo* (Chen et al., 2002; Chen and Lo, 2003; Lo, 2004), although a role in directed chemotaxis has not been shown. Zygotic and maternal mutants in *Drosophila* tensin are partially viable. Adult escapers have defects in wing expansion and show a blistered wing phenotype similar to some of the *Drosophila* integrin mutants (Lee et al., 2003). Contrary to this, RNAi of tensin resulted in a severe blockage of embryonic development. tensin mRNA did not appear to be heavily expressed early in embryonic development, but it may be required ubiquitously at low levels for proper development and maintenance of embryonic structures.

Pellino was originally identified in a two-hybrid screen for proteins that bind to the serine/threonine kinase Pelle (Grosshans et al., 1999). Interestingly, *Drosophila* Pelle is a positive regulator of larval hemocyte proliferation (Qiu et al., 1998). Ubiquitous overexpression of the Pvr ligand Pvf2 causes overproliferation of larval hemocytes (Qiu et al., 1998). Thus, Pellino may act downstream of Pvr and Pelle to regulate larval hemocyte proliferation. A link between Pellino and the PDGF receptor has not previously been demonstrated in mammalian systems.

Lnk is an adaptor protein with an N-terminal PH domain and a C-terminal SH2 domain. *Drosophila* Lnk has not been studied previously. In mammalian systems, the SH2 domain of Lnk has been shown to bind to the RTK c-Kit and thereby negatively regulate hematopoiesis (Nobuhisa et al., 2003). It is possible that Lnk interacts with Pvr in a similar fashion, negatively regulating Pvr-induced proliferation of hemocytes. Mutants in Lnk could be expected to have an

overabundance of larval hemocytes, similar to the Pvf2 overexpression phenotype described above.

CG17168 and CG1135 are both novel genes encoding proteins with a C-terminal FHA domain. FHA domains are similar to Smad domains and are generally found in proteins that bind serine/threonine kinases and translocate to the nucleus to activate transcription. The C-terminal half of the CG17168 protein is 60% identical and 75% similar to the human Smad Nuclear Interacting Protein 1 (SNIP1). The N-terminus is not conserved. The C-terminus of mammalian SNIP1 contains binding sites for Smad1 and Smad2 (Mad and Smox in *Drosophila*). The N-terminus of SNIP1 contains a nuclear localization sequence (NLS) and binding sites for the transcriptional co-activator CBP/p300 (Kim et al., 2000), but neither of these sequences is conserved in CG17168, suggesting that CG17168 may participate in Smad signaling, but is unlikely to be a full functional homolog of SNIP1. The C-terminal half of CG1135 shares 58% identity and 73% similarity with the human Microspherule protein 1 (MCRS1). The region of the CG1135 protein homologous to MCRS1 is sufficient for binding to Pvr. MCRS1 is a nucleolar protein that binds to the transcriptional activator Daxx. Links to the PDGF receptor, cell migration, or cell proliferation have not been shown for either SNIP1 or MCRS1. CG1135 is required to mediate the increase in Erk phosphorylation caused by overexpression of constitutively active Pvr, but not activation of endogenous Pvr. The Smad signaling pathway is also ectopically activated by gain-of-function torso (Li and Li, 2003).

Suppressors of Cytokine Signaling (SOCS) are negative regulators of Jak/Stat signaling. They are characterized by an SH2 domain and a C-terminal SOCS domain, which mediates ubiquitination. Presumably the SOCS proteins work to downregulate tyrosine-phosphorylated proteins by binding them and initiating ubiquitination and degradation. In *Drosophila* there are three Socs homologues: Socs16D, Socs36E, and Socs44A. In my two-hybrid screen for Pvr interactors, I pulled out two of the Socs homologues once each. They are both expressed in S2 cells and larval hemocytes, but inhibition of Socs16D and Socs44A by RNAi in embryos does not result in a hemocyte migration phenotype.

CG13289 and CG32406 are novel genes encoding proteins with an SH2 domain at the C-terminus. The N-termini of the encoded proteins have a low level of homology to each other, but not to any other proteins. The mRNAs are not expressed in S2 cells or in larval hemocytes.

CG32406 is expressed at low levels in embryonic hemocytes and by RNA in situ appears to be expressed only in a subset of cells in the embryonic CNS.

In summary, I have used a two-hybrid approach to identify proteins that bind to the intracellular domain of Pvr. Of 15 genes isolated, twelve are expressed in embryonic hemocyte-derived S2 cells and larval hemocytes. Embryonic mRNA expression patterns of none of these genes are the same as that of Pvr. In addition, RNAi of Pvr interactors in embryos either does not cause a hemocyte migration defect or causes such severe defects in embryogenesis that hemocyte migration cannot be analyzed. In S2 cells, drk is required downstream of Pvr for activation of Erk MAP kinase. It could be interesting to see whether activated Pvr and drk physically interact in S2 cells and whether drk is phosphorylated when Pvr is activated. One could also determine which tyrosine in Pvr is required for drk binding. To determine which other pathway members are required downstream of Pvr for Erk activation, one could perform RNAi on Sos; small G proteins Ras, Rac, Rho, and Cdc42; Raf homologues pole hole and Raf2; MEKK homologs Mekk1 and Pk92B; and MEK homologues Dsor1, Dsor3, and licorne.

Considering that none of the Pvr-interacting proteins had hemocyte migration phenotypes when expression of the corresponding genes were disrupted by RNAi, further study is required to determine whether the binding of these proteins to Pvr is physiologically relevant in any way. It is possible that RNAi did not completely eliminate the corresponding mRNAs, and enough mRNA remained post-injection to provide functional protein. Similarly, it is possible that there is redundancy in the pathway downstream of Pvr and removal of a single gene is not enough to generate a phenotype. To get around these problems, RNAi of the candidate interactors could be examined in a sensitized background where the Pvr pathway is already weakened but not broken, as in a Pvr hypomorph. In mutagenizing Pvr, I generated two hypomorphic alleles. One is Pvr^{KO8}, a genomic rearrangement of the Pvr locus that has not been fully molecularly mapped. The other is Pvr^{1067}, in which a glycine is mutated to serine in a part of the second immunoglobulin domain that is alternatively spliced.

The requirement of signaling components downstream of mammalian PDGFRs has been deduced in large part by determining which tyrosines in PDGFR are required for various processes and which proteins bind to those tyrosines when they are phosphorylated. The knowledge of which tyrosines are required in PDGFR cannot be applied to our understanding of Pvr function, as those tyrosines are not conserved. However, it would be highly enlightening to

know which tyrosines in Pvr are phosphorylated upon ligand binding, and which tyrosines are required for hemocyte migration. With Y-F Pvr mutants in hand, one could use the two-hybrid system or in vivo binding in S2 cells to determine where on Pvr the various Pvr-interacting proteins bound. A correlation could then be made between tyrosines required for binding a certain protein and tyrosines required for function in hemocyte migration.

MATERIALS AND METHODS

Construction of two-hybrid bait

The intracellular domain of Pvr was digested out of cDNA clone SD03874 with EcoRI and HincII. This fragment was cloned into the EcoRI and SmaI sites of pRS26DBD (Ethan Ford, Leonard Guarente) to created DBD-Pvrpartial. PRS26DBD contains the URA3 selectable marker, the ADH full-length promoter, and the Gal4 DNA-binding domain. The EcoRI site in Pvr is 150 bp downstream of the start of the intracellular domain. The remaining 150 bp fragment was amplified using SD03874 as a template and primers 5'-ATAGAATTCCTCGCCGTGCGCTACC-3' and 5'-CCTCGTTGTCAGCCGTCGC-3'. The latter primer is downstream of the endogenous EcoRI site in Pvr. The resulting PCR product was digested with EcoRI (underlined sequence) and cloned into the EcoRI site in DBD-Pvrpartial to create DBD-Pvr. Clones with the PCR product inserted in the correct orientation were identified by sequencing. DBD-PvrKA was created by site-directed mutagenesis using the QuikChange II XL kit (Stratagene) and primers 5'-ACCACGGTGGCCGTCGCAATGGTCAAGGCGACG-3' and its complement. The underlined sequence is an alanine codon. This sequence reads AAA in wild type Pvr, endoding lysine.

Construction of pAc-lambda-Pvr

A 2.8 kb BglII/BglII fragment was excised from SD03874 to create Pvr-intra. Pvrintra contains sequences encoding the Pvr transmembrane domain and the entire intracellular domain. The transmembrane and intracellular domains of Pvr were excised from Pvr-intra as a 2.1 kb BglII/StuI fragment. Sequences encoding the lambda cI repressor were excised from pBS-lambda-HtI (Alan Michelson) as a 0.6 kb BglII/Not fragment

lambda-Pvr. pAc5.1/V5-His B (Invitrogen) was modified by inserting an oligonucleotide 5'-TCGAGTCTAGAGTATACTACGTACGCCGC-3' annealed to 5'-GGCGTACGTAGTATACTCTAGAC-3' between the XhoI and SacII sites to create pAc5.1/V5-His D. pAc5.1/V5-His D was digested with NotI and BsaAI (underlined sequence) and ligated to the lambda cI and Pvr-intra fragments.

Library screening

Drosophila melanogaster embryo MATCHMAKER cDNA library was obtained from Clontech. The library contained 3.0 x 10^6 independent clones with an cDNA size range of 0.5-3 kb. The library was amplified once according to the manufacturer's protocol. 400 ml of YPDA medium was inoculated with PJ69-4A (James et al., 1996) and grown overnight. Cells from 300 OD600 units of culture were pelleted and suspended in 1.2 L of fresh YPDA and grown to OD_{600}=1.0. The cells were pelleted, suspended in 300 ml sterile water, repelleted, and suspended in 12 ml 100 mM lithium acetate. The cells were incubated at 30°C for 15 min and pelleted again. The cells were suspended in a solution of 33% PEG-8000, 100 mM Lithium acetate, 38.4 mg unsonicated single-stranded salmon sperm DNA (Sigma), 240 μg library DNA, and 360 μg DBD-Pvr in a total volume of 43.2 ml, incubated at 30°C for 30 min and heat-shocked at 42°C for 60 min. The cells were pelleted and suspended in 20 ml TE/1.2 M Sorbitol. The transformation was spread on 50 SC-leu,ura,his plates supplemented with 5 mM 3-aminotriazole. 2 μl of the transformation was spread on SC-leu.ura plates to determine transformation efficiency. One transformation resulted in 2.9 x 10^6 co-transformed colonies and another similar transformation resulted in 7.1 x10^6 co-transformed colonies. Positive colonies were patched onto SD-leu,ura,his,ade plates supplemented with 40 mM X-α-Gal.

RT-PCR

Embryonic hemocytes were FACS sorted using a Cytomation MoFlo high speed sorter at the MIT Flow Cytometry Core Facility from Pxn-Gal4,UAS-GFP embryos that had been gently homogenized in phosphate-buffered saline. Total RNA was isolated from 1.4x10^5 GFP-positive cells. Total RNA was isolated from 7x10^5 S2 cells with the RNAqueous-4PCR kit and subsequently treated with DNase (Ambion). Larval hemocyte RNA was a gift of Guilherme Neves and Andy Chess. RNAs were reverse-transcribed using the RETROscript kit (Ambion).

PCR was performed with the same gene-specific primers that were used to make dsRNA templates.

RNA in situ hybridization

Templates for in situ hybridization probes were amplified by PCR using the same primer sequences as were used for making dsRNA templates, except that the T7 sequence on the forward primers were replaced with T3 sequence 5'-AATTAACCCTCACTAAAGGGAGA-3'. RNA was transcribed using the MAXIscript kit (Ambion) and labeled by incorporation of digoxygenin-11-UTP. RNA in situs were performed as described (Lehmann and Tautz, 1994).

dsRNA synthesis for RNA interference

Templates for dsRNA synthesis were amplified by PCR using primers with the T7 sequence 5'-TAATACGACTCAGTATAGGGAGA-3' at the 5' end. The gene-specific sequences of the primers were as follows: Socs44A, 5'-TTACGCCGGCCATCTGTC-3' and 5'-CTCTGGAAGACCAGCTCC-3'; CG17168, 5'-AGCGAAACAAAGAGCGGGAC-3' and 5'-TCGTGGAGCAGAACATACTCGC-3'; Pli, 5'-CGTCAAGCGTTCCAAGCACTAC-3' and 5'-GCGTGGTATAACCGCGTGTTC-3'; dock, 5'-AAGCACGGCAAATCTCAGGAC-3' and 5'-TGGCACTCGCATTACGATAGG-3'; CG1135, 5'-TCGGAACAACCAAAACTTGAGC-3' and 5'-TTGACCAGGAAGGTGAAGCG-3'; Ork1, 5'-TCTTCGCTGGCGATCAAACG-3' and 5'-GGCAGCCTTATCGACTTTGTGG-3'; CG32406, 5'-CATCGACAGCAAGTTCGGTGAC-3' and 5'-TCTCCATGTTCTTGGCACGC-3'; CG13289, 5'-TCTCCGATGGCTATGTGAACG-3' and 5'-CCATACATCTCGAAGTCCGCTC-3'; tensin, 5'-CAATTTGCCCGTAGTTCGTCC-3' and 5'-TGGTTTCTTGTCAGACTCGCC-3'; krz, 5'-TTTCGGTACGGACGTGAAGACC-3' and 5'-ACGCTGAGCAGGATTGGTAATG-3'; Lnk, 5'-AGAGTTTTACACGCCGCACAAG-3' and 5'-AATGGTGAGCCGCAAATGC-3'; Socs16D, 5'-TGAACGGGACGTTGATAACGG-3' and 5'-AATGCGAACTGTCGCTCTCCAC-3'; drk, 5'-AGGAAGCGATTGCCAAACACG-3' and 5'-GGCGTCACATAAGTTGCTGG-3'; vav, 5'-GATGCAAGGTGTGCCAGATCAG-3' and 5'-TGCTCCTGCACATACTCCTTGG-3'; Shc, 5'-TCGACTTCCTCGCCTACATAGC-3' and 5'-ATCTTTGGTTCGGACCACGC-3'. cDNAs isolated from the yeast two-hybrid screen were used as PCR templates. Pvf1 dsRNA template was PCR amplified from genomic DNA using

primers 5'-TGTCCGTGTCCGCTGAG-3' and 5'-TCGTCCACCCAATACTTGTTC-3' with T7 sequences at the 5' ends. Pvf 2 and Pvf3 dsRNA templates were amplified by RT-PCR from S2 cell RNA. Primers for Pvf2 were 5'-GCATTTGACAGTGTTGAAAGAGC-3' and 5'-CAGATTGGGATTCCGATTTGG-3' with T7 5' ends. Primers for Pvf3 were 5'-AAGAAGGAGGACCAGTTGG-3' and 5'-TGTAGGATGGCTGTTCGTG-3' with T7 5' ends. dsRNAs were transcribed with the MEGAscript T7 High Yield Transcription kit (Ambion). Complementary transcripts were annealed by heating to 65°C for 30 min and slowly cooling to room temperature.

MAP kinase activation assays

S2 cells were plated at 10^6 cells/ml in 2 ml Schneider's *Drosophila* medium supplemented with 10% FBS (Gibco) in 6-well plates. Cells were grown at 24°C overnight and transfected with 1 μg each dsRNA and/or pAc-lambda-Pvr plasmid DNA using FuGENE 6 Transfection Reagent (Roche). Transfected cells were grown for an additional two days before assays were performed. For experiments using conditioned media to activate Pvr, cells were starved overnight in Schneider's *Drosophila* medium lacking FBS. Cells were subsequently washed and incubated in control media (fresh Schneider's media with FBS) or conditioned media (media taken from cells that had been cultured for 7-10 days) for 10 minutes. For experiments using lambda-Pvr, cells were not starved or treated with conditioned media. In both types of experiments, cells were washed in phosphate-buffered saline and lysed in 400 μl MAPK lysis buffer (20 mM Tris, pH 7.5, 150 mM NaCl, 1% Triton X-100, 1 mM sodium orthovanadate, 10 mM sodium α-glycerophosphate, 5 mM NaF, 5 mM sodium pyrophosphate, with complete protease inhibitor cocktail (Roche)). Proteins from 30 μl of soluble lysate fraction were separated by 10% SDS-PAGE and transferred to Hybond-P membrane (Amersham). Membranes were probed with monoclonal antibody against diphosphorylated ERK-1&2 (anti-dpErk; Sigma) diluted 1:5000 and subsequently stripped and reprobed with polyclonal antiserum against ERK-1,ERK-2 (Sigma) diluted 1:40,000. Primary antibody was detected with HRP-conjugated goat anti-mouse or goat anti-rabbit secondaries (Jackson ImmunoResearch) and ECL-Plus (Amersham). Bands were quantitated from developed film using UnScan-It software. The intensity of anti-dpErk bands was normalized against the intensity of the corresponding anti-Erk bands. This ratio was

divided by the ratio from a control lane in the same Western blot. Therefore, all Erk activation values are expressed as a fraction of the level of activation of a control sample.

RNAi of embryos

Pxn-Gal4,UAS-GFP flies were a gift of Michael Galko and Mark Krasnow. Embryos were collected for 1 hour on molasses agar plates and injected with dsRNAs at 2-6 $\mu g/\mu l$ suspended in injection buffer (0.1 mM sodium phosphate pH 6.8, 5 mM KCl). Embryos were aged at room temperature for 17 hours and examined by fluorescence microscopy on a Zeiss Axioplan 2 upright microscope.

REFERENCES

Alderton, F., Rakhit, S., Kong, K. C., Palmer, T., Sambi, B., Pyne, S., and Pyne, N. J. (2001). Tethering of the platelet-derived growth factor beta receptor to G-protein-coupled receptors. A novel platform for integrative signaling by these receptor classes in mammalian cells. J Biol Chem *276*, 28578-28585.

Anand-Apte, B., Zetter, B. R., Viswanathan, A., Qiu, R. G., Chen, J., Ruggieri, R., and Symons, M. (1997). Platelet-derived growth factor and fibronectin-stimulated migration are differentially regulated by the Rac and extracellular signal-regulated kinase pathways. J Biol Chem *272*, 30688-30692.

Arvidsson, A. K., Rupp, E., Nanberg, E., Downward, J., Ronnstrand, L., Wennstrom, S., Schlessinger, J., Heldin, C. H., and Claesson-Welsh, L. (1994). Tyr-716 in the platelet-derived growth factor beta-receptor kinase insert is involved in GRB2 binding and Ras activation. Mol Cell Biol *14*, 6715-6726.

Aspenstrom, P. (2002). The WASP-binding protein WIRE has a role in the regulation of the actin filament system downstream of the platelet-derived growth factor receptor. Exp Cell Res *279*, 21-33.

Auger, K. R., Songyang, Z., Lo, S. H., Roberts, T. M., and Chen, L. B. (1996). Platelet-derived growth factor-induced formation of tensin and phosphoinositide 3-kinase complexes. J Biol Chem *271*, 23452-23457.

Chen, H., Duncan, I. C., Bozorgchami, H., and Lo, S. H. (2002). Tensin1 and a previously undocumented family member, tensin2, positively regulate cell migration. Proc Natl Acad Sci U S A *99*, 733-738.

Chen, H., and Lo, S. H. (2003). Regulation of tensin-promoted cell migration by its focal adhesion binding and Src homology domain 2. Biochem J *370*, 1039-1045.

Cho, N. K., Keyes, L., Johnson, E., Heller, J., Ryner, L., Karim, F., and Krasnow, M. A. (2002). Developmental control of blood cell migration by the Drosophila VEGF pathway. Cell *108*, 865-876.

Choudhury, G. G., Karamitsos, C., Hernandez, J., Gentilini, A., Bardgette, J., and Abboud, H. E. (1997). PI-3-kinase and MAPK regulate mesangial cell proliferation and migration in response to PDGF. Am J Physiol *273*, F931-938.

Derman, M. P., Toker, A., Hartwig, J. H., Spokes, K., Falck, J. R., Chen, C. S., Cantley, L. C., and Cantley, L. G. (1997). The lipid products of phosphoinositide 3-kinase increase cell motility through protein kinase C. J Biol Chem *272*, 6465-6470.

Duchek, P., Somogyi, K., Jekely, G., Beccari, S., and Rorth, P. (2001). Guidance of cell migration by the Drosophila PDGF/VEGF receptor. Cell *107*, 17-26.

Goto, A., Kumagai, T., Kumagai, C., Hirose, J., Narita, H., Mori, H., Kadowaki, T., Beck, K., and Kitagawa, Y. (2001). A Drosophila haemocyte-specific protein, hemolectin, similar to human von Willebrand factor. Biochem J *359*, 99-108.

Grosshans, J., Schnorrer, F., and Nusslein-Volhard, C. (1999). Oligomerisation of Tube and Pelle leads to nuclear localisation of dorsal. Mech Dev *81*, 127-138.

Hall, A. B., Gakidis, A. M., Gao, S., Wilsbacher, J., Swat, W., and Brugge, J. S. (2003). Vav family proteins play a critical role in multiple macrophage functions. Molecular Biology of the Cell *14*, 212a.

Heino, T. I., Karpanen, T., Wahlstrom, G., Pulkkinen, M., Eriksson, U., Alitalo, K., and Roos, C. (2001). The Drosophila VEGF receptor homolog is expressed in hemocytes. Mech Dev *109*, 69-77.

Higaki, M., Sakaue, H., Ogawa, W., Kasuga, M., and Shimokado, K. (1996). Phosphatidylinositol 3-kinase-independent signal transduction pathway for platelet-derived growth factor-induced chemotaxis. J Biol Chem *271*, 29342-29346.

Hinton, D. R., He, S., Graf, K., Yang, D., Hsueh, W. A., Ryan, S. J., and Law, R. E. (1998). Mitogen-activated protein kinase activation mediates PDGF-directed migration of RPE cells. Exp Cell Res *239*, 11-15.

Hobson, J. P., Rosenfeldt, H. M., Barak, L. S., Olivera, A., Poulton, S., Caron, M. G., Milstien, S., and Spiegel, S. (2001). Role of the sphingosine-1-phosphate receptor EDG-1 in PDGF-induced cell motility. Science *291*, 1800-1803.

Hooshmand-Rad, R., Claesson-Welsh, L., Wennstrom, S., Yokote, K., Siegbahn, A., and Heldin, C. H. (1997). Involvement of phosphatidylinositide 3'-kinase and Rac in platelet-derived growth factor-induced actin reorganization and chemotaxis. Exp Cell Res *234*, 434-441.

Hornstein, I., Mortin, M. A., and Katzav, S. (2003). DroVav, the Drosophila melanogaster homologue of the mammalian Vav proteins, serves as a signal transducer protein in the Rac and DER pathways. Oncogene *22*, 6774-6784.

James, P., Halladay, J., and Craig, E. A. (1996). Genomic libraries and a host strain designed for highly efficient two-hybrid selection in yeast. Genetics *144*, 1425-1436.

Jiang, B., Yamamura, S., Nelson, P. R., Mureebe, L., and Kent, K. C. (1996). Differential effects of platelet-derived growth factor isotypes on human smooth muscle cell proliferation and migration are mediated by distinct signaling pathways. Surgery *120*, 427-431; discussion 432.

Kallin, A., Demoulin, J. B., Nishida, K., Hirano, T., Ronnstrand, L., and Heldin, C. H. (2004). Gab1 contributes to cytoskeletal reorganization and chemotaxis in response to platelet-derived growth factor. J Biol Chem.

Kim, R. H., Wang, D., Tsang, M., Martin, J., Huff, C., de Caestecker, M. P., Parks, W. T., Meng, X., Lechleider, R. J., Wang, T., and Roberts, A. B. (2000). A novel smad nuclear interacting protein, SNIP1, suppresses p300-dependent TGF-beta signal transduction. Genes Dev *14*, 1605-1616.

Kundra, V., Anand-Apte, B., Feig, L. A., and Zetter, B. R. (1995). The chemotactic response to PDGF-BB: evidence of a role for Ras. J Cell Biol *130*, 725-731.

Kundra, V., Escobedo, J. A., Kazlauskas, A., Kim, H. K., Rhee, S. G., Williams, L. T., and Zetter, B. R. (1994). Regulation of chemotaxis by the platelet-derived growth factor receptor-beta. Nature *367*, 474-476.

Lee, S. B., Cho, K. S., Kim, E., and Chung, J. (2003). blistery encodes Drosophila tensin protein and interacts with integrin and the JNK signaling pathway during wing development. Development *130*, 4001-4010.

Lehmann, R., and Tautz, D. (1994). In situ hybridization to RNA. Methods Cell Biol *44*, 575-598.

Li, J., and Li, W. X. (2003). Drosophila gain-of-function mutant RTK torso triggers ectopic Dpp and STAT signaling. Genetics *164*, 247-258.

Li, W., Hu, P., Skolnik, E. Y., Ullrich, A., and Schlessinger, J. (1992). The SH2 and SH3 domain-containing Nck protein is oncogenic and a common target for phosphorylation by different surface receptors. Mol Cell Biol *12*, 5824-5833.

Lo, S. H. (2004). Tensin. Int J Biochem Cell Biol *36*, 31-34.

Nobuhisa, I., Takizawa, M., Takaki, S., Inoue, H., Okita, K., Ueno, M., Takatsu, K., and Taga, T. (2003). Regulation of hematopoietic development in the aorta-gonad-mesonephros region mediated by Lnk adaptor protein. Mol Cell Biol *23*, 8486-8494.

Obenauer, J. C., Cantley, L. C., and Yaffe, M. B. (2003). Scansite 2.0: Proteome-wide prediction of cell signaling interactions using short sequence motifs. Nucleic Acids Res *31*, 3635-3641.

Qiu, P., Pan, P. C., and Govind, S. (1998). A role for the Drosophila Toll/Cactus pathway in larval hematopoiesis. Development *125*, 1909-1920.

Roman, G., He, J., and Davis, R. L. (2000). kurtz, a novel nonvisual arrestin, is an essential neural gene in Drosophila. Genetics *155*, 1281-1295.

Ronnstrand, L., and Heldin, C. H. (2001). Mechanisms of platelet-derived growth factor-induced chemotaxis. Int J Cancer *91*, 757-762.

Rozakis-Adcock, M., McGlade, J., Mbamalu, G., Pelicci, G., Daly, R., Li, W., Batzer, A., Thomas, S., Brugge, J., Pelicci, P. G., and et al. (1992). Association of the Shc and Grb2/Sem5

SH2-containing proteins is implicated in activation of the Ras pathway by tyrosine kinases. Nature *360*, 689-692.

Torgler, C. N., Narasimha, M., Knox, A. L., Zervas, C. G., Vernon, M. C., and Brown, N. H. (2004). Tensin stabilizes integrin adhesive contacts in Drosophila. Dev Cell *6*, 357-369.

Vanhaesebroeck, B., and Alessi, D. R. (2000). The PI3K-PDK1 connection: more than just a road to PKB. Biochem J *346 Pt 3*, 561-576.

Wennstrom, S., Hawkins, P., Cooke, F., Hara, K., Yonezawa, K., Kasuga, M., Jackson, T., Claesson-Welsh, L., and Stephens, L. (1994a). Activation of phosphoinositide 3-kinase is required for PDGF-stimulated membrane ruffling. Curr Biol *4*, 385-393.

Wennstrom, S., Siegbahn, A., Yokote, K., Arvidsson, A. K., Heldin, C. H., Mori, S., and Claesson-Welsh, L. (1994b). Membrane ruffling and chemotaxis transduced by the PDGF beta-receptor require the binding site for phosphatidylinositol 3' kinase. Oncogene *9*, 651-660.

Whetton, A. D., Lu, Y., Pierce, A., Carney, L., and Spooncer, E. (2003). Lysophospholipids synergistically promote primitive hematopoietic cell chemotaxis via a mechanism involving Vav 1. Blood *102*, 2798-2802.

CONCLUSIONS AND FUTURE DIRECTIONS

Tyrosine phosphorylation plays a key role in the regulation of the signaling cascades that control cell migration and tissue development. I have studied the roles of two receptors, a receptor tyrosine phosphatase, Ptp69D, and a receptor tyrosine kinase, Pvr, in axon guidance and cell migration contributing to the development of the nervous system. In addition to describing the involvement of these two receptors in nervous system development, I have sought to understand the mechanisms by which they guide migrating cells or navigating axons. Ptp69D's involvement in axon guidance has been described previously, but how it is activated and the proteins it interacts with in axon targeting were unknown. Conversely, receptor tyrosine kinase activation is well understood, and much is known about the signaling pathways downstream of PDGFRs in cell migration in cultured cells. However, the role of Pvr and its homologs in nervous system development and cell migration in the animal was not well understood.

Both Ptp69D and Pvr are involved in the development of the *Drosophila* nervous system. Ptp69D is involved in the guidance of axons in both the embryonic CNS and in the developing eye. It is thought that Ptp69D might regulate adhesion, rather than directly influencing growth cone attraction or repulsion. Pvr mutants also have defects in embryonic CNS morphogenesis, namely the mispositioning of longitudinal glia and the axon tracts in the CNS. However, these defects are not due to axon guidance errors or even defects in cell migration within the CNS. Rather, they are an indirect result of the failure of hemocytes to migrate out of the CNS. Hemocytes are blood cells that have macrophage-like properties, engulfing pathogens and dead cell debris. When the hemocytes are unable to engulf cell corpses either due to mispositioning or phagocytosis defects, the longitudinal glia become mispositioned. The longitudinal glia have phagocytic activity, much like the microglia in mammalian systems. I have hypothesized that in the absence of macrophages, the longitudinal glia converge on the midline to engulf the cell debris remaining from the apoptotic deaths of the midline glia. The longitudinal axon tracts in Pvr mutant embryos are positioned closer to the midline than in wild type, but there is no ectopic midline crossing, suggesting that axon guidance in Pvr mutants is normal. The mispositioning of the longitudinal axon tracts could be a result of the mispositioning of the longitudinal glia, as these glia are used to guide the axons as they grow out.

Cell migration and axon guidance are highly similar processes, involving the remodeling of the cytoskeleton to form protrusions from the cell and the stabilization of protrusions in a given direction. Cell migration and axon guidance primarily involve two types of modification: polymerization, depolymerization, or branching of the actin or microtubule cytoskeleton, and changes in adhesion, whether that be in cell-cell contacts or adhesion to the extracellular matrix. RPTPs and the PDGFR have been shown to regulate both types of modifications. I have sought to gain further understanding in the signaling pathways regulated by PTP69D and Pvr in axon guidance and cell migration by identifying proteins that they bind to and genetically interact with.

I have focused on the role of Ptp69D in photoreceptor axon guidance, seeking to identify genetic interactors and enzymatic substrates. Ptp69D loss of function or expression of dominant negative Ptp69D causes R1-R6 axons to shoot through their target, the lamina, and terminate with the R8s in the medulla. By expressing a truncated form of Ptp69D, I found that Ptp69D is likely to be activated by heterodimerization with another protein. I found the receptor tyrosine kinases Src and Abl to be positive effectors of Ptp69D signaling, while the EGF receptor and its downstream effector, Ras, were negative effectors of Ptp69D signaling. Src has been shown to be activated by mammalian RPTPs through dephosphorylation of a C-terminal inhibitory phosphotyrosine. Src is a key regulator of focal adhesion formation, and Ptp69D is also thought to regulate adhesion. It would be interesting to see whether Src is activated by Ptp69D and whether Ptp69D is recruited to focal adhesion sites at the lamina. The genetic relationship between Src and Ptp69D also needs to be pursued further.

By expressing dominant negative or dominant active Egfr and Ras in post-mitotic neurons, I found that the Egfr/Ras pathway is likely to be involved in outgrowth of the photoreceptor axons. Ptp69D may antagonize the Egfr/Ras pathway to stop axons at the lamina. To test this hypothesis, other members of the Egfr pathway such as drk, Shc, and Sos could be examined for a role in photoreceptor axon outgrowth. These pathway components could also be examined for genetic modification of the Ptp69D dominant negative phenotype. Both MAPK and other small GTPases such as Rac can be activated downstream of Ras. One could examine dominant negative and dominant active Rac, Rho, and Cdc42 for effects in photoreceptor axon outgrowth, and examine loss of function Erk, Rac, Rho, and Cdc42 for modification of the Ptp69D dominant negative phenotype. Ptp69D dominant negative could be combined with the

other dominant negative or active pathway components to determine the point in the Egfr pathway at which Ptp69D acts.

I used a biochemical approach to identify proteins that bind to the Ptp69D substrate trap. PR2, a cytoplasmic tyrosine kinase, was found to bind specifically to the Ptp69D substrate trap. The *C. elegans* homolog of PR2, ARK-1, negatively regulates the Egfr pathway. Mutants in PR2 do not yet exist, but could be made using the recently developed gene disruption technology. With mutants in hand, one could examine PR2 mutants for R1-R6 targeting defects, the genetic relationship between Ptp69D and PR2 in R1-R6 targeting, and the genetic relationship between PR2 and Egfr pathway components. The biochemical interaction between Ptp69D and PR2 could also be further analyzed to identify the tyrosine on PR2 that is dephosphorylated by Ptp69D and the functional role of that phosphotyrosine.

Other proteins were also found to bind the Ptp69D substrate trap, but were not pursued further to determine whether the interaction was specific. These include Lasp, Nmda1, CG7635, CG11009, belle, and lingerer. An additional approach to identify proteins that interact with Ptp69D would be to use both substrate-trapping domains in a yeast two-hybrid interaction trap, co-expressing Src or Abl to phosphorylate potential prey proteins.

To investigate the signaling pathways downstream of Pvr, I used the intracellular domain as bait in a two-hybrid interaction trap. I identified 15 proteins that bind kinase-active Pvr, but not kinase-dead Pvr. Various of these fifteen proteins or their mammalian counterparts are involved in MAPK activation (drk, Shc), cell migration (vav, dock), hematopoiesis (Pli, Lnk), GPCR signaling (kurtz), focal adhesion signaling (tensin), or downregulation of proteins through ubiquitination (Socs16D, Socs44A, Lnk). These would all be reasonable functions for Pvr signaling proteins, as either Pvr itself or the PDGFR has been shown to be involved in all of these processes. In addition, Pvr is regulated by endocytosis and may also be regulated by ubiquitination. Twelve of the 15 interactors are expressed in larval hemocytes, embryonic hemocytes, and S2 cells, although none have embryonic in situ patterns that overlap with Pvr. I found that drk is required for Pvr-dependent Erk activation, which is consistent with the role of Grb2 in mammalian cells. However, none of the putative Pvr interactors had defects in hemocyte migration when their expression was reduced by RNAi. It is possible that while RNAi of each interactor on its own gave no migration phenotype, they would give a phenotype in a

Pvr-compromised background. This could be achieved either with a Pvr hypomorph (Pvr^{KO8} or Pvr^{1067}) or by expression of Pvr dominant negative, which gives a partially penetrant hemocyte migration phenotype.

Initial studies of mammalian PDGFR involved identification of SH2 binding sites, determination of which proteins bound which sites, and mutation of those sites to determine which binding proteins were required for various functions. The same approach could be taken with Pvr. The tyrosines in Pvr could be mutated to phenylalanine to determine which sites are required for binding the various interactors. Mutant versions lacking the relevant tyrosines could then be expressed in embryos to determine whether they rescue the Pvr mutant hemocyte migration defect. In combination with loss of function data, this would enable us to determine which Pvr-binding proteins signal downstream of Pvr in migrating hemocytes.

Pvr is involved in cell proliferation as well as migration. Overexpression of Pvf2 in larvae results in overproliferation of the larval hemocytes. It would be interesting to see whether addition of recombinant Pvfs to cell growing in culture could enhance their rate of proliferation. If such an assay could be developed, the Pvr-binding proteins could be examined for a requirement in Pvr-dependent cell proliferation in culture. Lnk and Pellino are particularly likely to have roles in hemocyte proliferation, as Lnk has been shown to negatively regulate hematopoiesis in mammals, and the serine/threonine kinase Pelle, which binds Pellino, has been shown to regulate larval hemocyte proliferation in Drosophila.

In summary, I have identified some of the proteins that may act downstream of Ptp69D and Pvr in axon guidance and cell migration. Further study of these interactions should yield insight into the pathways that regulate these processes in vivo.

APPENDIX A. Additional Pvr mutant phenotypes not described in Chapter 3.

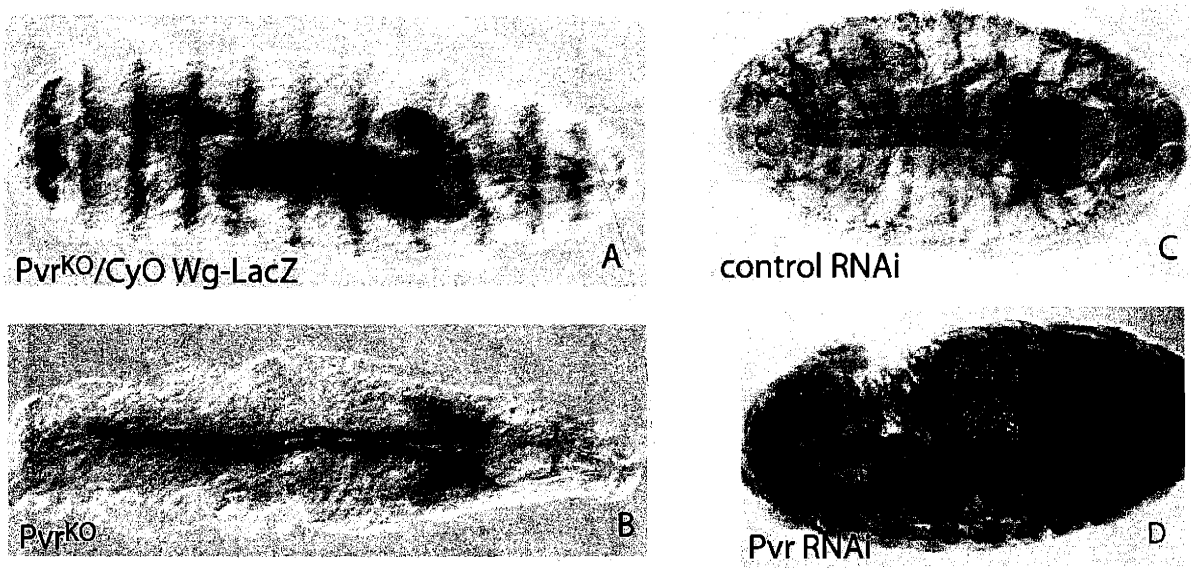

Figure A1. Pvr is required for germband retraction and nerve cord condensation. (A-B) Late stage 17 embryos stained with mAb BP102 to visualize CNS axons and anti-β-galactosidase to distinguish heterozygous (*Pvr*^{KO}/CyO Wg-LacZ) from homozygous (*Pvr*^{KO}/*Pvr*^{KO}) embryos. (A) In *Pvr* heterozygotes just prior to hatching, the nerve cord has condensed to ~1/3 of the length of the embryo. (B) In *Pvr*^{KO} embryos, the nerve cord does not condense and stays extended the entire length of the embryo. (C-D) Early stage 17 embryos stained with anti-Fasciclin II antibody to visualize longitudinal axons in the CNS and motor axons, (C) In control injected embryos, germband retraction is complete and the nerve cord has begun to condense. (D) In embryos injected with Pvr dsRNA, 7% of injected embryos fail to complete germband retraction, even though other features of embryogenesis such as gut development and motor axon extension proceed normally. (80% of injected embryos complete germband retraction, but fail to condense the nerve cord, as in (B).)

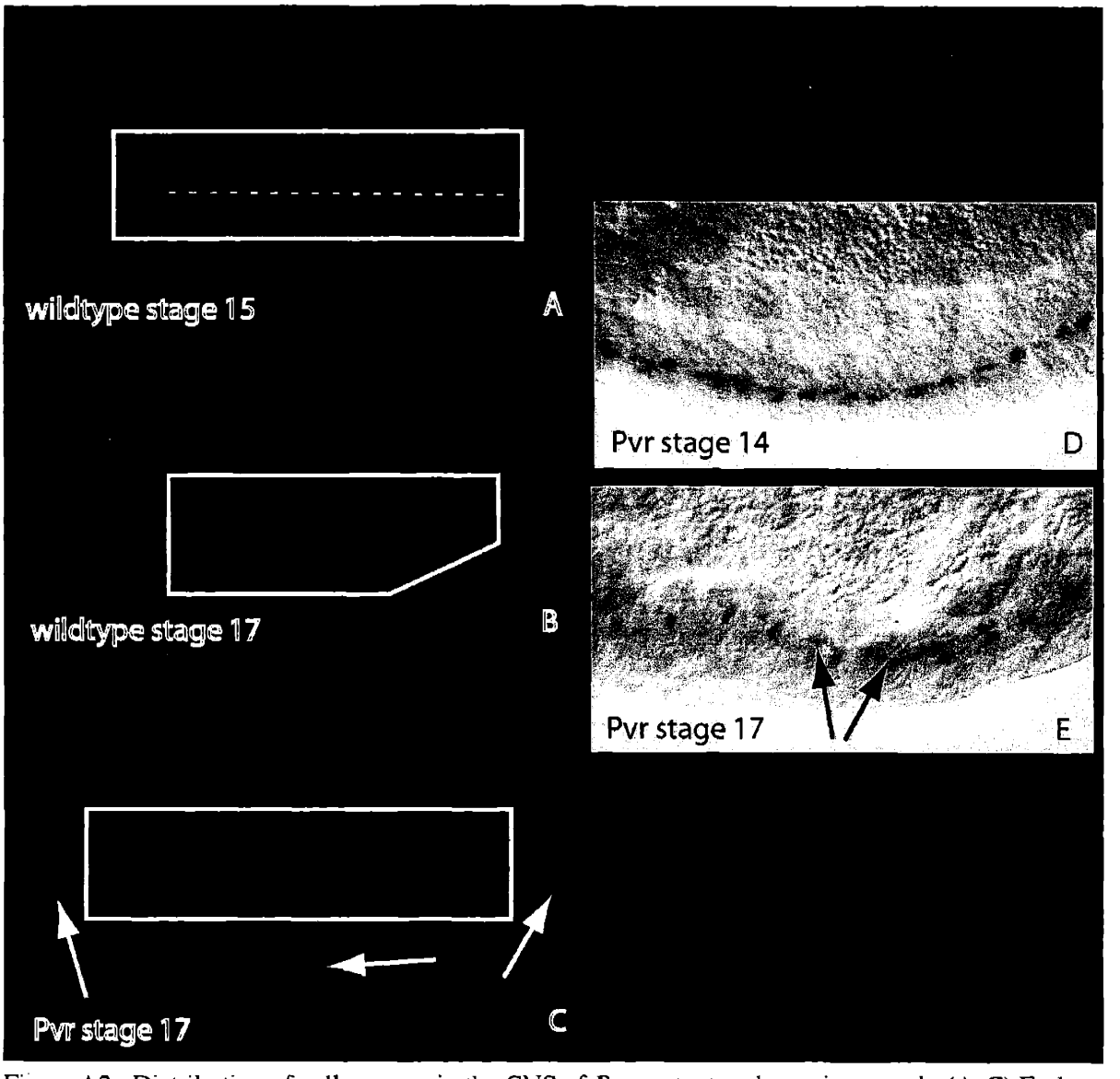

Figure A2. Distribution of cell corpses in the CNS of *Pvr* mutant embryos is normal. (A-C) Embryos were stained with acridine orange, which stains the nuclei of apoptotic cells, but not live cells. The CNS is outlined in white. (A) Stage 15, wildtype. A row of apoptotic cells can be seen down the midline (above dashed line). These are dying midline glia. There are also clumps of apoptotic cells elsewhere in the embryo (arrows). The midline glia have been engulfed by stage 17 in wildtype embryos (B) and are no longer visible by acridine orange staining. Other apoptotic cells can be seen scattered around the CNS, but the corpses that were visible elsewhere in the embryo have all been engulfed. (C) In *Pvr* mutant embryos, clumps of dead cells can be seen at various places in the embryo at stage 17 (arrows), indicative of a failure of the macrophages to scavenge the corpses. However, in the CNS, no dead midline glia remain, suggesting that they have been engulfed by another cell type or that they have been otherwise removed. (D-E) The death of midline glia proceeds normally in *Pvr* mutant embryos, as there are normal numbers of midline glia present in Pvr^{KO} embryos at stage 14 (D) and at stage 17 (E; arrows). Midline glia were marked with slit-LacZ.

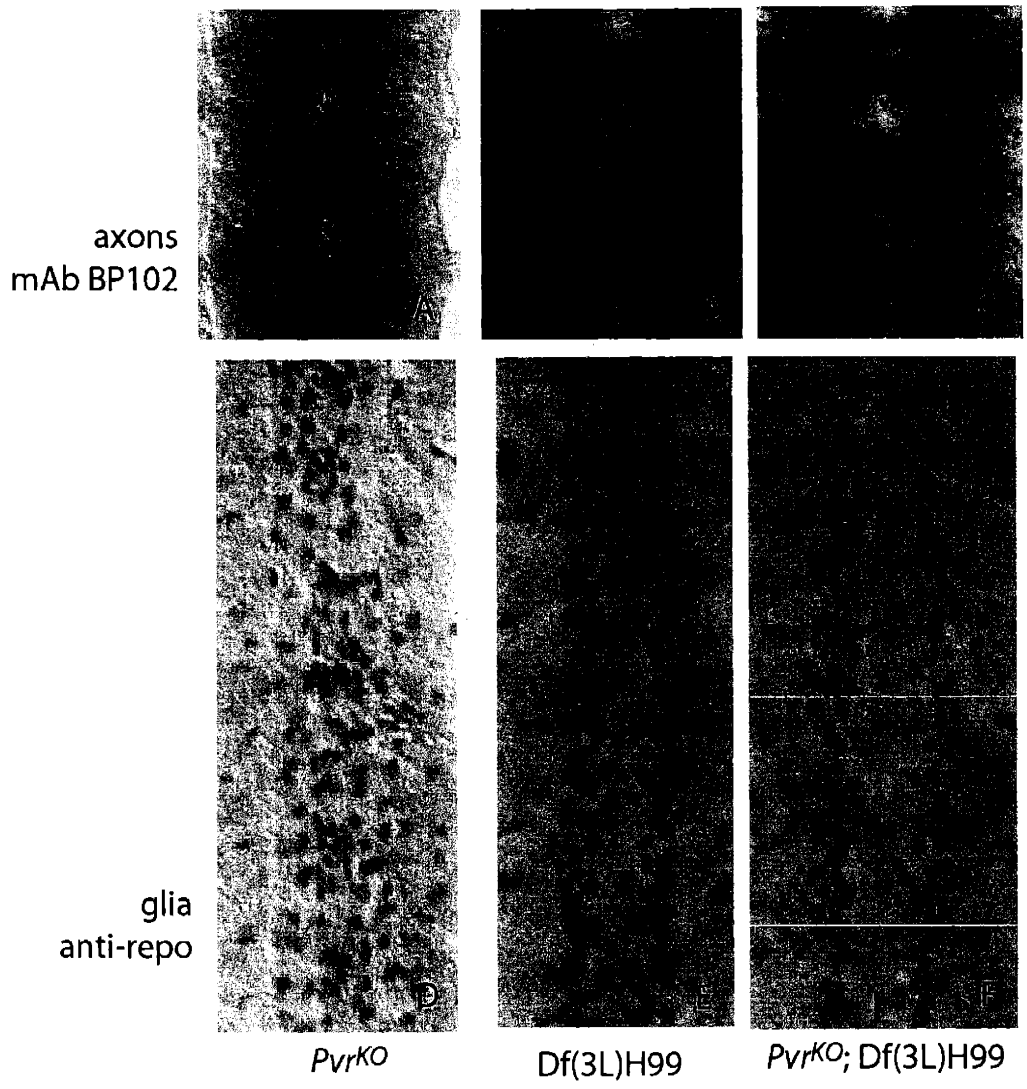

Figure A3. Blocking cell death suppresses the *Pvr* mutant CNS phenotypes. (A-C) CNS axons were stained with mAb BP102. (D-F) Longitudinal glia were stained with anti-repo antibody. (A,D) Pvr^{KO}. (B,E) Df(3L)H99, a deficiency that removes the cell death activators reaper, hid, and grim, in which all embryonic cell deaths are suppressed. These embryos have uncontracted nerve cords (not shown), but otherwise do not phenocopy Pvr mutants. The CNS in these embryos is wider than in wildtype due to the presence of extra neurons. (C,F) Pvr^{KO}; Df(3L)H99. Both the axon tract positioning defect and the longitudinal glia positioning defect observed in *Pvr* mutants were suppressed by blocking cell death. However, the widening of the CNS seen in Df(3L)H99 embryos is also suppressed.

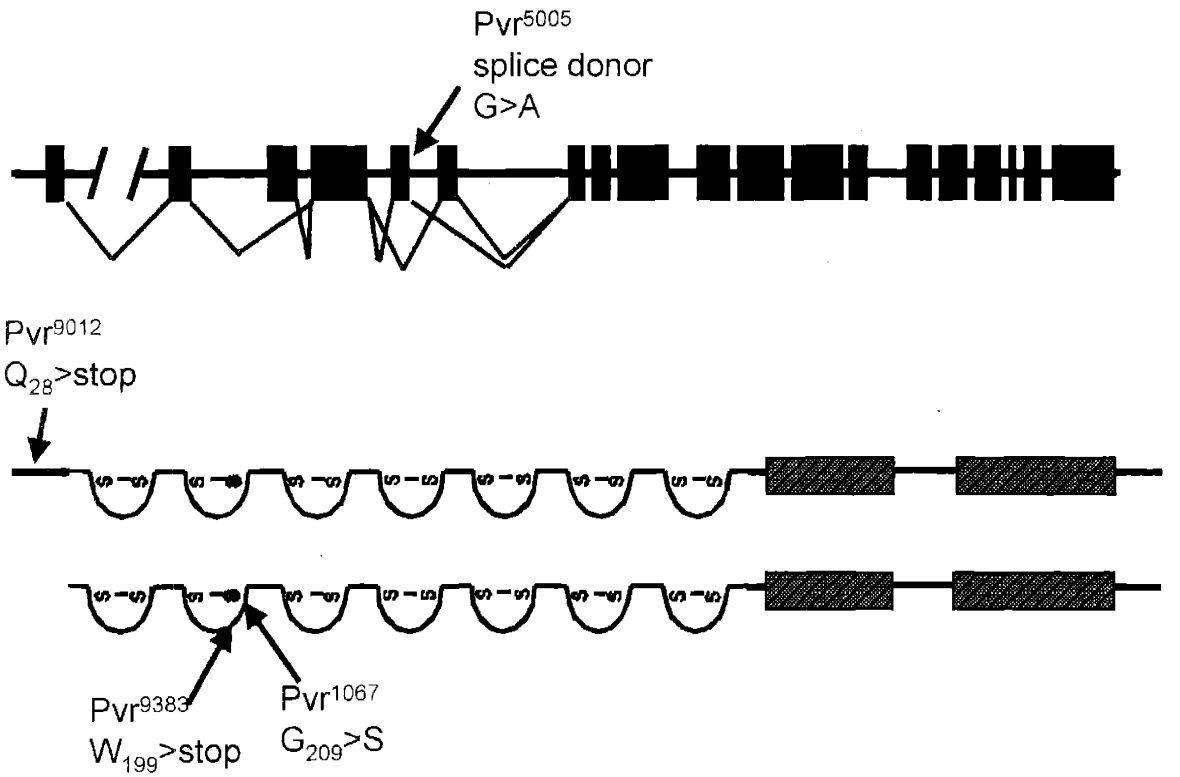

Figure A4. Several alleles of *Pvr* obtained from the EMS mutagenesis were in regions of putative alternative splicing. The locations and nature of these mutations are indicated in the figure. *Pvr*^{9012} is a nonsense mutation before the first Ig domain. An alternative first exon excludes this portion of the protein. *Pvr*^{9383} and *Pvr*^{1067} are nonsense and missense mutations respectively in the second half of the second Ig domain, which is encoded by an alternatively spliced region of the gene. *Pvr*^{1067} is a hypomorph, as a small percentage of *Pvr*^{1067}/Df(2L)Pvr hemizygous animals survive to adulthood. *Pvr*^{5005} is a mutation in the splice donor site of the first of three alternatively spliced exons encoding the second Ig domain. *Pvr*^{9383}, *Pvr*^{1067}, and *Pvr*^{5005} all affect the same alternatively spliced exon. This exon has not been found in the same mRNA as the first exon that contains the *Pvr*^{9012} lesion. However, *Pvr*^{9012} failed to complement the lethality of *Pvr*^{9383} and *Pvr*^{5005}, suggesting that these two alternatively spliced exons are found together in an as-yet undetected mRNA that is crucial for viability.

APPENDIX B. Fly strains constructed.

GMR-69D-loop: A Ptp69D dsRNA construct expressed in the eye with the GMR promoter. Homozygotes do not have any R1-R6 photoreceptor targeting defects

UAS-Δ69D: A fusion of the lambda repressor protein to the transmembrane and intracellular domain of Ptp69D, under the control of the Gal4 UAS. This chimeric protein should be constitutively dimerized. This does not give any axon guidance phenotype when crossed to GMR-Gal4.

GMR-srcDA3: The intracellular domain of Ptp69D with both phosphatase domains having the substrate-trapping D-A mutation, fused to the Src myristoylation sequence, which targets proteins to the apical surface of photoreceptors. One insertion of this contruct resulted in flies with rough eyes, but the other insertions had no phenotype.

FRT, $Ptp69D^{3A}$/TM6b

elav-Gal4, UAS-CS3, 8ex34?/TM6b: Ptp69D with both phosphatase domains having the catalytically inactivating C-S mutation, driven by the postmitotic neuronal promoter elav. These recombinants may or may not have the Ptp69D deletion Df(3L)8ex34.

$Ptp69D^{A6A}$, Ras85D/TM6b: Double mutant Ptp69D and Ras chromosome.

$Ptp69D^{A6A}$, Abl^2/TM6b: Double mutant Ptp69D and Abl^2 chromosome.

Abl^1, 23/5 /TM6b: The Abl^1 allele recombined with ro-tauLacZ, which causes expression of Δ-galactosidase in R2-R5.

$Ptp69D^{A6A}$, $Src64^{P1}$/TM6b: Double mutant Ptp69D and Src64 chromosome.

Pvr^{KO2}; $Ptp69D^{A6A}$/ CyO, TM3 hs-GFP

Vgr-KO DDNA, BDBA, BDBB: The starting strains for creating the Pvr knock-out.

slit-LacZ; Pvr^{KO1}/CyO A405: Δ-galactosidase expressed in midline glia, Pvr mutant.

Pvr^{KO2}/CyO; UAS-Pvr/TM6b: Strain for performing Pvr rescue experiments.

PvrKO, UAS-p35/ CyO Kr-GFP: A strain for blocking apoptosis in a subset of cells (by expression of p35) in a Pvr mutant background.

Pvr^{KO1}, elav-Gal4, Ki/ CyO, TM3 hs-GFP: elav-Gal4 drives expression of UAS constructs in postmitotic neurons

Pvr^{KO1}, sim-Gal4/ CyO Kr-GFP: sim-Gal4 drives expression of UAS constructs in midline glia and neurons

Pvr^{KO1}, slit-Gal4/ CyO Kr-GFP: slit-Gal4 drives expression of UAS constructs in midline glia

Pvr^{KO2}; $comm^{\Delta e39}$ / CyO, TM3 hs-GFP

elav-Gal4, UAS-Pvr, Ki/ TM6b Ubx-LacZ

Pvr^{KO}; Df(3R)H99/ CyO, TM3 hs-GFP: Df(3L)H99 deletes the cell death activators reaper, hid, and grim.

Pvr^{KO}; undertaker/ CyO, TM3 hs-GFP: undertaker is a gene required for hemocyte phagocytosis (Natalie Franc).

ACKNOWLEDGMENTS

I'd like to thank Paul Garrity for all of his encouragement and support. Thanks to Frank Gertler, Terry Orr-Weaver, and Bob Horvitz for challenging me, encouraging me, and giving me superb advice when I needed it most. I received technical help from Myles Robichaux, Candice Thomas, Caleb Kennedy, and Paul Phelps. I was supported through a Centocor Fellowship provided by Michael Wall and Hubert Schoemaker. Tim Tayler, Rita Khodosh, Jessica Whited, and Mark Rosenzweig have been like family to me over the past seven years. Thanks for being a sounding board for my ideas and my struggles. Thanks to my parents, David and Sandra Robertson, for supporting me in this endeavor since the beginning, and for always trying to understand what I was working on even when it was impossible. Saving the best for last, the most thanks goes to my husband Andrew for keeping me sane, for listening to my day every day even when he didn't understand most of the words I was saying, for celebrating with me through the good times and empathizing with me through the rough times. Thanks to everyone who made this possible for me.